



HAL
open science

L'analyse spatiale des extrêmes à partir d'une unique réalisation : un point de vue géostatistique

Marine Demangeot

► **To cite this version:**

Marine Demangeot. L'analyse spatiale des extrêmes à partir d'une unique réalisation : un point de vue géostatistique. Applications [stat.AP]. Université Paris sciences et lettres, 2020. Français. NNT : 2020UPSLM032 . tel-03078592

HAL Id: tel-03078592

<https://pastel.hal.science/tel-03078592>

Submitted on 16 Dec 2020

HAL is a multi-disciplinary open access archive for the deposit and dissemination of scientific research documents, whether they are published or not. The documents may come from teaching and research institutions in France or abroad, or from public or private research centers.

L'archive ouverte pluridisciplinaire **HAL**, est destinée au dépôt et à la diffusion de documents scientifiques de niveau recherche, publiés ou non, émanant des établissements d'enseignement et de recherche français ou étrangers, des laboratoires publics ou privés.



THÈSE DE DOCTORAT
DE L'UNIVERSITÉ PSL

Préparée à MINES ParisTech

**L'analyse spatiale des extrêmes à partir d'une unique
réalisation : un point de vue géostatistique**

**Spatial extremes with a single realization: a geostatistical
point of view**

Soutenue par

Marine DEMANGEOT

Le 05 Octobre 2020

École doctorale n°621

**Ingénierie des Systèmes,
Matériaux, Mécanique, En-
ergétique**

Spécialité

**Géostatistique et probabil-
ités appliquées**



Composition du jury :

Liliane BEL Professeure, AgroParisTech	<i>Présidente</i>
Clément DOMBRY Professeur, Université de Franche-Comté	<i>Rapporteur</i>
Marco OESTING Assistant Professor, University of Stuttgart	<i>Rapporteur</i>
Jean-Noël BACRO Professeur, Université de Montpellier	<i>Examineur</i>
Gwladys TOULEMONDE Maître de conférences, Université de Montpellier	<i>Examinatrice</i>
Erwan KOCH Assistant Professor, EPFL Lausanne	<i>Examineur</i>
Emilie CHAUTRU Chargée de recherche, MINES ParisTech	<i>Examinatrice</i>
Hans WACKERNAGEL Directeur de recherche, MINES ParisTech	<i>Directeur de thèse</i>

SPATIAL EXTREMES WITH A SINGLE REALIZATION: A GEOSTATISTICAL POINT OF VIEW



Thèse de doctorat

MINES ParisTech, PSL University - Centre de Géosciences - Equipe Géostatistique
Télécom Paris - Centre IDS - Equipe S2A

August 2020

Travaux encadrés par Hans Wackernagel et Emilie Chautru

Financements MINES ParisTech - Télécom Paris

Il est impossible que l'improbable n'arrive jamais.

– Emil Gumbel (1891-1966)

ABSTRACT - RÉSUMÉ

ABSTRACT

Spatial extreme value theory helps model and predict the frequency of extreme events in a spatial context like, for instance, extreme precipitations, extreme temperatures or high concentrations of pollution in the air. It is well adapted to time series, when the spatial object under study is observed through time. However, in some cases, such types of data cannot be accessed: only one or just a few records are made available. This is the case, for instance, in mining resources estimation, soil contamination evaluation or any other applications where the phenomenon of interest either varies too slowly across time to hope for a decent time series, or is too expensive to sample from. This situation is rarely addressed in the spatial extremes community, contrary to Geostatistics, which typically deals with such issues. The aim of this thesis is to make some connections between both disciplines, in order to better handle the study of spatial extreme events when having only one set of spatial observations.

We first focus on the concept of integral range. Intimately related to the ergodic and mixing properties, it is a geostatistical parameter that characterizes the statistical fluctuations of a stationary random field at large scale. When the latter is max-stable, we show that its extremal coefficient function (ECF) is closely related to the integral range of the corresponding exceedance field above a threshold. This approach allows to retrieve and complete previous results established in a spatial risk context. It also has the advantage of revealing a new expression for the extremal coefficient function that depends on the variogram of the exceedance field.

From this, we move to proposing a new nonparametric estimator of the ECF. Its asymptotic properties are derived when it is computed from a single and partially observed realization of a stationary max-stable random field. Specifically, considering both infill and increasing domain asymptotics, and under some assumptions on the aforementioned integral range, we prove that it is consistent and asymptotically normal. This illustrates the relevance of geostatistical tools for enriching extreme value analysis.

Finally, we develop a novel algorithm to perform exact simulations in a continuous domain of storm processes with deterministic shape function. It distinguishes itself from most existing algorithms, which apply to simulation domains made of a finite number of points. In this regard, it allows for easier investigation about the geometry of realizations of such processes. This is of particular interest when the geometric feature under study involves different scales of observation.

Key words: Spatial extreme value theory, Extremal coefficient function, Geostatistics, Integral range, Single realization, Simulation algorithm.

RÉSUMÉ

La théorie spatiale des valeurs extrêmes permet de modéliser et prédire la fréquence d'évènements extrêmes ayant une étendue spatiale comme, par exemple, des pluies ou des températures extrêmes, ou encore de fortes concentrations de polluants dans l'air. Elle s'adapte bien aux données temporelles, lorsque le phénomène spatial étudié est observé plusieurs fois dans le temps. Cependant, nous n'avons parfois pas accès à de telles données: seulement un ou quelques enregistrements sont disponibles. C'est le cas, par exemple, des études sur l'estimation des ressources minières ou sur l'évaluation de la pollution des sols et plus généralement de toute recherche dont l'objet d'étude varie très peu au cours du temps ou pour lequel le coût d'échantillonnage est trop élevé. Ce cas de figure est très peu abordé par la communauté des extrêmes. Au contraire, c'est un cadre d'analyse auquel la Géostatistique s'intéresse particulièrement. Les travaux réalisés au cours de cette thèse ont pour objectif d'établir des connexions mathématiques entre ces deux disciplines afin de mieux appréhender les évènements extrêmes, lorsque le phénomène spatial sous-jacent n'est observé qu'une seule fois.

Nous nous intéressons, dans un premier temps, au concept de portée intégrale. Intrinsèquement lié aux propriétés d'ergodicité et de mélange, ce paramètre issu de la théorie géostatistique caractérise les fluctuations statistiques, à large échelle, d'un champ aléatoire stationnaire. Lorsque ce dernier est un champ max-stable, nous montrons que sa fonction coefficient extrémal (ECF) est fortement liée à la portée intégrale du champ des excès, au dessus d'un certain seuil, correspondant. Cette approche permet de retrouver et de compléter des résultats précédemment établis dans un contexte de risque spatialisé. Elle met également en évidence une nouvelle expression de la fonction coefficient extrémal qui dépend du variogramme du champ des excès.

À partir de cette formule, nous proposons un nouvel estimateur non-paramétrique de l'ECF. Ses propriétés asymptotiques sont établies lorsqu'il est évalué à partir d'une unique réalisation, partiellement observée, d'un champ stationnaire max-stable. En particulier, lorsque le nombre d'observations se densifie en même temps que le champ d'observation grandit, et sous certaines hypothèses concernant la portée intégrale susmentionnée, nous montrons qu'il est consistant et asymptotiquement normal. Il est donc pertinent d'utiliser les outils géostatistiques pour enrichir l'analyse des valeurs extrêmes.

Finalement, nous développons un nouvel algorithme permettant de simuler, en continu, des processus aléatoires tempête pour lesquels la fonction de forme est déterministe. Il se distingue donc de la plupart des algorithmes existants qui s'utilisent exclusivement lorsque le domaine de simulation est composé d'un nombre fini de points. À cet égard, il permet d'étudier plus facilement la géométrie des réalisations de tels processus. Cela est particulièrement intéressant quand la caractéristique géométrique étudiée mêle différentes échelles d'observation.

Mots clés: Théorie spatiale des valeurs extrêmes, Fonction coefficient extrémal, Géostatistique, Portée intégrale, Réalisation unique, Algorithme de simulation.

PUBLICATIONS

SUBMITTED FOR PUBLICATION

M. Demangeot, R. Carnec, E. Chautru, C. Lantuéjoul, *Continuous simulation of storm processes*, 2020

TO BE SUBMITTED

M. Demangeot, E. Chautru, A. Sabourin, *Estimation of the extremal coefficient function based on a single observation*, 2021

M. Demangeot, E. Chautru, E. Koch, *Integral range for spatial risk assessment*, 2021

REMERCIEMENTS

Le meilleur pour la fin. Ainsi s'achève, pour moi, la rédaction de ce manuscrit de thèse. La tâche s'avère pourtant plus ardue qu'il n'y paraît : les mots seront-ils à la hauteur de toute la gratitude et la joie que j'éprouve lorsque je pense aux nombreuses personnes qui m'ont accompagnée dans cette aventure ?

Pour commencer, je souhaite remercier chaleureusement les membres de mon jury de thèse d'avoir accepté d'évaluer mon travail. Merci aux rapporteurs Clément Dombry et Marco Oesting pour la lecture attentive de mon manuscrit mais aussi pour tous les échanges que nous avons eus durant la thèse et qui m'ont été extrêmement bénéfiques. Merci aussi à ma présidente de jury, Liliane Bel, ainsi qu'aux autres examinateur·rice·s, Jean-Noël Bacro, Gwladys Toulemonde et Erwan Koch, pour leurs remarques pertinentes et leurs conseils avisés. J'en profite pour remercier Erwan d'avoir accepté de collaborer avec nous et pour toutes les discussions intéressantes qui s'en sont suivies, et pour celles encore à venir. Enfin, merci à tou·te·s pour votre disponibilité, votre bienveillance et vos encouragements pour la suite.

Je souhaite ensuite adresser un immense merci à mon encadrante de thèse Emilie. Je suis honorée d'avoir été ta première doctorante et je te remercie pour la confiance que tu m'as accordée en acceptant ma candidature à ce sujet de thèse. Merci pour tout l'accompagnement prodigué au cours de ces quatre dernières années. Un accompagnement scientifique d'une admirable rigueur dans l'univers fascinant des valeurs extrêmes, mais également très pédagogique : grâce à ton aide, je crois maintenant tenir le bon bout des présentations orales – je n'oublie pas les exercices théâtraux conseillés – et de la rédaction en anglais. Et surtout un accompagnement d'une extrême humanité qui a su me rassurer et m'encourager dans les nombreux moments de doute et de questionnement traversés. Travailler avec toi m'a aidée à affirmer mon envie de faire de la recherche : pour cela **merci**. La *mini-toi* que je suis espère maintenant que nous continuerons à collaborer ensemble. Je remercie aussi vivement Anne Sabourin qui a su trouvé des financements à Télécom afin que ma thèse puisse être prolongée. La collaboration qui s'en est suivie a été pour moi une riche expérience.

Ce doctorat a également été l'occasion de découvrir l'extrême richesse scientifique de la Géostatistique car j'ai eu la chance et le plaisir d'effectuer mon travail de recherche au sein de l'équipe de Géostatistique des Mines de Paris. Aussi, j'aimerais maintenant remercier l'ensemble des membres de cette équipe pour leur accueil, leur disponibilité et leur bienveillance. Merci à Hans, mon directeur de thèse à qui je dois ma première rencontre avec la communauté des extrêmes à Lausanne : tu as toujours su avoir des mots encourageants à mon égard. Merci Didier pour ton entrain communicatif ainsi que pour ton aide avec RGéostat : toujours prêt à voler à la rescousse des doctorants en détresse. Merci Fabien d'avoir répondu présent lorsque les soucis de programmation pointaient leur nez, mais aussi pour ton enthousiasme, ton énergie et les quelques parties de jeux de société partagées (je n'oublie pas que tu m'as tuée à Time bomb...). Merci à Nicolas pour tous tes encouragements et pour avoir partagé avec moi ton expérience passée en tant que doctorant : nos discussions m'ont aidée à ne pas me laisser submerger par le bien connu syndrome de l'imposteur. Merci aussi à Xavier, Chantal et Jacques d'avoir

été attentif-ve-s au bon déroulement de cette thèse et d'avoir toujours pris le temps de me conseiller. Merci ensuite à Gaëlle pour avoir su apporter une réponse à mes questions d'ordre géostatistique mais également pour les discussions autour d'une tasse de thé et, quelques fois, d'un bon gâteau fait maison. Je n'oublie pas non plus Thomas avec qui j'ai fait mes premiers pas dans l'univers de la Géostatistique, Cachou et nos aventures pédestres ainsi que Serge : merci pour les échanges que nous avons pu avoir ensemble. Un immense merci Nathalie – et en son temps Isabelle – pour toute la bonne humeur, la bienveillance et le bien-être que tu apportes à cette équipe : les *tea time* vont beaucoup me manquer. Enfin, *last but not least*, un merci infini à Lantu qui a toujours laissé sa porte ouverte, tôt le matin comme le tard le soir, aux nombreuses questions mathématiques que je me posais et qui à chaque fois, craie en main, a pris le temps d'y répondre avec rigueur, minutie et justesse. Je te suis extrêmement reconnaissante pour toute cette aide et plus généralement pour ton implication dans ce travail de thèse qui, sans toi, n'aurait pas la même allure. En particulier, je suis très honorée d'avoir pu collaborer avec toi, Emilie et Rémi (que je remercie au passage pour son excellent travail aussi bien computationnel que mathématique) sur la problématique de simulation des processus tempêtes : cette enrichissante et enthousiaste expérience m'encourage aujourd'hui à poursuivre dans la recherche. Merci également pour tous les « à-côtés » non mathématiques mais néanmoins très précieux que l'on a pu partager. À quand la prochaine excursion dans la forêt de Fontainebleau ?

D'autres spécimens hantent le bâtiment B du centre de Géosciences. Venant des quatre coins du monde, c'est par exemple le cas des étudiant-e-s du master CFSG avec qui il a toujours été agréable de discuter. J'ai une pensée particulière pour Hector, Esteban, Cécile, Marie-Cécile, Zhuldyz, Catalina et William. Cependant des créatures, plus mystérieuses encore, rôdent dans ses couloirs. Elles se réunissent quelquefois dans le hall et sous l'œil sévère du patriarche chantent, paraît-il, ses louanges : ce sont bien-sûr les doctorant-e-s de Géostat. Je suis sincèrement heureuse d'avoir pu vivre cette aventure en votre compagnie ! À commencer par Léa, avec qui j'ai eu le plaisir de partager mon bureau mais également les « joies » de la dernière ligne droite. Puis Jean et Laure, mes camarades PFP et bien plus encore, qui m'ont appris que la géologie, au final, c'était grave stylé. Alan, une présence réconfortante le matin quand j'arrivais, qui m'a fait redécouvrir le français : finalement eras tú el professor. Mathieu et Luc mes petits frères de thèse et Mike, toujours souriant, dont les visites à Fontainebleau m'enchantaient. Ricardo, mon presque colocataire qui a pris le temps d'écouter mes problèmes mathématiques. Mais aussi Jihane, Anna et Hugo. Merci à vous pour toute la joie que vous m'avez apportée. J'espère que la force de Georges ne nous tiendra jamais trop loin les un-e-s des autres (malgré nos désaccords gustatifs concernant la coriandre). Enfin, je ne puis terminer là sans évoquer un Géodoctorant (ou un encadrant, c'est selon) qui nous a accordé le privilège quasi quotidien de sa visite : le dénommé Robin. Merci bien-sûr pour le fameux lemme, mais surtout, merci d'avoir égayé mes journées avec tes apparitions furtives (mama ?) et d'avoir accompagné nos calculs, tard le soir, avec ta guitare.

Toutes ces illustres personnes font bien-sûr partie d'un plus vaste groupe de joyeux lurons : les doctorant-e-s & cie de Fontainebleau. En premier lieu, je pense à mon cher binôme de la DopaTeam Aurélien, adorable et attentionné avec nous tou-te-s (quoiqu'en dise Nico) : ta présence m'a été d'un grand réconfort. Merci à notre prédécesseur Sébastien qui avait rassemblé autour de lui un groupe soudé de doctorant-e-s : débiter sa thèse dans une si sympathique ambiance a été une chance ! Merci aussi à notre successeur Bob d'avoir repris le flambeau même si le succès de Dopalloween ne lui laissait plus

trop le choix : t'as géré! Je pense ensuite aux apparitions de bôôté légendaire de JB, à l'écoute et aux conseils bienveillants de Vaia, aux discussions paisibles avec Léonardo, Samy ou Amin, de retour dans le transilien R. Merci à Albane, Paule, Thibaut, Martin, Eric et François pour nos footings plus ou moins réguliers, quelques fois ponctués par l'apparition soudaine d'une biche ou d'un faon, au loin dans les fourrés, mais aussi à Elodie pour les séances de basket que tu as organisées. Angélique et Bibiche, je reste toujours époustoufflée par votre formidable interprétation de *Confessions nocturnes* et par votre incroyable motivation dès qu'il s'agit d'aller boire un coup; heureusement c'est également le cas de beaucoup d'autres ici. Merci Nicolas, notre petit rayon de soleil belge, pour ton enthousiasme sans faille et l'attention que tu portes aux gens autour de toi. Une pensée supplémentaire pour Guinnesse qui est décidément beaucoup trop mignonne. Je n'oublie pas non plus l'Audace de Kiki, l'humour fin de Léo, les visites bellifontaines de Paul et Xavier après un détour par Champagne-sur-Seine, et toutes les doctorant-e-s et affilié-e-s que j'ai eu la chance de pouvoir rencontrer : Alexandra, Loïc, Alexandre, Manon, Kaiwen, Théo, Andrès, Pierre, Eirini, Aurélien B, Hugues, Clément, Maëlle, Rémi, Shuaitao, Mathias, Nicolo, Deniz, Michelle, Tianyou, Hao, Michelle, Simona et bien d'autres encore. J'emporte avec moi des souvenirs précieux de tous ces merveilleux moments que j'ai passé avec vous, que ce soit un tarot (parfois à 10), une soirée jeux, une foulée impériale, une randonnée, une piste de ski dévalée, une raquette partagée, une bière au Glasgow, un apéro au canal, un karaoké, une soirée rock endiablée, une initiation au tricot... bref, la liste est longue. À très vite pour de nouvelles aventures!

Au sein de cet univers bellifontain, je souhaiterais enfin remercier Isabelle Olzenski ainsi que les autres membres de la Délégation qui veillent au bien vivre ensemble sur le site. Merci ensuite à Véronique Lachasse de prendre soin des doctorant-e-s, à Hervé Chauris et Jesus Angulo pour leurs encouragements, à Corinne pour le sourire qu'elle arbore tous les midis et aux membres de la DSI qui font un super travail. J'ai eu plaisir également à discuter avec bon nombre d'entre vous : Agnès, Alexandrine, Etienne, Beatriz Petr, Jean-Louis et Aurélien Baudin pour n'en citer que quelques-un-e-s.

Cette thèse m'a aussi permis de faire de belles rencontres en conférences. I thus would like to send kind regards to the extreme phd students I've met during the past four years : Jasper, Phyllis, Laura, Corina, Jon, Emilie, Florian, Andrea, Amir, Hamid and many more. Une mention spéciale pour Emilie avec qui j'ai effectué mes études en Statistiques et que j'ai eu l'immense plaisir de retrouver dans la communauté des extrêmes.

J'aimerais maintenant non plus m'attarder sur les nouvelles amitiés que j'ai tissées lors de ce doctorat mais sur de plus anciennes relations qui ont été, ces dernières années, très importantes pour moi et que je souhaite saluer. Je pense à Adrien, mon ancien tuteur de stage chez EDF, qui m'a encouragée à poursuivre en thèse, ainsi qu'à toute la troupe des Renardières. *Faute de mieux*, je pense aussi à la team Basket et aux rires qui ponctuent nos après-midi jeux : pour la peine, je vous graoute toutes. Merci aux *Filles* de l'Ensaï qui embellissent ma vie depuis maintenant sept ans, et ce même à distance. En particulier merci Angélique, ma coloc' adorée, pour ton enthousiasme débordant et la justesse de tes mots. Merci Nicoleta pour tes câlins réconfortants et tes encouragements énergiques. Et merci Manon d'être là depuis un bon bout de temps maintenant et pour tout ce que tu partages avec moi. Je vous kiffe grave les meufs! Merci aussi aux autres ami-e-s Ensaiens pour les bons moments partagés, et ceux encore à venir, à commencer par mon filleul Vasile puis Camille, Fabien, JB, Cornelia, David mais aussi

Adrian, Alex, Mathias, Benjamin et de nombreuses autres personnes. Je remercie ensuite Juliette, mon autre coloc' adorée, pour la joie que tu m'apportes et pour toutes les multiples attentions dont tu fais preuve à mon égard. Je remercie également la Brigade Temporelle pour toutes nos missions sauvetages, même celles qui échouent, et notamment Marie pour ton amitié que je chéris maintenant depuis 25 ans. Enfin, remontons aux origines : merci à la fabuleuse Team Sud – Coco, Alex, Julia, Bastien, Bryan, Nico, les Lucie et Ludivine – d'être toujours dans les parages. En particulier, merci aux plus ancien-ne-s, les *Alice Reynaud-sard*, dont l'amitié est l'un de mes trésors les plus précieux.

Si je termine cette thèse, c'est aussi grâce à de nombreux enseignant-e-s parmi lesquel-le-s Marcin Pulkowski avec qui j'ai découvert la beauté des Mathématiques, François Coquet qui m'a encouragée à oser et Myriam Vimond qui a toujours été disponible et de très bon conseil. Merci à tous ces professeur-e-s pour leur patience et l'énergie qu'ils déploient à élever nos consciences et à aiguïser nos réflexions.

La fin approchant, les lecteur-trice-s averti-e-s devineront sans surprise à qui s'adressent les prochains remerciements. De tout cœur, merci à ma famille pour tous ces moments que je ne rappellerai pas ici mais auxquels je pense très fort. La joie que me procure l'accomplissement de cette thèse n'est rien comparée à celle toute particulière que j'éprouve à partager votre vie. Enfin, Houssam, merci pour tout le courage et le réconfort que tu m'as apporté dans cette aventure. Merci d'avoir pris soin de moi dans la dernière (et un peu longue) ligne droite de cette thèse. Et tout simplement, merci pour le bonheur que m'a procuré ta présence ces dernières années. J'espère que, longtemps encore, tu auras envie de me manger car il y a mille autres aventures que j'aimerais maintenant vivre avec toi... \o/.

CONTENTS

I	INTRODUCTION	1
I.1	Motivation	1
I.2	Outline of the thesis	2
1	WHAT ARE SPATIAL EXTREMES	5
1.1	Extreme events, a statistical issue	6
1.1.1	Definition: extreme or not extreme that is the question	6
1.1.2	Estimating with few observations	7
1.2	Univariate extreme value theory	10
1.2.1	Normalized maxima: max-stable distributions	10
1.2.2	Peaks over threshold: the generalized Pareto distribution	13
1.2.3	An illustrative example	16
1.3	Spatial extremes: all about dependence	18
1.3.1	Random field: a brief presentation	19
1.3.2	Max-stable random fields	22
1.3.3	Extremal coefficient function: dependence in extremes	24
1.4	Estimating extreme events with spatial data	26
1.4.1	With repetitions of the spatial process: the standard framework	26
1.4.2	With a single observation: a geostatistical specificity	28
1.4.3	A specific issue: top-cut model and extreme value theory	32
2	FROM GEOSTATISTICS TO EVT: INTEGRAL RANGE AND EXTREMAL COEFFICIENT FUNCTION	35
2.1	Setting	36
2.1.1	Stochastic integrals	36
2.1.2	Convergence to \mathbb{R}^d	37
2.2	The integral range	38
2.2.1	Background	38
2.2.2	Definition and interpretation	41
2.2.3	Estimation	46
2.3	Connecting the integral range with the extremal coefficient function	50
2.3.1	Main results	53
2.3.2	Examples	57
2.3.3	Illustrations	61
2.4	Applications in a spatial risk context	69

2.4.1	Some context	69
2.4.2	The integral range, a relevant tool	71
2.5	Discussion	72
2.6	Proofs	74
2.6.1	Integral range and nonnegative correlation function	74
2.6.2	Correlation function behaviour	74
2.6.3	Finite integral equivalence	75
2.6.4	Mixing and mean-ergodicity properties	80
2.6.5	M2 process with Cauchy density shape function	83
2.7	Supplements about Van-Hove sequences	84
3	ESTIMATION OF THE EXTREMAL COEFFICIENT FUNCTION BASED ON A SINGLE OBSERVATION	89
3.1	Introduction	89
3.2	Settings	90
3.3	A new nonparametric variogram based estimator	91
3.3.1	Covariance or variogram ?	91
3.3.2	Nonparametric kernel estimator of the variogram: definition and as- sumptions	94
3.3.3	Asymptotic properties	98
3.4	Numerical experiments	101
3.4.1	Experimental protocol	101
3.4.2	Tracking consistency and asymptotic normality	103
3.4.3	Comparison with the F-madogram estimator	104
3.5	Discussion	109
3.6	Proofs and supplements	111
3.6.1	Finite integral range: a sufficient condition	111
3.6.2	Continuity: an adequate assumption	115
3.6.3	Finite integrale range: an alternative condition	118
3.6.4	Ergodicity in the covariance	122
4	CONTINUOUS SIMULATION OF STORM PROCESSES	125
4.1	Introduction	126
4.2	Notation and setting	127
4.3	An algorithm for continuous simulation	129
4.3.1	Contribution of the inner process	129
4.3.2	Contribution of the outer process	130
4.3.3	Efficient computation of maxima	134
4.4	Examples	135
4.4.1	Gaussian storms	135

4.4.2	Student storms	137
4.4.3	Power exponential storms	138
4.5	Discussion	140
4.5.1	On the covering	140
4.5.2	About the simulation domain	141
4.5.3	Improving computation efficiency	141
4.5.4	Random storms	142
4.6	Conclusion	143
4.7	Proofs	143
4.7.1	Distribution of \dot{s}	143
4.7.2	Domains of influence of power exponential storms	145
	BIBLIOGRAPHY	149

ACRONYMS

MATHEMATICAL ABBREVIATIONS

EVT	Extreme value theory
RF	Random field
SRF	Stationary random field
i.i.d.	Independent and identically distributed
c.d.f.	Cumulative distribution function
p.d.f.	Probability distribution function

INTRODUCTION

I.1 MOTIVATION

In 2012, the Intergovernmental Panel on Climate Change (IPCC) published a special report entitled *Managing the risks of extreme events and disasters to advance climate change adaptation* (see [IPCC, 2012](#)), in which they stated

« It is *likely* that the frequency of heavy precipitation or the proportion of total rainfall from heavy rainfalls will increase in the 21st century over many areas of the globe. »

More generally, as suggested by both observational and numerical climate models, the frequency, intensity and spatial extent of weather and climate extremes such as high rainfalls, heat waves or windstorms will increase in the future. Hence, it is of primary interest to improve our apprehension of spatial extreme events, in order to better assess the related risks. In such a context, the spatial extreme value theory is particularly relevant: it helps model and predict the frequency of extreme events in a spatial context.

Even if climate extreme events are likely to be more frequent, they are still rare events, by definition. Consequently, the main issue when studying them from a statistical point of view is that the amount of related data is limited. Furthermore, it is often needed to infer extremal behaviours well beyond the range of observed data. Based on some specific models, among which the so-called *max-stable* models, the extreme value theory basically uses the largest observations to perform such extrapolations. One approach, linked to the max-stable models, is to work with maxima, for instance monthly or annual (pointwise) maxima of temperatures over a region. If the temperatures are recorded over a long period, this results in a time series of maxima. Hence, since climatic data are generally observed through time, spatial analysis of climatic extremes often deals with time series. However, as mentioned in [Naveau et al. \(2009\)](#), climate is defined by the atmospheric scientists as the behaviour of the atmosphere over a long period of time. Instead of monthly or annual maxima, it thus may be interesting to consider maxima over a longer period. This is done *e.g.* in [Naveau et al. \(2009\)](#) when studying the Bourgogne precipitation data set, which regroups 51-year maxima of daily precipitation recorded at 146 weather station locations. At each location, they consider the maxima of precipitation over the whole observed period. The resulting data set is thus made of a single set of spatial observations. Actually, such a framework is rarely addressed in the spatial extremes

community and, as specified in [Naveau et al. \(2009\)](#), there is a need to theoretically investigate the estimation of extreme events in this context. On the contrary, Geostatistics typically deals with such issues. The aim of this thesis is therefore to make some connections between this discipline and the spatial extreme value theory in order to better handle the study of extremes when having only one spatial set of data.

I.2 OUTLINE OF THE THESIS

[Chapter 1](#) is dedicated to the introduction of spatial extreme value theory. For readers who are unfamiliar with the statistical study of extreme events, we first discuss the specificities of these events. Basic results and objects from univariate extreme value theory are also presented, and a toy example is provided to illustrate the relevance of the theory when assessing extremal behaviours. Then, max-stable processes are introduced together with the extremal coefficient function. This function is a bivariate measure of spatial extreme dependence, which is at the center of this PhD. Finally, we address the question of estimating spatial extreme events when the phenomenon under study is observed only once. In this regard, basic tools and concepts from Geostatistics are reminded.

[Chapter 2](#) centres on the concept of integral range. Intimately related to the ergodic and mixing properties, it is a geostatistical parameter that helps characterize the statistical fluctuations of a stationary random field at large scale. A detailed account of this quantity is first given. In particular, we introduce a new method to estimate it, which slightly differs from the procedure originally proposed by [Lantuéjoul \(1991\)](#). Then, when the random field is simple max-stable, we show that its extremal coefficient function is closely related to the integral range of the corresponding exceedance field I_z above a positive threshold z . In particular, we find a necessary and sufficient condition on the former so that the latter is finite. This condition is investigated for standard max-stable models, then illustrated on simulations. It is also related to the ergodic and mixing properties of simple max-stable processes. Finally, we show that this work allows to retrieve and complete previous results established by [Koch \(2017\)](#) in a spatial risk context.

From the work of [Chapter 2](#), a new nonparametric estimator of the extremal coefficient function is proposed in [Chapter 3](#). It is based on the kernel variogram estimator of I_z studied in [García-Soidán et al. \(2004\)](#) and [García-Soidán \(2007\)](#). From their work, we derive asymptotic properties of our estimator when it is computed from a single spatial set of observations. Namely, under some assumptions, we show that it is asymptotically consistent and normal.

Some of these assumptions concern the aforementioned integral range. This confirms the relevance of geostatistical tools to enrich extreme value analysis, especially when estimating starting with a single realization of the spatial process. These results are then illustrated by numerical experiments and a comparison with the F-madogram estimator proposed in [Cooley et al. \(2006\)](#) is performed.

Independently of the other chapters, [Chapter 4](#) focuses on the simulation of specific storm processes. These processes constitute prototype models for spatial extremes. They are classically simulated on a finite number of points within a given domain. We propose a new algorithm that allows to perform such a task in continuous domains like hyperrectangles or hyperballs, in arbitrary dimension. This consists in generating basic ingredients that can subsequently be used to assign a value at any point of the simulation field. Such an approach is particularly appropriate to investigate the geometrical properties of storm processes. Particular attention is paid to efficiency: by introducing and exploiting the notion of domain of influence of each storm, the running time is considerably reduced. Besides, most parts of the algorithm are designed to be parallelizable. This algorithm is used to perform several illustrative simulations in the other chapters.

WHAT ARE SPATIAL EXTREMES

Résumé *Ce chapitre est une introduction à la théorie spatiale des valeurs extrêmes. Pour les lecteurs non familiers avec l'étude statistique des événements extrêmes, la notion d'extrême est d'abord détaillée. Des éléments de la théorie des valeurs extrêmes sont ensuite rappelés, notamment les approches de maxima par blocs et d'excès au dessus d'un seuil. Un exemple numérique illustrant la pertinence de cette théorie pour étudier des événements extrêmes est également fourni. Par la suite, le chapitre se concentre sur les extrêmes spatiaux et en particulier sur les champs aléatoires max-stables. Dans la méthode des maxima par blocs, ces derniers apparaissent naturellement comme limite de maxima ponctuels de champs aléatoires indépendants et identiquement distribués (i.i.d.). La fonction coefficient extrémal est aussi introduite: cette fonction bivariable constitue la principale mesure de dépendance des champs max-stables. Elle est au centre des travaux présentés dans ce document. Les principaux travaux d'estimation de la fonction coefficient extrémal sont effectués sur la base d'observations i.i.d. ou qui se répètent dans le temps. Peu de travaux se sont intéressés à son estimation à partir d'une unique réalisation, partiellement observée, du champ max-stable considéré. Cette question et plus largement celle de l'estimation à partir d'un unique jeu d'observations spatialisées sont discutées à la fin de ce chapitre. À cet égard, des éléments et concepts de base issus de la Géostatistique sont rappelés.*

Spatial extreme value theory, as a branch of extreme value theory (EVT), helps model and predict the frequency of extreme events in a spatial context. The objective of this chapter is first to introduce the specificity of extreme events from a statistical point of view. Then, basic results and mathematical objects from univariate and spatial EVT are presented. This includes the extremal coefficient function, which is at the center of the works exposed in [Chapter 2](#) and [Chapter 3](#). The first three sections are mostly addressed to readers who are unfamiliar with extreme value theory. They lay the groundwork before getting into the heart of the matter in the last section. There, we tackle the issue of estimating spatial extreme events when the phenomenon of interest is observed only once. To the best of our knowledge, this situation has rarely been investigated in the spatial extremes literature. Geostatistics, on the other hand, typically deals with unique phenomena. By making fruitful connections between both disciplines, we aspire to better handle the study of extreme events when having only one set of spatial observations.

1.1 EXTREME EVENTS, A STATISTICAL ISSUE

1.1.1 *Definition: extreme or not extreme that is the question*

As remarked by [Stephenson \(2008\)](#),

« extreme events are generally easy to recognize but difficult to define »,

partly because there is no unique definition for what is meant by *extreme*, and deciding what makes an event extreme or not highly depends on the field of study (see e.g. [McPhillips et al., 2018](#)). Extreme value theory aims to help these different disciplines to analyse, from a statistical point of view, what they call extreme events. Therefore, we consider the quite general definition hereunder.

Definition 1.1 – *Extreme event*. A event is said to be extreme when the two following conditions are verified:

- (i) it is a **rare event**, i.e. its probability of occurrence is very low,
- (ii) the underlying phenomenon takes **very high (or very low) values**.

By way of illustration, here are some examples of extreme events:

- the main shock of L'Aquila earthquake, in 2009, that was rated 6.3 on the Richter magnitude scale,
- Hurricane Harvey, a category 4 hurricane that affected a large area in Central America and Eastern United States in August 2017,
- the french record-breaking temperature, 45.9 degrees Celsius, recorded on the 28th of June 2019 in a southern town called Gallargues-le-Montueux,
- the stock market crash on Monday, 19th October 1987, known as *Black Monday*.

Notice that these four examples also had a high impact: they caused severe financial or material damages and/or many deaths. According to [Definition 1.1](#), an extreme event is not necessary high-impact and interest can also be in studying phenomena such as long human life span or sport records (see e.g. [Einmahl and Magnus, 2008](#) and [Einmahl et al., 2019](#)). More detailed examples of extreme events can be found, for instance, in [Beirlant et al. \(2004\)](#), [Dey and Yan \(2016\)](#), or [Embrechts et al. \(1997\)](#). Formally, suppose that the phenomenon of interest, e.g. the sea level at a specific location, can be modeled by a random variable X with density function f . Extreme value theory focuses on the right and left tails of f , where it usually takes very low values (cf. [Figure 1.1](#)). Although defining what belongs to the tail highly depends on the current study, the areas of concern are usually over (resp. below) the 90% (resp. 10%)

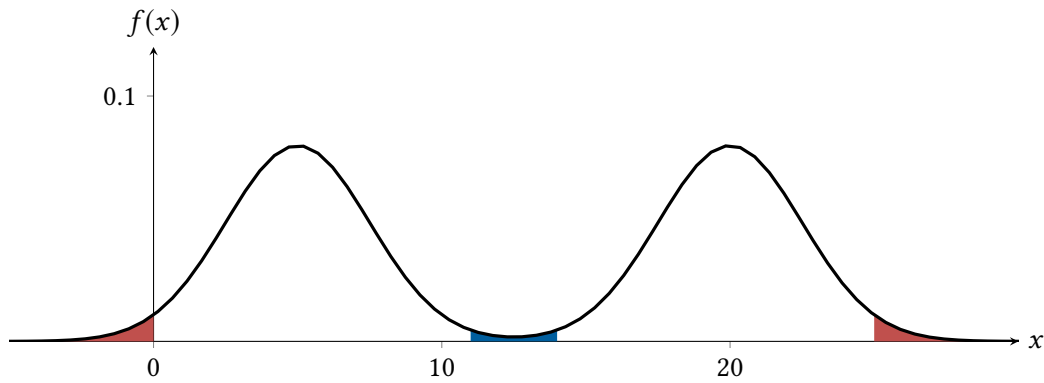


FIGURE 1.1 – A density function $f = f_1 + f_2$, where f_1 and f_2 are the density functions associated with the Gaussian distributions $\mathcal{N}(5, 2.5)$ and $\mathcal{N}(20, 2.5)$, respectively. The extreme value theory is interested in the tail of f (red area) and not in its centred part, even if f takes low values (blue area).

quantile (see e.g. IPCC, 2012, page 116 about climate extremes).

In practice, the phenomena under study are typically complex and depend on multivariate parameters. For instance, the sea level can be divided into several components like the mean sea level, the tide level and the surge level. Extreme sea levels may be observed when one or several of these components reach high values. As pointed out by Tawn (1992), possible dependence between the components must be taken into account. In addition, a lot of extreme events such as heavy rainfalls and heatwaves are spatial in nature; extremes may appear in clusters over a region, and this spatial dependency must also be considered. Due to the possible multivariate or spatial characteristics of extreme events, EVT is also concerned with the tail behavior of random vectors or random fields. For instance, let the sea level at two specific locations be modeled by the random variables X_1 and X_2 with joint density function f . Attention is paid to the tail parts of f , where at least X_1 or X_2 takes extreme values.

In the following, without any loss of generality (cf. Remark 1.7), we shall focus exclusively on the right tail of the distribution. In this context, the goal may be to estimate quantities such as exceedance probabilities above very high thresholds, where very few or even no data are observed. In such a situation, standard statistical tools are no longer relevant.

1.1.2 Estimating with few observations

In this subsection we illustrate with a specific example why standard statistical methods are inappropriate when studying extreme events.

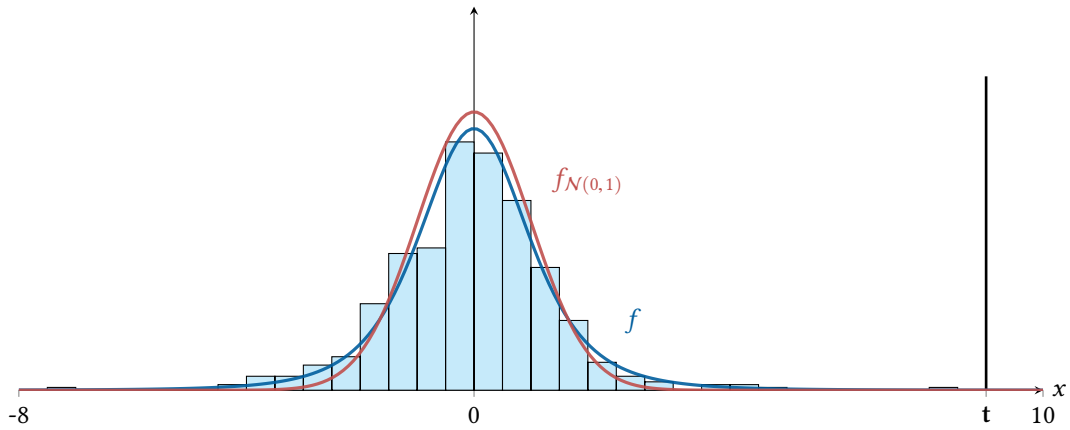


FIGURE 1.2 – Histogram of the sample of size 500 drawn from a Student distribution $\mathcal{T}(4)$ (in lightblue). The density functions f of the Student distribution $\mathcal{T}(4)$ (in blue) and $f_{\mathcal{N}(0,1)}$ of the standard Gaussian distribution $\mathcal{N}(0, 1)$ (in red) are displayed for comparison, as well as the threshold $t = 9$.

Turning back to the univariate case, let $\mathcal{T}(4)$ denote the Student distribution with 4 degrees of freedom, and take a random variable $X \sim \mathcal{T}(4)$. Denote by f its density function, set $t \in (0, +\infty)$ a very high threshold and consider the event $\{X > t\}$ (cf. Figure 1.2). According to Definition 1.1, $\{X > t\}$ is an extreme event. In a risk management context, suppose now that we are interested in assessing its probability $\mathbf{P}[X > t] =: \bar{F}(t)$; \bar{F} stands for *the survival function*. Assume that 500 independent realizations of X are observed, providing the histogram displayed in Figure 1.2.

First, notice its bell shape: the standard normal distribution $\mathcal{N}(0, 1)$ seems to be a good candidate to model the data. However, if the laws $\mathcal{N}(0, 1)$ and $\mathcal{T}(4)$ have similar behaviour in the sample range, this is not the case in tail regions: as shown in Figure 1.3, the corresponding survival functions $\bar{F}_{\mathcal{N}(0,1)}$ and \bar{F} have respectively a light and a heavy right-tail. The difference between the two tails is also illustrated by Figure 1.4, which compares the quantile functions of both distributions. This is why usual parametric estimation methods may fail when considering extreme events, especially when they are based on Gaussian distributions. Since a Gaussian density function always has a light-tail (see Beirlant et al., 2004), this could lead, as in the present example, to a serious underestimation of the probabilities associated to extreme events. In a risk management context, the consequences could be catastrophic; Salmon (2009) found such Gaussian underestimation to be one of the causes of the global economic crisis of 2008.

Of course, parametric adjustment is not the only option, and we could also estimate $\mathbf{P}[X > t]$ with a non-parametric method. However, there is no observation beyond the threshold t ; the exceedance probability would be arbitrarily set to 0. The problem of not observing enough extreme data was also encountered by the Delta committee, in the Netherlands. They were asked to find an appropriate level for the dikes after the severe storm surge on February 1953,

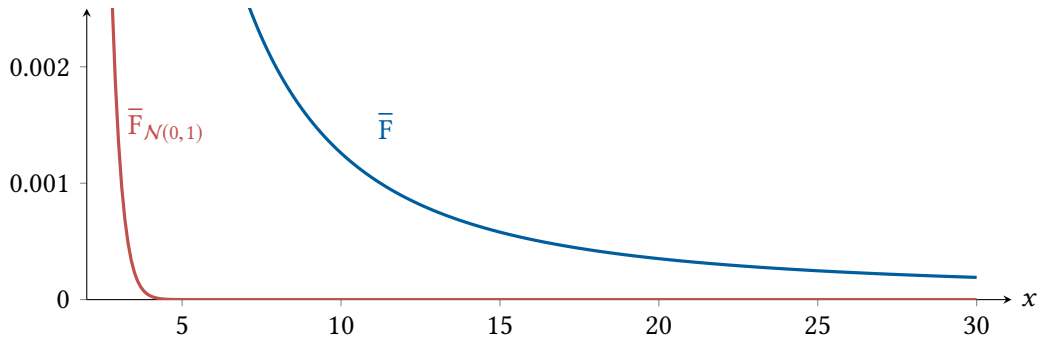


FIGURE 1.3 – Survival functions of the Student distribution $\mathcal{T}(4)$ (in blue) and the standard normal distribution $\mathcal{N}(0, 1)$ (in red).

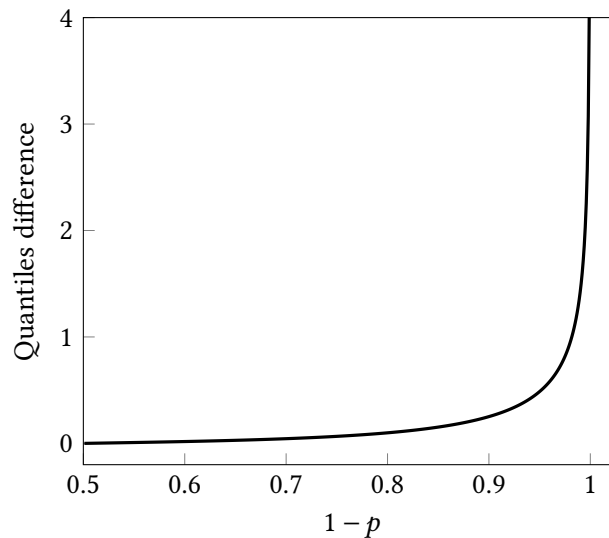


FIGURE 1.4 – Difference between the quantiles of order $1 - p$ of the Student distribution $\mathcal{T}(4)$ and the standard normal distribution $\mathcal{N}(0, 1)$. This difference dramatically increases as $1 - p$ tends to 1.

which caused extensive flooding in several parts of the country, killing nearly 2000 people. In particular, they had to determine the height of the dikes so that the probability of a flood, in a given year, is 10^{-4} ; this corresponds to a quantile of order $1 - 10^{-4}$. However, high tide water level had been recorded only for the past 100 years; it was impossible to estimate this quantile using only these data, without making some assumptions on the underlying distribution. Since we are interested in extreme values, an idea would be, after suitable assumptions on f , to use the largest observations of the sample to extrapolate the tail of the distribution beyond the latter. This is one of the purposes of extreme value theory: by studying the fluctuations of maxima, it helps choose a model for the tail among a family of models that are appropriate when studying extreme events. This theory is introduced next in the univariate then in the spatial case.

1.2 UNIVARIATE EXTREME VALUE THEORY

Three approaches have been developed to study tails of distributions; they are based on max-stable distributions, generalized pareto distributions and point processes, respectively. Since we do not make use of the third approach in this thesis, we shall not introduce it. We invite the interested reader to consult *e.g.* Chapter 7 in Coles (2001) for a comprehensive introduction. We focus instead on the first two approaches, which are usually presented when investigating univariate extremes. The following notation will be needed.

Equality in distribution is denoted by $\stackrel{d}{=}$ and the indicator function of any condition C is written $1\{C\}$. Let X be a real-valued random variable with probability distribution \mathbf{P}_X , cumulative distribution function (c.d.f.) F and probability density function (p.d.f.) f . In the sequel, we shall write equivalently $X \sim \mathbf{P}_X$, $X \sim F$ or $X \sim f$. In addition, for any $n \in \mathbb{N}^*$, let X_1, \dots, X_n be independent real-valued random variables with common c.d.f. F , modelling some observations of the phenomenon of interest. Recall that $\bar{F} = 1 - F$ is the corresponding survival function. For every $k \in \{1, \dots, n\}$, we shall denote $X_{(k)}$ the k th order statistic related with the vector (X_1, \dots, X_n) , *i.e.* $X_{(1)} \leq \dots \leq X_{(n)}$. In particular, $X_{(1)} = \min(X_1, \dots, X_n)$ and $X_{(n)} = \max(X_1, \dots, X_n)$. Finally, define the right endpoint of F as

$$x^* := \sup \{x \in \mathbb{R} : F(x) < 1\} \in \mathbb{R} \cup \{+\infty\}.$$

1.2.1 Normalized maxima: max-stable distributions

Theoretical foundations

The first approach considers that the largest observations are approximately governed by the law of the maximum $X_{(n)}$ with c.d.f. F^n . Typically, in the same spirit as the Central Limit Theorem for the sum $\sum_{k=1}^n X_k$, we would like to know the possible limit distributions for $X_{(n)}$, after normalization, as $n \rightarrow +\infty$. Notice that the normalization is necessary since $X_{(n)} \rightarrow x^*$ a.s. when $n \rightarrow +\infty$, *i.e.* the distribution of $X_{(n)}$ degenerates to a point mass on x^* . To do so, first consider the following definition.

Definition 1.2 – *Distributions of the same type.* Two cumulative distribution functions F and G are of the same type if there exist constants $a > 0$ and $b \in \mathbb{R}$ such that for any $x \in \mathbb{R}$

$$F(x) = G(ax + b).$$

Then, the limit distributions of the normalized maximum are characterized by the next theorem.

Theorem 1.3 – *Limit distributions for maxima (Fisher and Tippett, 1928; Gnedenko, 1943).* Suppose there exist sequences of real numbers $a_n > 0$ and $b_n \in \mathbb{R}$ such that

$$\lim_{n \rightarrow +\infty} \mathbf{P} \left[\frac{X_{(n)} - b_n}{a_n} \leq x \right] = G(x), \quad (1.1)$$

for any $x \in \mathbb{R}$ at which G is continuous and where G is a non-degenerate distribution. Then G is called a *generalized extreme value* (GEV) if it is of the same type as one of the following three seminal distributions:

- the Fréchet distribution $\Phi_\gamma : x \in \mathbb{R} \mapsto \exp \{-x^{-1/\gamma}\} \mathbf{1}\{x > 0\}$ with $\gamma > 0$,
- the Gumbel distribution $\Lambda : x \in \mathbb{R} \mapsto \exp \{-e^{-x}\}$,
- the Weibull distribution $\Psi_\gamma : x \in \mathbb{R} \mapsto \mathbf{1}\{x > 0\} + \exp \{-(-x)^{1/\gamma}\} \mathbf{1}\{x \leq 0\}$ with $\gamma < 0$.

In von Mises (1936) and Jenkinson (1955) a synthetic representation of GEV distributions is proposed. They are of the same type as the following parametric distribution, defined for $\gamma \in \mathbb{R}$ with support $\mathcal{S} := \{x \in \mathbb{R} : 1 + \gamma x > 0\}$:

$$\forall x \in \mathcal{S} \quad G_\gamma(x) := \begin{cases} \exp \left\{ -(1 + \gamma x)^{-1/\gamma} \right\} & \text{if } \gamma \neq 0, \\ \exp \{-e^{-x}\} & \text{if } \gamma = 0. \end{cases} \quad (1.2)$$

With this new representation in mind, Theorem 1.3 states that though different choices of normalizing sequences could lead to a non-degenerate limit in Eq. (1.1), the latter is of fixed type defined by Eq. (1.2) (see also Resnick, 1987, Proposition 0.2). It depends on the parameter $\gamma \in \mathbb{R}$, referred to as the *extreme value index* (EVI). If such normalizing sequences exist, then F is said to be in the *maximum domain of attraction* (MDA) of G_γ , abbreviated $F \in \text{MDA}(G_\gamma)$. Its right-tail decay regime is controlled by the EVI, which defines three categories of maximum domains of attraction depending on its sign.

- If $\gamma > 0$, then F is said to be in the *Fréchet* maximum domain of attraction. It has a polynomial tail decay and its upper endpoint $x^* = +\infty$. This encompasses heavy-tailed distributions like Pareto or Student laws.
- If $\gamma = 0$, then F is said to be in the *Gumbel* maximum domain of attraction. It has an exponential tail decay. This includes light-tailed distributions like Normal or Lognormal laws.
- If $\gamma < 0$, then F is said to be in the *Weibull* maximum domain of attraction. Its upper tail is bounded: $x^* < +\infty$. This is the case, for instance, of the c.d.f. of the Uniform distribution on some closed interval.

Observe that the limit distribution of F is of the same type as a Fréchet, Gumbel or Weibull distribution iff F belongs to the respective MDA. These seminal distributions are displayed with

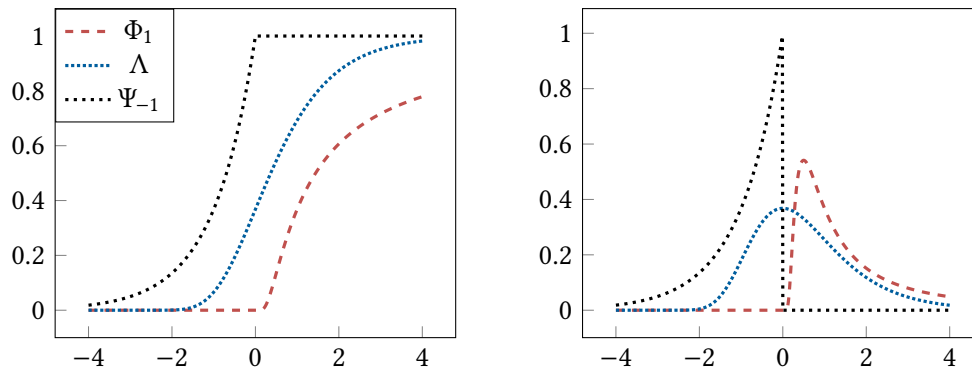


FIGURE 1.5 – Cumulative distribution functions (left) and probability distribution functions (right) of the standard Fréchet, Gumbel and Weibull distributions; their right tails are respectively heavy, light and bounded.

their corresponding p.d.f. in Figure 1.5 for particular values of γ . The maximum domain of attractions and adequate normalizing sequences of some classical distributions can be found in Beirlant et al. (2004, pages 59,62,72) or in Embrechts et al. (1997, pages 153-157).

Remark 1.4 Some light-tailed distributions F with bounded upper tail can belong to the Weibull maximum domain of attraction. Conversely, F can have a bounded upper tail and satisfy $F \in \text{MDA}(G_0)$. We shall also point out that some distributions belong to neither of these three maximum domains of attraction. It is the case *e.g.* for many common discrete distributions such as the geometric, Poisson and negative binomial distributions. This is also the case for Log-Pareto distributions, which are identified as *super-heavy-tailed* (Cormann and Reiss, 2009). In fact, for every $\gamma \in \mathbb{R}$, necessary and sufficient conditions have been investigated to guarantee that $F \in \text{MDA}(G_\gamma)$. The interested reader may refer *e.g.* to Resnick (1987).

It turns out that the class of GEV distributions coincides with that of the so-called max-stable distributions, defined hereunder (Embrechts et al., 1997, Theorem 3.2.2).

Definition 1.5 – Max-stable distribution. Let $X \sim F$, with F a non-degenerate distribution. The c.d.f. F and the random variable X are called max-stable if, for any $n \in \mathbb{N}^*$, F^n is of the same type as F .

Remark 1.6 Given $n \in \mathbb{N}^*$ i.i.d. copies X_1, \dots, X_n of X , F^n is the c.d.f. of $X_{(n)}$. Therefore, F^n is of the same type as F iff there exist constants $a_n > 0$ and $b_n \in \mathbb{R}$ such that

$$\frac{X_{(n)} - b_n}{a_n} \stackrel{d}{=} X.$$

Max-stable distributions are the core element of this thesis.

Practical aspects

We shall now demonstrate how GEV distributions can be used to model the tail of F . Assume that there exists $\gamma \in \mathbb{R}$ such that $F \in \text{MDA}(G_\gamma)$. Then, there exist sequences of real numbers $a_n > 0$ and $b_n \in \mathbb{R}$ such that

$$\forall x \in \mathbb{R} \quad \lim_{n \rightarrow +\infty} F^n(a_n x + b_n) = G_\gamma(x).$$

Taking every point $x \in \mathbb{R}$ for which $G_\gamma(x) \in (0, 1)$, it follows that

$$\lim_{n \rightarrow +\infty} n \log \{F(a_n x + b_n)\} = \log \{G_\gamma(x)\},$$

which implies that $\lim_{n \rightarrow +\infty} F(a_n x + b_n) = 1$ and ultimately $\lim_{n \rightarrow +\infty} a_n x + b_n = +\infty$. Using a Taylor expansion of the logarithm, we obtain

$$\bar{F}(a_n x + b_n) \sim -\frac{1}{n} \log \{G_\gamma(x)\} \quad \text{as } n \rightarrow +\infty.$$

Therefore, given some large enough $n \in \mathbb{N}^*$ and $x \in \mathbb{R}$, the tail of F can be approximated as follows:

$$\bar{F}(x) \approx -\frac{1}{n} \log \left\{ G_\gamma \left(\frac{x - b_n}{a_n} \right) \right\}. \quad (1.3)$$

If we were to observe a non-negligible number of independent repetitions of $X_{(n)}$, many classical estimation techniques could be used to assess γ , a_n and b_n (Beirlant et al., 2004). In practice, such observations can be created artificially by dividing the original sample of size $n \in \mathbb{N}^*$ into subsamples of size $m < n$ and taking their respective maxima: this is the so-called *block maxima method*. Classical conditions on m are necessary to guarantee the good properties of the ensuing estimators: $m = m(n) \rightarrow +\infty$ and $m/n \rightarrow 0$ as $n \rightarrow +\infty$. Practically, they mean that the number of blocks should be large enough to provide precise estimates (*i.e.* with low variance) but small enough not to include false maxima (non-extreme realizations), which would bias the estimation.

Before introducing the second approach, based on the generalized Pareto distribution, we shall conclude this subsection with the following comment.

Remark 1.7 – Studying the minimum. Since $X_{(1)} = -\max(-X_1, \dots, -X_n)$, the results presented above can be readily used to study minima and model the left-tail of distributions.

1.2.2 *Peaks over threshold: the generalized Pareto distribution*

In the previous approach, the statistical analysis of extremes was based on $X_{(n)}$. However, as remarked in Beirlant et al. (2004),

« It would be unrealistic to assume that only the maximum of a sample contains valuable information about the tail of the distribution. Other large order statistics could do this as well. »

Further, using the block maxima method on a dataset with a block size $n \in \mathbb{N}^*$, sufficiently large so that the approximation (1.3) be good enough, may lead to a significant loss of information, see e.g. [Madsen et al. \(1997\)](#). By modelling exceedances over high threshold, the approach presented hereafter takes into account the largest order statistics when analysing the tail of a distribution. It is thus generally referred to as the *Peaks-Over-Threshold* (POT) method.

Let $X \sim F$, fix a threshold $t \in \mathbb{R}$ and consider the random variable $X - t \mid X > t$. Similarly to the previous approach with $X_{(n)}$, we are interested in the limit distribution of $X - t \mid X > t$ as $t \rightarrow x^*$. First, we introduce the following theorem, found for instance in [de Haan and Ferreira \(2006, Theorem 1.1.6, page 10\)](#).

Theorem 1.8 Let $\gamma \in \mathbb{R}$ and consider the random variable X with c.d.f. F having upper endpoint x^* . The following two assertions are equivalent:

- (i) $F \in \text{MDA}(G_\gamma)$,
- (ii) there exists a measurable function $m : \mathbb{R} \rightarrow (0, +\infty)$ such that for all $x \in \mathbb{R}$ satisfying $1 + \gamma x > 0$,

$$\lim_{t \rightarrow x^*} \frac{\bar{F}(t + xm(t))}{\bar{F}(t)} = \begin{cases} (1 + \gamma x)^{-1/\gamma} & \text{if } \gamma \neq 0, \\ \exp\{-x\} & \text{if } \gamma = 0. \end{cases}$$

Since for any $x \in (0, +\infty)$ and $t < x^*$

$$\frac{\bar{F}(t + xm(t))}{\bar{F}(t)} = \mathbf{P} \left[\frac{X - t}{m(t)} > x \mid X > t \right],$$

condition (i) in [Theorem 1.8](#) implies that for all $x \in (0, +\infty)$ satisfying $1 + \gamma x > 0$,

$$\lim_{t \rightarrow x^*} \mathbf{P} \left[\frac{X - t}{m(t)} > x \mid X > t \right] = \begin{cases} (1 + \gamma x)^{-1/\gamma} & \text{if } \gamma \neq 0, \\ \exp\{-x\} & \text{if } \gamma = 0. \end{cases} \quad (1.4)$$

It exhibits possible limit distributions, after scaling, for $X - t \mid X > t$. Every distribution of the same type as the limit distribution in [Eq. \(1.4\)](#) is called a *generalized Pareto distribution* (see [Definition 1.9](#)), abbreviated GPD. Like max-stable distributions, its right-tail is controlled by the EVI $\gamma \in \mathbb{R}$. Actually, [Balkema and de Haan \(1974\)](#) showed that when $x^* = +\infty$, the generalized Pareto distributions are the only possible non-degenerate limits for the distribution of $(X - t)/m(t) \mid X > t$, as $t \rightarrow x^*$. Such distributions are characterized by the *threshold stability* property: if the random variable Y has a GPD with finite right endpoint y^* , then for any threshold $t' < y^*$, the exceedance $Y - t' \mid Y > t'$ has a GPD too.

Definition 1.9 – *Generalized Pareto distribution.* Let H be a c.d.f. and $\gamma \in \mathbb{R}$. The former is a generalized Pareto distribution (GPD) if it is of the same type as H_γ defined by

$$H_\gamma(x) = \begin{cases} 1 - (1 + \gamma x)^{-1/\gamma} & \text{when } \gamma \neq 0 \\ 1 - \exp\{-x\} & \text{when } \gamma = 0, \end{cases}$$

for any $x \in (0, +\infty)$ such that $1 + \gamma x > 0$. The c.d.f. H_γ is called the standard generalized Pareto distribution.

Now, fix a high threshold $t < x^*$ and assume that (i) is satisfied. The Eq. (1.4) gives the following approximation:

$$\mathbf{P}[X - t > x \mid X > t] \approx \begin{cases} \left(1 + \gamma \frac{x}{m(t)}\right)^{-1/\gamma} & \text{when } \gamma \neq 0 \\ \exp\left\{-\frac{x}{m(t)}\right\} & \text{when } \gamma = 0, \end{cases} \quad (1.5)$$

i.e. the excess $X - t > x \mid X > t$ is approximatively distributed according to a GPD. Writing $\zeta_t = \bar{F}(t)$, it follows from Eq. (1.5) that, for every $x > t$,

$$\bar{F}(x) \approx \begin{cases} \zeta_t \left(1 + \gamma \frac{x - t}{m(t)}\right)^{-1/\gamma} & \text{when } \gamma \neq 0 \\ \zeta_t \exp\left\{-\frac{x - t}{m(t)}\right\} & \text{when } \gamma = 0. \end{cases} \quad (1.6)$$

Hence, the exceedance probability $\bar{F}(x)$ may be evaluated by estimating ζ_t , $m(t)$ and γ . In the same way, we could also evaluate the probability $\mathbf{P}[X - t > x \mid X > t]$ in Eq. (1.5); in a reinsurance context, this typically represents the probability that a claim lies in a given interval, knowing that the latter has already exceeded the level t . Usually, ζ_t is estimated using the empirical cumulative distribution function. As for $m(t)$ and γ , there exist different methods of estimation, and they are only based on the observations exceeding the threshold t in the sample, see e.g. Beirlant et al. (2004). Thus, choosing t raises similar problems as for the choice of the size blocks in the block maxima method: a high value of t guarantees that the approximation (1.5) is good enough but may result in too few exceedances, hence producing high variance estimators. On the contrary, for small t , the estimators become biased. There exist several methods that help choosing the threshold t , see e.g. Coles (2001) for the common graphical ones or Scarrott and MacDonald (2012) for a more exhaustive review of these existing methods. One of them is detailed in the following subsection.

In the last two subsections, we have presented the basis of univariate extreme value theory that provides a class of models to enable the extrapolation from observed levels to unobserved

levels. Such models have the huge advantage to be based on a family of finite-dimensional parametric distributions. Before illustrating this theory in the next subsection, we shall end this part with the following comment from [Coles \(2001\)](#):

It is easy to be cynical about this strategy, arguing that extrapolation of models to unseen levels requires a leap of faith, even if the models have an underlying asymptotic rationale. There is no simple defense against this criticism, except to say that applications demand extrapolation, and that it is better to use techniques that have a rationale of some sort. This argument is well understood and, notwithstanding objections to the general principle of extrapolation, there are no serious competitor models to those provided by extreme value theory.

1.2.3 An illustrative example

Consider again the $n = 500$ realizations x_1, \dots, x_n drawn from $X \sim \mathcal{T}(4)$ in [Subsection 1.1.2](#), with c.d.f. F . We want to estimate the tail of F using the POT method presented in the previous subsection. First, we shall assume that there exists $\gamma \in \mathbb{R}$ such that $F \in \text{MDA}(G_\gamma)$. Hence, for a adequate threshold $t \in \mathbb{R}$, the survival function \bar{F} satisfies [Eq. \(1.6\)](#) for any $x > t$. Before evaluating the parameters ζ_t , $m(t)$ and γ , we thus have to choose a threshold t_0 so that the approximation [\(1.6\)](#) be good enough, but at the same time, as low as possible to have enough observations beyond t_0 when estimating these parameters. For this purpose, we use a graphical method based on the so-called *mean excess function* $\mathbb{E}[X - t \mid X > t]$, defined for $t < x^*$. Suppose that t is high enough so that the standard GPD may be considered as a valid model for $(X - t)/m(t) \mid X > t$. Consequently, $\mathbb{E}[X - t \mid X > t]$ is infinite when $\gamma \geq 1$ and is equal to $m(t)/(1 - \gamma)$ when $\gamma < 1$. Consider another threshold $t < t' < x^*$. From the threshold stability property of GPD and e.g. [Theorem 4.1 in Coles \(2001\)](#), it is easy to show that

$$\mathbb{E}[X - t' \mid X > t'] = \frac{m(t) + \gamma t'}{1 - \gamma}, \quad (1.7)$$

for $\gamma < 1$. In particular, the map $t' \in (t, x^*) \mapsto \mathbb{E}[X - t' \mid X > t']$ is linear. Then, for any $t < x^*$, let n_t stands for the number of realizations exceeding t' . If $\gamma < 1$, the function

$$e_n : t \mapsto \frac{1}{n_t} \sum_{i=1}^n (x_i - t) \mathbf{1}\{X_i > t\},$$

that gives the empirical estimate of $\mathbb{E}[X - t \mid X > t]$ for any $t < x^*$, can thus be expected to be approximatively linear in t , at least when t is high enough for the GPD to provide a valid approximation to the excess distribution. Since $F \in \text{MDA}(G_{0.25})$ (see e.g. [Beirlant et al. \(2004\)](#), page 59), this suggests a graphical method for choosing the threshold t_0 : we can choose t_0 such that $e_n(x)$ is approximately linear for $x \geq t_0$. Notice that, in case we did not know that $\gamma < 1$, we could also have estimated γ for different high thresholds in order to

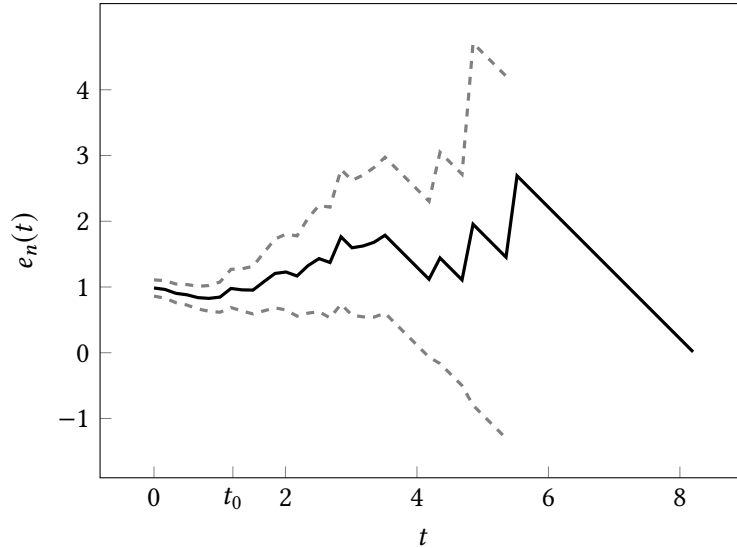


FIGURE 1.6 – Mean residual life plot (black line) with associated 95% confidence intervals (dashed gray line), where $t_0 = 1.2$. The confidence intervals are not plotted for thresholds t above which there are too few observations.

check this condition. Hence, we plot e_n against $t < x^*$ in Figure 1.6 with 95% confidence intervals based on the approximate normality of sample means: this is the *mean residual life plot*. In practice, the interpretation of a mean residual life plot is not always simple, since we are looking for approximate linearity. In Figure 1.6, the graph is approximately linear from $t \approx 1.2$ to $t \approx 3.8$, beyond which it decays until $t \approx 4$, then seems again to linearly increase. It thus could be tempting to choose $t_0 = 4$, however there are only 6 observations above this threshold: based on such limited amount of data, the estimate e_n and the associated confidence intervals are thus unreliable. In addition, this would leave too few data to make meaningful inference afterwards. Accordingly, this is probably better to set $t_0 = 1.2$, which is exceeded by 63 observations. Of course, this is an approximate choice and it is recommended to compare final estimates across a variety of t_0 -values. This is not done here but it is also highly recommended to compare different methods for choosing t_0 .

Once t has been set, it remains to estimate ζ_t , $m(t)$ and γ from the data. The former is evaluated using the empirical survival function \bar{F}_n , which gives the following estimate:

$$\hat{\zeta}_t = \frac{1}{n} \sum_{i=1}^n \mathbf{1}\{x_{(i)} > t\},$$

whereas the latter two are estimated by maximum likelihood, see e.g. Coles (2001, page 80). In particular, we obtain $\hat{\gamma} \approx 0.18$, which is close to 0.25. Using Eq. (1.6), the tail of the extreme estimator $\hat{\bar{F}}$ is finally computed and displayed in Figure 1.7, as well as the tail of \bar{F} and those of the estimators \bar{F}_n and $\bar{F}_{\mathcal{N}(0,1)}$ mentioned in Subsection 1.1.2. It appears that the former performs better than the last two, thus illustrating the relevance of extreme value theory when studying extreme events.

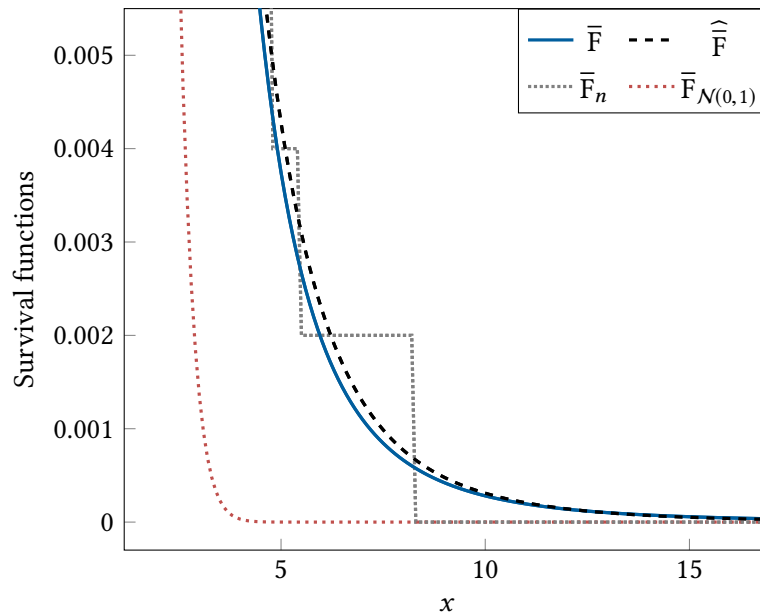


FIGURE 1.7 – Survival function of the Student distribution $\mathcal{T}(4)$ (blue curve) as well as its extreme estimator (black dashed curve), its empirical survival function (grey densely dotted curve) and the survival function of the standard normal distribution $\mathcal{N}(0, 1)$ (red dotted curve).

1.3 SPATIAL EXTREMES: ALL ABOUT DEPENDENCE

As pointed out in the first section, a lot of extreme events are spatial in extent and, with the prospect for future climate change, statistical modelling of spatial extremes have developed remarkably in the last decades. In contrast to the univariate framework, it aims to apprehend the spatial dependence of such extreme events, it is thus based on the study of random fields. Several approaches to modelling spatial extremes have been proposed so far, see *e.g.* [Davison et al. \(2012\)](#) for a description of three main types of statistical models. In this thesis we shall focus on the widely used max-stable processes, which represent a functional extension to max-stable distributions introduced in [Subsection 1.2.1](#). Notice that there also exist functional extensions to the generalized pareto distribution described in [Subsection 1.2.2](#) that are not presented here, see *e.g.* [Ferreira and de Haan \(2014\)](#), [Dombry and Ribatet \(2015\)](#), [Tawn et al. \(2018\)](#) and [de Fondeville \(2018, chapter 4\)](#). After a brief review of the concept of random fields, in the next paragraph, we thus introduce max-stable random fields. Under relatively mild assumptions, the latter admit a nice representation, known as the spectral characterization, from which a particular measure of spatial dependence is built: the extremal coefficient function. This useful tool, we shall focus on in [Chapter 2](#) and [Chapter 3](#), is detailed in the last subsection.

1.3.1 Random field: a brief presentation

Let $(\Omega, \mathcal{F}, \mathbb{P})$ be a complete probability space and set $d \in \mathbb{N}^*$. Let also the Euclidean space \mathbb{R}^d and \mathbb{R} be equipped with their respective Borel σ -algebra $\mathcal{B}_{\mathbb{R}^d}$ and $\mathcal{B}_{\mathbb{R}}$. Elements of \mathbb{R}^d are written in bold. In addition, the distance separating two points \mathbf{x} and $\mathbf{y} \in \mathbb{R}^d$ is written $\|\mathbf{x} - \mathbf{y}\|$. We shall also denote G^d the set of all real-valued functions defined on \mathbb{R}^d and \mathcal{G}^d the so-called *cylinder σ -algebra* generated by the cylinder sets of the form $\{f \in G^d : f(\mathbf{x}_j) \in B_j, j = 1, \dots, m\}$, where $m \in \mathbb{N}^*$, $\mathbf{x}_1, \dots, \mathbf{x}_m \in \mathbb{R}^d$ and $B_1, \dots, B_m \in \mathcal{B}_{\mathbb{R}}$. In the sequel, we always consider real-valued random fields (abbreviated RF) on \mathbb{R}^d , which can be defined

(i) either as a measurable mapping from $(\Omega, \mathcal{F}, \mathbb{P})$ into (G^d, \mathcal{G}^d) ,

(ii) or as a collection of real-valued random variables with index set \mathbb{R}^d ,

see e.g. Adler (1981). We shall mention that, in the sequel, random fields are sometimes simply called processes. Let X be such a process. This is thus convenient to consider the latter as the map

$$\begin{aligned} X : \Omega \times \mathbb{R}^d &\rightarrow \mathbb{R} \\ (\omega, \mathbf{x}) &\mapsto X(\omega, \mathbf{x}), \end{aligned}$$

since this recovers both definitions (i) and (ii). Indeed, for any $\mathbf{x} \in \mathbb{R}^d$

$$\begin{aligned} X(\mathbf{x}) : \Omega &\rightarrow \mathbb{R} \\ \omega &\mapsto X(\mathbf{x}, \omega) \end{aligned}$$

is a real-valued random variable: this corresponds to (ii). On the contrary, when fixing $\omega \in \Omega$, the sample path

$$\begin{aligned} \mathbb{R}^d &\rightarrow \mathbb{R} \\ \mathbf{x} &\mapsto X(\mathbf{x}, \omega), \end{aligned}$$

can be viewed as a realization of X , according to (i). Considering again the definition (i), it is known that the law of X , i.e. the pushforward probability measure \mathbb{P}_X on (G^d, \mathcal{G}^d) , is characterized by its finite-dimensional distributions, that is all the probability measures $\mathbb{P}_{\mathbf{x}_1, \dots, \mathbf{x}_k}^X$, where $k \in \mathbb{N}^*$ and $\mathbf{x}_1, \dots, \mathbf{x}_k \in \mathbb{R}^d$, defined by

$$\mathbb{P}_{\mathbf{x}_1, \dots, \mathbf{x}_k}^X(B_1 \times \dots \times B_k) = \mathbb{P}[X(\mathbf{x}_1) \in B_1, \dots, X(\mathbf{x}_k) \in B_k],$$

for any $B_1, \dots, B_k \in \mathcal{B}_{\mathbb{R}}$. Indeed, as it is shown in e.g. Breiman (1992, Proposition 12.12), two processes X and Y on \mathbb{R}^d have the same law if and only if they have the same finite-dimensional distributions. In this case, we write $X \stackrel{f.d.d.}{=} Y$. In addition, let $(Y_n)_{n \in \mathbb{N}^*}$ be a sequence of RF's on \mathbb{R}^d ; it is said to converge to X in finite-dimensional distribution, as $n \rightarrow +\infty$, if

$$\mathbb{P}_{\mathbf{x}_1, \dots, \mathbf{x}_k}^{Y_n}(B_1 \times \dots \times B_k) \xrightarrow{n \rightarrow +\infty} \mathbb{P}_{\mathbf{x}_1, \dots, \mathbf{x}_k}^X(B_1 \times \dots \times B_k),$$

for any $k \in \mathbb{N}^*$, $\mathbf{x}_1, \dots, \mathbf{x}_k \in \mathbb{R}^d$ and $B_1, \dots, B_k \in \mathcal{B}_{\mathbb{R}}$. It is then denoted by $X \xrightarrow{f.d.d.} Y$. We shall now introduce the next two definitions. The first one gives a stronger notion of equality between stochastic processes than equality in finite-dimensional distribution and the second one defines a notion of continuity for stochastic processes; these notions are both used in the following.

Definition 1.10 – *Modification of a stochastic process.* Let X and Y be two RF's on \mathbb{R}^d , that are defined on the same probability space $(\Omega, \mathcal{F}, \mathbb{P})$. The RF X is said to be a *modification* (or a *version*) of Y if

$$\mathbb{P}[X(\mathbf{x}) = Y(\mathbf{x})] = 1,$$

for any $\mathbf{x} \in \mathbb{R}^d$.

Definition 1.11 – *Continuity in probability.* A RF X on \mathbb{R}^d is said *stochastically continuous* or *continuous in probability* if for any $\mathbf{x} \in \mathbb{R}^d$,

$$X(\mathbf{x}_0) \xrightarrow{\mathbb{P}} X(\mathbf{x}) \text{ as } \mathbf{x}_0 \rightarrow \mathbf{x},$$

i.e.

$$\lim_{\mathbf{x}_0 \rightarrow \mathbf{x}} \mathbb{P}[|X(\mathbf{x}_0) - X(\mathbf{x})| > \epsilon] = 0,$$

for any $\epsilon > 0$.

By construction, random fields are relevant tools to stochastically model spatial events, and consequently to study spatial extreme events. Consider, for instance, a precipitation field modelled by the RF X on \mathbb{R}^2 and let $n \in \mathbb{N}^*$. As mentioned at the beginning of the section, the spatial extreme analysis aims to apprehend the spatial dependence of extreme events. Suppose we observe X at k specific locations $\mathbf{x}_1, \dots, \mathbf{x}_k \in \mathbb{R}^2$. It could be interesting *e.g.* to evaluate the probability that the rainfall amount exceeds a critical level $z \in \mathbb{R}_+$ in at least one location, *i.e.*

$$1 - \mathbb{P}[X(\mathbf{x}_1) \leq z, \dots, X(\mathbf{x}_k) \leq z]. \quad (1.8)$$

Consider now a measurable and bounded subset $V \subset \mathbb{R}^2$. It may also be of great interest to estimate the probability that the total rainfall amount over V be more than some threshold $z \in \mathbb{R}_+$, *i.e.*

$$\mathbb{P}\left[\int_V X(\mathbf{x}) d\mathbf{x} > z\right], \quad (1.9)$$

or the probability that the largest "pointwise" rainfall amount on V be more than $z \in \mathbb{R}_+$, *i.e.*

$$\mathbb{P}\left[\sup_{\mathbf{x} \in V} X(\mathbf{x}) > z\right], \quad (1.10)$$

when these probabilities are well-defined, see [Remark 1.12](#). Since the latter involve the dependence structure of the process X , estimating them thus goes beyond the framework of the univariate extreme value theory. The probability in [Eq. \(1.8\)](#) only includes a countable number of margins of X ; it could be assessed using the multivariate extreme analysis (see e.g. [Beirlant et al. \(2004\)](#) for a very thorough introduction to multivariate extreme modelling), but such framework does not take into account the spatial characteristics of the underlying phenomenon. Evaluating the probabilities in [Eq. \(1.9\)](#) or [Eq. \(1.10\)](#) are more challenging since it requires the knowledge of the distribution of $(X(\mathbf{x}))_{\mathbf{x} \in V}$. It thus call for spatial extreme investigation or, in other words, for functional extreme analysis. The latter can be seen as a generalization of the multivariate settings and has the advantage to take into account the spatial features of the phenomenon. Hence we shall not introduce multivariate extreme value theory in the sequel and only concentrate on the so-called functional extreme value theory. In particular, we whall focus on max-stable processes, which have become, in the last decades, a prevalent tool for modelling spatial extremes, specifically in environmental sciences; they are introduced in the next subsection.

Remark 1.12 – *About measurability of some events.* Let X be a RF on \mathbb{R}^d . Let also $V \subset \mathbb{R}^d$ be a measurable and bounded and z be a positive threshold. By construction of the σ -algebra \mathcal{G}^d ,

$$\left\{ f \in G^d : \int_V f(\mathbf{x}) d\mathbf{x} > z \right\} \quad \text{and} \quad \left\{ f \in G^d : \sup_{\mathbf{x} \in V} f(\mathbf{x}) > z \right\}$$

may not be in \mathcal{G}^d , and consequently, the probabilities [Eq. \(1.9\)](#) and [Eq. \(1.10\)](#) are not necessarily well-defined. To work around these difficulties, the concept of (joint) measurability and separability have to be introduced. The measurability assumption, detailed in [Section 2.1](#), guarantees that the stochastic integral

$$\begin{aligned} \Omega &\rightarrow \mathbb{R} \\ \omega &\mapsto \int_V X(\mathbf{x}, \omega) d\mathbf{x} \end{aligned}$$

is a well-defined random variable, when X has \mathbb{P} -almost surely (a.s.) locally integrable sample paths. The separability assumption ensures that $\left\{ f \in G^d : \sup_{\mathbf{x} \in V} f(\mathbf{x}) > z \right\}$ is a measurable set; since such set is not studied in the following, we shall not go into further details but we refer to e.g. [Adler \(1981\)](#) for a very short and comprehensive introduction to the concept of separability and to [Billingsley \(1995\)](#) for a more detailed discussion.

1.3.2 Max-stable random fields

We shall begin by giving the definition of a max-stable RF.

Definition 1.13 – *Max-stable processes*. Let Z be a RF on \mathbb{R}^d . It is said to be *max-stable* if there exist sequences of positive functions $(\alpha_n)_{n \in \mathbb{N}^*}$ and real-valued functions $(\beta_n)_{n \in \mathbb{N}^*}$ such that, for any $n \in \mathbb{N}^*$,

$$\left(\max_{i \in \{1, \dots, n\}} \frac{Z_i(\mathbf{x}) - \beta_n(\mathbf{x})}{\alpha_n(\mathbf{x})} \right)_{\mathbf{x} \in \mathbb{R}^d} \stackrel{f.d.d.}{=} (Z(\mathbf{x}))_{\mathbf{x} \in \mathbb{R}^d},$$

where Z_1, \dots, Z_n are *i.i.d.* copies of Z .

We shall stress that all finite dimensional distributions of a max-stable process Z are multivariate extreme distributions (see *e.g.* [Beirlant et al., 2004](#)), in particular its margins are all max-stable random variables. Consider *i.i.d.* copies X_1, \dots, X_n of a RF X on \mathbb{R}^d . From the multivariate extreme value theory, we know that if there exist sequences of positive functions $(a_n)_{n \in \mathbb{N}^*}$ and real-valued functions $(b_n)_{n \in \mathbb{N}^*}$ such that

$$\left(\max_{i \in \{1, \dots, n\}} \frac{X_i(\mathbf{x}) - b_n(\mathbf{x})}{a_n(\mathbf{x})} \right)_{\mathbf{x} \in \mathbb{R}^d} \xrightarrow{f.d.d.} (Z(\mathbf{x}))_{\mathbf{x} \in \mathbb{R}^d}, \quad (1.11)$$

where Z has non degenerate margins, then Z is a max-stable processes, see *e.g.* [de Haan \(1984\)](#). Hence, max-stable processes arise as the pointwise maxima taken over an infinite number of appropriately rescaled *i.i.d.* random fields: they thus provide suitable models when studying, for n large enough, the partial maxima process $\left(\max_{i \in \{1, \dots, n\}} X_i(\mathbf{x}) \right)_{\mathbf{x} \in \mathbb{R}^d}$. This is a statistical motivation for using max-stable processes for modelling spatial extremes. As in the univariate case, the convergence in (1.11) can also help estimate probabilities such as [Eq. \(1.8\)](#) (for the probabilities (1.9) and (1.10), stronger convergence is needed, see [Remark 1.15](#)). Indeed, according to [Eq. \(1.11\)](#), we have the following practical approximation, for n large enough,

$$\mathbf{P}[X(\mathbf{x}_1) \leq z_1, \dots, X(\mathbf{x}_k) \leq z_k]^n \approx \mathbf{P}\left[Z(\mathbf{x}_1) \leq \frac{z_1 - b_n(\mathbf{x}_1)}{a_n(\mathbf{x}_1)}, \dots, Z(\mathbf{x}_k) \leq \frac{z_k - b_n(\mathbf{x}_k)}{a_n(\mathbf{x}_k)}\right], \quad (1.12)$$

where $k \in \mathbb{N}^*$, $\mathbf{x}_1, \dots, \mathbf{x}_k \in \mathbb{R}^d$ and $z_1, \dots, z_k \in \mathbb{R}$. Recall that, for any $j \in \{1, \dots, n\}$, the margin $Z(\mathbf{x}_j)$ above has a GEV distribution depending on the EVI $\gamma(\mathbf{x}_j) \in \mathbb{R}$ and, as mentioned in [Subsection 1.2.1](#), the latter, as well as the parameters $a_n(\mathbf{x}_j)$ and $b_n(\mathbf{x}_j)$, can be estimated using methods described *e.g.* in [Beirlant et al. \(2004\)](#). Hence, it is convenient to transform X so that Z has common margins; this allows for separating the assessment of the dependence structure of Z from the evaluation of its margins. A widely used choice is to standardize X so that Z has *unit Fréchet margins*, *i.e.* for any $\mathbf{x} \in \mathbb{R}^d$ and $z \in (0, +\infty)$,

$$\mathbf{P}[Z(\mathbf{x}) \leq z] = e^{-1/z};$$

in particular $Z(\mathbf{x})$ has infinite moments. Such max-stable process is referred to as a *simple max-stable* process. From now on, unless otherwise specified, we shall assume that the max-stable RF Z is simple. This assumption is very convenient since, in this case, Z has the following representation.

Theorem 1.14 – *Spectral characterization, see e.g. de Haan (1984).* Let $(Z(\mathbf{x}))_{\mathbb{R}^d}$ be a simple max-stable process which is continuous in probability. It can be written

$$(Z(\mathbf{x}))_{\mathbf{x} \in \mathbb{R}^d} \stackrel{f.d.d.}{=} \left(\max_{i \geq 1} U_i Y_i(\mathbf{x}) \right)_{\mathbf{x} \in \mathbb{R}^d}, \quad (1.13)$$

where $(U_i)_{i \in \mathbb{N}^*}$ are the points of a Poisson point process on $(0, +\infty)$ with intensity $u^{-2} du$ and $(Y_i)_{i \in \mathbb{N}^*}$ are *i.i.d.* copies of a nonnegative RF Y on \mathbb{R}^d called *spectral process*, which is continuous in probability and such that $E[Y(\mathbf{x})] = 1$, for every $\mathbf{x} \in \mathbb{R}^d$.

In order to better understand this representation, the following interpretation, due to Smith (1990), may be considered, even though it has no theoretical justification. For any $i \in \mathbb{N}^*$, $U_i Y_i(\mathbf{x})$ may be interpreted as the amount of rainfall at position \mathbf{x} from a storm of magnitude U_i with spatial extent driven by Y_i . Hence, max-stable processes may be seen as the pointwise rainfall maxima over an infinite number of storms. The spectral representation in Theorem 1.14 is very useful. Indeed, to estimate probabilities such as (1.8), we need to assess the dependence structure of Z , in particular its finite-dimensional distributions. It can be shown that the latter depends on the RF Y in Eq. (1.13):

$$\mathbb{P}[Z(\mathbf{x}_1) \leq z_1, \dots, Z(\mathbf{x}_k) \leq z_k] = \exp \left\{ -\mathbb{E} \left[\max_{i \in \{1, \dots, k\}} \frac{Y(\mathbf{x}_i)}{z_i} \right] \right\}, \quad (1.14)$$

where $k \in \mathbb{N}^*$, $\mathbf{x}_1, \dots, \mathbf{x}_k \in \mathbb{R}^d$ and $z_1, \dots, z_k \in (0, +\infty)$, see e.g. Ribatet (2013). Now let $\mathbf{x} = \{\mathbf{x}_1, \dots, \mathbf{x}_k\}$ and $\mathbf{z} = \{z_1, \dots, z_k\}$. The Eq. (1.14) can be rewritten

$$\mathbb{P}[Z(\mathbf{x}_1) \leq z_1, \dots, Z(\mathbf{x}_k) \leq z_k] = \exp \{-V_{\mathbf{x}}(\mathbf{z})\},$$

where $V_{\mathbf{x}}(\mathbf{z}) = \mathbb{E} \left[\max_{i \in \{1, \dots, k\}} \frac{Y(\mathbf{x}_i)}{z_i} \right]$ is the exponent function linked to the so-called exponent measure, see e.g. Beirlant et al. (2004). We shall stress that the exponent measure, and more generally, the dependence structure of Z , cannot be characterized parametrically. In practice, however, the standard approach is to fit a flexible parametric model for the former. In a spatial context, this amounts to assume a specific form for the RF Y ; some examples are given in Subsection 2.3.2. Notice that, despite this parametric approach, the complexity of max-stable processes makes inference difficult for high-dimensional data (Castruccio et al., 2016). Some methods such as composite likelihood (see e.g. Padoan et al. (2010) or Huser and Davison (2013)) have been proposed to reduce the computational difficulties, otherwise an attractive alternative is to use peaks-over-threshold analysis.

The spectral representation in [Theorem 1.14](#) is thus very convenient since it helps build models for max-stable processes. Despite its complex form, which involves pointwise maximum of an infinite number of functions, it is also very helpful when simulating max-stable processes; we refer to [Oesting et al. \(2015\)](#) for more details about simulation algorithms. This representation is used in [Schlather and Tawn \(2003\)](#) to introduce a bivariate measure of the spatial dependence of a max-stable process: the extremal coefficient function.

Remark 1.15 – *Convergence and sample continuous processes.* Although the convergence in finite-dimensional distributions in [Eq. \(1.11\)](#) is useful when estimating the probability [\(1.8\)](#), it does not help assess the probabilities [\(1.9\)](#) and [\(1.10\)](#) since the latter necessitate the knowledge of the distribution of $(X(\mathbf{x}))_{\mathbf{x} \in V}$ and not only the finite-dimensional distribution of X . To evaluate them, we thus need a stronger convergence: the weak convergence. When requiring such convergence instead of the finite-dimensional distribution convergence in [Eq. \(1.11\)](#), it is usually assume that X , and consequently Z , has continuous sample paths, see e.g. [Ferreira et al. \(2012\)](#) or [Engelke et al. \(2018\)](#). This guarantees that X , as defined in [\(i\)](#), is valued in a metric space, a situation in which weak convergence is well-studied. In this thesis, we are not interested in evaluating probabilities that involve the distribution of $(X(\mathbf{x}))_{\mathbf{x} \in V}$ for some set $V \subset \mathbb{R}^d$, hence we do not need such assumptions. Nonetheless, the results obtained in this work also holds under these assumptions.

1.3.3 Extremal coefficient function: dependence in extremes

Let Z be again a simple max-stable RF on \mathbb{R}^d , which is continuous in probability, and suppose that we want to obtain some information about its dependence structure but without assuming any specific model. Due to high-dimensional distributional complexity the study of the dependence is thus commonly limited to the bivariate distributions, *i.e.* for any $\mathbf{x}, \mathbf{y} \in \mathbb{R}^d$, we focus on the spatial dependence between the margins $Z(\mathbf{x})$ and $Z(\mathbf{y})$. Notice that the multivariate extreme value theory provides several measures of the dependence between $Z(\mathbf{x})$ and $Z(\mathbf{y})$ (see e.g. [Bacro and Toulemonde \(2013\)](#)) but the latter do not take explicitly into account the spatial characteristics of the underlying phenomenon. Assume, for instance, that Z is (strictly) stationary, *i.e.* its finite finite-dimensional distributions are shift-invariant, see [Eq. 1.17](#). Some examples of simple stationary max-stable processes are given in [Subsection 2.3.2](#). Hence, a measure of the spatial dependence between $Z(\mathbf{x})$ and $Z(\mathbf{y})$ shall depend on the distance separating \mathbf{x} and \mathbf{y} . Recall now that Z has unit-Fréchet margins: its expectation and its variance are infinite, *i.e.* $E[Z(\mathbf{x})] = +\infty$ and $\text{Var}[Z(\mathbf{x})] = +\infty$ for any $\mathbf{x} \in \mathbb{R}^d$. This precludes from considering the covariance function or the variogram usually studied in spatial statistics, see

e.g. [Chilès and Delfiner \(2012\)](#). When Z is stationary, [Schlather and Tawn \(2003\)](#) introduces the so-called extremal coefficient function (ECF) θ defined by

$$\theta : \mathbf{h} \in \mathbb{R}^d \mapsto \mathbb{E}[\max(Y(\mathbf{0}), Y(\mathbf{h}))], \quad (1.15)$$

where Y is the spectral process defined in [Eq. \(1.13\)](#), and which satisfies

$$\mathbb{P}[Z(\mathbf{0}) \leq z, Z(\mathbf{h}) \leq z] = \exp\left\{-\frac{\theta(\mathbf{h})}{z}\right\}$$

for any $\mathbf{h} \in \mathbb{R}^d$, $z \in (0, +\infty)$. In particular, according to the Tonelli's theorem, if Y is $(\mathcal{F} \otimes \mathcal{B}_{\mathbb{R}^d}, \mathcal{B}_{\mathbb{R}})$ -measurable then so is θ . The ECF is a spatial extension of the extremal coefficient introduced in [Smith \(1990\)](#); it summarizes the strength of dependence between pairs of sites separated by the same distance and therefore, its estimation is of primary interest in spatial extreme value theory. It is easy to show from [Eq. \(1.15\)](#) that, for any $\mathbf{h} \in \mathbb{R}^d$,

$$1 \leq \theta(\mathbf{h}) \leq 2, \quad (1.16)$$

where $\theta(\mathbf{h}) = 1$ corresponds to (a.s.) equality between $Z(\mathbf{0})$ and $Z(\mathbf{h})$ whereas $\theta(\mathbf{h}) = 2$ corresponds to independence. We shall remark that, for any $\mathbf{h} \in \mathbb{R}^d$ satisfying $\theta(\mathbf{h}) \neq 2$,

$$\lim_{z \rightarrow +\infty} \mathbb{P}[Z(\mathbf{h}) > z | Z(\mathbf{0}) > z] = 2 - \theta(\mathbf{h}) > 0.$$

Hence stationary simple max-stable RF's, and more generally max-stable RF's, are not suitable for modelling asymptotic independent events, *i.e.* events that become independent as they become more and more extreme, see e.g. [Bacro and Toulemonde \(2013\)](#) and references therein for more details about asymptotic independence. The next theorem, proposed by [Schlather and Tawn \(2003\)](#), gives some properties of the ECF that are used in the thesis.

Theorem 1.16 – [Schlather and Tawn \(2003\)](#). Let Z be a stationary simple max-stable process defined on \mathbb{R}^d and consider its extremal coefficient function θ . The following assertions hold.

- (i) The function $2 - \theta$ is positive-semidefinite.
- (ii) θ is not differentiable at the origin unless $\theta(\mathbf{h}) = 1$ for every $\mathbf{h} \in \mathbb{R}^d$.
- (iii) If $d > 1$ and if Z is isotropic, then θ has at most a jump at the origin and is continuous elsewhere.

Notice that the property (i) guarantees that $\theta - 1$ is conditionally negative-semidefinite, that is for any $n \in \mathbb{N}^*$ and $(\lambda_1, \dots, \lambda_n) \in \mathbb{R}^n \setminus \{0\}$ such that $\sum_{i=1}^n \lambda_i = 0$, then

$$\sum_{i=1}^n \sum_{j=1}^n \lambda_i \lambda_j [\theta(\mathbf{x}_i - \mathbf{x}_j) - 1] \leq 0,$$

for every $\mathbf{x}_1, \dots, \mathbf{x}_n \in \mathbb{R}^d$. Consequently, it is a valid variogram for a stationary random field, see e.g. [Chilès and Delfiner \(2012\)](#). This may help readers that are more familiar with the geostatistic theory than the functional extreme analysis to apprehend the extremal coefficient function as a measure of spatial dependence.

Once the max-stable RF's have been introduced, we shall address the question of estimating extreme events with spatial data.

1.4 ESTIMATING EXTREME EVENTS WITH SPATIAL DATA

The standard estimation procedures stemming from the extreme value theory theoretically require *i.i.d.* replications of the process under study. When dealing with spatial data, it is impossible to have access to *i.i.d.* observations and, as next detailed, we often have to work with temporal repetitions of the object under study. In some cases, even time series are not available: the phenomenon is recorded only once. This situation is rarely addressed in the spatial extremes community, contrary to Geostatistics, which typically deals with such issue. On the other hand, Geostatistics barely makes use of the mathematics tools developed by the extreme value theory. Hence, it seems interesting to make some connexions between both disciplines in order to better handle the estimation of extreme events when having only one set of spatial observations; it would be, for instance, extremely valuable to exploit such connexion when using the so-called *top-cut* model in Geostatistics.

1.4.1 *With repetitions of the spatial process: the standard framework*

First, consider again the univariate case: let X be a random variable satisfying [Eq. \(1.1\)](#), i.e. its c.d.f. F is in the domain of attraction of some GEV distribution. As mentioned in [Subsection 1.2.1](#), when observing *i.i.d.* repetitions of X , many classical estimation techniques can be used to assess some quantity of interest by employing the block maxima method. When studying extreme events, we often deal with temporal data, e.g. daily temperatures or daily rainfall amounts. However, temporal independence is usually an unrealistic assumption; extreme conditions often persist over several consecutive observations. Is the GEV model still appropriate to study extremes in such a case? This question has been investigated for stationary time series. Let $(X_i)_{i \in \mathbb{N}}$ be a (strictly) stationary sequence of random variables i.e., for any $k, h \in \mathbb{N}$ and for every $i_1 < \dots < i_k \in \mathbb{N}$, the laws of the vectors $(X_{i_1}, \dots, X_{i_k})$ and $(X_{i_1+h}, \dots, X_{i_k+h})$ are identical. Suppose also that it satisfies some mixing condition ensuring that long-range dependence at extremes levels is weak, i.e. the events $\{X_i > u\}$ and $\{X_j > u\}$ are approximately independent provided that the threshold $u \in \mathbb{R}$ is high enough

and that the moments $i, j \in \mathbb{N}$ are separated by a long time period. It can be shown that if $\max(X_1, \dots, X_n)$, after renormalization, converges to a non-degenerate distribution G , as $n \rightarrow +\infty$, then G is a GEV distribution. We refer to [Leadbetter \(1983\)](#) for more mathematical details. In such situation, the GEV model thus remains pertinent to investigate extreme events. The block maxima method then consists in dividing the time serie in sequential blocks. Again, this method faces the usual bias-variance tradeoff: the number of observations in each block must be large enough so that the maximum over these observations may be approximated by a max-stable random variable. Annual maxima are, for instance, frequently examined. In addition, large blocks guarantee that all the resulting max-stable random variables may be considered as independent. On the other hand, the number of blocks, *i.e.* the number of *i.i.d.* max-stable random variables, also needs to be large to correctly conduct standard inference methods as *e.g.* the likelihood-based inference.

Actually, such procedure is also used when dealing with spatial extremes. Let $(X_i)_{i \in \mathbb{N}}$ be a sequence of stationary RF's on some domain $V \subset \mathbb{R}^d$, which are observed through time. The sequence may represent, for instance, daily temperatures over a region V of interest. Suppose that we are interested in studying the extremal behaviour of the annual maxima of these temperatures. It is then usually assumed that the sequence fulfils [Eq. \(1.11\)](#), *i.e.* the point-wise maxima taken over an infinite number of properly rescaled processes of such sequence is a max-stable RF. A maxima block method is then used to assess the characteristics of this max-stable RF. Such procedure has been exploited, for instance, to analyse extreme precipitations (see *e.g.* [Coles \(1993\)](#); [Coles and Tawn \(1996\)](#); [Smith and Stephenson \(2009\)](#); [Naveau et al. \(2009\)](#); [Padoan et al. \(2010\)](#); [Davison et al. \(2012\)](#); [Davison et al. \(2019\)](#); [Castro-Camilo and Huser \(2019\)](#)), maximum wind speeds (see *e.g.* [Coles and Walshaw \(1994\)](#); [Ribatet \(2013\)](#)), annual maximum temperatures (see *e.g.* [Davison and Gholamrezaee \(2012\)](#)) or high concentrations of pollution in the air (see *e.g.* [Vettori et al. \(2018\)](#)). Since the main max-stable models studied in the literature are stationary, thus so are, in general, the max-stable models considered in such studies; this assumption simplifies the study of their dependence structure. Some works have investigated the modelling of non-stationarity in the dependence structure (see *e.g.* [Huser and Genton \(2016\)](#)) of a max-stable process. We shall also point out that, when looking at high threshold exceedances instead of maxima, spatial extreme events may be modelled using Generalized Pareto processes. Since we only focus, in this work, on stationary max-stable processes, this is not detailed here.

In some situations, the spatial phenomenon of interest is recorded only once. Since spatial independence assumption is usually just as unrealistic as temporal independence assumption, how to manage estimations in such context ? As explained next, this question is rarely considered in spatial extremes, whereas Geostatistics typically deals with such issue.

1.4.2 With a single observation: a geostatistical specificity

The specificity of Geostatistics, as a branch of spatial statistics, is that it deals with regionalized phenomena modelled by random fields that are observed only once, see e.g. [Chilès and Delfiner \(2012\)](#) for a thorough state of the art of the geostatistical approach. That is the case, for instance, in mining resources estimation, soil contamination evaluation or any other applications where the phenomenon of interest either varies too slowly across time to hope for a decent time series, or is too expensive to sample from. To overcome this difficulty when estimating, it appears that a certain form of spatial homogeneity of the phenomenon under study needs to be assumed. When considering the associated random field, such homogeneity translates into some stationarity assumptions, which allow us to replace repeatability in time, which is not available, by repetition in space. We shall distinguish three types of stationarity.

Definition 1.17 – Strict stationarity. Let Z be a RF on \mathbb{R}^d . It is said to be (*strictly*) *stationary* if, for any $\mathbf{h}, \mathbf{x}_1, \dots, \mathbf{x}_k \in \mathbb{R}^d$ and $z_1, \dots, z_k \in (0, +\infty)$ with $k \in \mathbb{N}^*$,

$$\mathbf{P}[Z(\mathbf{x}_1) \leq z_1, \dots, Z(\mathbf{x}_k) \leq z_k] = \mathbf{P}[Z(\mathbf{x}_1 + \mathbf{h}) \leq z_1, \dots, Z(\mathbf{x}_k + \mathbf{h}) \leq z_k],$$

i.e. the finite finite-dimensional distributions of Z are invariant under an arbitrary translation of the points by a vector \mathbf{h} . In the sequel, a stationary RF is abbreviated SRF.

Definition 1.18 – Second-order stationarity . Let Z be a RF on \mathbb{R}^d . It is said to be *second-order stationary* (or *weakly stationary*) if, for any $\mathbf{x}, \mathbf{h} \in \mathbb{R}^d$,

- $\mathbf{E}[Z(\mathbf{x})] = \mu < +\infty$,
- $\text{Cov}[Z(\mathbf{x}), Z(\mathbf{x} + \mathbf{h})] = C(\mathbf{h}) < +\infty$,

where $\mu \in \mathbb{R}$ and $C : \mathbb{R}^d \rightarrow \mathbb{R}$ is called the *covariance function*. That is, the (pointwise) expectation of Z is constant over \mathbb{R}^d and the covariance between two margins only depends on the distance between them. In the sequel, a second-order stationary RF is abbreviated second-order SRF.

Definition 1.19 – Intrinsic stationarity. Let Z be a RF on \mathbb{R}^d . It is said to be *intrinsically stationary* if, for any $\mathbf{h} \in \mathbb{R}^d$, the incremental process $Y_{\mathbf{h}}$ defined, for every $\mathbf{x} \in \mathbb{R}^d$, by

$$Y_{\mathbf{h}} := Z(\mathbf{x} + \mathbf{h}) - Z(\mathbf{x})$$

is a second-order SRF. It is then referred to as an intrinsic RF.

Notice that, when $E[(Z(\mathbf{x}))^2] < +\infty$ for every $\mathbf{x} \in \mathbb{R}^d$, strict stationarity implies second-order stationarity that implies, in turn, intrinsic stationarity.

Let Z be a RF on a domain $V \subset \mathbb{R}^d$, which models some spatial phenomenon and suppose we are interested in investigating the dependence structure of Z . When the latter is, at least, second-order stationary, we can try to assess its covariance function. However, the second-order stationarity assumption is sometimes too strong: the expectation of Z may not be stable in V and its (pointwise) variance might not be finite. To overcome this problem, the so-called *variogram* is thus introduced.

Definition 1.20 – Variogram. Let Z be an intrinsic RF on \mathbb{R}^d . Its *variogram* γ is defined by

$$\gamma(\mathbf{h}) := \frac{1}{2} \text{Var} [Z(\mathbf{0}) - Z(\mathbf{h})],$$

for every $\mathbf{h} \in \mathbb{R}^d$. It is sometimes called *semi-variogram*.

The variogram only needs Z to be intrinsically stationary to be well-defined. In addition, when Z is second order-stationary, it is possible to retrieve the covariance function from the latter by the following equality:

$$\gamma(\mathbf{h}) = C(\mathbf{0}) - C(\mathbf{h}), \quad (1.17)$$

for any $\mathbf{h} \in \mathbb{R}^d$. Further, as mentioned in [Chilès and Delfiner \(2012, page 32\)](#), the variogram does not require the knowledge of the expectation of Z to be calculated, see *e.g.* [Eq. \(1.18\)](#). On the contrary, the latter has to be estimated from the data in order to compute the covariance function, which introduces a bias. That is why Geostatistics mainly focuses on the variogram to grasp the spatial variability of a RF. We shall also mention that γ is conditionally negative-semidefinite, *i.e.* $-\gamma$ is conditionally positive-semidefinite, see *e.g.* [Chilès and Delfiner \(2012, page 63\)](#). When predicting Z at unobserved locations, this property guarantees that the variance of the kriging error is nonnegative.

Next, assume that Z is an intrinsic RF observed on a finite number $n \in \mathbb{N}^*$ of locations $\mathbf{x}_1, \dots, \mathbf{x}_n \in \mathbb{R}^d$. Suppose also that Z has constant expectation, *i.e.* $E[Z(\mathbf{x})] = \mu \in \mathbb{R}$, for every $\mathbf{x} \in \mathbb{R}^d$. The variogram becomes $\gamma(\mathbf{h}) = \frac{1}{2} E[(Z(\mathbf{h}) - Z(\mathbf{0}))^2]$, for any $\mathbf{h} \in \mathbb{R}^d$. [Mathéron \(1962\)](#) has proposed the following unbiased empirical estimator of the variogram, called *experimental variogram*:

$$\hat{\gamma}(\mathbf{h}) := \frac{1}{2|\mathbf{N}_{\mathbf{h}}|} \sum_{(\mathbf{x}_i, \mathbf{x}_j) \in \mathbf{N}_{\mathbf{h}}} (Z(\mathbf{x}_i) - Z(\mathbf{x}_j))^2, \quad (1.18)$$

for every $\mathbf{h} \in \mathbb{R}^d$, where $\mathbf{N}_{\mathbf{h}} := \{(\mathbf{x}_i, \mathbf{x}_j) : (\mathbf{x}_i - \mathbf{x}_j) = \mathbf{h}, i, j = 1, \dots, k\}$ and $|\mathbf{N}_{\mathbf{h}}|$ is the number of distinct pairs in $\mathbf{N}_{\mathbf{h}}$. We shall remark that, when the points x_1, \dots, x_k are irregularly

spaced in V , the set $N_{\mathbf{h}}$ is often taken as $N_{\mathbf{h}} = \{(\mathbf{x}_i, \mathbf{x}_j) : (\mathbf{x}_i - \mathbf{x}_j) \in T_{\mathbf{h}}, i, j = 1, \dots, k\}$, with $T_{\mathbf{h}}$ some tolerance region around \mathbf{h} . However, this estimator cannot be used directly for spatial prediction since it is not conditionally negative-semidefinite; it has to be adjusted. This is commonly done by fitting a parametric model on this experimental variogram, which satisfies the condition of conditionally negative-semidefiniteness, see *e.g.* [Desassis and Renard \(2012\)](#) and references therein. Hence, the experimental variogram is rather a tool to explore the spatial variability of the phenomenon of interest. In the vocabulary used by [Matheron \(1989\)](#), this is an *objective quantity*, *i.e.* it may be calculated from the values of a single realization over a domain, and not a *conventional quantity* the statement of which is neither decidable nor falsifiable in Popper's terminology, like the variogram γ or the expectation μ . That is why Matheron does not have investigate the asymptotic properties of (1.18)

Other estimators than the empirical variogram have been proposed in the literature and, for a few, their asymptotic properties have been established under some appropriate mixing conditions; see [Section 3.3](#). Indeed, under some stationarity assumptions, the possibility to perform statistical inference is always based on some mixing and more generally ergodic properties, in that the latter guarantee that estimators asymptotically converge, in some sense, towards the quantity to be estimated. The concept of ergodicity in the context of unique realization and, in particular, the notion of *mean-ergodicity* are discussed in [Matheron \(1989\)](#). The latter ensures, under second-order stationarity, that the spatial mean converges in quadratic mean to the expectation μ when the domain it is computed on becomes increasingly large. Related to this property, the notion of *integral range* is also introduced; this is a quantity that helps characterize the statistical fluctuations of a second-order stationary random field at large scale and, in some cases, it may be interpreted as the spatial scale of the phenomenon. These two concept are more detailed in the next chapter.

Now, let Z be a max-stable RF that is (partially) observed only once on some domain. For simplicity, we shall also assume that Z is stationary; the work presented in this thesis could constitute the basis of future developments where the strictly stationarity assumption would be relaxed. It would be nice to use the variogram and associated estimators to explore its dependence structure. Unfortunately, depending on the EVI of the margins of Z , we might have $E[Z(\mathbf{0})] = +\infty$ and $\text{Var}[Z(\mathbf{0})] = +\infty$, hence the variogram may not exist. This is *e.g.* the case for simple max-stable processes. Consider instead the extremal coefficient function θ introduced in the last section. Several estimators of the latter has been proposed in the literature, but they are generally used with temporal replications of Z , see [Chapter 3](#). Among them, the so-called nonparametric *F-madogram estimator*, suggested by [Cooley et al. \(2006\)](#),

has however been inspired by the geostatistical framework. Let F be the c.d.f. of $Z(\mathbf{0})$. It is based on the so-called F-madogram

$$v_F(\mathbf{h}) := \frac{1}{2} \mathbf{E} \left[|F(Z(\mathbf{h})) - F(Z(\mathbf{0}))| \right],$$

for every $\mathbf{h} \in \mathbb{R}^d$, which corresponds to the variogram of order 1 of the RF $(F(Z(\mathbf{x})))_{\mathbf{x} \in \mathbb{R}^d}$. We refer to [Chilès and Delfiner \(2012\)](#) for more details about variograms of order 1, also called madograms. This madogram can be estimated by an empirical estimator of the same type as [Eq. \(1.18\)](#) but this requires the knowledge of the c.d.f. F . In studies, both F and v_F are usually evaluated empirically from time series that are considered as approximatively *i.i.d.*. Sometimes, F is also estimated by fitting a GEV distribution from such replications. Hence, the applications conducted in spatial extreme studies generally involve time series, and to our knowledge, only [Bel et al. \(2008\)](#) and [Naveau et al. \(2009\)](#) have estimated the extremal coefficient function from a single realization of Z . The two papers focus on the same Bourgogne precipitation data set, which consists of 51-year maxima of daily precipitation recorded at 146 weather station locations. It was obtained from the Météo France research laboratory, which preprocessed the measurements so that the data can be assumed to be a realization of a stationary RF. Since the data are maxima computed over a long period of time, the latter is also supposed to be max-stable. From this data, [Bel et al. \(2008\)](#) compute different estimators of θ among which the F-madogram estimator. They also propose a nonlinear least squares madogram function based estimator which is a generalization of the latter. [Naveau et al. \(2009\)](#) also suggest an estimator that generalizes the F-madogram estimator. In both papers, the margins of the max-stable RF are evaluated empirically and the madograms are estimated using an empirical estimator of the same type as [Eq. \(1.18\)](#). Both analysis show that there exists a pairwise extremal dependence in the precipitation field, which is rather strong over the first 50 kilometers; such dependence thus needs to be taken into account *e.g.* when modelling extreme events in order to make scenarii for preventing flood. However, asymptotic properties of the aforementioned estimators have not been studied; as remarked in [Naveau et al. \(2009\)](#), it would be very interesting to establish the convergence of these estimators when the number of locations increases, either by increasing the density of points in a fix domain or by enlarging the domain size, or both. Actually, this is done in [Dombry and Eyi-Minko \(2012\)](#) when considering increasing domain asymptotics. Under a mixing condition, the asymptotic normality of some estimators of the ECF, among which the F-madogram estimator, is established. However, this result holds when the when the max-stable process is defined on \mathbb{Z}^d and, for all we know, no generalization to \mathbb{R}^d has been proposed so far.

Based on these considerations, it seems relevant to investigate the connexions between spatial extreme value theory and Geostatistics in order to better handle the study of spatial extremes when having a single observation. In this work, we mainly focus on the extremal coefficient function of a stationary max-stable random field. Recall that θ is a measure of the pairwise

extremal dependence. In the next chapter, we examine its relation with the integral range, since the latter can be interpreted, in some cases, as the spatial scale of the phenomenon. Then, in [Chapter 3](#), a new nonparametric estimator of θ is proposed and its asymptotic properties are derived when it is computing from a single and partially observed realization of a max-stable random field. More generally, the work presented in this thesis, and especially in [Chapter 2](#), is an invitation to think about the possibility of estimating, with some precision, relevant quantities from the extreme value theory, when having a single set of spatial observations. Such considerations may encourage the more frequent use of the extreme value theory in geostatistical modelling. For instance, as briefly developed in the next section, knowing how to evaluate the EVI from a unique observation might enrich the well-known top-cut model.

1.4.3 A specific issue: top-cut model and extreme value theory

Historically, Geostatistics has been developed to address mining resources estimation issues. In this section, we focus on ore deposits the grade distribution of which is heavy-tailed, typically gold deposits. Since high-values make the inference of first and second-order statistics (e.g. expectation, variance, variogram) nonrobust, they were usually cut down to some threshold and the estimation was performed using truncated grades. Consequently, the total amount of metal in a deposit was underestimated, which is not optimal from an investment point of view. A few years ago, [Rivoirard et al. \(2013\)](#) has proposed the so-called top-cut model to handle high values.

Let X be a stationary RF that models the grade in the ore deposit V and let $z_e \in (0, +\infty)$ be the threshold value, called top-cut grade, at which the grade is usually cut down to. Let also $m(z_e) := E[X(\mathbf{0})|X(\mathbf{0}) \geq z_e]$. [Rivoirard et al. \(2013\)](#) proposes to split X in three parts:

- the truncated grade $(\min(X(\mathbf{x}), z_e))_{\mathbf{x} \in V}$,
- the weighted indicator above the top-cut grade $((m(z_e) - z_e)\mathbf{1}\{X(\mathbf{x}) \geq z_e\})_{\mathbf{x} \in V}$,
- the residual $((X(\mathbf{x}) - m(z_e))\mathbf{1}\{X(\mathbf{x}) \geq z_e\})_{\mathbf{x} \in V}$,

which gives, for any $\mathbf{x} \in \mathbb{R}^d$,

$$X(\mathbf{x}) = \min(X(\mathbf{x}), z_e) + (m(z_e) - z_e)\mathbf{1}\{X(\mathbf{x}) \geq z_e\} + (X(\mathbf{x}) - m(z_e))\mathbf{1}\{X(\mathbf{x}) \geq z_e\}.$$

Then, they assume that there is no spatial correlation between the residual and the indicator or the truncated grade; when performing some predictions to unobserved locations, this allows for kriging separately the residual and cokriging the truncated grade and the indicator. This makes the study more robust since both truncated grade and indicator do not present high values. Besides, they suggest a method to find, if its exists, a minimal bound for the top-cut grade above which the aforementioned assumption is approximatively met. They also

propose to find, if it exists, a maximal bound for the top-cut grade above which the residual can be considered as a pure-nugget effect: in this case, the simple kriging of the residual is thus equal to 0.

The top-cut model thus takes into account the high values mainly through the conditional expectation $E[X(\mathbf{0}) - z_e | X(\mathbf{0}) \geq z_e] = m(z_e) - z_e$. In [Rivoirard et al. \(2013\)](#), the latter is estimated empirically by computing the mean of the excess of all the observations above z_e . However, this empirical mean may underestimate the expectation, especially since the distribution of X is supposed to be heavy tailed. Such expectation could be assessed using instead the extreme value theory. Assume that the c.d.f. of $X(\mathbf{0})$ is in the domain of attraction of some GEV distribution with EVI $\gamma \in \mathbb{R}$. According to [Eq. \(1.5\)](#), if z_e is high enough, then $X(\mathbf{0}) - z_e | X(\mathbf{0}) \geq z_e$ has (approximatively) a GPD distribution with shape parameter γ . If this distribution is known, then so is the expectation of $X(\mathbf{0}) - z_e | X(\mathbf{0}) \geq z_e$. Notice that, when $\gamma > 1$, the latter is infinite: this information cannot be used directly to predict grades at unobserved locations but it suggests that we may expect a high quantity of metal in the ore. The remaining issue is therefore: how to estimate the parameters of this GPD distribution, and in particular γ , when having a single and partial realization of X on V ? This question is left for future works.

FROM GEOSTATISTICS TO EVT: INTEGRAL RANGE AND EXTREMAL COEFFICIENT FUNCTION

Résumé Ce chapitre établit un lien entre la Géostatistique et la théorie spatiale des extrêmes à travers le concept de portée intégrale. Issu de la théorie géostatistique, ce paramètre caractérise les fluctuations, à large échelle, d'un champ aléatoire stationnaire. Il intervient notamment lorsqu'on cherche à évaluer l'espérance de ce dernier par la moyenne spatiale calculée sur une large fenêtre. Cette quantité est tout d'abord détaillée et une méthode pour l'estimer, qui diffère légèrement de celle proposée par [Lantuéjoul \(1991\)](#), est introduite. Ensuite, lorsque le champ stationnaire est max-stable simple, nous montrons que sa fonction coefficient extrémal est fortement liée à la portée intégrale du champ des excès, au dessus d'un certain seuil, correspondant. En particulier, nous donnons une condition nécessaire et suffisante sur l'ECF pour que la portée intégrale soit finie. Cette condition est reliée aux propriétés d'ergodicité et de mélange du champ max-stable. Elle est étudiée pour des modèles max-stables standards puis est illustrée sur des jeux de données simulés. Enfin, nous montrons que ce travail permet de retrouver et de compléter des résultats précédemment établis par [Koch \(2017\)](#) dans un contexte de risque spatialisé.

In many geostatistical applications (soil contamination evaluation, mining resources estimation), the physical phenomenon under study is interpreted as a particular realization of a stationary random field (SRF) with a finite expectation. A natural question that arises in such a context is whether this expectation can be estimated from a single realization. Part of the answer is brought by the concept of integral range introduced and studied by [Mathéron \(1989\)](#) and [Lantuéjoul \(1991\)](#). Intimately related to the ergodic and mixing properties, it is a geostatistical object that characterizes the statistical fluctuations of the random field at large scale. When the latter is max-stable, we show that its extremal coefficient function is closely related to the integral range of the corresponding indicator function above a threshold. This approach allows to retrieve and complete results established by [Koch \(2017\)](#) in a spatial risk context. It thereby illustrates the relevance of geostatistical tools to enrich extreme value analysis, especially when inference must be based on a single realization of the spatial process.

The chapter is structured as follows. We start off in [Section 2.1](#) with the introduction of a few notation and hypotheses, subsequently used when working with the integral range. A detailed account of this quantity is then given in [Section 2.2](#). In particular, we introduce a new method to estimate it, which slightly differs from the procedure originally proposed by [Lantuéjoul \(1991\)](#). In [Section 2.3](#), the connection between the integral range and the extremal coefficient function is investigated. The results, illustrated by numerical experiments, are then related to the ergodic and mixing properties of a simple max-stable SRF. In [Section 2.4](#), they are additionally linked to the work of [Koch \(2017\)](#). Assets, liabilities, natural extensions and required improvements of our work are finally listed and discussed in [Section 2.5](#). Technical proofs are postponed to [Section 2.6](#).

2.1 SETTING

Like in the previous chapter, let $(\Omega, \mathcal{F}, \mathbb{P})$ be a complete probability space and set $d \in \mathbb{N}^*$. The spaces \mathbb{R}^d and \mathbb{R} are equipped with their respective Borel σ -algebra $\mathcal{B}_{\mathbb{R}^d}$ and $\mathcal{B}_{\mathbb{R}}$. The origin of \mathbb{R}^d is $\mathbf{0}$ and elements of \mathbb{R}^d are still written in bold. Recall also that the Euclidean distance separating two points \mathbf{x} and \mathbf{y} of \mathbb{R}^d is written $\|\mathbf{x} - \mathbf{y}\|$, and that the indicator function of any condition C is denoted by $\mathbf{1}\{C\}$. In addition, for any measurable subset V of \mathbb{R}^d , let $|V|$ be its volume with respect to the Lebesgue measure in \mathbb{R}^d . We shall denote by \mathcal{K} the set of all compact subsets of \mathbb{R}^d and by \mathcal{B} the set of measurable bounded subsets of \mathbb{R}^d with positive volume. In the sequel, all random fields are supposed to be real-valued.

When working with the integral range, we shall deal with stochastic integrals and sequences of subsets of \mathbb{R}^d that converge to \mathbb{R}^d in a certain way. They are introduced in this section. All these concepts are introduced in the following subsections.

2.1.1 Stochastic integrals

Let Z be a random field (RF) defined on \mathbb{R}^d . To guarantee that the quantities we shall work with are well-defined, the following assumptions are required.

Assumption 2.1 Z is $(\mathcal{F} \otimes \mathcal{B}_{\mathbb{R}^d}, \mathcal{B}_{\mathbb{R}})$ -measurable.

Assumption 2.2 Z has \mathbb{P} -almost surely (a.s.) locally integrable sample paths.

The first assumption is necessary to apply Tonelli's theorem, which ensures that, for any $V \in \mathcal{B}$, the stochastic integral

$$\begin{aligned} \Omega &\longrightarrow \mathbb{R}_+ \cup \{+\infty\} \\ \omega &\longmapsto \int_V |Z(\mathbf{x}, \omega)| d\mathbf{x} \end{aligned}$$

is $(\mathcal{F}, \mathcal{B}_{\mathbb{R}})$ -measurable, making it a well-defined random variable. Now, the second assumption means that

$$\mathbf{P} \left[\left\{ \omega \in \Omega : \int_W |Z(\mathbf{x}, \omega)| d\mathbf{x} \text{ is finite for any } W \in \mathcal{K} \right\} \right] = 1, \quad (2.1)$$

which implies that

$$\mathbf{P} \left[\left\{ \omega \in \Omega : \int_V Z(\mathbf{x}, \omega) d\mathbf{x} \text{ is finite for any } V \in \mathcal{B} \right\} \right] = 1.$$

For any $V \in \mathcal{B}$, this allows us to define the \mathbf{P} -a.s. finite random variable

$$\begin{aligned} Z(V) &: \Omega \longrightarrow \mathbb{R} \\ \omega &\longmapsto \frac{1}{|V|} \int_V Z(\mathbf{x}, \omega) d\mathbf{x}. \end{aligned}$$

[Assumption 2.1](#) actually guarantees that, when all the expectations below exist,

$$\mathbf{E}[Z(V)] = \frac{1}{|V|} \int_V \mathbf{E}[Z(\mathbf{x}, \omega)] d\mathbf{x}.$$

2.1.2 Convergence to \mathbb{R}^d

The integral range is an asymptotic quantity obtained when considering sequences of subsets of \mathbb{R}^d that grow infinitely to \mathbb{R}^d in a certain way. To define such types of sequences, we first need to introduce a few definitions and notation. Let V and W be two non-empty, bounded, measurable subsets of \mathbb{R}^d . The translation of V by an element \mathbf{w} of W is written $V + \mathbf{w}$. Then, the Minkowski difference of V and W is defined as

$$V \ominus W := \bigcap_{\mathbf{w} \in W} V + \mathbf{w}.$$

Let now $\check{W} := \{-\mathbf{v} : \mathbf{v} \in W\}$ denote the symmetric of W with respect to the origin $\mathbf{0}$. The set $V \ominus \check{W}$ represents the erosion of V by the structuring element W (see [Figure 2.13](#) for an illustrative example). Let also $\mathbf{b}_V \in \mathbb{R}^d$ stand for the barycenter of V . For any $\lambda \in (0, +\infty)$, the set $\lambda_{\mathbf{b}} V$ corresponds to the image of V after applying the homothety with center $\mathbf{b} \in \mathbb{R}^d$ and ratio λ . When $\mathbf{b} = \mathbf{b}_V$, the latter is simply denoted by λV . In addition, we write $B_r(\mathbf{x})$ the closed ball of center $\mathbf{x} \in \mathbb{R}^d$ and radius $r \in (0, +\infty)$, with the simplification $B_r(\mathbf{0}) = B_r$.

Definition 2.3 Let $(V_n)_{n \in \mathbb{N}}$ be a sequence of sets in \mathcal{B} . It is written $V_n \uparrow \mathbb{R}^d$ if it converges to \mathbb{R}^d in the following sense:

- (i) $V_n \subset V_{n+1}$ for all $n \in \mathbb{N}$,
- (ii) $\bigcup_{n \in \mathbb{N}} V_n = \mathbb{R}^d$,
- (iii) $\lim_{n \rightarrow +\infty} \frac{|V_n \ominus \check{W}|}{|V_n|} = 1$, for any compact subset W of \mathbb{R}^d .

These conditions are not very restrictive. They are satisfied by sequences $(\lambda_n V)_{n \in \mathbb{N}}$ where $V \in \mathcal{B}$ contains a ball $B(\mathbf{b}_V, r)$ with radius $r \in (0, +\infty)$, and $(\lambda_n)_{n \in \mathbb{N}}$ is a nondecreasing sequence of positive real numbers that diverges to $+\infty$ as $n \rightarrow +\infty$. Such sequences typically include nondecreasing sequences of balls or hyperrectangles. Notice that (i) - (iii) imply that $|V_n| \rightarrow +\infty$ as $n \rightarrow +\infty$. The last two conditions have already been considered in Lantuéjoul (1991). By insuring that V_n grows in all directions as $n \rightarrow +\infty$, (ii) guarantees the covering of the whole space \mathbb{R}^d . Condition (iii) means that the effect of erosions becomes negligible as $n \rightarrow +\infty$. In effect, the subsets V_n cannot look like Swiss cheese, riddled with holes.

Example 2.4 – Swiss cheese sets. Set $d = 2$ and for any $n \in \mathbb{N}$, consider the square V_n of side $2n + 1$ and centre $\mathbf{0}$. Divide it into $2(2n + 1)$ non-overlapping squares of side 1, which are then perforated in the middle with a disk of diameter $1/(n + 1)$, like in Figure 2.1. Then, the sequence $(V_n)_{n \in \mathbb{N}}$ satisfies the conditions (i) and (ii) in Definition 2.3, but not condition (iii). Indeed, consider a square of side 1 that is centred in $\mathbf{0}$, from which the origin has been removed. The erosion of this set by the disk $B_{1/2}$ is an empty set, therefore so is the erosion of V_n by $B_{1/2}$, for any $n \in \mathbb{N}$. Consequently, $\lim_{n \rightarrow +\infty} \frac{|V_n \ominus B_{1/2}|}{|V_n|} = 0$.

We shall see in Section 2.7 that conditions (i) - (iii) hold, in particular, for Van Hove sequences of subsets. Such increasing sequences were used in a spatial extreme context by, for instance, Koch (2017, 2019) and Koch et al. (2018).

2.2 THE INTEGRAL RANGE

2.2.1 Background

In this section, let Z be a second-order SRF with expectation $\mu := E[Z(\mathbf{0})]$. Its variance is denoted by $\sigma^2 := \text{Var}[Z(\mathbf{0})]$ and its correlation function by $\rho : \mathbf{h} \in \mathbb{R}^d \mapsto \sigma^{-2} \text{Cov}[Z(\mathbf{0}), Z(\mathbf{h})] \in [-1, 1]$. As pointed out in the previous chapter, in many applications, only one realization of

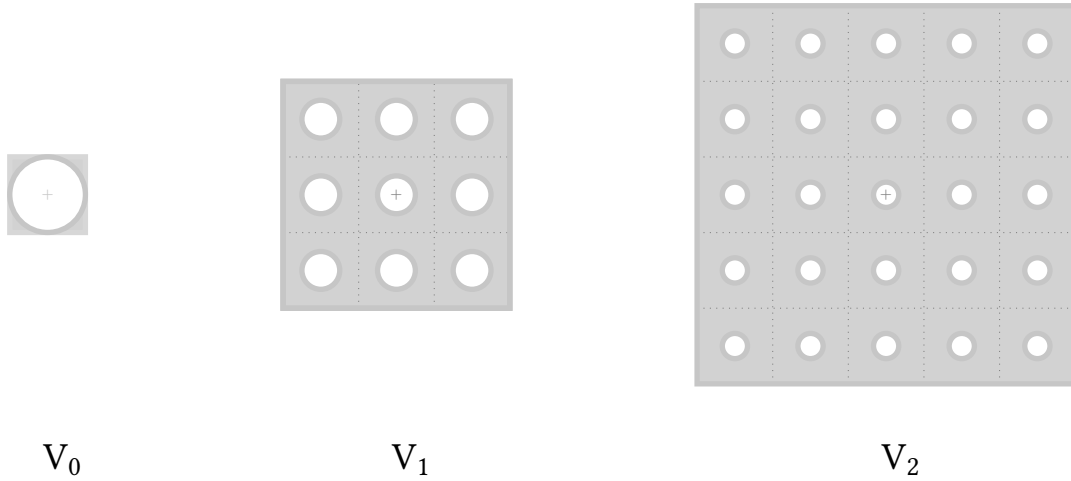


FIGURE 2.1 – The sets V_0 , V_1 and V_2 (grey area), all centred in $\mathbf{0}$ (grey cross). They are divided into 1×1 squares (dashed lines), which are in turn perforated by disks (in white).

Z is partially observed. Can we hope for a good estimation of μ in such situations? This question is of particular interest in the context of heterogeneous material studies. One important goal is to estimate effective physical or morphological properties of such material, which are then modelled by the expectation μ of some second-order RF. In general, producing several samples of the studied material is too expensive or too time consuming, and this estimation has to be performed using only one spatial set of observations. For instance, one might refer to [Azzimonti et al. \(2013\)](#) for the study of some optical properties, [Peyrega and Jeulin \(2013\)](#) for acoustic properties estimation, [Dirrenberger et al. \(2014\)](#) for a work on fibrous network and [Gasnier et al. \(2015\)](#) for the evaluation of thermoelastic behaviour of an explosive material.

Let $V_n \uparrow \mathbb{R}^d$ and, for any $n \in \mathbb{N}$, assume that Z is observed everywhere in V_n . The random variable $Z(V_n)$ is square integrable and, by stationarity, it is an unbiased estimator of μ :

$$\mathbb{E}[Z(V_n)] = \frac{1}{|V_n|} \int_{V_n} \mathbb{E}[Z(\mathbf{x})] d\mathbf{x} = \mu.$$

Its variance equals

$$\text{Var}[Z(V_n)] = \frac{\sigma^2}{|V_n|^2} \int_{V_n} \int_{V_n} \rho(\mathbf{x} - \mathbf{y}) d\mathbf{x} d\mathbf{y} = \frac{\sigma^2}{|V_n|} \int_{\mathbb{R}^d} \rho(\mathbf{h}) \frac{K_n(\mathbf{h})}{K_n(\mathbf{0})} d\mathbf{h}, \quad (2.2)$$

where, for any $\mathbf{h} \in \mathbb{R}^d$, $K_n(\mathbf{h}) := |V_n \cap (V_n + \mathbf{h})|$ is called the geometric covariogram of V_n . It is a measurable function of \mathbf{h} satisfying $K_n \leq K_n(\mathbf{0})$. Notice that $V_n \cap (V_n + \mathbf{h})$ can be viewed as the erosion of V_n by $\{0, \mathbf{h}\}$, i.e. $V_n \cap (V_n + \mathbf{h}) = V_n \ominus \{0, \mathbf{h}\}$. Thus, according to condition [\(iii\)](#) in [Definition 2.3](#):

$$\lim_{n \rightarrow +\infty} \frac{K_n(\mathbf{h})}{K_n(\mathbf{0})} = 1. \quad (2.3)$$

For practical use, we would like to have some kind of asymptotic consistency that does not involve i.i.d. replications of $Z(V_n)$. Typically, if $\text{Var}[Z(V_n)]$ were to vanish when the domain V_n becomes infinite (in the sense given in [Definition 2.3](#)), then $Z(V_n)$ would be an asymptotically consistent estimator of μ . However, it is not always the case. A classic counterexample, given in [Yaglom \(1987\)](#), is the RF Z defined for all $\mathbf{x} \in V_n$ by $Z(\mathbf{x}) = W$, with W a non-constant random variable. Hence, for any $n \in \mathbb{N}$ we have $Z(V_n) = W$, and $\text{Var}[(Z(V_n))]$ does not tend towards 0 as $n \rightarrow +\infty$. This is why the concept of ergodicity in the mean is introduced in a spatial context (see e.g. [Yaglom, 1987](#); [Lantuéjoul, 1991](#)).

Definition 2.5 Let $V_n \uparrow \mathbb{R}^d$. The second-order RF Z is said to be ergodic in the mean (or first-order ergodic) if $Z(V_n)$ converges to μ in quadratic mean:

$$\lim_{n \rightarrow +\infty} \text{Var}[Z(V_n)] = 0. \quad (2.4)$$

Remark 2.6 – Slutsky’s formula. An equivalent condition for [Eq. \(2.4\)](#) is the so-called Slutsky’s formula:

$$\lim_{n \rightarrow +\infty} \frac{1}{|V_n|} \int_{V_n} \text{Cov}[Z(\mathbf{0}), Z(\mathbf{h})] d\mathbf{h} = 0. \quad (2.5)$$

Indeed, applying the Cauchy-Schwarz inequality to

$$\text{Cov}\left[Z(\mathbf{0}), \frac{1}{|V_n|} \int_{V_n} Z(\mathbf{h}) d\mathbf{h}\right]$$

shows that [Eq. \(2.4\)](#) implies [Eq. \(2.5\)](#). The converse directly follows from [Eq. \(2.2\)](#). Consequently, a sufficient (but not necessary) condition for mean-ergodicity is

$$\lim_{\|\mathbf{h}\| \rightarrow +\infty} \rho(\mathbf{h}) = 0. \quad (2.6)$$

To the best of our knowledge, there does not exist any procedure to test the mean-ergodicity assumption when observing only one spatial set of observations. Two references were found in a discrete temporal setting, namely [Domowitz and El-Gamal \(1993\)](#) and [Domowitz and El-Gamal \(2001\)](#). In the following, we shall assume that Z satisfies [Eq. \(2.4\)](#).

Now, consider two sequences $V_n^1 \uparrow \mathbb{R}^d$ and $V_n^2 \uparrow \mathbb{R}^d$ such that $|V_n^1| = |V_n^2|$ for each $n \in \mathbb{N}$. The Cauchy-Schwarz inequality gives

$$0 \leq (\text{Cov}[Z(V_n^1), Z(V_n^2)])^2 \leq \text{Var}[Z(V_n^1)] \text{Var}[Z(V_n^2)].$$

Thus, the first-order ergodicity assumption is sufficient to yield

$$\lim_{n \rightarrow +\infty} \text{Cov}[Z(V_n^1), Z(V_n^2)] = 0. \quad (2.7)$$

It also guarantees that the expectation μ can be assessed from a single realization of Z with any desirable degree of accuracy, provided that the latter is observed on a sufficiently large domain. Precisely, by virtue of the Bienaymé-Chebychev inequality, it entails that for any $\epsilon \in (0, +\infty)$ and $\eta \in (0, 1]$ there exists $n_{\epsilon, \eta} \in \mathbb{N}$ such that for all $n \geq n_{\epsilon, \eta}$,

$$\mathbf{P}[|Z(V_n) - \mu| < \epsilon] > 1 - \eta.$$

However, the mean ergodicity property does not indicate how to choose $n \in \mathbb{N}$ to insure that $\text{Var}[Z(V_n)]$ is less than a pre-specified value. The concept of *integral range* is introduced for this purpose.

2.2.2 Definition and interpretation

Considering the mathematical setting described in the previous subsection, let $n \in \mathbb{N}$ and define

$$A_n := |V_n| \frac{\text{Var}[Z(V_n)]}{\sigma^2} \in (0, +\infty), \quad (2.8)$$

which is finite since V_n is a bounded set. Using Eq. (2.2), it can also be written

$$A_n = \int_{\mathbb{R}^d} \rho(\mathbf{h}) \frac{K_n(\mathbf{h})}{K_n(\mathbf{0})} d\mathbf{h}. \quad (2.9)$$

Definition 2.7 – Integral range. When it exists, the quantity

$$A := \lim_{n \rightarrow +\infty} A_n \quad (2.10)$$

is called the integral range of Z . It is nonnegative, possibly infinite, and can be considered as a d -volume (a length when $d = 1$, an area when $d = 2$, a volume when $d = 3$).

Historically, the term of *integral range* was introduced by [Matheron \(1989\)](#) to name the integral

$$\int_{\mathbb{R}^d} \rho(\mathbf{h}) d\mathbf{h}. \quad (2.11)$$

This quantity also appears in [Yaglom \(1987\)](#), but is not referred to as the integral range; it is called *correlation time* (or *integral time scale*) in a temporal framework, and *correlation area* (or *integral area scale*) when $d = 2$. The more general definition we use here was adopted by [Lantuéjoul \(1991\)](#). He actually showed that it coincides with Eq. (2.11) as long as ρ is integrable. Indeed, from Eq. (2.9), we have

$$A = \lim_{n \rightarrow +\infty} \int_{\mathbb{R}^d} \rho(\mathbf{h}) \frac{K_n(\mathbf{h})}{K_n(\mathbf{0})} d\mathbf{h}. \quad (2.12)$$

In addition, for any $n \in \mathbb{N}$ and any $\mathbf{h} \in \mathbb{R}^d$ the inequality $K_n(\mathbf{h})/K_n(\mathbf{0}) \leq 1$ holds by construction, and Eq. (2.3) states that $\lim_{n \rightarrow +\infty} K_n(\mathbf{h})/K_n(\mathbf{0}) = 1$. Thus, when ρ is integrable, the dominated convergence theorem can be used to exchange limit and integral operator in Eq. (2.12),

which establishes the result. As claimed in [Proposition 2.8](#), the converse holds when ρ is non-negative, but this is not true in the general case. Consider for instance $d = 1$ and $\rho = \cos$. This function is not integrable on \mathbb{R} . However, setting $n \in \mathbb{N}$ and $V_n = [-n, n]$, [Eq. \(2.3\)](#) entails

$$A_n = \frac{1}{2n} \int_{-n}^n \int_{-n}^n \cos(x-y) dx dy = \frac{2 \sin(2n)}{n},$$

which implies in turn that $A = 0$.

Proposition 2.8 Let Z be a second-order SRF, with measurable and nonnegative correlation function ρ . Its integral range A always exists and equals $\int_{\mathbb{R}^d} \rho(\mathbf{h}) d\mathbf{h} \in [0, +\infty]$.

We refer to [Subsection 2.6.1](#) for the proof. In fine, we shall point out that the limit in [Eq. \(2.10\)](#) exists for all usual isotropic covariance functions used in geostatistics, the values of which are given in [Lantuéjoul \(2002\)](#).

To obtain a more physical interpretation of this mathematical object, recall that $|V_n| \rightarrow +\infty$ and $\text{Var}[Z(V_n)] \rightarrow 0$ as $n \rightarrow +\infty$. The integral range A gives information about the behaviour of the variance $\text{Var}[Z(V_n)]$ with respect to $|V_n|$, for large domains V_n . Three cases shall be distinguished: when A is finite positive, null or infinite. The first situation turns out to be the most interesting in practice, since A can then be interpreted as the spatial scale of the phenomenon and helps control $\text{Var}[Z(V_n)]$ for large V_n .

2.2.2.1 Finite positive integral range

Assume that $A \in (0, +\infty)$. As $n \rightarrow +\infty$, the variance of $Z(V_n)$ is of order $|V_n|^{-1}$:

$$\text{Var}[Z(V_n)] \underset{n \rightarrow \infty}{\sim} \sigma^2 \frac{A}{|V_n|}. \quad (2.13)$$

Since $A \neq 0$, for some large enough $n \in \mathbb{N}$ we can find a positive integer $N = N_n$ such that $N \approx \frac{A}{|V_n|}$; it represents the number of disjoint subdomains of measure A contained in V_n . Then, [Eq. \(2.13\)](#) becomes

$$\text{Var}[Z(V_n)] \approx \frac{\sigma^2}{N}. \quad (2.14)$$

Take $\mathbf{x}_1, \dots, \mathbf{x}_N$ separately in each of the N blocks of volume A dividing V_n . [Lantuéjoul \(1991\)](#) remarks that if $Z(\mathbf{x}_1), \dots, Z(\mathbf{x}_N)$ are uncorrelated, in which case the blocks are said to be uncorrelated, the variance of $N^{-1} \sum_{i=1}^N Z(\mathbf{x}_i)$ would also be σ^2/N . Therefore, when the integral range is positive and finite, it can be physically interpreted as the scale of the phenomenon, while V_n is the scale of observation; we can judge how large V_n is with respect to A . Obviously, the bigger N , the lower $\text{Var}[Z(V_n)]$ and the more precise the estimation of $E[Z(\mathbf{0})]$. In practice, if we were to provide a good estimate of $A\sigma^2$ (see [Subsection 2.2.3](#)), the domain V_n could be chosen so that $\text{Var}[Z(V_n)]$ is smaller than a prespecified value. That is why the integral range

is used in heterogeneous material studies: it helps to define an optimal sample size, which can be extremely large with respect to the microscopic scale at which the study is conducted. An example of RF with finite positive integral range is given in [Example 2.9](#).

On the physical interpretation of Eq. (2.14) The analogy proposed by [Lantuéjoul \(1991\)](#) with a partition of V_n into N uncorrelated blocks provides a physical interpretation of the phenomenon. Nonetheless, in general, such subsets cannot be considered as uncorrelated. That is, for any two of these sub-blocks V_n^1 and V_n^2 and for any $(\mathbf{x}, \mathbf{y}) \in V_n^1 \times V_n^2$, there is no reason for the random variables $Z(\mathbf{x})$ and $Z(\mathbf{y})$ to be uncorrelated. Sufficient conditions to have (approximatively) no correlation would be that $\lim_{\|\mathbf{h}\| \rightarrow +\infty} \rho(\mathbf{h})$ exist, ρ be integrable and the distance between \mathbf{x} and \mathbf{y} be large enough. Indeed, when $\lim_{\|\mathbf{h}\| \rightarrow +\infty} \rho(\mathbf{h})$ exists

$$\int_{\mathbb{R}^d} \rho(\mathbf{h}) d\mathbf{h} < +\infty \Rightarrow \lim_{\|\mathbf{h}\| \rightarrow +\infty} \rho(\mathbf{h}) = 0. \quad (2.15)$$

The implication (2.15) is easily proven by contradiction: assume that $\lim_{\|\mathbf{h}\| \rightarrow +\infty} \rho(\mathbf{h}) = \ell \in \mathbb{R}^*$. Then, there exists $m \in (0, +\infty)$ such that ρ has a constant sign on $E_m := \{\mathbf{h} \in \mathbb{R}^d : \|\mathbf{h}\| \geq m\}$ and, for any $\mathbf{h} \in E_m$, $|\rho(\mathbf{h})| \geq |\ell/2|$. It follows that

$$\int_{\|\mathbf{h}\| \geq m} |\rho(\mathbf{h})| d\mathbf{h} \geq \int_{\|\mathbf{h}\| \geq m} \left| \frac{\ell}{2} \right| d\mathbf{h} = +\infty,$$

which contradicts the assumption that ρ is integrable. Consequently, when $\lim_{\|\mathbf{h}\| \rightarrow +\infty} \rho(\mathbf{h})$ exists and ρ is integrable, two blocks V_n^1 and V_n^2 may be considered as uncorrelated if they are quite far apart from each other.

Links with mixing The decrease to 0 of ρ when $\|\mathbf{h}\| \rightarrow +\infty$ is linked to the ergodic and mixing properties. For instance, when Z is a Gaussian second-order SRF, then $\lim_{\|\mathbf{h}\| \rightarrow +\infty} \rho(\mathbf{h}) = 0$ if and only if it is mixing (in the precise sense given later in [Definition 2.26](#)); this is proven in the one-dimensional case in [Maruyama \(1949\)](#). This equivalence holds because the law of a Gaussian SRF is characterized by its expectation and its covariance function, but it is most likely false in the general case. Indeed, the mixing property involves the finite-dimensional distributions of Z , which are more complex objects than the correlation function. According to [Eq. \(2.15\)](#), when $\lim_{\|\mathbf{h}\| \rightarrow +\infty} \rho(\mathbf{h})$ exists, the integrability of ρ , which entails that A is finite, thus implies that the Gaussian RF Z is mixing. This illustrates the potential link between integral range and mixing. Notice that the integrability of ρ is much more informative than the convergence of ρ to 0; it means that the latter vanishes fast enough to be integrable. This property may be an advantage when estimating from a single realization. We shall remark that, similarly to the correlation function of a Gaussian process, the extremal coefficient function (ECF) of a simple max-stable SRF is also related to the mixing property given in [Definition 2.26](#); this is detailed in the next section. This encourages us to look for some links between the integral

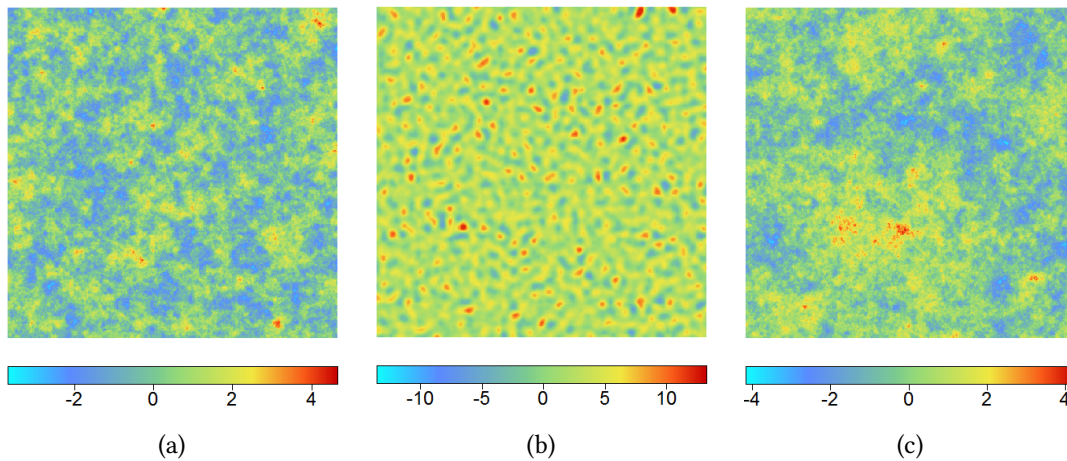


FIGURE 2.2 – Realizations of a Gaussian second-order SRF with: (a) exponential covariance function (positive integral range), (b) covariance function defined by Eq. (2.17) (null integral range) and (c) hyperbolic covariance function (infinite integral range), when the scale parameter a is 10, 20 and 10, respectively. The simulation field is 500×500 , with mesh size equal to 1.

range this function.

Example 2.9 – *Gaussian RF with finite positive integral range.* Let Z be a Gaussian second-order SRF with exponential covariance function C given, for any $\mathbf{h} \in \mathbb{R}^d$, by

$$C(\mathbf{h}) = \exp \left\{ -\frac{\|\mathbf{h}\|}{a} \right\},$$

where $a \in (0, +\infty)$ is a scale parameter. It is known that Z has a finite non-null integral range A (see Lantuéjoul, 2002). Figure 2.2(a) shows a realization of Z when $a = 10$, obtained with the R package `Randomfields`. At the scale of the simulation, it gives an impression of spatial homogeneity; we can hope to estimate the expectation μ of Z with quite good precision. Others examples of second-order SRF's with finite non-null integral range are given in Lantuéjoul (2002).

2.2.2.2 Null integral range

Assume that $A = 0$. From Eq. (2.10), it stems that $\text{Var}[Z(V_n)] \underset{n \rightarrow \infty}{=} o(|V_n|^{-1})$: the variance $\text{Var}[Z(V_n)]$ decreases faster than $|V_n|^{-1}$. Even though this is an ideal framework, knowing A does not help controlling the variance of $Z(V_n)$. To cope with this liability, in some situations, Lantuéjoul (1991) proposes to consider the following relation:

$$\text{Var}[Z(V_n)] \approx \sigma^2 \frac{k}{|V_n|^\alpha}, \quad (2.16)$$

where $k \in (0, +\infty)$ and $\alpha > 1$.

Example 2.10 – *Gaussian RF with null integral range.* Let Z be a Gaussian second-order SRF with covariance function C defined, for any $\mathbf{h} \in \mathbb{R}^d$, by

$$C(\mathbf{h}) = \exp \left\{ -\frac{|\mathbf{h}|^2}{a^2} \right\} \left(1 - \frac{|\mathbf{h}|^2}{a^2} \right), \quad (2.17)$$

with scale parameter $a \in (0, +\infty)$. It can be shown that this RF, which has been proposed by [Lantuéjoul \(2002\)](#), has a null integral range A . A realization of Z is displayed in [Figure 2.2\(b\)](#); it gives a strong impression of spatial homogeneity.

2.2.2.3 Infinite integral range

From [Eq. \(2.10\)](#), $|V_n|^{-1} \underset{n \rightarrow \infty}{=} o(\text{Var}[Z(V_n)])$: the variance $\text{Var}[Z(V_n)]$ decreases more slowly than $|V|^{-1}$. In this case, the integral range cannot be used to control $\text{Var}[Z(V_n)]$ and if the decrease of the variance is too slow, we can only expect to estimate μ with a very poor precision. When appropriate, [Lantuéjoul \(1991\)](#) suggested taking $\alpha < 1$ in [Eq. \(2.16\)](#). This relation is satisfied, in particular, by second-order RF's based on boolean random closed sets built from Poisson varieties ([Jeulin, 2011](#)). It was used in practice by, e.g., [Dirrenberger et al. \(2014\)](#).

Example 2.11 – *Gaussian RF with infinite integral range.* Let Z be a Gaussian second-order SRF with hyperbolic covariance function C given, for any $\mathbf{h} \in \mathbb{R}^d$, by

$$C(\mathbf{h}) = \frac{a}{a + \|\mathbf{h}\|},$$

with scale parameter $a \in (0, +\infty)$. It is known that Z has an infinite integral range A (see [Lantuéjoul, 2002](#)). [Figure 2.2\(c\)](#) shows a realization of Z , when $a = 10$. It has been simulated with the R package `Randomfields`. At the scale of the simulation, the realization seems to be less homogeneous than the one in [Figure 2.2\(a\)](#).

Before presenting a method to estimate the integral range, we shall end this subsection with two remarks.

Remark 2.12 – *The mean ergodicity assumption.* The assumption of mean ergodicity is not necessary to define the concept of integral range. Even so, it is preferable to work under this assumption otherwise, by definition, the integral range would be infinite.

Remark 2.13 – *On the necessity to consider $V_n \uparrow \mathbb{R}^d$.* The example below is taken from [Lantuéjoul \(1991\)](#). Set $p < d$. The restriction of Z to \mathbb{R}^p is also second-order stationary and first-order ergodic; if the limit in [Eq. \(2.12\)](#) exists, its integral range is well-defined.

It is possible that it is finite whereas it is infinite when considering the whole space \mathbb{R}^d . This is the case, for instance, when the correlation function associated to Z is defined by

$$\rho(\mathbf{h}) = \frac{1}{1 + \|\mathbf{h}\|^2}$$

for any $\mathbf{h} \in \mathbb{R}^3$. It is easy to show that the integral range computed in \mathbb{R}^3 is infinite, whereas it is finite when Z is restricted to \mathbb{R} . Set $n \in \mathbb{N}$. One may be attempted to estimate the expectation μ by $Z(V_n)$, where $V_n \subset \mathbb{R}$ is a very long segment of length $r_n \in (0, +\infty)$. The variance $\text{Var}[Z(V_n)]$ thus behaves like $1/r_n$. Now, let V_n be a ball in \mathbb{R}^3 with large radius r_n . Since the integral range is infinite in \mathbb{R}^3 , the variance $\text{Var}[Z(V_n)]$ decreases more slowly than $1/r_n^3$. Its explicit calculus shows that it behaves like $1/r_n^2$, see e.g. [Matheron \(1965, pages 56-57\)](#) for the computation of the geometric covariogram of a 3-ball. Thus, the variance of $Z(V_n)$ decreases faster in the second case, when the integral is infinite, than in the first case when it is finite. Now, let $(V_n)_{n \in \mathbb{N}}$ be a sequence of sets in \mathcal{B} . As shown with this example, when Z is isotropic, we can expect $\text{Var}[Z(V_n)]$ to decrease faster (or at the same speed) when V_n grows in all directions than when it increases only in certain directions, as $n \rightarrow +\infty$. That is why we choose to consider sequences $(V_n)_{n \in \mathbb{N}}$ of subsets in \mathbb{R}^d such that $\bigcup_{n \in \mathbb{N}} V_n = \mathbb{R}^d$ in [Definition 2.3](#). We want to ensure that V_n grows in all directions, and ideally at the same rate, as $n \rightarrow +\infty$. Accordingly, with no loss of generality, we could also have worked with sequences of subsets that lie in the positive orthants substituing [\(ii\)](#) in [Definition 2.3](#) by $\bigcup_{n \in \mathbb{N}} V_n = \mathbb{R}_+^d$, but it seems unintuitive in a spatial context. This is sometimes done in a one-dimensional framework, typically when dealing with time processes, see e.g. [Yaglom \(1987, pages 218\)](#). The situation is more complicated when Z is anisotropic and it may sometimes be better, in this case, to work with sequences of subsets that grow only in the anisotropy directions. Since we mainly focus on isotropic applications in the following, this investigation is left for future research.

2.2.3 Estimation

Let Z be a second-order SRF defined on \mathbb{R}^d and recall from the last subsection that, if the limit exists, its integral range is defined by

$$A = \lim_{n \rightarrow +\infty} A_n,$$

where for any $n \in \mathbb{N}$

$$A_n = |V_n| \frac{\text{Var}[Z(V_n)]}{\sigma^2} > 0.$$

In this subsection, we propose an algorithm to estimate A , starting from a single realization z of Z on a fixed domain $V \subset \mathcal{B}$. This set is supposed large enough to ensure that

$$\text{Var}[Z(V)] \approx \sigma^2 \frac{A}{|V|}, \quad (2.18)$$

if A exists and is finite. It is inspired from the algorithm proposed in [Lantuéjoul \(2002\)](#). The advantage of our method is that it is more user-friendly: the visual clues to draw conclusions about A are more explicit. Very briefly, each algorithm consists in plotting a given quantity versus a sequence of volumes. In [Lantuéjoul \(2002\)](#), it must be verified whether the points associated to the largest volumes are ranged on a straight line with slope -1 or not. With our procedure, we only need to check whether the curve is stabilizing or not, as the volumes become larger. Since the aim of this section is not to compare these two procedures, we shall not go into more details and let the interested reader refer to [Lantuéjoul \(2002\)](#).

Set $N \in \mathbb{N}^*$ and consider an increasing sequence of measurable subdomains $(V_n)_{n \in \{1, \dots, N\}}$ in V , with positive volume. Suppose first that A exists. If $A < +\infty$ then, when plotting A_n versus $|V_n|$, the curve should stabilize around A , as n becomes large enough. On the contrary, if $A = +\infty$, the curve must keep increasing. When A does not exist, it should probably oscillate as n grows. Fix $n \in \{1, \dots, N\}$. In practice, A_n is unknown and an estimation of the latter shall be plotted instead. The question is thus: how to estimate A_n for each subdomain V_n ? This amounts to evaluating $\text{Var}[Z(V_n)]$ and σ^2 . Assume that V_n divides V , i.e. V can be decomposed into an union of $k_n \in \mathbb{N}^*$ disjoint subdomains $V_n^1, \dots, V_n^{k_n}$, all congruent to V_n . Though this assumption seems quite restrictive, it is actually easy to build such sequences when V is an hyperrectangle; it suffices to find a partition of smaller and congruent hyperrectangular domains. Then, estimators of $\text{Var}[Z(V_n)]$ and σ^2 are respectively

$$S^2(V_n|V) := \frac{1}{k_n} \sum_{i=1}^{k_n} [Z(V_n^i) - Z(V)]^2$$

and

$$S^2(\cdot|V) := \frac{1}{|V|} \int_V [Z(\mathbf{x}) - Z(V)]^2 d\mathbf{x},$$

with

$$E[S^2(V_n|V)] = \text{Var}[Z(V_n)] - \text{Var}[Z(V)] \quad (2.19)$$

and

$$E[S^2(\cdot|V)] = \sigma^2 - \text{Var}[Z(V)]. \quad (2.20)$$

These expectations are called *dispersion variances* in Geostatistic, see e.g. [Matheron \(1971\)](#). Recall now that Z is supposed to be ergodic in the mean. Hence, when V is very large relatively to V_n , the term $\text{Var}[Z(V)]$ can be neglected in [Eq. \(2.19\)](#) and [Eq. \(2.20\)](#), and the following approximation holds:

$$E[S^2(V_n|V)] \approx \text{Var}[Z(V_n)] \quad \text{and} \quad E[S^2(\cdot|V)] \approx \sigma^2. \quad (2.21)$$

In other words, $S^2(V_n|V)$ and $S^2(\cdot|V)$ can be considered as unbiased estimators of $\text{Var}[Z(V_n)]$ and σ^2 . In practice, the realization z of Z is not observed everywhere on V but only in some

locations, therefore only discretized version of $S^2(V_n|V)$ and $S^2(\cdot|V)$ can be computed. Suppose that z is known in $K \in \mathbb{N}^*$ fixed locations x_1, \dots, x_K . Further, define $\bar{Z} := \frac{1}{K} \sum_{j=1}^K Z(x_j)$ and, for any $i \in \{1, \dots, k_n\}$, let K_n^i stand for the number of observations in subdomain V_n^i . Discretized versions of $S^2(V_n|V)$ and $S^2(\cdot|V)$ are

$$S_K^2(V_n|V) = \frac{1}{k_n} \sum_{i=1}^{k_n} \left[\frac{1}{K_n^i} \sum_{\substack{j \in \{1, \dots, N\} \\ x_j \in V_n^i}} Z(x_j) - \bar{Z} \right]^2 \quad (2.22)$$

and

$$S_K^2(\cdot|V) = \frac{1}{K} \sum_{j=1}^K [Z(x_j) - \bar{Z}]^2. \quad (2.23)$$

Assume now that the locations x_1, \dots, x_K form a regular grid G such that the number of observations K_n^i is the same for any $i \in \{1, \dots, k_n\}$; it is denoted by K_n . The estimators (2.22) and (2.23) have expectations

$$E [S_K^2(V_n|V)] = \text{Var} \left[\frac{1}{K_n} \sum_{x \in V_n^1 \cap G} Z(x) \right] - \text{Var} [\bar{Z}] \quad (2.24)$$

and

$$E [S_K^2(\cdot|V)] = \sigma^2 - \text{Var} [\bar{Z}]. \quad (2.25)$$

Hence, similarly to the continuous version, when V is very large relatively to V_n , they can be considered as unbiased estimators of $\text{Var} \left[\frac{1}{K_n} \sum_{x \in V_n^1 \cap G} Z(x) \right]$ and σ^2 . In addition, when K is very large, *i.e.* G is a dense grid, we can expect $S_K^2(V_n|V)$ to be an approximately unbiased estimator of $\text{Var} [Z(V_n)]$. It would be interesting to investigate the asymptotic properties of such estimators when considering *e.g.* infill asymptotics inside increasing domains. This is not done in the present work but related questions are examined *e.g.* in [Lahiri et al. \(1999\)](#), when the grid is irregular. Finally, for any $n \in \{1, \dots, N\}$, we write \hat{A}_n the estimator of A_n resulting from [Eq. \(2.22\)](#) and [Eq. \(2.23\)](#). Before illustrating this method of estimation with the examples below, we shall make the following comment.

Remark 2.14 – *On the choice of V and subdomains V_n^i .* At the beginning of this subsection, we required V to be large enough so that, when A exists and is finite, [Eq. \(2.18\)](#) is satisfied. Since A is unknown, we do not know, in practice, how to choose V . Imagine now that, when plotting \hat{A}_n versus $|V_n|$, for every $n \in \{1, \dots, N\}$, a increasing curve is observed. This may signify that either A is infinite or that V is not large enough to observe the curve stabilizing. It could also mean that the assumption of second-order stationarity is not valid. In such a situation, the choice of taking V larger shall be made on a case by case basis, taking into account the underlying phenomenon of interest and the financial

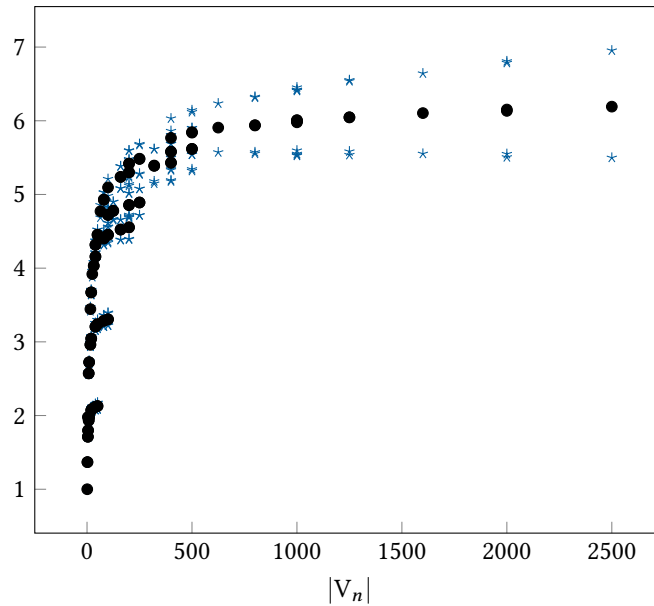


FIGURE 2.3 – The mean curve (black dots) and the corresponding 90% confidence envelope (blue stars) from Example 2.15. Several points lie on the same verticals; they correspond to rectangular subdomains with the same area but with different side lengths.

and technical constraints. We shall also make some general recommendations about the choice of the subdomains V_n . First, V shall be large with respect to the latter, so that the approximation (2.21) holds. At the same time, for any $n \in \{1, \dots, N\}$, the number k_n of subdomains V_n^i , which form a partition of V , as well as the number of observed locations $x_1, \dots, x_{k_n}^i$ in V_n^i must not be too small to compute the estimators $S_K^2(V_n|V)$ and $S_K^2(\cdot|V)$.

Example 2.15 – Finite non-null integral range. Let $d = 2$ and consider Z as in Example 2.9, with $a = 1$. By integrating the corresponding correlation function over \mathbb{R}^2 , it is easy to show that $A = 2\pi$. We generate 500 realizations of Z on a regular grid 1000×1000 , with unit mesh size. Then for each realization and for each $n \in \{1, \dots, N\}$, we estimate A_n with the previous algorithm. We constrain the sequence $(V_n)_{n \in \{1, \dots, N\}}$ so that each subdomain V_n is a rectangle with integer side lengths less than 100 and with $k_n \geq 30$. Figure 2.3 displays the mean curve obtained by averaging, for each $n \in \{1, \dots, N\}$, the 500 estimates \hat{A}_n . It also shows the corresponding 90% confidence envelopes built by computing, for each $n \in \{1, \dots, N\}$, the sample quantiles of order 0.05 and 0.95 of the 500 estimates \hat{A}_n . Notice that the three curves are stabilizing as $|V_n|$ increases, suggesting that the integral range is finite. Finally, the latter can be estimated, from a single realization, by the intercept of the linear regression model fitted only from the data $(|V_n|, \hat{A}_n)_{n \in \{1, \dots, N\}}$ for which $|V_n|$ is large enough. This is shown in Figure 2.4.

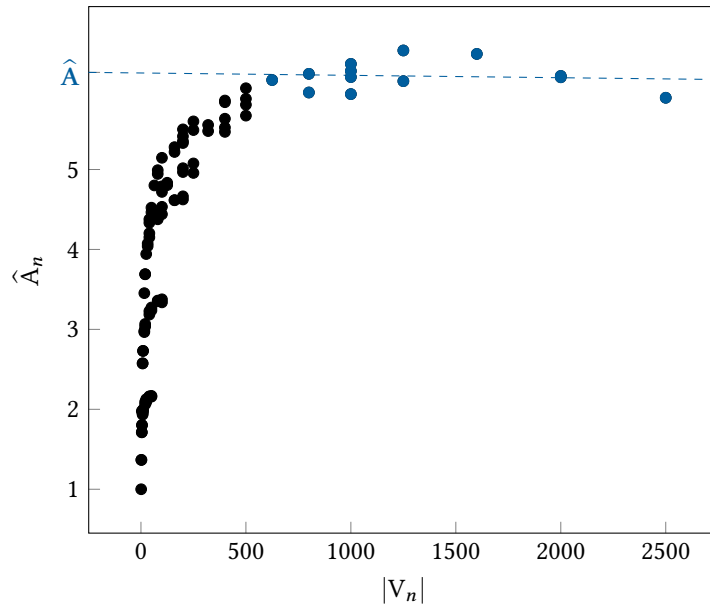


FIGURE 2.4 – The estimates \hat{A}_n as well as an estimate $\hat{A} = 6.215$ of the integral range $A = 2\pi$ computed from a single realization of the Gaussian process in [Example 2.15](#). The latter has been obtained by fitting a linear regression model (blue dashed line) from data lying strictly beyond threshold $|V_n| = 500$ (in blue).

Example 2.16 – Infinite integral range. Let $d = 2$ and consider Z as in [Example 2.11](#), with $a = 1$. It is easy to show that $A = +\infty$. We generate 500 realizations of Z on a regular grid 1000×1000 , with unit mesh size. Then, choosing the sequence $(V_n)_{n \in \{1, \dots, N\}}$ in the same way as in [Example 2.15](#), we estimate A_n with the previous algorithm for each realizations and for each $n \in \{1, \dots, N\}$. The curves displayed in [Figure 2.5](#) keep increasing as the volume $|V_n|$ grows, which is consistent with having $A = +\infty$.

Now, recall from [Eq. \(2.12\)](#) that the integral range can be written $\lim_{n \rightarrow +\infty} \int_{\mathbb{R}^d} \rho(\mathbf{h}) \frac{K_n(\mathbf{h})}{K_n(\mathbf{0})} d\mathbf{h}$, thus it is linked to the spatial dependence structure of the second-order SRF Z . When considering an appropriate max-stable RF, we expect it to be connected with the extremal coefficient function.

2.3 CONNECTING THE INTEGRAL RANGE WITH THE EXTREMAL COEFFICIENT FUNCTION

We shall now assume that Z is a simple max-stable SRF and write $\theta : \mathbb{R}^d \rightarrow [1, 2]$ its extremal coefficient function, which satisfies

$$\mathbf{P}[Z(\mathbf{0}) \leq z, Z(\mathbf{h}) \leq z] = \exp\left\{-\frac{\theta(\mathbf{h})}{z}\right\}$$

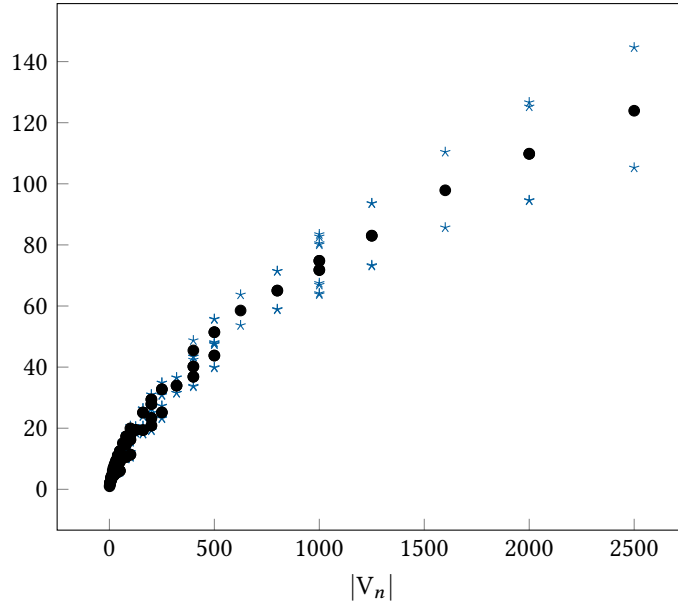


FIGURE 2.5 – The mean curve (black dots) and the corresponding 90% confidence envelope (blue stars) from Example 2.16.

for any $\mathbf{h} \in \mathbb{R}^d$ and any $z \in (0, +\infty)$, see Subsection 1.3.3. In addition, suppose that Z is continuous in probability; it admits the spectral representation given in Eq. (1.13). Notice that, by Lemma 2 in de Haan (1984), the associated spectral process Y is continuous in L^1 , therefore it is also continuous in probability. Hence, both Z and Y have a $(\mathcal{F} \otimes \mathcal{B}_{\mathbb{R}^d}, \mathcal{B}_{\mathbb{R}})$ -measurable modification; this is a known result from Doob (1990, Theorem 2.6). We shall point out that the proof is given for stochastic processes defined on \mathbb{R} but it can be generalized to higher dimensions. We also refer to Theorem 3.4 in Potthoff (2009) for a similar result when $d > 1$. That is why we additionally assume that both RF's Z and Y are $(\mathcal{F} \otimes \mathcal{B}_{\mathbb{R}^d}, \mathcal{B}_{\mathbb{R}})$ -measurable. As remarked in Subsection 1.3.3, the measurability of Y implies, in particular, that θ is $(\mathcal{B}_{\mathbb{R}^d}, \mathcal{B}_{\mathbb{R}})$ -measurable. More generally, Strokorb and Schlather (2015, Lemma 23) have shown that if Z is continuous in probability then θ is a continuous function.

As we pointed out in the first chapter, Z does not have finite expectation and variance; its integral range cannot be defined. In the next subsections, we consider instead the integral range of the indicator RF of Z above a threshold. This indicator field is stationary. It has finite first and second order moments, and satisfies both Assumption 2.1 and Assumption 2.2.

Set $z \in (0, +\infty)$ and let the SRF $\{I_z(\mathbf{x}) : \mathbf{x} \in \mathbb{R}^d\}$, referred to as the *exceedance field* in the sequel, be defined by

$$\forall \mathbf{x} \in \mathbb{R}^d \quad I_z(\mathbf{x}) := \mathbf{1}\{Z(\mathbf{x}) > z\}. \quad (2.26)$$

For any $\mathbf{x} \in \mathbb{R}^d$, the random variable $I_z(\mathbf{x})$ is Bernoulli-distributed with finite expectation $\mu_z := \mathbf{P}[Z(\mathbf{0}) > z] = 1 - \exp\{-1/z\}$ and variance $\sigma_z^2 := (1 - \exp\{-1/z\}) \exp\{-1/z\}$. For all $\mathbf{h} \in \mathbb{R}^d$, the covariance between $I_z(\mathbf{0})$ and $I_z(\mathbf{h})$ is given by

$$\text{Cov}[I_z(\mathbf{0}), I_z(\mathbf{h})] = \exp\{-\theta(\mathbf{h})/z\} - \exp\{-2/z\}, \quad (2.27)$$

with corresponding correlation function

$$\rho(\mathbf{h}, z) = \frac{\text{Cov}[I_z(\mathbf{0}), I_z(\mathbf{h})]}{\sqrt{\text{Var}[I_z(\mathbf{0})] \text{Var}[I_z(\mathbf{h})]}} = \frac{\exp\left\{\frac{2 - \theta(\mathbf{h})}{z}\right\} - 1}{\exp\{1/z\} - 1}. \quad (2.28)$$

Because $1 \leq \theta(\mathbf{h}) \leq 2$, the correlation function is valued in $[0, 1]$. From Eq. (2.27), we shall remark that an estimator of the covariance function $C_z : \mathbf{h} \in \mathbb{R}^d \rightarrow \text{Cov}[I_z(\mathbf{0}), I_z(\mathbf{h})]$ immediately provides an estimator of θ . This is used in Chapter 3 to propose a new non-parametric estimator of the ECF.

Now, for fixed $\mathbf{h} \in \mathbb{R}^d$, write $\rho_{\mathbf{h}}$ the map $z \in (0, +\infty) \mapsto \rho(\mathbf{h}, z) \in [0, 1]$. Alternatively, for fixed $z \in (0, +\infty)$, denote by ρ_z the function $\mathbf{h} \in \mathbb{R}^d \mapsto \rho(\mathbf{h}, z) \in [0, 1]$. The two following propositions exhibit the behavior of both functions.

Proposition 2.17 Let $z \in (0, +\infty)$. The map ρ_z is a continuous (thus measurable) nonnegative function.

Proposition 2.18 Let $\mathbf{h} \in \mathbb{R}^d$. The map $\rho_{\mathbf{h}}$ is a continuous (thus measurable) nonnegative and nondecreasing function with limits $\lim_{z \rightarrow 0} \rho_{\mathbf{h}}(z) = 1 \{\theta(\mathbf{h}) = 1\}$ and $\lim_{z \rightarrow +\infty} \rho_{\mathbf{h}}(z) = 2 - \theta(\mathbf{h})$.

We refer to Subsection 2.6.2 for both proofs. Now, let $V_n \uparrow \mathbb{R}^d$ and consider the integral range associated with I_z , given by

$$A_z := \lim_{n \rightarrow +\infty} A_{z,n}, \quad (2.29)$$

where, for every $n \in \mathbb{N}$,

$$A_{z,n} := |V_n| \frac{\text{Var}[I_z(V_n)]}{\sigma_z^2}. \quad (2.30)$$

According to the last subsection, if A_z is finite and nonzero, then the exceedance probability $\mathbf{P}[Z(\mathbf{0}) > z]$ can be estimated from a single realization of I_z , with a chosen precision that depends on the domain V_n of observation, $n \in \mathbb{N}$. This may be of great interest for insurance companies that want to assess some risks, e.g. the risk of flood at a given location. In addition, ρ_z is nonnegative for every $z \in (0, +\infty)$: when the integral range is finite, this means that the latter converges fast enough to 0 to be integrable.

For any $z \in (0, +\infty)$, we are thus interested in situations where the integral range A_z is finite. The latter is linked to the correlation function of I_z and so is θ . In the next subsection, we give a condition on the ECF so that A_z is finite.

2.3.1 Main results

The next theorem establishes necessary and sufficient conditions on the extremal coefficient function of Z so that the integral range A_z is finite.

Theorem 2.19 – *Finite integral equivalence.* Let Z be a simple max-stable SRF with extremal coefficient function θ and, for any $z \in (0, +\infty)$, denote by A_z the integral range of the associated exceedance field I_z . The following assertions are equivalent:

- (i) $\exists z \in (0, +\infty) \quad A_z < +\infty,$
- (ii) $\forall z \in (0, +\infty) \quad A_z < +\infty,$
- (iii) $A_\infty := \int_{\mathbb{R}^d} 2 - \theta(\mathbf{h}) \, d\mathbf{h} < +\infty.$

If these conditions are fulfilled, the mapping $z \in (0, +\infty) \mapsto A_z \in [0, +\infty)$ is continuous and nondecreasing with $\lim_{z \rightarrow 0} A_z = 0$ and $\lim_{z \rightarrow +\infty} A_z = A_\infty$.

We refer to [Subsection 2.6.3](#) for the proof. The implication (iii) \Rightarrow (ii), is mentioned in [Spodarev \(2014, page 11\)](#), when substituting A_z by $\int_{\mathbb{R}^d} \rho_z(\mathbf{h}) \, d\mathbf{h}$ in (ii). In a slightly different form, this statement is also proven in [Koch \(2017, Theorem 3\)](#), in a spatial risk context, but again without referring to the concept of the integral range. As a consequence, the proofs are completely different; our proof being, for instance, shorter. We refer to [Subsection 2.4.2](#) for more details.

From [Lemma 2.38](#), we know that, for any $z \in (0, +\infty)$,

$$A_z = \int_{\mathbb{R}^d} \rho(\mathbf{h}, z) \, d\mathbf{h}. \quad (2.31)$$

Recall now from [Chapter 1](#) that $2 - \theta$ is, in some sense, an extreme values analogue of the correlation function. Thus, assertion (iii) is not surprising. For some models, the latter is easy to check. For instance, if $\theta(\mathbf{h})$ is bounded above by a constant strictly less than 2 then (iii) is not satisfied. It is also sometimes possible to bound above $\int_{\mathbb{R}^d} 2 - \theta(\mathbf{h}) \, d\mathbf{h}$ by a finite quantity. We refer to [Subsection 2.3.2](#) for specific examples. In the particular case of Moving Maxima processes (M2 processes), we found a necessary and sufficient condition so that $\int_{\mathbb{R}^d} 2 - \theta(\mathbf{h}) \, d\mathbf{h} < +\infty$. First, let us introduce such RF's.

Definition 2.20 – *M2 processes*. Let Z be a SRF defined on \mathbb{R}^d . It is called a M2 process if

$$\forall \mathbf{x} \in \mathbb{R}^d \quad Z(\mathbf{x}) = \max_{(T,S) \in \Pi} T f(\mathbf{x} - S), \quad (2.32)$$

where Π is a Poisson process on $(0, +\infty) \times \mathbb{R}^d$ with intensity $t^{-2} dt ds$ and $f : \mathbb{R}^d \rightarrow \mathbb{R}_+$ is the so-called (deterministic) *shape function*, which is measurable, nonnegative and satisfies $\int_{\mathbb{R}^d} f(\mathbf{x}) d\mathbf{x} = 1$. Its ECF is then given by

$$\theta(\mathbf{h}) = \int_{\mathbb{R}^d} \max(f(\mathbf{y}), f(\mathbf{y} + \mathbf{h})) d\mathbf{y},$$

see e.g. [Schlather and Tawn \(2003, Equation 9\)](#).

Any M2 process is a simple max-stable SRF, see [Schlather \(2002, Theorem 1\)](#). As remarked in [Subsection 1.3.2](#), $Tf(\mathbf{x} - S)$ may be interpreted as the amount of rainfall at position \mathbf{x} from a storm of magnitude T and shape f ; the storm being additionally centred in S . That is why such a process is sometimes also called *storm process* and its shape function f is referred to as a storm. Let us also recall the next standard definition.

Definition 2.21 Let Σ be a symmetric and positive-semidefinite $d \times d$ matrix, and consider the norm $\|\cdot\|_{\Sigma}$ associated with the inner product induced by the matrix Σ , i.e. $\|\mathbf{h}\|_{\Sigma} = \sqrt{\mathbf{h}^T \Sigma \mathbf{h}}$, where \mathbf{h}^T designates the transpose of \mathbf{h} . A function $f : \mathbb{R}^d \rightarrow \mathbb{R}_+$ is said to be Σ -radially symmetric and non-increasing if $f(\mathbf{x}) = f_0(\|\mathbf{x}\|_{\Sigma})$ for every $\mathbf{x} \in \mathbb{R}^d$, where the map $f_0 : \mathbb{R}_+ \rightarrow \mathbb{R}_+$ is non-increasing. When Σ is the identity matrix, f is simply said to be radially symmetric and non-increasing.

Let Z be a M2 process with Σ -radially symmetric and non-increasing shape function f . The following corollary gives a necessary and sufficient condition on Z so that the integral range A_z of the corresponding exceedance field is finite.

Corollary 2.22 Let Z be a M2 process on \mathbb{R}^d and A_z be the integral range of the corresponding exceedance field above a threshold $z \in (0, +\infty)$. Let also Σ be a symmetric and positive-semidefinite $d \times d$ matrix, and $X = (X_1, \dots, X_d) \sim f$, where f is the associated shape function in [Eq. \(2.32\)](#). If f is Σ -radially symmetric and non-increasing, then the following propositions are equivalent

- (i) $\forall z \in (0, +\infty) \quad A_z < +\infty,$
- (ii) $E\{\|X\|^d\} < +\infty,$
- (iii) $\forall i \in \{1, \dots, d\} \quad E[|X_i|^d] < +\infty.$

In addition, when Σ is the identity matrix,

$$A_\infty := \int_{\mathbb{R}^d} 2 - \theta(\mathbf{h}) d\mathbf{h} = 2 \omega_d E\{\|X\|^d\}.$$

We refer to [Subsection 2.6.3](#) for the proof and to [Subsection 2.3.2](#) for specific examples. Additionally, from [Dombry and Eyi-Minko \(2012, page 3798\)](#), we know that a necessary condition for A_z to be finite is

$$\limsup_{\|\mathbf{h}\| \rightarrow +\infty} \frac{\ln(f(\mathbf{h}))}{\ln(\|\mathbf{h}\|)} < -k_d,$$

with $k_1 = 3$ and $k_d = 2(d+1)$ for $d \geq 2$. Before going further, let us make the following remark.

Remark 2.23 – Null integral ranges. If there exists $z \in (0, +\infty)$ such that $A_z = 0$ then, for all $z \in (0, +\infty)$, $A_z = 0$. Indeed, let $z \in (0, +\infty)$ and assume that $A_z = 0$. From [Eq. \(2.31\)](#), this is equivalent to $\rho(\mathbf{h}, z) = 0$ for almost every $\mathbf{h} \in \mathbb{R}^d$, i.e. $\theta(\mathbf{h}) = 2$ for almost every $\mathbf{h} \in \mathbb{R}^d$. The last equality does not depend on z and implies that $A_z = 0$ for all $z \in (0, +\infty)$.

We can also deduce ergodic and mixing properties of Z from condition [\(iii\)](#) in [Theorem 2.19](#). Let $Z = (Z(x))_{x \in \mathbb{R}^d}$ be a SRF. The definitions of the classical notions of ergodicity and mixing for Z are given below; both formulations are employed e.g. in [Kabluchko and Schlather \(2010, Definition 2.1\)](#) in the one-dimensional case or in [Bradley \(1993a, page 1921\)](#) and [Wang et al. \(2013, page 216\)](#) when extending to the multidimensional case. An equivalent definition, which gives conditions on the σ -field of invariants sets, can be sometimes found in the literature, see e.g. [Cressie \(1993, page 54\)](#) or [Adler \(1981, page 143\)](#).

Definition 2.24 – Ergodic property. Let $m, p \in \mathbb{N}^*$ and $V_n \uparrow \mathbb{R}^d$. The SRF Z is called ergodic if

$$\begin{aligned} \lim_{n \rightarrow +\infty} \frac{1}{|V_n|} \int_{V_n} \mathbf{P}[(Z(\mathbf{x}_1), \dots, Z(\mathbf{x}_m)) \in A, (Z(\mathbf{y}_1 + \mathbf{h}), \dots, Z(\mathbf{y}_p + \mathbf{h})) \in B] d\mathbf{h} \\ = \mathbf{P}[(Z(\mathbf{x}_1), \dots, Z(\mathbf{x}_m)) \in A] \mathbf{P}[(Z(\mathbf{y}_1), \dots, Z(\mathbf{y}_p)) \in B], \end{aligned} \quad (2.33)$$

for any $\mathbf{x}_1, \dots, \mathbf{x}_m, \mathbf{y}_1, \dots, \mathbf{y}_p \in \mathbb{R}^d$ and any Borel sets $A \subset \mathbb{R}^m$ and $B \subset \mathbb{R}^p$.

The ergodic property means that the event $\{(Z(\mathbf{x}_1), \dots, Z(\mathbf{x}_m)) \in A\}$ and the event $\{(Z(\mathbf{y}_1 + \mathbf{h}), \dots, Z(\mathbf{y}_p + \mathbf{h})) \in B\}$ become, on spatial average, asymptotically independent.

Remark 2.25 If Z has finite second order moments and satisfies [Eq. \(2.33\)](#) then it is ergodic in the mean. This is a consequence of the von Neumann's mean ergodic theorem extended to \mathbb{R}^d , see [Wiener \(1939\)](#) or [Dunford \(1939a,b\)](#).

The mixing property defined next is a stronger notion of asymptotic independence.

Definition 2.26 – *Mixing property.* Let $m, p \in \mathbb{N}^*$ and $\mathbf{h} \in \mathbb{R}^d$. The SRF Z is called mixing if

$$\begin{aligned} \lim_{\|\mathbf{h}\| \rightarrow +\infty} \mathbf{P}[(Z(\mathbf{x}_1), \dots, Z(\mathbf{x}_m)) \in A, (Z(\mathbf{y}_1 + \mathbf{h}), \dots, Z(\mathbf{y}_p + \mathbf{h})) \in B] \\ = \mathbf{P}[(Z(\mathbf{x}_1), \dots, Z(\mathbf{x}_m)) \in A] \mathbf{P}[(Z(\mathbf{y}_1), \dots, Z(\mathbf{y}_p)) \in B], \end{aligned}$$

for any $\mathbf{x}_1, \dots, \mathbf{x}_m, \mathbf{y}_1, \dots, \mathbf{y}_p \in \mathbb{R}^d$ and any Borel set $A \subset \mathbb{R}^n$ and $B \subset \mathbb{R}^m$.

Remark 2.27 As mentioned above, mixing is a stronger notion of asymptotically independence than ergodicity: if Z is mixing then it is ergodic too. This can easily be established like in the proof of the Cesàro mean convergence theorem.

Remark 2.28 Let Z be a SRF. If Z is mixing (resp. ergodic) then I_z is mixing (resp. ergodic) too, for any $z \in (0, +\infty)$.

In a one-dimensional framework ($d = 1$), ergodic and mixing properties of max-stable SRF's have been studied extensively by [Stoev \(2008, 2010\)](#), [Kabluchko \(2009\)](#) and [Kabluchko and Schlather \(2010\)](#). It has been shown that such properties can be characterized by some conditions on the extremal coefficient function, see e.g. Theorem 3.1 and 3.2 in [Kabluchko and Schlather \(2010\)](#). It seems that these results can be generalized to higher dimensions ($d > 1$). This is done in [Wang et al. \(2013\)](#) for ergodicity, and this is claimed by [Dombry and Kabluchko \(2017\)](#) for both ergodic and mixing properties. However, the proof of the extension to higher dimensions is not provided in the paper.

Theorem 2.29 – [Stoev \(2008\)](#), [Kabluchko and Schlather \(2010\)](#). Let Z be a simple max-stable SRF on \mathbb{R}^d with extremal coefficient function θ and $V_n \uparrow \mathbb{R}^d$. The following two propositions hold :

- (i) Z is ergodic if and only if $\lim_{n \rightarrow +\infty} \frac{1}{|V_n|} \int_{V_n} 2 - \theta(\mathbf{h}) d\mathbf{h} = 0$,
- (ii) Z is mixing if and only if $\lim_{\|\mathbf{h}\| \rightarrow +\infty} 2 - \theta(\mathbf{h}) = 0$.

First, notice that

$$\lim_{\|\mathbf{h}\| \rightarrow +\infty} 2 - \theta(\mathbf{h}) = 0 \Rightarrow \lim_{n \rightarrow +\infty} \frac{1}{|V_n|} \int_{V_n} 2 - \theta(\mathbf{h}) d\mathbf{h} = 0,$$

which is coherent with [Remark 2.25](#). The second proposition in [Theorem 2.29](#) is not surprising. Indeed, $\lim_{\|\mathbf{h}\| \rightarrow +\infty} \theta(\mathbf{h}) = 2$ means that the margins $Z(\mathbf{0})$ and $Z(\mathbf{h})$ are asymptotically independent. Now, from [Resnick \(1987, Corollary 5.25\)](#), the margins of Z are pairwise independent if and only if, for any $n \in \mathbb{N}^*$ and any $\mathbf{x}_1, \dots, \mathbf{x}_n \in \mathbb{R}^d$, the random variables $Z(\mathbf{x}_1), \dots, Z(\mathbf{x}_n)$

are mutually independent. Hence, some properties of the finite-dimensional distributions of Z can be characterized in term of θ . However, contrary to the correlation function of a Gaussian RF, we shall stress that the ECF does not determine the law of Z .

The two propositions in [Theorem 2.29](#) help deduce ergodic and mixing properties from [Theorem 2.19](#). Let Z be as in [Theorem 2.19](#) and assume that the conditions [\(i\)-\(iii\)](#) are fulfilled. In particular, [\(iii\)](#) implies that

$$\lim_{n \rightarrow +\infty} \frac{1}{|V_n|} \int_{V_n} 2 - \theta(\mathbf{h}) d\mathbf{h} = 0,$$

i.e. Z is ergodic and therefore so is I_z for any $z \in (0, +\infty)$. Furthermore, if we assume that

$\lim_{\|\mathbf{h}\| \rightarrow +\infty} \theta(\mathbf{h})$ exists then [\(iii\)](#) also gives

$$\lim_{\|\mathbf{h}\| \rightarrow +\infty} 2 - \theta(\mathbf{h}) = 0, \tag{2.34}$$

i.e. Z is mixing and thus so is I_z , $z \in (0, +\infty)$. This last implication can be proven in the same way as the one in [Eq. \(2.15\)](#). Similarly to the Gaussian case, a finite integral range A_z is thus a stronger condition than the ergodic and mixing properties.

In addition, proposition [\(ii\)](#) in [Theorem 2.29](#) also helps show the following result.

Proposition 2.30 – *Mixing and mean-ergodicity properties.* Set $z \in (0, +\infty)$ and let Z be an isotropic and simple max-stable SRF on \mathbb{R}^d , with extremal coefficient function θ . If $\lim_{\|\mathbf{h}\| \rightarrow +\infty} \theta(\mathbf{h})$ exists then I_z is mean-ergodic if and only if Z is mixing.

This proposition modestly generalizes Corollary 3 in [Koch \(2017\)](#), who obtains this result when Z is defined on \mathbb{R}^2 . To prove this result, we have also extended Corollary 1 in [Koch \(2017\)](#), which only involves disks or squares, to more general sets. Both proofs are deferred to [Subsection 2.6.4](#). As it is noticed in [Koch \(2017\)](#), under the conditions of [Proposition 2.30](#), Z (or I_z) is mixing if and only if it is ergodic. This equivalence may be retrieved using [Theorem 2.29](#). We shall now give some examples of max-stable SRF's that satisfy or not the conditions in [Theorem 2.19](#).

2.3.2 Examples

To illustrate [Theorem 2.19](#) we provide several well-known models of simple max-stable SRF's that either satisfy or do not satisfy the conditions [\(i\)-\(iii\)](#). Realizations of such processes are shown in [Figure 2.6](#).

Example 2.31 – Smith process. The Smith process was first considered by [Smith \(1990\)](#). It is a stationary M2 process with shape function f satisfying $f(\mathbf{x}) = \varphi_{\Sigma, d}(\mathbf{x})$ for any $\mathbf{x} \in \mathbb{R}^d$, where $\varphi_{\Sigma, d}$ stands for the density function of a centred Gaussian d -variate vector with covariance matrix Σ . When Σ is the identity matrix, the density function is simply denoted by φ_d , and by φ in the unidimensional case. For any $\mathbf{h} \in \mathbb{R}^d$, the ECF is thus given by (see Eq. 3.1 in [Smith, 1990](#))

$$\theta(\mathbf{h}) = 2\Phi\left(\frac{\|\mathbf{h}\|_{\Sigma^{-1}}}{2}\right),$$

where Φ corresponds to the standard normal cumulative distribution function. It follows that

$$\begin{aligned} 0 \leq \int_{\mathbb{R}^d} 2 - \theta(\mathbf{h}) \, d\mathbf{h} &= 2 \int_{\mathbb{R}^d} \int_{\mathbb{R}_+} \varphi(t) \mathbf{1}\{2t \geq \|\mathbf{h}\|_{\Sigma^{-1}}\} \, dt d\mathbf{h} \\ &= 2 \int_{\mathbb{R}_+} \varphi(t) \int_{\mathbb{R}^d} \mathbf{1}\{2t \geq \|\mathbf{h}\|_{\Sigma^{-1}}\} \, d\mathbf{h} dt, \end{aligned}$$

where the last equality is a consequence of Fubini-Tonelli theorem. Since all norms are equivalent in \mathbb{R}^d , there exists $C \in (0, +\infty)$ such that, for every $\mathbf{h} \in \mathbb{R}^d$, $\|\mathbf{h}\|_{\Sigma^{-1}} \geq C\|\mathbf{h}\|$. Thus,

$$\int_{\mathbb{R}^d} \mathbf{1}\{2t \geq \|\mathbf{h}\|_{\Sigma^{-1}}\} \, d\mathbf{h} \leq \int_{\mathbb{R}^d} \mathbf{1}\{2t \geq C\|\mathbf{h}\|\} \, d\mathbf{h}. \quad (2.35)$$

Switching to hyperspherical coordinates in the integral on the right hand side, [Eq. \(2.35\)](#) becomes

$$\int_{\mathbb{R}^d} \mathbf{1}\{2t \geq \|\mathbf{h}\|_{\Sigma^{-1}}\} \, d\mathbf{h} \leq \omega_d \left(\frac{2t}{C}\right)^d,$$

where ω_d represents the volume of the unit d -ball. Consequently,

$$0 \leq \int_{\mathbb{R}^d} 2 - \theta(\mathbf{h}) \, d\mathbf{h} \leq \frac{2^{d+1}\omega_d}{C^d} \int_{\mathbb{R}_+} t^d \varphi(t) \, dt < +\infty, \quad (2.36)$$

since φ is even and all moments of a standard Gaussian random variable are finite. The assumption [\(iii\)](#) in [Theorem 2.19](#) is thus satisfied by a Smith process. Observe that, when Σ equals the identity matrix I_d , [Eq. \(2.36\)](#) becomes

$$\int_{\mathbb{R}^d} 2 - \theta(\mathbf{h}) \, d\mathbf{h} = 2^{d+1}\omega_d \int_{\mathbb{R}_+} t^d \varphi(t) \, dt = 4(2\pi)^{\frac{d}{2}} \frac{\Gamma(d)}{d \left[\Gamma\left(\frac{d}{2}\right)\right]^2}, \quad (2.37)$$

where Γ stands for the Gamma distribution. Since f is Σ^{-1} -radially symmetric and non-increasing, all these results can also be retrieved from [Corollary 2.22](#).

Example 2.32 – M2 process with Cauchy density shape function. Let Z be an isotropic stationary M2 process defined on \mathbb{R}^d , where the shape function f is the multivariate

Cauchy density function with location vector $m = \mathbf{0}$ and scale matrix Σ ; it is symmetric and positive-semidefinite. Precisely, for every $\mathbf{h} \in \mathbb{R}^d$,

$$f(\mathbf{h}) = \left[\Gamma\left(\frac{1}{2}\right) \pi^{\frac{d}{2}} \sqrt{\det(\Sigma)} \right]^{-1} \frac{\Gamma\left(\frac{d+1}{2}\right)}{\left[\pi \left(1 + \|\mathbf{h}\|_{\Sigma^{-1}}^2\right) \right]^{\frac{d+1}{2}}}, \quad (2.38)$$

where $\det(\Sigma)$ denotes the determinant of Σ . Let $X \sim f$ and denote by X^T its transpose. It is known that, for any $\mathbf{h} \in \mathbb{R}^d$, the random variable $X^T \mathbf{h}$ is distributed according to an univariate Cauchy distribution, see e.g. [Lee et al. \(2014, Theorem 1\)](#). In the same way, the bivariate distribution of a Smith process is calculated in [Smith \(1990, Equation 3.1\)](#). It can be found that, for any $\mathbf{h} \in \mathbb{R}^d$,

$$\theta(\mathbf{h}) = 2G\left(\frac{\|\mathbf{h}\|_{\Sigma^{-1}}}{2}\right),$$

where G stands for the c.d.f. of a standard Cauchy distribution, see [Subsection 2.6.5](#) for the proof. Let $g : x \in \mathbb{R} \mapsto [\pi(1+x^2)]^{-1}$ be the associated density function, and contrary to the previous example, consider $C \in (0, +\infty)$ such that $\|\mathbf{h}\|_{\Sigma^{-1}} \leq C\|\mathbf{h}\|$ for every $\mathbf{h} \in \mathbb{R}^d$. Then,

$$0 \leq \frac{2^{d+1}\omega_d}{C^d} \int_{\mathbb{R}_+} t^d g(t) dt \leq \int_{\mathbb{R}^d} 2 - \theta(\mathbf{h}) d\mathbf{h}. \quad (2.39)$$

The integral on the left hand side is infinite, thus so is that on the right hand side. As a result, assumption [\(iii\)](#) in [Theorem 2.19](#) is not fulfilled by the max-stable SRF Z . Again, since f is Σ^{-1} -radially symmetric and non-increasing, this result can also be established from [Corollary 2.22](#). Notice however that, since $\theta(\mathbf{h}) \rightarrow 2$ as $\|\mathbf{h}\| \rightarrow +\infty$, Z is mixing according to [Theorem 2.29](#). More generally, it is known from [Dombry and Kabluchko \(2017, Theorem 3\)](#) that any M2 process with locally bounded sample paths is mixing.

Example 2.33 – Extremal Gaussian process. Introduced first by [Schlather \(2002\)](#), the extremal Gaussian process is a simple max-stable SRF where the spectral process Y in [Eq. \(1.13\)](#) is given by

$$\forall \mathbf{x} \in \mathbb{R}^d \quad Y(\mathbf{x}) = \sqrt{\frac{\pi}{2}} \max(0, W(\mathbf{x})),$$

where W is a Gaussian SRF with standard Gaussian margins and correlation function ρ . For any $\mathbf{h} \in \mathbb{R}^d$, the ECF is thus given by (see e.g. [Schlather and Tawn, 2003](#))

$$\theta(\mathbf{h}) = 1 + \sqrt{\frac{1 - \rho(\mathbf{h})}{2}}.$$

Recall now that ρ is a positive-semidefinite function. If it is isotropic, then $\rho(\mathbf{h}) \geq -1/d$ for any $\mathbf{h} \in \mathbb{R}^d$ (see [Matérn, 1986](#), page 13). Thus, when $d > 1$, we obtain that

$$\forall \mathbf{h} \in \mathbb{R}^d \quad \theta(\mathbf{h}) \leq 1 + \sqrt{\frac{d+1}{2d}} < 2. \quad (2.40)$$

Hence, according to [Theorem 2.29](#), the extremal Gaussian process is neither mixing nor ergodic. In addition, [\(i\)-\(iii\)](#) are not satisfied. From [Eq. \(2.27\)](#), we could also have remarked that

$$\text{Var} [I_z(V_n)] = \frac{1}{|V_n|^2} \int_{\mathbb{R}^d} K_n(\mathbf{h}) (\exp\{-\theta(\mathbf{h})/z\} - \exp\{-2/z\}) d\mathbf{h},$$

for any $z \in (0, +\infty)$. Since $\int_{\mathbb{R}^d} K_n(\mathbf{h}) d\mathbf{h} = |V_n|^2$, it follows from [Eq. \(2.40\)](#) that

$$\text{Var} [I_z(V_n)] \geq \exp\{-c/z\} - \exp\{-2/z\} > 0,$$

where $c = 1 + \sqrt{\frac{d+1}{2d}}$. Thus, I_z is not mean-ergodic, neither is Z , which is ultimately not mixing. We shall remark that, under some conditions, [Proposition 2.42](#) gives an expression for $\lim_{n \rightarrow +\infty} \text{Var} [I_z(V_n)]$.

Example 2.34 – *Brown-Resnick processes*. First introduced by [Brown and Resnick \(1977\)](#) and then generalized by [Kabluchko et al. \(2009\)](#), the Brown-Resnick process is a simple max-stable SRF where the spectral process Y in [Eq. \(1.13\)](#) is given by

$$\forall \mathbf{x} \in \mathbb{R}^d \quad Y(\mathbf{x}) = \exp \left\{ W(\mathbf{x}) - \frac{\sigma_W^2(\mathbf{x})}{2} \right\}, \quad (2.41)$$

where $(W(\mathbf{x}))_{\mathbf{x} \in \mathbb{R}^d}$ is an intrinsically Gaussian RF such that $E[Y(\mathbf{x})] = 0$ and $\sigma_W^2(\mathbf{x}) = \text{Var} [W(\mathbf{x})]$ for all $\mathbf{x} \in \mathbb{R}^d$. Its distribution depends only on its semivariogram defined by

$$\forall \mathbf{x}, \mathbf{h} \in \mathbb{R}^d \quad \gamma(\mathbf{h}) = \frac{1}{2} \text{Var} [W(\mathbf{x} + \mathbf{h}) - W(\mathbf{x})]. \quad (2.42)$$

For every $\mathbf{h} \in \mathbb{R}^d$, the ECF is thus equal to

$$\theta(\mathbf{h}) = 2\Phi \left(\sqrt{\frac{\gamma(\mathbf{h})}{2}} \right),$$

where Φ still denotes the cumulative distribution function of the standard normal distribution (see [Kabluchko et al., 2009](#), page 2063). Hence, if γ is bounded above by a constant $c < +\infty$ then so is θ by a constant $\tilde{c} < 2$. Then, like in the previous example, for any $z \in (0, +\infty)$ the excess RF I_z is not mean-ergodic and Z is neither mixing nor ergodic. In addition, [\(i\)-\(iii\)](#) are not satisfied. This is the case for the so-called *geometric Gaussian process* (see e.g. [Davison et al., 2012](#)) where W is a stationary Gaussian RF with variance

$\text{Var}[W(\mathbf{x})] = \sigma_W^2 < +\infty$, for any $\mathbf{x} \in \mathbb{R}^d$. According to Eq. (1.17), θ is then bounded above by $2\Phi(\sigma_W/2) < 2$. On the contrary, if $\lim_{\|\mathbf{h}\| \rightarrow +\infty} \gamma(\mathbf{h}) = +\infty$ then $\lim_{\|\mathbf{h}\| \rightarrow +\infty} \theta(\mathbf{h}) = 2$, i.e. Z is mixing. Further, Dombry and Kabluchko (2018, Example 11) remark that (iii) is satisfied provided that the following condition is met:

$$\liminf_{\|\mathbf{h}\| \rightarrow +\infty} \frac{\gamma(\mathbf{h})}{\ln(\|\mathbf{h}\|)} > 4d.$$

We try next to recover the behaviour of the integral ranges A_z , for $z \in (0, +\infty)$, of these max-stable SRF's, using the estimation method proposed in Subsection 2.2.3.

2.3.3 Illustrations

Set $d = 2$ and consider the following max-stable SRF's, some realizations of which are displayed in Figure 2.6:

- (i) a Smith process with shape function φ_2 ;
- (ii) a M2 process with Cauchy density shape function as in Eq. 2.32;
- (iii) an extremal Gaussian process with $\rho(\mathbf{h}) = \exp\{-\|\mathbf{h}\|\}$, for any $\mathbf{h} \in \mathbb{R}^2$;
- (iv) a geometric Gaussian process where the semivariogram γ in Eq. (2.42) satisfies $\gamma(\mathbf{h}) = 1 - \exp\{-\sqrt{\|\mathbf{h}\|}\}$, for any $\mathbf{h} \in \mathbb{R}^2$. This corresponds to a stable covariance function with parameter $\alpha = 1/2$.

Each of these processes is simulated 200 times on a regular grid 1500×1500 with unit mesh size, see Remark 2.36 for more details on the simulation algorithms. Let the thresholds z_1 and z_2 be equal to the median and the third quartile of a unit Fréchet distribution, respectively. That is $z_1 \approx 1.44$ and $z_2 \approx 3.48$. For any simulation of the max-stable SRF, the exceedance fields I_{z_1} and I_{z_2} are then computed. Let V be a 1500×1500 square and, as in Example 2.15 and Example 2.16, set $N \in \mathbb{N}^*$ such that all the domains of the sequence $(V_n)_{n \in \{1, \dots, N\}}$, which divide V , are rectangles with (integer) side lengths less than 150 and with $k_n \geq 30$. For $n \in \{1, \dots, N\}$, the quantities $A_{z_1, n}$ and $A_{z_2, n}$ are finally evaluated using the method proposed in Subsection 2.2.3. The left graphics in Figure 2.7 and Figure 2.9 display the mean curve obtained by avering the 200 estimates $\hat{A}_{z_1, n}$, for each $n \in \{1, \dots, N\}$. It also shows the corresponding 90% confidence envelope built by computing, for each $n \in \{1, \dots, N\}$, the sample quantiles of order 0.05 and 0.95 of the 200 estimates $\hat{A}_{z_1, n}$. The same information is shown in the right graphics when considering the threshold z_2 . Figure 2.7 is consistent with the expected results. The stabilization of the curves in Figure 2.7(a) suggests that the integral ranges A_{z_1} and A_{z_2} are finite for the Smith process, with $A_{z_1} \leq A_{z_2}$. Notice also that, as anticipated, the mean curves for both thresholds z_1 and z_2 are lower than the limits $A_\infty : \int_{\mathbb{R}^d} 2 - \theta(\mathbf{h}) d\mathbf{h} = 4\pi$ (see Eq. (2.37)). In Figure 2.7(b), the increasing curves indicate that they are possibly infinite for

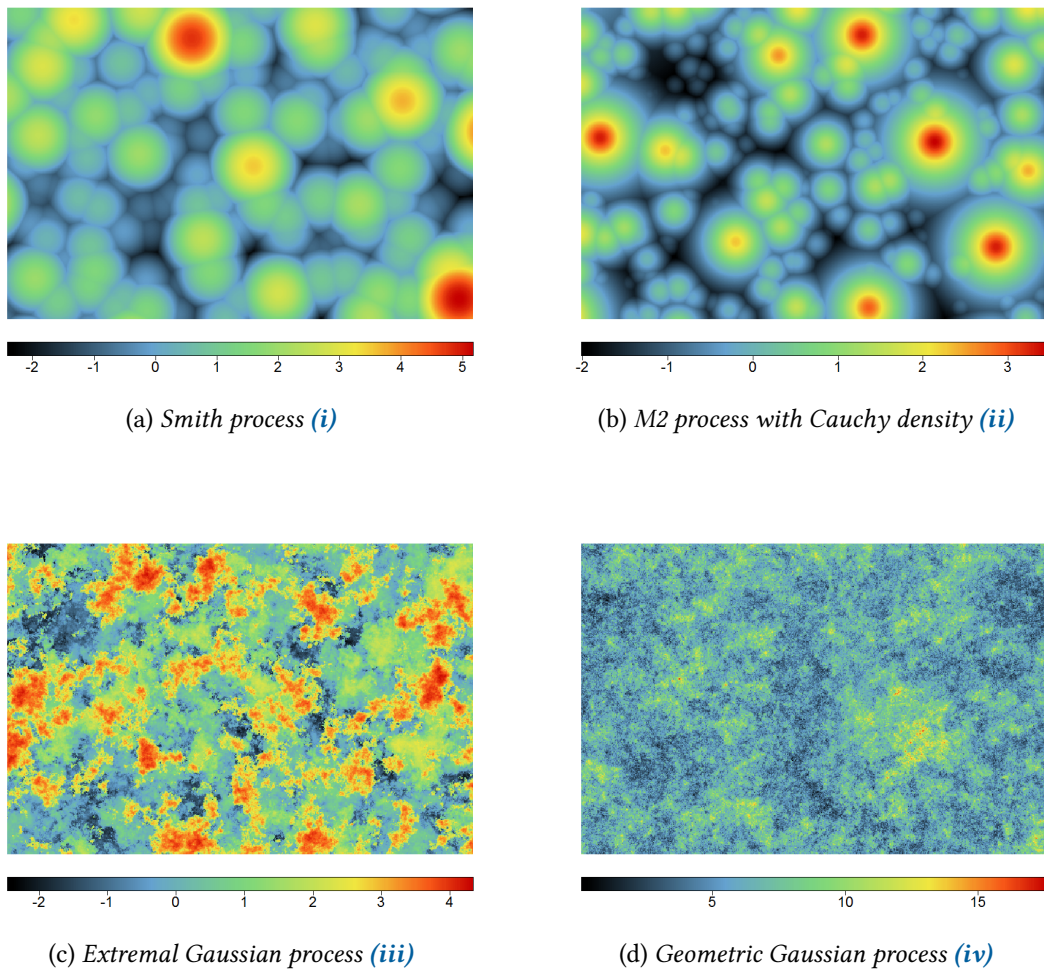


FIGURE 2.6 – Realizations of max-stable RF's on a grid 600×400 , with mesh size equal to 0.05. For viewing purposes, the processes have been transformed to obtain margins with standard Gumbel distribution Λ (see Theorem 1.3)

the M2 process with Cauchy density shape function. Notice that the 90% confidence envelope is large; that is why it looks like the mean curve is flattening for large volumes. When it is plotted without the confidence band, the positive trend is more evident (see [Figure 2.8](#)).

On the contrary, [Figure 2.9](#) contradicts what has been shown in the previous subsection, since it suggests that A_{z_1} and A_{z_2} are finite for the extremal and the geometric Gaussian processes. The reason for this inconsistency is that the exceedance fields associated with these max-stable SRF's are not mean-ergodic. Indeed, recall that, for any $z \in (z_1, z_2)$ and any $n \in \{1, \dots, N\}$, the estimation of $A_{z,n}$ requires the evaluation of $\text{Var} [I_z(V_n)]$ and σ_z^2 (see [Eq. \(2.30\)](#)). In accordance with the estimation method proposed in [Subsection 2.2.3](#), the latter are estimated by a discretized version of

$$S_z^2(V_n|V) = \frac{1}{k_n} \sum_{i=1}^{k_n} [I_z(V_n^i) - I_z(V)]^2$$

and

$$S_z^2(\cdot|V) = \frac{1}{|V|} \int_V [I_z(\mathbf{x}) - I_z(V)]^2 d\mathbf{x},$$

the expectations of which are respectively

$$E [S_z^2(V_n|V)] = \text{Var} [I_z(V_n)] - \text{Var} [I_z(V)], \quad (2.43)$$

and

$$E [S_z^2(\cdot|V)] = \sigma_z^2 - \text{Var} [I_z(V)]. \quad (2.44)$$

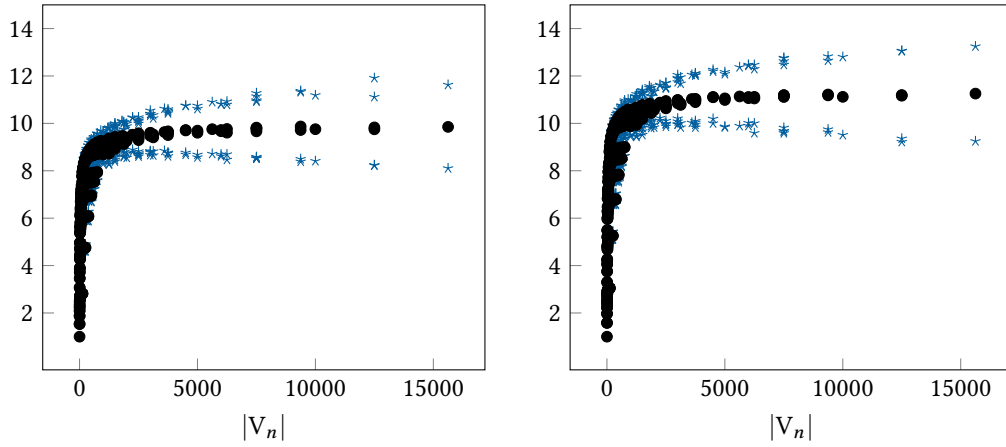
By construction of $(V_n)_{n \in \{1, \dots, N\}}$, the square V can be considered as very large relatively to each V_n . As already mentioned, when I_z is mean-ergodic, the variance $\text{Var} [I_z(V)]$ can be omitted in [Eq. \(2.43\)](#) and [Eq. \(2.44\)](#), so that $S_z^2(V_n|V)$ and $S_z^2(\cdot|V)$ may be considered as unbiased estimators of the variances. On the contrary, when I_z is not mean-ergodic, it cannot be neglected; this is illustrated next. We set $z = z_1$ and, for each max-stable SRF [\(i\)-\(iv\)](#), we compute, from the 200 simulations, an empirical estimate of σ_z^2 , $\text{Var} [I_z(V)]$ and $\text{Var} [I_z(V_n)]$, for different squares $V_n \subset V$ (see [Remark 2.35](#) for more details). This provides empirical estimates of the relative differences of variances

$$\frac{\text{Var} [I_z(V_n)] - \text{Var} [I_z(V)]}{\text{Var} [I_z(V_n)]} \quad (2.45)$$

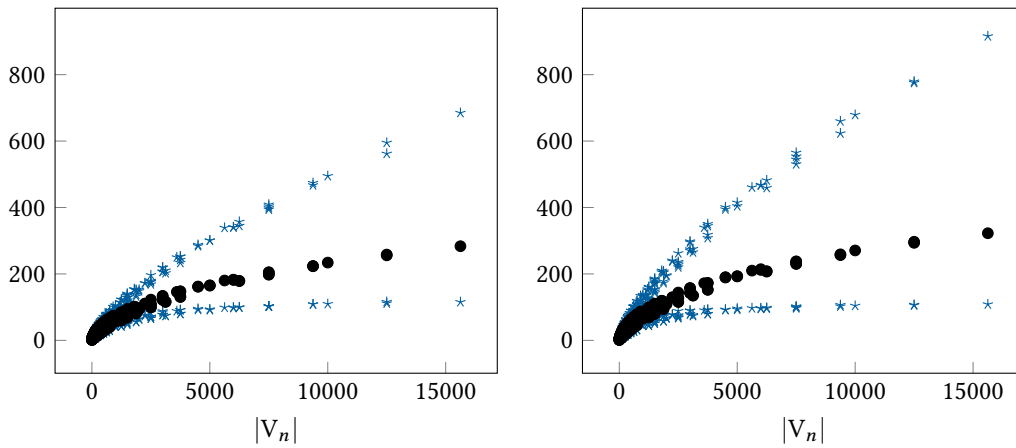
and

$$\frac{\sigma_z^2 - \text{Var} [I_z(V)]}{\sigma_z^2}, \quad (2.46)$$

which are plotted in [Figure 2.10](#). For the Smith process and the M2 process with Cauchy density chape function, these relative differences are very close to 1, even for large subdomains V_n . On the contrary, for the extremal and geometric Gaussian processes, the relative difference [\(2.46\)](#) is further away from 1 and, most importantly, the relative difference [\(2.45\)](#) rapidly decreases to 0. This sharp decrease entails, in average, a very large underestimation



(a) *Smith process*



(b) *M2 process with Cauchy density shape function*

FIGURE 2.7 – The mean curve (black dots) and the corresponding 90% confidence envelope (blue stars) for thresholds z_1 (on the left) and z_2 (on the right). They are computed from 200 simulations of each max-stable SRF (i) (on the top) and (ii) (on the bottom), on a grid 1500×1500 with mesh size equal to 1. Several points lie on the same verticals; they correspond to rectangular subdomains with same area but with different side lengths.

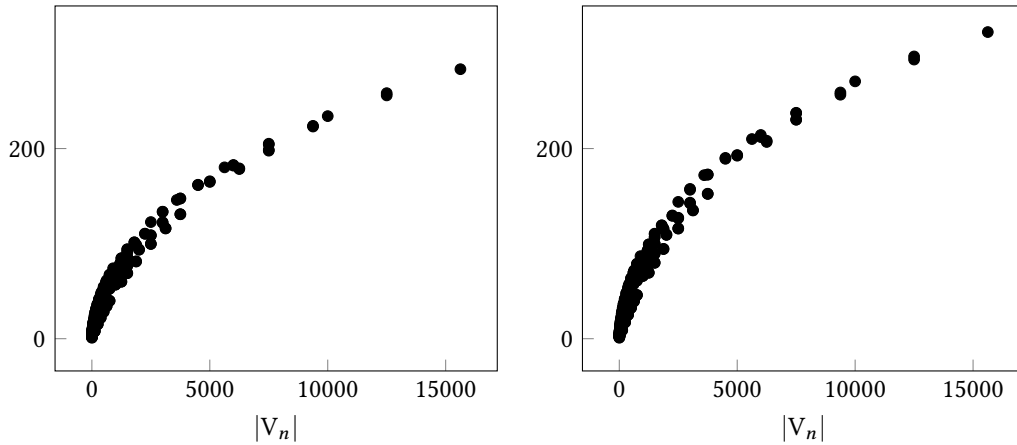
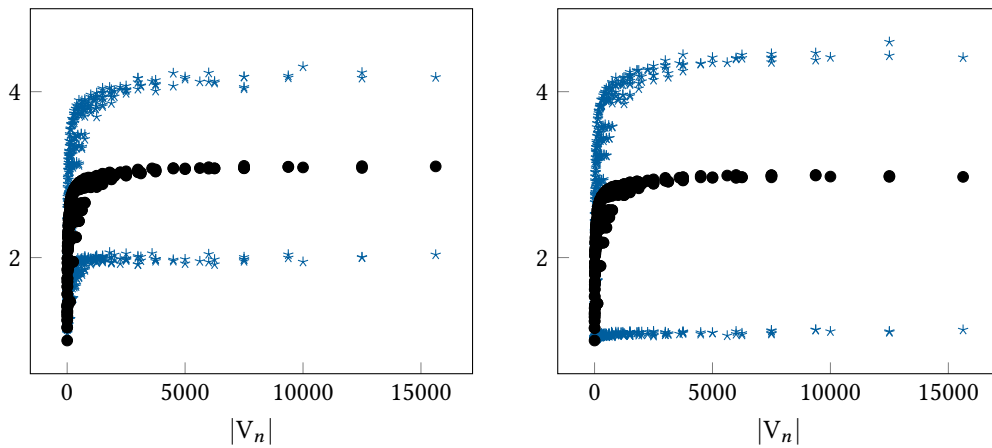
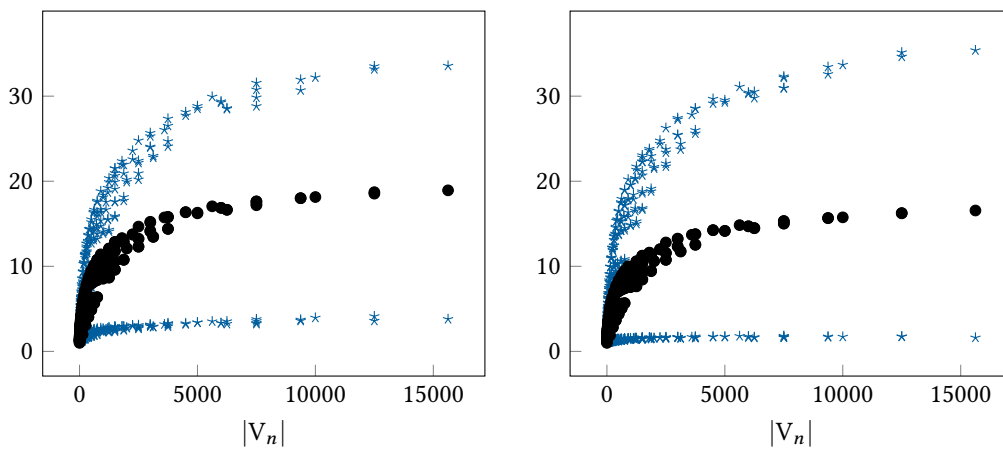


FIGURE 2.8 – The mean curve for thresholds z_1 (on the left) and z_2 (on the right) for the max-stable RF (ii). It is computed from 200 simulations of this process on a grid 1500×1500 with mesh size equal to 1.



(a) Extremal Gaussian process



(b) Geometric Gaussian process

FIGURE 2.9 – The mean curve (black dots) and the corresponding 90% confidence envelope (blue stars) for thresholds z_1 (on the left) and z_2 (on the right). They are computed from 200 simulations of max-stable SRF's (iii) (on the top) and (iv) (on the bottom), on a grid 1500×1500 with mesh size equal to 1.

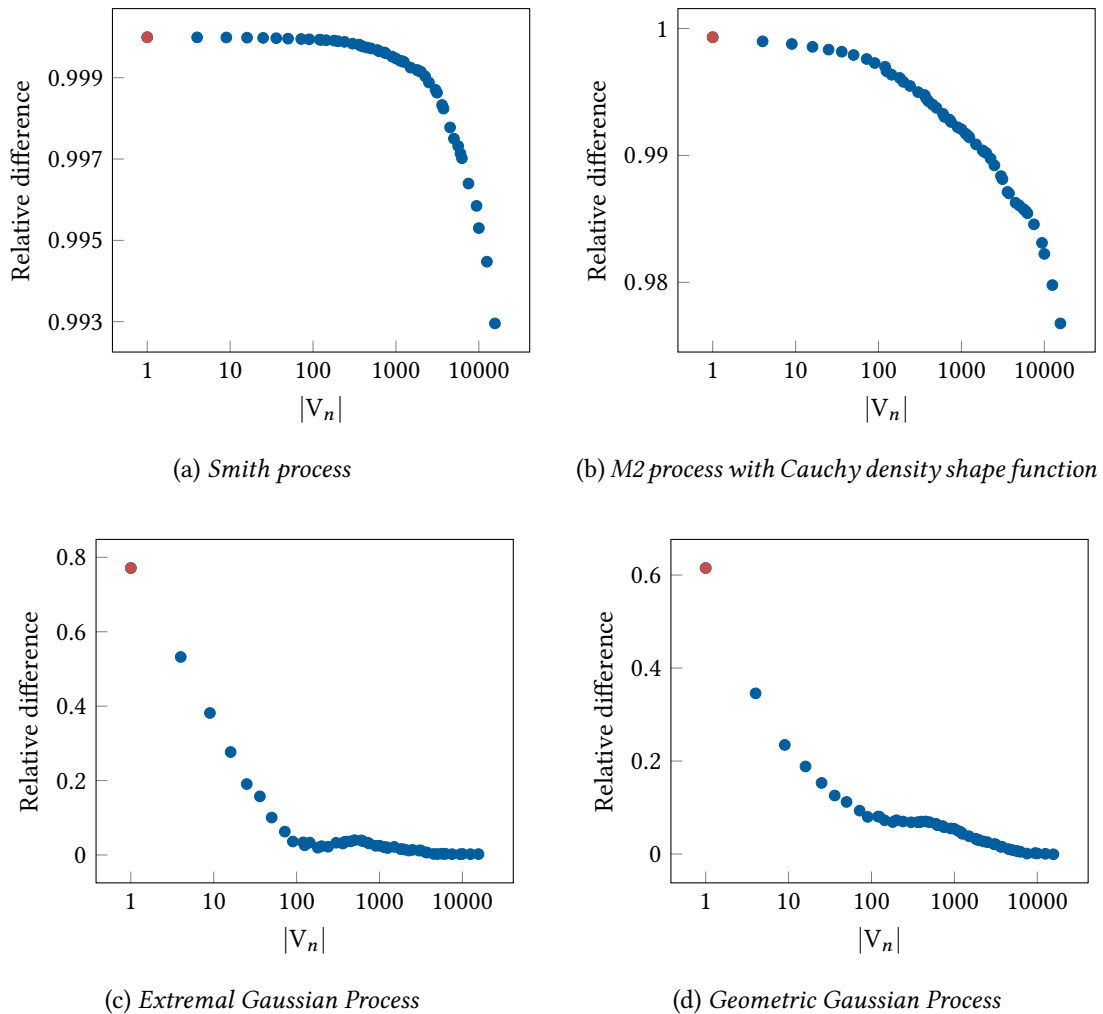


FIGURE 2.10 – Empirical estimates of the relative difference of variances (2.45) (blue dots), when $z = z_1$. For a better visualization, a logarithmic scale is used for the x-axis. By construction of the grid, the red dot with coordinate $|V_n| = 1$ actually corresponds to the relative difference of variances (2.46), see Remark 2.35.

of $\text{Var}[I_z(V_n)]$, when the latter is evaluated from a single realization of Z by (a discretized version of) $S_z^2(V_n|V)$. Thus, it may compensate for the increase of $|V_n|$ when n grows, thereby explaining the stabilization of the curves in Figure 2.9. Using *i.i.d.* observations to estimate $A_{z,n}$ obviously avoids this problem. From the previous empirical estimates of σ_z^2 and $\text{Var}[I_z(V_n)]$, we compute an empirical estimate of $A_{z,n}$, for the max-stable processes (iii) and (iv), and for threshold $z \in \{z_1, z_2\}$. It is displayed in Figure 2.11 for the different squares $V_n \subset V$: the increasing curves suggest that the integral ranges A_{z_1} and A_{z_2} are infinite for both max-stable processes, which is now consistent with the results that have been established in the previous subsection.

Remark 2.35 – Empirical estimates. Recall that V is a square of side 1500. We select $n = 50$ different squares $V_n \subset V$ with side length less than 150 and such that $k_n \geq 30$. In

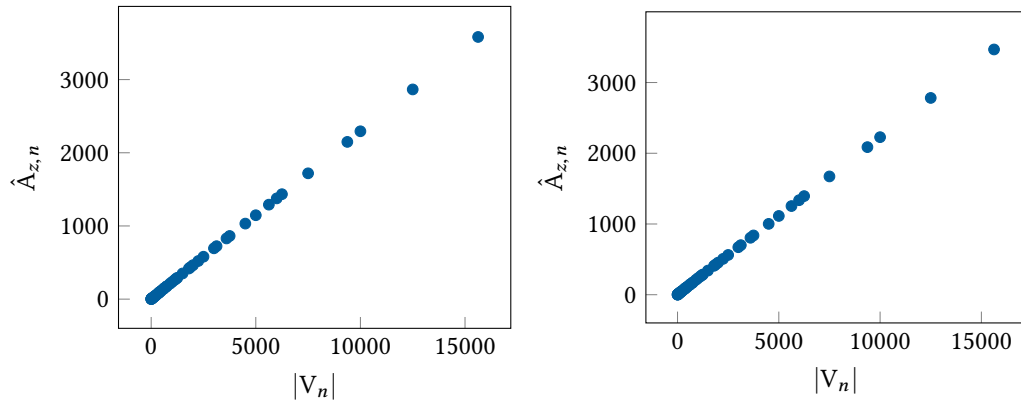
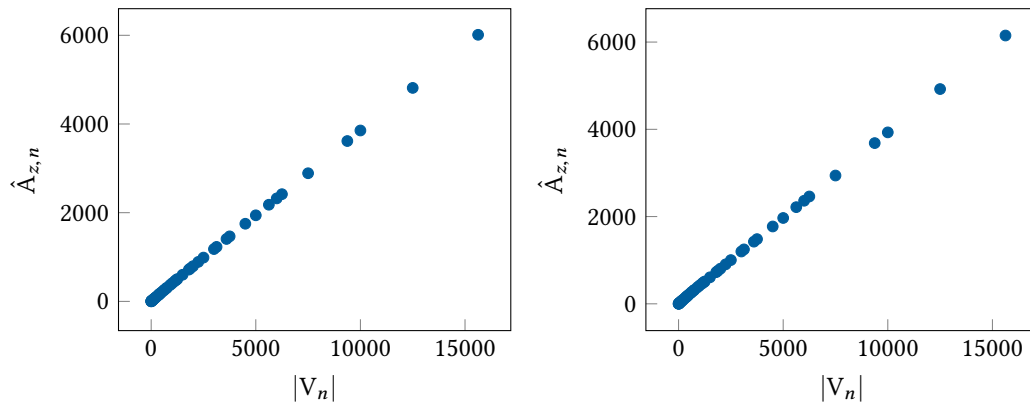
(a) *Extremal Gaussian process*(b) *Geometric Gaussian process*

FIGURE 2.11 – Empirical estimates $\hat{A}_{z,n}$ of the integral range A_z for thresholds $z = z_1$ (on the left) and $z = z_2$ (on the right), computed from 200 simulations of max-stable SRF's (iii) (on the top) and (iv) (on the bottom), on a grid 1500×1500 mesh size equal to 1.

particular $|V_1| = 1$. Now, let $n \in \{1, \dots, 50\}$ and $z \in (0, +\infty)$. For each max-stable process **(i)-(iv)**, we want to estimate $\text{Var}[I_z(V_n)]$ using the *i.i.d.* information from the 200 simulations. For this, we fix in each simulation the same square V_n to compute an empirical and unbiased estimation of this variance. Notice that, since the simulations are performed on a grid G , we cannot compute $I_z(V_n)$ but only a discretized version of it, *i.e.* $\sum_{i=1}^{K_n} I_z(x_i)$, if we suppose that $V_n \cap G = \{x_1, \dots, x_{K_n}\}$. Hence, we actually perform an empirical estimation of the variance of this discretized version, that we consider also as an empirical estimation of $I_z(V_n)$. We shall also point out that, when $|V_n| = 1$, then $V_n \cap G$ is reduced to a single point, since the mesh size of the grid is equal to 1. In practice, estimating $\text{Var}[I_z(V_n)]$ when $|V_n| = 1$ thus amounts to estimating σ_z^2 .

Remark 2.36 – Simulation algorithms. We shall make some comments about the algorithms used to generate realizations of the max-stable RF's **(i)-(iv)**. The first process is simulated exactly by the algorithm proposed in [Oesting et al. \(2018\)](#), which is based on a normalized spectral representation. This algorithm is easy to use for M2 processes and it is implemented in the package `Randomfields` in R. We also use the package `Randomfields` to simulate the RF's **(iii)** and **(iv)**. For the former process, it is based on the algorithm proposed in [Schlather \(2002\)](#). Since the spectral process Y associated with Z is not a.s. bounded, it is approximated by a bounded one; this results in non-exact simulations. Even so, as shown in [Oesting et al. \(2015\)](#), the accuracy of this procedure is quite good. For the process **(iv)**, the package uses an appropriate method within those discussed in [Oesting et al. \(2012\)](#). The latter do not produce exact simulations either. Hence, we shall at least check whether the margins are (approximately) unit Fréchet. We generate 1000 realizations of the RF **(iv)** on a grid 50×50 , with mesh size equal to 0.2. Then, we randomly pick a point in each realization and, for better visualisation, we consider its logarithm. This results in a vector of 1000 values, the empirical quantiles of which are compared to the quantiles of the standard Gumbel distribution Λ in [Figure 2.12](#). Let θ be the ECF of the process **(iv)**. The figure also shows an estimation of the latter, computed from the 1000 realizations. This estimation is obtained by using the F-madogram estimator (see [Chapter 3](#)), which is computed with the function `fmadogram` of the package `SpatialExtremes` in R. These two graphs indicate that the procedure gives quite accurate results. We shall remark that [Dombry et al. \(2016\)](#) propose an algorithm, based on the so-called extremal functions, which carries out exact simulations of max-stable RF's, including the Brown-Resnick processes. However, their algorithm can become very time-consuming when simulating on a dense grid; that is why we do not use it for the geometric Gaussian process. Alternatively, we also have developed an algorithm to perform exact simulations of M2 processes with radially symmetric and non-increasing

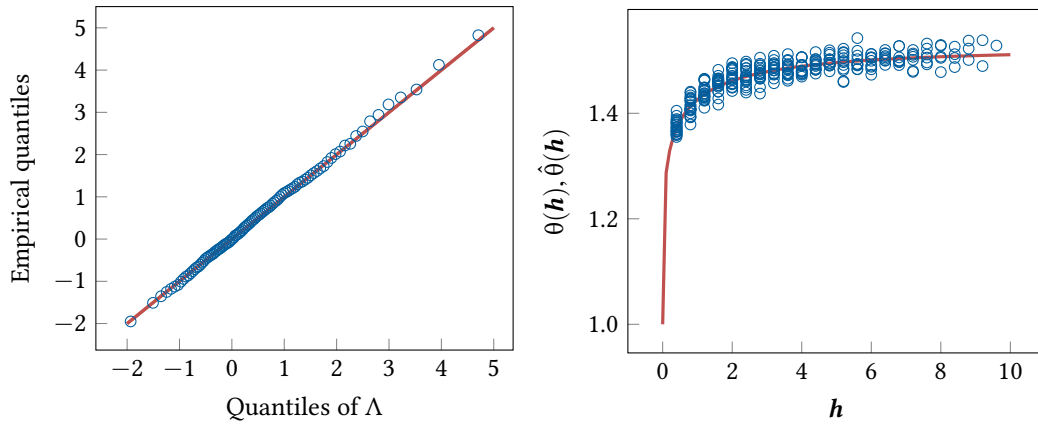


FIGURE 2.12 – Diagnostic plots based on 1000 realizations of the max-stable process (iv) on a grid 50×50 , with mesh size equal to 0.2. On the left: Q-Q plot of the empirical distribution (after logarithmic transformation) against the standard Gumbel distribution Λ . On the right: the ECF θ (red line) in comparison to an empirical estimation $\hat{\theta}$ (blue circles), computed from the F-madogram estimator. We select 25 locations on the grid 50×50 , which remain the same in each simulation. Then, for each pair of points, we calculate the F-madogram estimator using all the realizations. Several points lie on the same verticals: they correspond to pairs of locations that are separated by the same distance.

shape function and, contrary to the first procedure, it has been designed for simulating in a continuous domain of \mathbb{R}^d , see Chapter 4. We use it to obtain realizations of the RF (ii).

We shall now detail how the concept of integral range and the results in Theorem 2.19 relate to the work in Koch (2017).

2.4 APPLICATIONS IN A SPATIAL RISK CONTEXT

2.4.1 Some context

In August 2017, Hurricane Harvey affected a large area in Central America and Eastern United States especially Texas and Louisiana, and caused at least 107 deaths. It is one of the costliest tropical cyclones on record, inflicting 125 billion USD in damage. A few weeks later, a little further to the South, Hurricane Irma caused at least 134 deaths and extensive damage exceeding 64.8 billion USD in value. An accurate evaluation of the environmental risk is thus of great importance for civil authorities and for the insurance and reinsurance industries, especially its spatial characteristics. For insurance companies, this is related to the question of spatial diversification. Recently, Koch (2017) propose a new notion of spatial risk measure that takes into account the spatial dependence in risk assessment. It is summarized hereinafter.

Let the process $(Z(\mathbf{x}))_{\mathbf{x} \in \mathbb{R}^2}$ model an environmental variable, which may be a source of risk (e.g. the temperature, the wind speed or the rainfall amount). Consider also a damage function D such that, for every $\mathbf{x} \in \mathbb{R}^2$, $D(Z(\mathbf{x}))$ represents the (economic) cost induced by Z at the location \mathbf{x} . It is assumed that $(D(Z(\mathbf{x})))_{\mathbf{x} \in \mathbb{R}^2}$ satisfies [Assumption 2.1](#) and [Assumption 2.2](#). The spatial risk measure introduced by [Koch \(2017\)](#) is based on the spatial aggregation of the damage field over a region of interest:

$$\begin{aligned} \mathcal{R}_\Pi : \mathcal{B} &\rightarrow \mathbb{R} \\ V &\mapsto \Pi \left[\frac{1}{|V|} \int_V D(Z(\mathbf{x})) d\mathbf{x} \right], \end{aligned}$$

where Π is a classical risk measure, e.g. the variance, the value-at-risk or the expected short-fall. The paper also proposes a set of axioms regarding the spatial properties of the risk measure \mathcal{R}_Π . One of them is the so-called asymptotic spatial homogeneity of order $-\alpha$, with $\alpha \in (0, +\infty)$. Let $\lambda \in (0, +\infty)$ and $V \in \mathcal{B}$, and recall that λV corresponds to the image of V after applying the homothety with center \mathbf{b}_V . This axiom states that

$$\lim_{\lambda \rightarrow +\infty} \mathcal{R}_\Pi(\lambda V) = K_1 + K_2 \lambda^{-\alpha} + o(\lambda^{-\alpha}), \quad (2.47)$$

where the constants $K_1 \in \mathbb{R}$ and $K_2 \in \mathbb{R}^*$ may depend on V . This equation helps quantify the rate of spatial diversification when the region of interest becomes large. Depending on the value on α , it may be relevant, for an insurance company, to extend its activity to a new geographical region.

Suppose now that Z is a simple stationary max-stable process with ECF θ . It may represent, for instance, annual maxima of daily precipitation. Let also D be the indicator function above a threshold $z \in (0, +\infty)$ and Π stand for the variance. Then, \mathcal{R}_Π becomes

$$\forall V \in \mathcal{B} \quad \mathcal{R}_\Pi(V) = \text{Var} [I_z(V)]; \quad (2.48)$$

it is noted \mathcal{R}_2 in the sequel. In addition, define

$$\varsigma := \sqrt{\int_{\mathbb{R}^2} \text{Cov} [I_z(\mathbf{0}), I_z(\mathbf{h})] d\mathbf{h}}.$$

We shall recall that the covariance function of I_z is given in [Eq. \(2.27\)](#). It is proven in [Koch \(2017, Theorem 3\)](#) that if

$$\int_{\mathbb{R}^2} 2 - \theta(\mathbf{h}) d\mathbf{h} < +\infty,$$

then \mathcal{R}_2 satisfies [Eq. \(2.47\)](#) with $\alpha = 2$, $K_1 = 0$ and $K_2 = \frac{\varsigma^2}{|V|}$. This result is equivalent to the implication [\(iii\) \$\Rightarrow\$ \(i\)](#) in [Theorem 2.19](#); this stems from the link between the integral range A_z and the axiom of spatial homogeneity of order -2 .

2.4.2 The integral range, a relevant tool

Set $z \in (0, +\infty)$ and let again Z be a simple max-stable SRF in \mathbb{R}^2 with exceedance field I_z . The correlation function and the variance of the latter are respectively denoted by ρ_z and σ_z^2 . Consider also a mapping $g : \mathbb{R} \rightarrow \mathbb{R}$ and let $a \in \mathbb{R}$. As detailed *e.g.* in Koch (2017, Appendix A.7), if for any nondecreasing sequence $(\lambda_n)_{n \in \mathbb{N}}$ of positive real numbers satisfying

$$\lim_{n \rightarrow +\infty} \lambda_n = +\infty, \quad \lim_{n \rightarrow +\infty} g(\lambda_n) = a,$$

then $\lim_{\lambda \rightarrow +\infty} g(\lambda) = a$. Hence, for any convex set $V \in \mathcal{B}$, the risk measure \mathcal{R}_2 in Eq. (2.48) satisfies the axiom of spatial homogeneity of order -2 , with $K_1 = 0$ and $K_2 = \frac{\sigma_z^2}{|V|}$ if and only if

$$\text{Var} [I_z(\lambda_n V)] \underset{n \rightarrow \infty}{\sim} \frac{\sigma_z^2}{\lambda_n^2 |V|} \int_{\mathbb{R}^2} \rho_z(\mathbf{h}) d\mathbf{h},$$

for any nondecreasing sequence $(\lambda_n)_{n \in \mathbb{N}}$ of positive real numbers such that $\lim_{n \rightarrow +\infty} \lambda_n = +\infty$. That is, if and only if the integral range A_z is finite (see Eq. (2.13))

The concept of asymptotic homogeneity is larger than the notion of integral range, but working with the latter has many advantages. First, the proof of the implication (iii) \Rightarrow (i) in Theorem 2.19 is shorter and slightly easier than the proof of Theorem 3, proposition 3 in Koch (2017), and does not require to work with convex sets in \mathcal{B} . This is mainly because the properties of a sequence $V_n \uparrow \mathbb{R}^d$ are exploited. Further, A_z may be estimated with the method provided in Subsection 2.2.3 without making any assumption on the simple max-stable SRF Z , except that it is mean-ergodic. Indeed, we shall recall that its estimation in the case of processes that are not mean-ergodic is problematic since it may lead to the wrong conclusion. In addition, when A_z is finite, it can be used to assess the variance of $I_z(V)$ when estimating $\mu_z = \mathbb{P}[Z((0)) > z]$ from a single realization of Z on a large enough domain V . This may be of great interest for insurance companies that want to evaluate some risks at a given location, *e.g.* the risk of flood.

Recently, Koch (2019, Theorem 6) extended the results in Koch (2017, Theorem 3) to a more general damage field $(D(Z(\mathbf{x})))_{\mathbf{x} \in \mathbb{R}^2}$ than the exceedance field we have focused on. In particular, it is not assumed to be stationary anymore, but only second-order stationary. It would be interesting to retrieve this result when using the integral range. More generally, it would be useful to better study the integral range of a second-order SRF Z . Questions of interest are for instance: in which case the integral range is finite whereas the correlation function of Z is not integrable? What does a null integral range say about the process Z ? This should be investigated in a joint work with Erwan Koch. This ongoing collaboration mainly aims to introduce the concept of integral range in an insurance context.

2.5 DISCUSSION

The integral range is a geostatistical object that helps characterize the statistical fluctuations of a (second-order) stationary random field at large scale. When it is finite and does not vanish, it can be interpreted as the spatial scale of this field, which is ultimately first-order ergodic. Let Z be a simple max-stable SRF and fix a threshold $z \in (0, +\infty)$. We have found that the integral range A_z of the corresponding exceedance field above z is intimately related to the extremal coefficient function θ of Z . In [Theorem 2.19](#), we revealed a sufficient and necessary condition on the latter to guarantee that the former is finite. This condition has been illustrated on a collection of standard max-stable models. It has also been linked to the ergodic and mixing properties of max-stable processes. When $\lim_{\|\mathbf{h}\| \rightarrow +\infty} \theta(\mathbf{h})$ exists, we showed that if A_z is finite then Z is mixing, and thus ergodic. At first glance, such a result is not common, except for Gaussian fields. We can then surmise that a finite integral range is a useful condition when studying Z from only one set of spatial observations. As shown in the next chapter, this is for instance a sufficient condition to ensure the consistence and the asymptotic normality of a new nonparametric estimator of the ECF, when it is computed from a single and partially observed realization of Z . In addition, [Theorem 2.19](#) completes results established by [Koch \(2017\)](#) in a spatial risk context, but which do not refer to the concept of integral range. This illustrates the relevance of geostatistical tools for enriching extreme value analysis.

We have also provided a method to assess A_z , with no prior knowledge on the ECF. This procedure has been tested on simulated data. When Z is mean-ergodic, it performs well. However, recall that the process has been simulated on large and dense grids. Except in some studies like the heterogeneous material studies, the data are generally sparse. In such a case, the method is likely to fail: this should be empirically and theoretically investigated in future works. Furthermore, it has been shown that the procedure of estimation is not robust to the violation of the mean-ergodicity assumption. Indeed, when Z is not mean-ergodic, the results indicate that the integral range seems to be finite, thus leading to the wrong conclusion. As pointed out before, there does not exist any procedure to test the mean-ergodicity assumption when observing only one realization of a spatial process, hence we currently do not know how to overcome this difficulty.

We shall now suggest some natural extensions of the work presented in this chapter. First, we think that [Theorem 2.19](#) can be readily extended to *max-infinitely divisible* (max-i.d.) processes. Introduced by [Balkema and Resnick \(1977\)](#), this class of processes regroups each RF Z such that, for any $n \in \mathbb{N}^*$, there exists a process Y satisfying

$$Z \stackrel{f.d.d.}{=} \max_{i \in \{1, \dots, n\}} Y_i,$$

where Y_1, \dots, Y_n are *i.i.d.* replications of Y . This typically includes max-stable RF's. Actually, the equivalence between pairwise independence and mutual independence of the finite dimensional distributions holds for max-id process and not only for max-stable processes (see [Resnick, 1987](#), Proposition 5.24). Besides, similarly to the extremal coefficient function, [Kabluchko and Schlather \(2010\)](#) also show that the bivariate distribution of a stationary max-id RF Z relates to its ergodic and mixing properties. That is why we conjecture that the results in [Theorem 2.19](#) can be generalized to such processes. It would also be interesting to establish similar results for Generalized Pareto processes. This is suggested by the "threshold stability property" of A_z revealed in [Theorem 2.19](#): for fixed $z \in (0, +\infty)$, A_z is finite if and only if it is finite for every $z \in (0, +\infty)$.

It would also be worth improving the results established in this chapter. In [Corollary 2.22](#), we give a necessary and sufficient condition on a M2 process Z so that $\int_{\mathbb{R}^d} 2 - \theta(\mathbf{h}) d\mathbf{h}$, and thus A_z , is finite. More generally, is it possible to better identify the max-stable processes for which $A_z < +\infty$? Consider a stationary Brown-Resnick RF Z , the distribution of which depends on the semivariogram γ . According to [Dombry and Kabluchko \(2018, Example 11\)](#), $\int_{\mathbb{R}^d} 2 - \theta(\mathbf{h}) d\mathbf{h}$ is finite provided that the following condition is met:

$$\liminf_{\|\mathbf{h}\| \rightarrow +\infty} \frac{\gamma(\mathbf{h})}{\ln(\|\mathbf{h}\|)} > 4d.$$

In the one-dimensional case, this condition guarantees that the process has a mixed moving maxima representation, see [Kabluchko et al. \(2009, Remark 15\)](#). We can then wonder if a stationary max-stable RF Z for which A_z is finite always has a mixed moving maxima representation. Notice that the converse is false, since we have shown that a M2 process with Cauchy density shape function has infinite integral range A_z . Let Y be the spectral process associated to Z . From [Dombry and Kabluchko \(2017, Theorem 3\)](#), one idea would be to verify if the following implication is true:

$$\int_{\mathbb{R}^d} 2 - \theta(\mathbf{h}) d\mathbf{h} < +\infty \quad \Rightarrow \quad \lim_{\|\mathbf{h}\| \rightarrow +\infty} Y(\mathbf{h}) = 0 \quad a.s.$$

or, at least, to determine which conditions guarantee this result. As shown in [Dombry and Kabluchko \(2018\)](#), when Z has a.s. continuous sample paths, the condition $\lim_{\|\mathbf{h}\| \rightarrow +\infty} Y(\mathbf{h}) = 0$ implies that Z is strongly β -mixing (in the sense given in the paper). This brings up another question: how the concept of integral range relates to mixing coefficients such as the α -mixing, the β -mixing or the ϱ -mixing coefficients. For two subsets $V_1, V_2 \subset \mathbb{R}^d$, they measure how much $(Z(\mathbf{x}))_{\mathbf{x} \in V_1}$ and $(Z(\mathbf{x}))_{\mathbf{x} \in V_2}$ differ from independence (see e.g. [Doukhan \(1994\)](#) for a thorough review of mixing theory). When working with a unique realization, some studies required that these coefficients vanish fast enough to 0 when the distance between V_1 and V_2 goes to infinity. This generally guarantees that the studied estimator are asymptotically normal, see e.g. [Lahiri et al. \(1999\)](#), or [Dombry and Eyi-Minko \(2012\)](#).

2.6 PROOFS

2.6.1 Integral range and nonnegative correlation function

Before tackling its proof, [Proposition 2.8](#) is recalled for convenience.

Proposition Let Z be a second-order SRF, with measurable and nonnegative correlation function ρ . Its integral range A always exists and equals $\int_{\mathbb{R}^d} \rho(\mathbf{h}) d\mathbf{h} \in [0, +\infty]$.

Proof. Let $V_n \uparrow \mathbb{R}^d$. By assumption, the correlation function ρ is measurable. nonnegative, thus $\int_{\mathbb{R}^d} \rho(\mathbf{h}) d\mathbf{h}$ always exists and is valued in $[0, +\infty]$. Let us consider both the case $\int_{\mathbb{R}^d} \rho(\mathbf{h}) d\mathbf{h} < +\infty$ and $\int_{\mathbb{R}^d} \rho(\mathbf{h}) d\mathbf{h} = +\infty$ separately. First, assume that $\int_{\mathbb{R}^d} \rho(\mathbf{h}) d\mathbf{h}$ is finite. As stated by Theorem 2 p.401 in [Lantuéjoul \(1991\)](#), it implies that A exists and equals $\int_{\mathbb{R}^d} \rho(\mathbf{h}) d\mathbf{h}$. Now, assume that $\int_{\mathbb{R}^d} \rho(\mathbf{h}) d\mathbf{h} = +\infty$. If the integral range A exists, recall from [Eq. \(2.12\)](#) that it is defined as

$$A = \lim_{n \rightarrow +\infty} \int_{\mathbb{R}^d} \rho(\mathbf{h}) \frac{K_n(\mathbf{h})}{K_n(\mathbf{0})} d\mathbf{h}.$$

For any $n \in \mathbb{N}$, the map $\mathbf{h} \mapsto \rho(\mathbf{h}) K_n(\mathbf{h})/K_n(\mathbf{0})$ is a nonnegative measurable function of \mathbf{h} and for fixed $\mathbf{h} \in \mathbb{R}^d$, $\lim_{n \rightarrow +\infty} \rho(\mathbf{h}) K_n(\mathbf{h})/K_n(\mathbf{0}) = \rho(\mathbf{h})$ according to [Eq. \(2.3\)](#). Therefore, by Fatou's lemma,

$$0 \leq \int_{\mathbb{R}^d} \rho(\mathbf{h}) d\mathbf{h} \leq \liminf_{n \rightarrow \infty} \int_{\mathbb{R}^d} \rho(\mathbf{h}) \frac{K_n(\mathbf{h})}{K_n(\mathbf{0})} d\mathbf{h}.$$

By assumption, $\int_{\mathbb{R}^d} \rho(\mathbf{h}) d\mathbf{h}$ is infinite thus, so are $\liminf_{n \rightarrow \infty} \int_{\mathbb{R}^d} \rho(\mathbf{h}) \frac{K_n(\mathbf{h})}{K_n(\mathbf{0})} d\mathbf{h}$ and ultimately $\lim_{n \rightarrow +\infty} \int_{\mathbb{R}^d} \rho(\mathbf{h}) \frac{K_n(\mathbf{h})}{K_n(\mathbf{0})} d\mathbf{h}$. The integral range A_z exists and equals $\int_{\mathbb{R}^d} \rho(\mathbf{h}) d\mathbf{h}$.

In fine, it has be shown that $\int_{\mathbb{R}^d} \rho(\mathbf{h}) d\mathbf{h}$ always exists and is valued in $[0, +\infty]$ thus so does A . In addition, we always have $A_z = \int_{\mathbb{R}^d} \rho(\mathbf{h}, z) d\mathbf{h}$. ■

2.6.2 Correlation function behaviour

Let Z be a simple max-stable SRF. For fixed $\mathbf{h} \in \mathbb{R}^d$, recall that $\rho_{\mathbf{h}}$ stands for the function $z \in (0, +\infty) \mapsto \rho(\mathbf{h}, z) \in [0, 1]$, where ρ is defined by [Eq. \(2.28\)](#). Alternatively, for fixed $z \in (0, +\infty)$, ρ_z denotes the map $\mathbf{h} \in \mathbb{R}^d \mapsto \rho(\mathbf{h}, z) \in [0, 1]$. We can now tackle the proof of [Proposition 2.17](#) and [Proposition 2.18](#), which are recalled for convenience.

Proposition Let $z \in (0, +\infty)$. The map ρ_z is a continuous (thus measurable) nonnegative function.

Proof. Set $z \in (0, +\infty)$ and recall that Z is assumed to be stochastically continuous. The nonnegativeness of ρ_z is straightforward. Its continuity follows from the continuity of the function θ , see [Strokorb and Schlather \(2015, Lemma 23\)](#). In some cases, (almost everywhere) continuity may also be established from [Theorem 1.16](#) and [Kabluchko and Schlather \(2010, Proposition 1\)](#) when $d \geq 2$ and $d = 1$, respectively. ■

Proposition Let $\mathbf{h} \in \mathbb{R}^d$. The map $\rho_{\mathbf{h}}$ is a continuous (thus measurable) nonnegative and nondecreasing function with limits $\lim_{z \rightarrow 0} \rho_{\mathbf{h}}(z) = 1 \{\theta(\mathbf{h}) = 1\}$ and $\lim_{z \rightarrow +\infty} \rho_{\mathbf{h}}(z) = 2 - \theta(\mathbf{h})$.

Proof. Continuity and nonnegativeness are straightforward. Let us analyze the variations of $\rho_{\mathbf{h}}$. For any $z \in (0, +\infty)$,

$$\rho_{\mathbf{h}}(z) = \frac{\exp\left\{\frac{2 - \theta(\mathbf{h})}{z}\right\} - 1}{\exp\{1/z\} - 1}.$$

When \mathbf{h} is such that $\theta(\mathbf{h}) = 1$ (resp. $\theta(\mathbf{h}) = 2$), then $\rho_{\mathbf{h}}$ is constant equal to 1 (resp. 0). Alternatively, when \mathbf{h} is such that $1 < \theta(\mathbf{h}) < 2$, then $\rho_{\mathbf{h}}$ is differentiable with derivative

$$\rho'_{\mathbf{h}}(z) = \frac{\exp\{1/z\}}{z^2 (\exp\{1/z\} - 1)^2} \left[(\theta(\mathbf{h}) - 1) \exp\left\{\frac{2 - \theta(\mathbf{h})}{z}\right\} - (\theta(\mathbf{h}) - 2) \exp\left\{\frac{1 - \theta(\mathbf{h})}{z}\right\} - 1 \right]$$

for any $z \in (0, +\infty)$. The part in front of the brackets is positive. Denote by $f_{\mathbf{h}}(z)$ the part within the brackets. The function $f_{\mathbf{h}} : (0, +\infty) \rightarrow \mathbb{R}$ is differentiable, with derivative

$$f'_{\mathbf{h}}(z) = \frac{(\theta(\mathbf{h}) - 2)(1 - \theta(\mathbf{h}))}{z^2} \left[\exp\left\{\frac{1 - \theta(\mathbf{h})}{z}\right\} - \exp\left\{\frac{2 - \theta(\mathbf{h})}{z}\right\} \right], \quad z \in (0, +\infty),$$

which is always negative since $0 < 1 < \theta(\mathbf{h}) < 2$. Therefore, $f_{\mathbf{h}}$ is decreasing. Because it also tends towards 0 as $z \rightarrow +\infty$, it is positive. Consequently, so is $\rho'_{\mathbf{h}}$ and $\rho_{\mathbf{h}}$ is ultimately increasing.

In fine, for all $\mathbf{h} \in \mathbb{R}^d$, the nonnegative continuous function $\rho_{\mathbf{h}}$ is nondecreasing, bounded from above by $\lim_{z \rightarrow +\infty} \rho_{\mathbf{h}}(z) = 2 - \theta(\mathbf{h})$ and from below by $\lim_{z \rightarrow 0} \rho_{\mathbf{h}}(z) = 1 \{\theta(\mathbf{h}) = 1\}$. ■

2.6.3 Finite integral equivalence

Before handling [Theorem 2.19](#) and [Corollary 2.22](#), we start by establishing two intermediate results, which are introduced herein-after. The first lemma gives a condition on the set $\mathcal{D} = \{\mathbf{h} \in \mathbb{R}^d : \theta(\mathbf{h}) = 1\}$, where θ still denotes the extremal coefficient function of a simple max-stable SRF Z , so that its volume is null.

Proposition 2.37 The set $\mathcal{D} = \{\mathbf{h} \in \mathbb{R}^d : \theta(\mathbf{h}) = 1\}$ is a measurable set. In addition, if it exists $\mathbf{h} \in \mathbb{R}^d$ such that $\theta(\mathbf{h}) \neq 1$ then $|\mathcal{D}| = 0$.

Proof. First, we shall prove that \mathcal{D} is measurable. Consider the sequence $(z_n)_{n \in \mathbb{N}}$ of positive real numbers such that $\lim_{n \rightarrow +\infty} z_n = 0$. Let $n \in \mathbb{N}$. From [Proposition 2.17](#), we know that the map ρ_{z_n} is measurable. In addition, for any $\mathbf{h} \in \mathbb{R}^d$, we have $\lim_{n \rightarrow +\infty} \rho_{\mathbf{h}}(z_n) = 1 \{\theta(\mathbf{h}) = 1\}$ by continuity of the function $\rho_{\mathbf{h}}$, see [Proposition 2.18](#). Consequently, the map $\mathbf{h} \in \mathbb{R}^d \mapsto 1 \{\theta(\mathbf{h}) = 1\}$ is measurable as the pointwise limit of a sequence of measurable functions, therefore so is \mathcal{D} . Now, assume that it exists $\mathbf{h} \in \mathbb{R}^d$ such that $\theta(\mathbf{h}) \neq 1$. From Theorem 3 in [Schlather and Tawn \(2003\)](#), it implies that the extremal coefficient function θ is not differentiable, and thus non locally constant, at the origin. We recall that $\theta(\mathbf{0}) = 1$. Let us prove that $|\mathcal{D}| = 0$ by first assuming the converse. This means that it exists a non degenerate d -dimensional interval $\mathcal{I} \subset \mathbb{R}^d$ such that $\theta(\mathbf{h}) = 1$, for any $\mathbf{h} \in \mathcal{I}$. Let $\mathcal{A} \subset \mathbb{R}^d$ be a neighbourhood of $\mathbf{0}$ such that it exists $\mathbf{v} \in \mathbb{R}^d$ satisfying $\mathcal{A} + \mathbf{v} \subset \mathcal{I}$ and set $\mathbf{h} \in \mathcal{A}$. Then consider $\mathbf{y}, \mathbf{x} \in \mathbb{R}^d$ such that $\mathbf{y} - \mathbf{x} = \mathbf{h}$. By definition of \mathcal{A} , it exists $\mathbf{h}_1, \mathbf{h}_2 \in \mathcal{I}$ whose difference $\mathbf{h}_1 - \mathbf{h}_2$ is also equal to \mathbf{h} , and thus $\mathbf{x} + \mathbf{h}_1 = \mathbf{y} + \mathbf{h}_2$. Since $\theta(\mathbf{h}_1) = \theta(\mathbf{h}_2) = 1$, we have a.s. $Z(\mathbf{x}) = Z(\mathbf{x} + \mathbf{h}_1)$ and $Z(\mathbf{y}) = Z(\mathbf{y} + \mathbf{h}_2)$. By transitivity of the a.s. equality, it follows that $Z(\mathbf{x}) = Z(\mathbf{y})$ a.s., i.e. $\theta(\mathbf{h}) = 1$. The previous equality holds for any $\mathbf{h} \in \mathcal{A}$ and thus contradicts the non-differentiability of θ in $\mathbf{0}$. Consequently $|\mathcal{D}| = 0$. \blacksquare

The second intermediate result claims that A_z is either finite or infinite for every $z \in (0, +\infty)$.

Lemma 2.38 If there exists $z > 0$ such that $A_z < +\infty$ (resp. $= \infty$), then $A_z < +\infty$ (resp. $= \infty$) for all $z \in (0, +\infty)$.

Proof. For fixed $z_1 \in (0, +\infty)$ assume that $A_{z_1} < +\infty$ and let $z_2 \in (0, +\infty)$.

- When $z_2 \leq z_1$, as stated by [Proposition 2.18](#), the function $\rho_{\mathbf{h}}$ is nonnegative and nondecreasing, hence $0 \leq \rho(\mathbf{h}, z_2) \leq \rho(\mathbf{h}, z_1)$. Thus, according to [Proposition 2.8](#), $0 \leq A_{z_2} \leq A_{z_1} < +\infty$.
- When $z_2 > z_1$, the inequalities $0 \leq \exp\left\{\frac{2 - \theta(\mathbf{h})}{z_2}\right\} - 1 \leq \exp\left\{\frac{2 - \theta(\mathbf{h})}{z_1}\right\} - 1$ hold. In addition, from [Proposition 2.8](#), $A_{z_1} < +\infty$ is equivalent to $\int_{\mathbb{R}^d} \exp\left\{\frac{2 - \theta(\mathbf{h})}{z}\right\} - 1 d\mathbf{h} < +\infty$. As a consequence, $0 \leq A_{z_2} \leq A_{z_1} < +\infty$.

We prove the infinity case by contraposition. \blacksquare

We are now fully equipped to prove [Theorem 2.19](#), the statement of which is recalled below.

Theorem – Finite integral equivalence. Let Z be a simple max-stable SRF with extremal coefficient function θ and, for any $z \in (0, +\infty)$, denote by A_z the integral range of the associated exceedance field I_z . The following assertions are equivalent:

- (i) $\exists z \in (0, +\infty) \quad A_z < +\infty,$
- (ii) $\forall z \in (0, +\infty) \quad A_z < +\infty,$
- (iii) $A_\infty := \int_{\mathbb{R}^d} 2 - \theta(\mathbf{h}) \, d\mathbf{h} < +\infty.$

If these conditions are fulfilled, the mapping $z \in (0, +\infty) \mapsto A_z \in [0, +\infty)$ is continuous and nondecreasing with $\lim_{z \rightarrow 0} A_z = |\mathcal{D}|$ and $\lim_{z \rightarrow +\infty} A_z = A_\infty$, where $\mathcal{D} := \{\mathbf{h} \in \mathbb{R}^d : \theta(\mathbf{h}) = 1\}$.

Proof. We shall start by proving the equivalence between (i), (ii) and (iii), then assuming that these conditions are true, we shall finally study the variations of the integral range A_z with $z \in (0, +\infty)$.

Proof that (i) is equivalent to (ii). According to Lemma 2.38, (i) implies (ii) which proves the equivalence.

Proof that (ii) implies (iii). Assume that (ii) holds and consider the case where $z = 1$. Using the power series characterization of the exponential function, for any $\mathbf{h} \in \mathbb{R}^d$ we have

$$(e - 1) \rho_1(\mathbf{h}) = \exp\{2 - \theta(\mathbf{h})\} - 1 = \sum_{n=1}^{+\infty} \frac{1}{n!} (2 - \theta(\mathbf{h}))^n.$$

All the terms of this serie are nonnegative, thus $(e - 1) \rho_1(\mathbf{h})$ is greater than its first term $2 - \theta(\mathbf{h})$. According to Proposition 2.8, (ii) holds if and only if $\int_{\mathbb{R}^d} \rho_z(\mathbf{h}) \, d\mathbf{h} < +\infty$, for any $z \in (0, +\infty)$. Hence, it directly follows that

$$\int_{\mathbb{R}^d} 2 - \theta(\mathbf{h}) \, d\mathbf{h} \leq (e - 1) \int_{\mathbb{R}^d} \rho_1(\mathbf{h}) \, d\mathbf{h} < +\infty.$$

Proof that (iii) implies (ii). Assume that (iii) holds and recall that $\mathcal{D} = \{\mathbf{h} \in \mathbb{R}^d : \theta(\mathbf{h}) = 1\}$ is a measurable set, see Proposition 2.37. For all $\mathbf{h} \in \mathbb{R}^d$, Proposition 2.18 establishes that the nonnegative continuous function $\rho_{\mathbf{h}}$ is nondecreasing, bounded from above by $\lim_{z \rightarrow +\infty} \rho_{\mathbf{h}}(z) = 2 - \theta(\mathbf{h})$ and from below by $\lim_{z \rightarrow 0} \rho_{\mathbf{h}}(z) = \mathbf{1}_{\{\theta(\mathbf{h}) = 1\}}$. Hence, for all $z \in (0, +\infty)$, we have $\rho_0 \leq \rho_z \leq \rho_\infty$ with $\rho_0 : \mathbf{h} \in \mathbb{R}^d \mapsto \mathbf{1}_{\{\theta(\mathbf{h}) = 1\}} \in \{0, 1\}$ and $\rho_\infty : \mathbf{h} \in \mathbb{R}^d \mapsto 2 - \theta(\mathbf{h})/1 \in [0, 1]$. Recalling that (iii) holds, we have

$$|\mathcal{D}| = \int_{\mathbb{R}^d} \rho_0(\mathbf{h}) \, d\mathbf{h} \leq \int_{\mathbb{R}^d} \rho_z(\mathbf{h}) \, d\mathbf{h} \leq \int_{\mathbb{R}^d} \rho_\infty(\mathbf{h}) \, d\mathbf{h} < +\infty.$$

Using Proposition 2.8, we can conclude that $A_z < +\infty$ for any $z \in (0, +\infty)$.

Study of the function $z \in (0, +\infty) \mapsto A_z$. Assume that (i)–(iii) are true. We know from Proposition 2.8 that (i) implies $A_z = \int_{\mathbb{R}^d} \rho(\mathbf{h}, z) \, d\mathbf{h}$ for any $z \in (0, +\infty)$. We have

just seen that for all $\mathbf{h} \in \mathbb{R}^d$, the function $\rho_{\mathbf{h}}$ is nondecreasing, therefore so is the map $z \in (0, +\infty) \mapsto A_z$. The latter is also continuous as a consequence of the dominated convergence theorem, see e.g. Theorem 16.8 p.112 in Billingsley (1995). First, we know from Proposition 2.17 and Proposition 2.18 that for fixed $z \in (0, +\infty)$, the map ρ_z is measurable and for all $z \in (0, +\infty)$, $\mathbf{h} \in \mathbb{R}^d$, $|\rho(z, \mathbf{h})| \leq 2 - \theta(\mathbf{h})$ where, by (iii), the map $\mathbf{h} \mapsto 2 - \theta(\mathbf{h})$ is integrable on \mathbb{R}^d . The key element to remember is that the function $\rho_{\mathbf{h}}$ is continuous for any $\mathbf{h} \in \mathbb{R}^d$, i.e., for any $z \in (0, +\infty)$ and for any sequence $(z_n)_{n \in \mathbb{N}}$ of positive real numbers such that $\lim_{n \rightarrow +\infty} z_n = z$, we have $\lim_{n \rightarrow +\infty} \rho_{\mathbf{h}}(z_n) = \rho_{\mathbf{h}}(z)$. Thus, applying the dominated convergence theorem to the sequence of function $(\rho_{z_n})_{n \in \mathbb{N}}$ we obtain that the map $z \in (0, +\infty) \mapsto A_z$ is continuous for any $z \in (0, +\infty)$. Recalling now that the function $\rho_{\mathbf{h}}$ is bounded from above by $\lim_{z \rightarrow +\infty} \rho_{\mathbf{h}}(z) = 2 - \theta(\mathbf{h})$ and from below by $\lim_{z \rightarrow 0} \rho_{\mathbf{h}}(z) = 1 \{\theta(\mathbf{h}) = 1\}$, it follows that $\lim_{z \rightarrow +\infty} A_z = A_\infty$ and $\lim_{z \rightarrow 0} A_z = |\mathcal{D}|$ where $\mathcal{D} := \{\mathbf{h} \in \mathbb{R}^d : \theta(\mathbf{h}) = 1\}$. Finally, since (iii) means that there exists $\mathbf{h} \in \mathbb{R}^d$ such that $\theta(\mathbf{h}) \neq 1$, Proposition 2.37 holds and $\lim_{z \rightarrow 0} A_z = 0$. ■

Remark 2.39 – Alternative proof. We shall present another proof for the equivalence (ii) \Leftrightarrow (iii) (or equivalently (i) \Leftrightarrow (iii)), which may be easier than the one given above.

Proof that (i) implies (iii). Set $z \in (0, +\infty)$ and assume that (ii) holds. By convexity of the exponential function, $(y - x) \exp\{x\} \leq \exp\{y\} - \exp\{x\}$, for any $x, y \in \mathbb{R}$, and therefore,

$$0 \leq \frac{2 - \theta(\mathbf{h})}{z} \exp\{-2/z\} \leq \exp\{-\theta(\mathbf{h})/z\} - \exp\{-2/z\},$$

for every $\mathbf{h} \in \mathbb{R}^d$. Besides, according to Proposition 2.8, (i) is equivalent to

$$\int_{\mathbb{R}^d} \rho_z(\mathbf{h}) \, d\mathbf{h} < +\infty.$$

It follows that

$$\int_{\mathbb{R}^d} 2 - \theta(\mathbf{h}) \, d\mathbf{h} \leq \int_{\mathbb{R}^d} \exp\{-\theta(\mathbf{h})/z\} - \exp\{-2/z\} \, d\mathbf{h} = \sigma_z^2 \int_{\mathbb{R}^d} \rho_z(\mathbf{h}) \, d\mathbf{h} < +\infty.$$

Proof that (iii) implies (i). Set $z \in (0, +\infty)$ and consider the function $x \in \mathbb{R} \mapsto |x| \exp\{|x|\} - |\exp\{x\} - 1|$. It can be easily shown that the latter is nonnegative, and consequently, for every $\mathbf{h} \in \mathbb{R}^d$,

$$0 \leq \left| \exp\left\{\frac{2 - \theta(\mathbf{h})}{z}\right\} - 1 \right| \leq \frac{|2 - \theta(\mathbf{h})|}{z} \exp\left\{\frac{|2 - \theta(\mathbf{h})|}{z}\right\}.$$

Since $2 - \theta(\mathbf{h}) \geq 0$, it follows that

$$0 \leq \exp\left\{\frac{2 - \theta(\mathbf{h})}{z}\right\} - 1 \leq \frac{2 - \theta(\mathbf{h})}{z} \exp\{2/z\}.$$

Hence,

$$(\exp\{1/z\} - 1) \int_{\mathbb{R}^d} \rho_z(\mathbf{h}) d\mathbf{h} \leq \frac{\exp\{1/z\} - 1}{z} \exp\{2/z\} \int_{\mathbb{R}^d} 2 - \theta(\mathbf{h}) d\mathbf{h} < +\infty,$$

and using [Proposition 2.8](#), we can conclude that $A_z < +\infty$.

Now, let us now prove [Corollary 2.22](#) which is recalled below for convenience.

Corollary Let Z be a M2 process on \mathbb{R}^d and A_z be the integral range of the corresponding exceedance field above a threshold $z \in (0, +\infty)$. Let also Σ be a symmetric and positive-semidefinite $d \times d$ matrix, and $X = (X_1, \dots, X_d) \sim f$, where f is the associated shape function in [Eq. \(2.32\)](#). If f is Σ -radially symmetric and non-increasing, then the following proposition are equivalent

- (i) $\forall z \in (0, +\infty) \quad A_z < +\infty$,
- (ii) $E\{\|X\|^d\} < +\infty$,
- (iii) $\forall i \in \{1, \dots, d\} \quad E[|X_i|^d] < +\infty$.

In addition, when Σ is the identity matrix,

$$A_\infty := \int_{\mathbb{R}^d} 2 - \theta(\mathbf{h}) d\mathbf{h} = 2\omega_d E\{\|X\|^d\}.$$

Proof. Let Z be a M2 process. By definition, $\theta(\mathbf{h}) = \int_{\mathbb{R}^d} \max(f(\mathbf{y}), f(\mathbf{y} + \mathbf{h})) d\mathbf{y}$, for any $\mathbf{h} \in \mathbb{R}^d$ (see [Definition 2.20](#)). We thus have

$$\int_{\mathbb{R}^d} 2 - \theta(\mathbf{h}) d\mathbf{h} = \int_{\mathbb{R}^d} \int_{\mathbb{R}^d} \min(f(\mathbf{u}), f(\mathbf{u} + \mathbf{h})) d\mathbf{u} d\mathbf{h} = \int_{\mathbb{R}^d} \int_{\mathbb{R}^d} \min(f(\mathbf{u}), f(\mathbf{u} + \mathbf{h})) d\mathbf{h} d\mathbf{u},$$

where the last inequality is obtained by using the Fubini-Tonelli theorem. With substitution $\mathbf{v} = \mathbf{h} + \mathbf{u}$, it yields

$$\int_{\mathbb{R}^d} 2 - \theta(\mathbf{h}) d\mathbf{h} = \int_{\mathbb{R}^d} \int_{\mathbf{v}: f(\mathbf{u}) \geq f(\mathbf{v})} f(\mathbf{v}) d\mathbf{v} d\mathbf{u} + \int_{\mathbb{R}^d} \int_{\mathbf{v}: f(\mathbf{u}) < f(\mathbf{v})} f(\mathbf{u}) d\mathbf{v} d\mathbf{u}. \quad (2.49)$$

Hence, $\int_{\mathbb{R}^d} 2 - \theta(\mathbf{h}) d\mathbf{h} < +\infty$ if and only if both integrals in [Eq. \(2.49\)](#) are finite. Now, let Σ be a symmetric and positive-semidefinite $d \times d$ matrix, and suppose that the shape function f is Σ -radially symmetric and non-increasing (see [Definition 2.21](#)); it means that the level sets of f are d -ellipsoids centred in $\mathbf{0}$. Considering the first part of [Eq. \(2.49\)](#), it yields

$$\begin{aligned} \int_{\mathbb{R}^d} \int_{\mathbf{v}: f(\mathbf{u}) \geq f(\mathbf{v})} f(\mathbf{v}) d\mathbf{v} d\mathbf{u} &= \int_{\mathbb{R}^d} \int_{\mathbb{R}^d} f(\mathbf{v}) \mathbf{1}\{\|\mathbf{u}\|_\Sigma \leq \|\mathbf{v}\|_\Sigma\} d\mathbf{v} d\mathbf{u} \\ &= \int_{\mathbb{R}^d} f(\mathbf{v}) \int_{\mathbb{R}^d} \mathbf{1}\{\|\mathbf{u}\|_\Sigma \leq \|\mathbf{v}\|_\Sigma\} d\mathbf{u} d\mathbf{v} \end{aligned}$$

Besides, since all norms are equivalent in \mathbb{R}^d , there exist $C_1, C_2 \in (0, +\infty)$ such that, for any $\mathbf{u} \in \mathbb{R}^d$, $C_1\|\mathbf{u}\| \leq \|\mathbf{u}\|_\Sigma \leq C_2\|\mathbf{u}\|$. Thus, for any $\mathbf{v} \in \mathbb{R}^d$,

$$0 \leq \int_{\mathbb{R}^d} \mathbf{1}\{C_2\|\mathbf{u}\| \leq C_1\|\mathbf{v}\|\} d\mathbf{u} \leq \int_{\mathbb{R}^d} \mathbf{1}\{\|\mathbf{u}\|_\Sigma \leq \|\mathbf{v}\|_\Sigma\} d\mathbf{u} \leq \int_{\mathbb{R}^d} \mathbf{1}\{C_1\|\mathbf{u}\| \leq C_2\|\mathbf{v}\|\} d\mathbf{u}.$$

Write $X = (X_1, \dots, X_d)$ the random vector with probability density distribution f and let ω_d represents the volume of the unit d -ball. It then follows

$$0 \leq \omega_d \left(\frac{C_1}{C_2} \right)^d \mathbb{E} \left[\|X\|^d \right] \leq \int_{\mathbb{R}^d} f(\mathbf{v}) \int_{\mathbb{R}^d} \mathbf{1}_{\{\|\mathbf{u}\|_{\Sigma} \leq \|\mathbf{v}\|_{\Sigma}\}} d\mathbf{u} d\mathbf{v} \leq \omega_d \left(\frac{C_2}{C_1} \right)^d \mathbb{E} \left[\|X\|^d \right]. \quad (2.50)$$

Notice that the same bounds also hold for the second part of Eq. (2.49). Since

$$\sum_{i=1}^d \mathbb{E} \left[|X_i|^d \right] \leq \mathbb{E} \left[\|X\|^d \right] \leq d^{d/2} \mathbb{E} \left[\max(|X_1|^d, \dots, |X_d|^d) \right] \leq d^{d/2} \sum_{i=1}^d \mathbb{E} \left[|X_i|^d \right],$$

it thus follows that

$$\int_{\mathbb{R}} 2 - \theta(\mathbf{h}) d\mathbf{h} < +\infty \Leftrightarrow \mathbb{E}\{\|X\|^d\} < +\infty \Leftrightarrow \forall i \in \{1, \dots, d\}, \mathbb{E}\{|X_i|^d\} < +\infty. \quad (2.51)$$

In fine, when Σ is the identity matrix, remark that the bounds in Eq. (2.50) are equal, and therefore

$$\int_{\mathbb{R}} 2 - \theta(\mathbf{h}) d\mathbf{h} = 2\omega_d \mathbb{E}\{\|X\|^d\}. \quad (2.52)$$

■

Remark 2.40 In the more general case where the level sets of f are d -dimensional ellipsoids centred in $c \in \mathbb{R}^d$, i.e. for all $\mathbf{x} \in \mathbb{R}^d$, $f(\mathbf{x}) = f_0((\mathbf{x} - c)^t \Sigma (\mathbf{x} - c))$, where $f_0 : \mathbb{R}_+ \rightarrow \mathbb{R}_+$ is non-increasing, the results Eq. (2.51) and Eq. (2.52) still hold.

2.6.4 Mixing and mean-ergodicity properties

Before handling Proposition 2.30 we shall first prove the two following intermediate results.

Proposition 2.41 For any $A \in \mathcal{B}$, denote by f_A the probability distribution function of the Euclidean distance between two independent points uniformly distributed on A . For any $A \in \mathcal{B}$, any $\lambda \in (0, +\infty)$ and any distance $t \in (0, +\infty)$, it thus holds

$$f_{\lambda A}(\lambda t) = \frac{1}{\lambda} f_A(t),$$

Proof. For any $A \in \mathcal{B}$, denote by F_A the cumulative distribution function associated to f_A . Since $f_A = f_{A+y}$ for every $A \in \mathcal{B}$, every $y \in \mathbb{R}^d$, it is enough to prove Proposition 2.41 only for sets $A \in \mathcal{B}$ with barycenter $\mathbf{b}_A = \mathbf{0}$. Consider such a set and let $\lambda \in (0, +\infty)$. For every $x \in \mathbb{R}^d$, $t \in (0, +\infty)$, we shall first remark that

$$|\lambda A \cap B(\mathbf{x}, t)| = |\lambda A \cap \lambda_0 B(\mathbf{x}/\lambda, t/\lambda)| = |\lambda_0 (A \cap B(\mathbf{x}/\lambda, t/\lambda))| = \lambda^d |A \cap B(\mathbf{x}/\lambda, t/\lambda)|, \quad (2.53)$$

The last inequality comes from the Lebesgue measure properties. Now, let X and Y be two independent random variables uniformly distributed on λA . For any distance $t \in (0, +\infty)$, we thus have

$$F_{\lambda A}(t) = \mathbf{P}[\|X - Y\| \leq t] = \int_{\lambda A} \frac{|\lambda A \cap B(\mathbf{x}, t)|}{|\lambda A|^2} d\mathbf{x} = \frac{1}{\lambda^{2d}} \int_{\lambda A} \frac{|A \cap B(\mathbf{x}/\lambda, t/\lambda)|}{|A|^2} d\mathbf{x},$$

according to Eq. (2.53). Then, the substitution $\mathbf{u} = \mathbf{x}/\lambda$ in the last integral gives

$$F_{\lambda A}(t) = \int_A \frac{|A \cap B(\mathbf{u}, t/\lambda)|}{|A|^2} d\mathbf{u},$$

i.e. $F_{\lambda A}(t) = F_A(t/\lambda)$ for any $t \in (0, +\infty)$. Consequently, $f_{\lambda A}(\lambda t) = \frac{1}{\lambda} f_A(t)$ for any $t \in (0, +\infty)$. ■

Now, Proposition 2.41 enables us to generalize Corollary 1 in Koch (2017), which considered only increasing sequence of disks or squares in \mathbb{R}^2 , to higher dimensions and to set $A \in \mathcal{B}$. This is what is presented in the next proposition, the proof of which is entirely inspired by the one in Koch (2017).

Proposition 2.42 Let Z be a simple max-stable and isotropic SRF defined on \mathbb{R}^d , with ECF θ . Since the latter is radially symmetric, there exists a function $\theta_0 : (0, +\infty) \rightarrow [1, 2]$ such that $\theta(\mathbf{h}) = \theta_0(\|\mathbf{h}\|)$ for every $\mathbf{h} \in \mathbb{R}^d$. Now, consider a set $A \in \mathcal{B}$ with barycentre $\mathbf{b}_A \in \mathbb{R}^d$ and a threshold $z \in (0, +\infty)$. If $\lim_{\|\mathbf{h}\| \rightarrow +\infty} \theta(\mathbf{h})$ exists then

$$\lim_{\lambda \rightarrow +\infty} \text{Var}[I_z(\lambda A)] = \exp\left\{-\frac{\lim_{\lambda \rightarrow +\infty} \theta_0(\lambda)}{z}\right\} - \exp\left\{\frac{2}{z}\right\}.$$

Proof. Let $A \in \mathcal{B}$ with barycentre $\mathbf{b}_A \in \mathbb{R}^d$ and $\lambda \in (0, +\infty)$. Since A is bounded, there exists a ball $B_r(\mathbf{b}_A)$, with $r \in (0, +\infty)$, such that $A \subset B_r$. Consequently, $\lambda A \subset \lambda B_{\lambda r}(\mathbf{b}_A)$ and $f_{\lambda A}(t) = 0$ for, at least, any real $t > 2\lambda r$. Now let $z \in (0, +\infty)$ and recall from Eq. (2.27) that

$$\text{Var}[I_z(\lambda A)] = \frac{1}{|\lambda A|^2} \int_{\lambda A} \int_{\lambda A} \exp\left\{-\frac{\theta(\|\mathbf{x} - \mathbf{y}\|)}{z}\right\} - \exp\left\{\frac{2}{z}\right\} d\mathbf{x} d\mathbf{y}. \quad (2.54)$$

Notice also that $|\lambda A|^2$ can be thought of as the non discrete analogous of counting the total number of pairs of points in λA in the finite case. Similarly, $|\lambda A|^2 f_{\lambda A}(t)$ can be thought of as the number of pairs of points separated by the distance $t \in (0, +\infty)$ in λA . Since θ is radially symmetric, the right side of Eq. (2.54) may be thus rewritten

$$\int_0^{2\lambda r} f_{\lambda A}(t) \left(\exp\left\{-\frac{\theta_0(t)}{z}\right\} - \exp\left\{\frac{2}{z}\right\} \right) dt,$$

and given Proposition 2.41, Eq. (2.54) becomes

$$\text{Var}[I_z(\lambda A)] = \int_0^{2r} f_A(t) \left(\exp\left\{-\frac{\theta_0(\lambda t)}{z}\right\} - \exp\left\{\frac{2}{z}\right\} \right) dt.$$

Now, as shown in [Remark 2.44](#), f_A is bounded above by $2\pi^{d-1}/|A|$. This allows us to use the Lebesgue's dominated convergence Theorem to get

$$\begin{aligned} \lim_{\lambda \rightarrow +\infty} \int_0^{2r} f_A(t) \left(\exp \left\{ -\frac{\theta_0(\lambda t)}{z} \right\} - \exp \left\{ \frac{2}{z} \right\} \right) dt = \\ \int_0^{2r} f_A(t) \left(\exp \left\{ -\frac{\lim_{\lambda \rightarrow +\infty} \theta_0(\lambda)}{z} \right\} - \exp \left\{ \frac{2}{z} \right\} \right) dt. \end{aligned}$$

Since f_A is a density function, we finally obtain

$$\lim_{\lambda \rightarrow +\infty} \text{Var} [I_z(\lambda A)] = \exp \left\{ -\frac{\lim_{\lambda \rightarrow +\infty} \theta_0(\lambda)}{z} \right\} - \exp \left\{ \frac{2}{z} \right\}.$$

■

Using [Proposition 2.42](#) we can now tackle the proof of [Proposition 2.30](#) which is actually the same as in [Koch \(2017\)](#), see [Remark 2.43](#) for some comments. Let first recall, for convenience, the statement of [Proposition 2.30](#).

Proposition – *Mixing and mean-ergodicity properties.* Set $z \in (0, +\infty)$ and let Z be a simple max-stable and isotropic SRF on \mathbb{R}^d , with extremal coefficient function θ . If $\lim_{\|\mathbf{h}\| \rightarrow +\infty} \theta(\mathbf{h})$ exists then the following propositions are equivalent:

- (i) Z is mixing ,
- (ii) I_z is mean-ergodic .

Proof. Set $z \in (0, +\infty)$. We already know that (i) implies (ii), see [Remark 2.25](#) and [Remark 2.28](#). Let us prove the opposite implication and assume (ii). If $\lim_{\|\mathbf{h}\| \rightarrow +\infty} \theta(\mathbf{h})$ exists, then [Proposition 2.42](#) gives

$$\exp \left\{ -\frac{\lim_{\lambda \rightarrow +\infty} \theta_0(\lambda)}{z} \right\} - \exp \left\{ \frac{2}{z} \right\} = 0,$$

i.e. $\lim_{\lambda \rightarrow +\infty} \theta_0(\lambda) = 2$, which means that Z is mixing, see [Theorem 2.29](#). ■

Remark 2.43 To prove [Proposition 2.30](#), it was sufficient to generalize Corollary 1 in [Koch \(2017\)](#) to higher dimensions only, and not to any set $A \in \mathcal{B}$. We carried out anyway this last generalization, hoping that it may be helpful in future works.

Remark 2.44 Let $A \in \mathcal{B}$ and f_A be the density function defined in Proposition 2.41 with corresponding cumulative distribution function F_A . The latter depends on the geometric covariogram K_A of A , introduced in Subsection 2.2.1. Indeed, for any $t \in (0, +\infty)$

$$F_A(t) = \int_A \frac{|A \cap B(\mathbf{x}, t)|}{|A|^2} d\mathbf{x} = \frac{1}{|A|^2} \int_{\mathbb{R}^d} \int_{\mathbb{R}^d} \mathbf{1}\{\|\mathbf{x} - \mathbf{y}\| \leq t\} \mathbf{1}\{\mathbf{x} \in A\} \mathbf{1}\{\mathbf{y} \in A\} d\mathbf{x} d\mathbf{y},$$

which becomes, with substitution $\mathbf{h} = \mathbf{x} - \mathbf{y}$ in the last integral,

$$F_A(t) = \frac{1}{|A|^2} \int_{\mathbb{R}^d} \mathbf{1}\{\|\mathbf{h}\| \leq t\} K_A(\mathbf{h}) d\mathbf{h}. \quad (2.55)$$

By converting Eq. (2.55) into hyperspherical coordinates, we get

$$F_A(t) = \frac{1}{|A|^2} \int_0^t \int_{[0, \pi]^{d-2} \times [0, 2\pi)} K_A(tx_s) ds dt,$$

where

- $\mathbf{s} = (s_1, \dots, s_{n-1})$,
- $x_s = (\cos(s_1), \sin(s_1) \cos(s_2), \sin(s_1) \sin(s_2) \cos(s_3), \dots, (\sin(s_1), \dots, \sin(s_{n-1})))$.

Hence,

$$f_A(t) = \frac{1}{|A|^2} \int_{[0, \pi]^{d-2} \times [0, 2\pi)} K_A(tx_s) ds dt$$

and is bounded above by $2\pi^{d-1}/|A|$ since $K_A(\mathbf{h})/|A| \leq 1$ for any $\mathbf{h} \in \mathbb{R}^d$.

2.6.5 M2 process with Cauchy density shape function

In this part, we shall prove the next proposition.

Proposition 2.45 Let Z be an isotropic stationary M2 process defined on \mathbb{R}^d where the shape function f is the multivariate Cauchy density function specified by Eq. (2.38). Its extremal coefficient function θ is thus given, for every $\mathbf{h} \in \mathbb{R}^d$, by

$$\theta(\mathbf{h}) = 2G\left(\frac{\|\mathbf{h}\|_{\Sigma^{-1}}}{2}\right),$$

where G stands for the c.d.f. of a standard univariate Cauchy distribution.

Proof. Set $\mathbf{h} \in \mathbb{R}^d$ and remember from Definition 2.20 that

$$\begin{aligned} \theta(\mathbf{h}) &= \int_{\mathbb{R}^d} \max(f(\mathbf{y}), f(\mathbf{y} + \mathbf{h})) d\mathbf{y} \\ &= \int_{\mathbb{R}^d} f(\mathbf{y}) \mathbf{1}\{f(\mathbf{y}) > f(\mathbf{y} + \mathbf{h})\} d\mathbf{y} + \int_{\mathbb{R}^d} f(\mathbf{y}) \mathbf{1}\{f(\mathbf{y}) > f(\mathbf{y} - \mathbf{h})\} d\mathbf{y} \\ &= \mathbf{P}[f(X) \geq f(X + \mathbf{h})] + \mathbf{P}[f(X) \geq f(X - \mathbf{h})], \end{aligned}$$

where $X \sim f$. Since f is Σ^{-1} -radially symmetric and non-increasing, $f(X) \geq f(X + \mathbf{h})$ if and only if

$$X^T \Sigma^{-1} X < (X + \mathbf{h})^T \Sigma^{-1} (X + \mathbf{h}),$$

which occurs if and only if

$$X^T \Sigma^{-1} \mathbf{h} > -\frac{\mathbf{h}^T \Sigma^{-1} \mathbf{h}}{2}.$$

Since

$$\frac{X^T \Sigma^{-1}}{\sqrt{\mathbf{h}^T \Sigma^{-1} \mathbf{h}}}$$

is standard Cauchy distributed (see e.g. Lee et al., 2014), it follows that

$$\mathbf{P}[f(X) \geq f(X + \mathbf{h})] = G\left(\frac{\|\mathbf{h}\|_{\Sigma^{-1}}}{2}\right).$$

Similarly, it can be shown that $\mathbf{P}[f(X) \geq f(X - \mathbf{h})] = G(\|\mathbf{h}\|_{\Sigma^{-1}}/2)$, which concludes the proof. \blacksquare

2.7 SUPPLEMENTS ABOUT VAN-HOVE SEQUENCES

Let us introduce or recall some notation. In the following, \mathbb{R}^d is equipped with the distance d . For any measurable subset V of \mathbb{R}^d , we shall denote by \bar{V} its closure, by $\overset{\circ}{V}$ its interior, and by ∂V its boundary. Its translation by a vector $\mathbf{x} \in \mathbb{R}^d$ is written $V + \mathbf{x} := \{\mathbf{v} + \mathbf{x} : \mathbf{v} \in V\}$ and, for any $\mathbf{x} \in \mathbb{R}^d$, the distance $d(\mathbf{x}, V) := \inf\{d(\mathbf{x}, \mathbf{v}) : \mathbf{v} \in V\}$ stands for the distance between \mathbf{x} and V . The Minkowski sum and difference of two bounded measurable subsets V and W of \mathbb{R}^d are respectively defined as

$$V \oplus W := \bigcup_{\mathbf{w} \in W} V + \mathbf{w} \quad \text{and} \quad V \ominus W := \bigcap_{\mathbf{w} \in W} V + \mathbf{w}.$$

Recall now that \check{W} denotes the symmetric of W with respect to the origin $\mathbf{0}$. The sets $V \oplus \check{W}$ and $V \ominus \check{W}$ represent respectively the dilation and the erosion of V by the structuring element W . For a more intuitive expression, notice that

$$V \oplus \check{W} = \left\{ \mathbf{x} \in \mathbb{R}^d : (W + \mathbf{x}) \cap V \neq \emptyset \right\} \quad \text{and} \quad V \ominus \check{W} = \left\{ \mathbf{x} \in \mathbb{R}^d : W + \mathbf{x} \subset V \right\}.$$

See Figure 2.13 for an illustrative example in two dimensions.

We present now the concept of a Van-Hove sequence as it is defined in Koch et al. (2018).

Definition 2.46 Let $(V_n)_{n \in \mathbb{N}}$ be a sequence of sets in \mathcal{B} . It is called a Van Hove sequence if it converges to \mathbb{R}^d in the following sense:

- (i) $V_n \subset V_{n+1}$, for all $n \in \mathbb{N}$,
- (ii) $\bigcup_{n \in \mathbb{N}} V_n = \mathbb{R}^d$, and

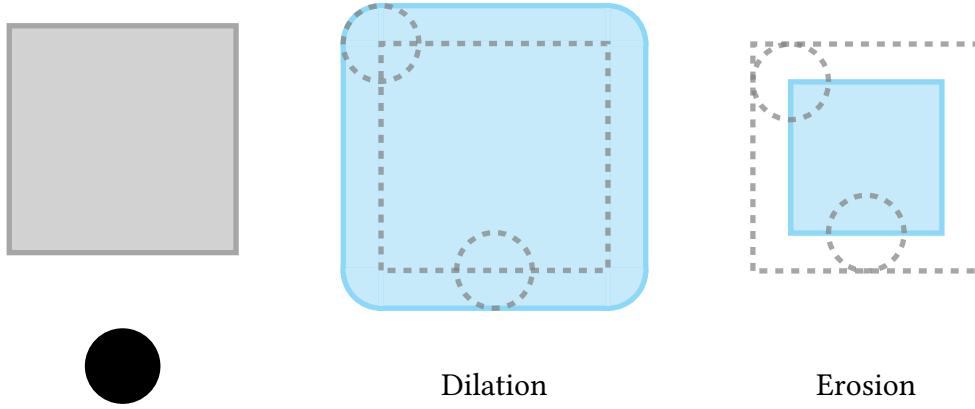


FIGURE 2.13 – Dilatation and erosion (blue area) of a 3×3 square (gray area) by the disk $B_{1/2}$ (black disk).

$$(iii) \quad \lim_{n \rightarrow +\infty} \frac{|\partial V_n \oplus B_r|}{|V_n|} = 0, \quad \text{for all } r \in (0, +\infty).$$

This convenient concept has been used in different fields such as dynamical systems theory (see e.g. Lee et al., 2002; Moody and Strungaru, 2004; Lenz and Stollmann, 2005), thermodynamics (see e.g. Catto et al., 1998; Ruelle, 2004), stochastic geometry (see e.g. Baake et al., 2009; Spodarev, 2014) or spatial extreme value theory (see e.g. Koch, 2017; Koch et al., 2018; Koch, 2019). Notice that this definition is more constraining than the one we propose to characterize the convergence to \mathbb{R}^d (see Definition 2.3). As it is shown in Proposition 2.47, the condition (iii) is stronger than our third condition. It means that the boundary of V_n becomes negligible in front of its interior as $n \rightarrow +\infty$. An example of sequence that does not fulfilled (iii) in Definition 2.46 but satisfies (iii) in Definition 2.3 is given at the end of the section.

Proposition 2.47 Let $(V_n)_{n \in \mathbb{N}}$ be a sequence of bounded measurable subsets of \mathbb{R}^d with positive volume satisfying (iii) in Definition 2.46. Then for any compact subset W of \mathbb{R}^d ,

$$\lim_{n \rightarrow +\infty} \frac{|V_n \ominus \check{W}|}{|V_n|} = 1.$$

Proposition 2.47 holds, in particular, for a Van-Hove sequence. Before proving Proposition 2.47, we establish the following lemmas.

Lemma 2.48 Let V be a non-empty subset of \mathbb{R}^d and $\mathbf{x} \in \mathbb{R}^d$. If $\mathbf{x} \notin \overset{\circ}{V}$ then

$$d(\mathbf{x}, \partial V) = d(\mathbf{x}, \bar{V}).$$

Proof. By definition $\partial V \subset \bar{V}$, thus $d(\mathbf{x}, \bar{V}) \leq d(\mathbf{x}, \partial V)$ for any $\mathbf{x} \in \mathbb{R}^d$. Let us prove the converse inequality. The closure \bar{V} is a closed subset, hence there exists $\mathbf{y} \in \bar{V}$ such that

$d(\mathbf{x}, \mathbf{y}) = d(\mathbf{x}, \bar{\mathbf{V}})$. Let $\epsilon > 0$ and assume that $B_\epsilon(\mathbf{y}) \subsetneq \bar{\mathbf{V}}$. There exists $\tilde{\mathbf{y}} \in \bar{\mathbf{V}}$ closer to \mathbf{x} than \mathbf{y} which is impossible by definition of \mathbf{y} , therefore $B_\epsilon(\mathbf{y}) \subset \bar{\mathbf{V}}$. This is true for all $\epsilon > 0$, thus $\mathbf{y} \notin \overset{\circ}{\bar{\mathbf{V}}}$, that is $\mathbf{y} \in \partial V$. Consequently $d(\mathbf{x}, \partial V) \leq d(\mathbf{x}, \bar{\mathbf{V}})$ which concludes the proof. ■

Lemma 2.49 Let V be a measurable bounded subset of \mathbb{R}^d and $r \in \mathbb{R}_+^*$. Then

$$\partial V \oplus B_r = (\bar{V} \oplus B_r) \setminus (\overset{\circ}{V} \ominus B_r).$$

Proof. The equality is immediate if $\overset{\circ}{V}_n = \emptyset$, so we shall assume $\overset{\circ}{V}_n \neq \emptyset$ in the sequel. To prove the equality of the two subsets, we shall prove the double inclusion.

Proof that $\partial V_n \oplus B_r \subset (\bar{V} \oplus B_r) \setminus (\overset{\circ}{V} \ominus B_r)$ It stems from the inclusion properties of Minkowski addition, cf. e.g. [Molchanov \(2017, p.565\)](#)

Proof that $(\bar{V} \oplus B_r) \setminus (\overset{\circ}{V} \ominus B_r) \subset \partial V_n \oplus B_r$ By contradiction: let us assume that there exists $\mathbf{x} \in \left((\bar{V} \oplus B_r) \setminus (\overset{\circ}{V} \ominus B_r) \right) \cap (\partial V_n \oplus B_r)^c$. In particular, $\mathbf{x} \in (\partial V_n \oplus B_r)^c$ implies that $d(\mathbf{x}, \partial V_n) > r$, i.e.

$$B_r(\mathbf{x}) \cap \partial V = \emptyset \tag{2.56}$$

Now, we shall consider both the cases $\mathbf{x} \notin \overset{\circ}{V}_n$ and $\mathbf{x} \in \overset{\circ}{V}_n$ separately. First, assume $\mathbf{x} \notin \overset{\circ}{V}_n$. As stated in [Lemma 2.48](#), $d(\mathbf{x}, \bar{V}) = d(\mathbf{x}, \partial V) > r$, i.e. $\mathbf{x} \notin \bar{V} \oplus B_r$ which is impossible. On the other hand, suppose $\mathbf{x} \in \overset{\circ}{V}_n$. By assumption, $\mathbf{x} \notin \overset{\circ}{V} \ominus B_r$, i.e. $B_r(\mathbf{x}) \not\subset \overset{\circ}{V}_n$. Thus there exists $\mathbf{y} \in B_r(\mathbf{x})$ such that $\mathbf{y} \in (\overset{\circ}{V})^c$. Then, notice that $\mathbf{y} \in B_r(\mathbf{x})$ implies $d(\mathbf{y}, \bar{V}) \leq r$ and that $d(\mathbf{y}, \bar{V}) = d(\mathbf{y}, \partial V)$, according to [Lemma 2.48](#). As a consequence $d(\mathbf{y}, \partial V) \leq r$, hence $B_r(\mathbf{x}) \cap \partial V \neq \emptyset$ which contradicts [Eq. \(2.56\)](#). The inclusion $(\bar{V} \oplus B_r) \setminus (\overset{\circ}{V} \ominus B_r) \subset \partial V_n \oplus B_r$ is proved. ■

Proof of Proposition 2.47. We shall start by proving the proposition when $W = B_r$ for some positive r . Let $n \in \mathbb{N}$. By definition we have $\overset{\circ}{V}_n \ominus B_r \subset V_n \ominus B_r \subsetneq V_n \subsetneq V_n \oplus B_r \subset \bar{V}_n \oplus B_r$, hence $0 \leq |V_n| - |V_n \ominus B_r| \leq |\bar{V}_n \oplus B_r| - |\overset{\circ}{V}_n \ominus B_r|$. By [Lemma 2.49](#), the right hand part of this last inequality corresponds exactly to $|\partial V_n \oplus B_r|$. It was assumed to be dominated by $|V_n|$ as $n \rightarrow +\infty$, therefore so is $|V_n| - |V_n \ominus B_r|$. This implies that $\lim_{n \rightarrow +\infty} \frac{|V_n \ominus B_r|}{|V_n|} = 1$, which is true for any $r \in (0, +\infty)$.

We shall now consider any compact $W \subset \mathbb{R}^d$. Again, let $n \in \mathbb{N}$. Since W is compact in \mathbb{R}^d , thus so is its symmetric $\check{W} := \{-\mathbf{w} : \mathbf{w} \in W\}$ and consequently there exists $\mathbf{w} \in W$ and $r \in (0, +\infty)$ such that $\check{W} + \mathbf{w} \subset B_r$. In particular, it implies that $V_n \ominus B_r \subset V_n \ominus (\check{W} + \mathbf{w})$, cf. e.g. [Matheron \(1975\)](#). By construction $\check{W} + \mathbf{w}$ contains $\{0\}$, thus $V_n \ominus (\check{W} + \mathbf{w}) \subset V_n$. As a consequence

$$1 \geq \frac{|V_n \ominus (\check{W} + \mathbf{w})|}{|V_n|} \geq \frac{|V_n \ominus B_r|}{|V_n|},$$

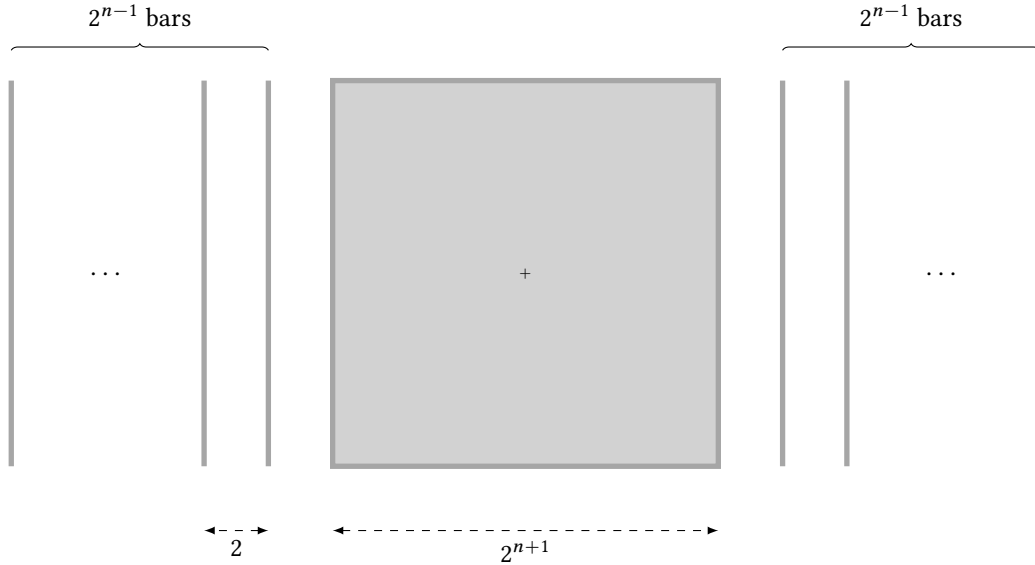


FIGURE 2.14 – The sets V_n centered in $\mathbf{0}$ (grey area). It is the union of a $2^{n+1} \times 2^{n+1}$ square and of 2^n vertical bars of length 2^{n+1} . The bars are equally spaced and regularly placed on each side of the square.

where $\frac{|V_n \ominus (\check{W} + \mathbf{w})|}{|V_n|} = \frac{|(V_n \ominus \check{W}) + \mathbf{w}|}{|V_n|} = \frac{|V_n \ominus \check{W}|}{|V_n|}$. Finally, since we have seen that $\lim_{n \rightarrow +\infty} \frac{|V_n \ominus B_r|}{|V_n|} = 1$, using the squeeze theorem we obtain that $\lim_{n \rightarrow +\infty} \frac{|V_n \ominus \check{W}|}{|V_n|} = 1$ as well. ■

Example 2.50 Sequence that does not satisfy the Van Hove conditions This example is taken from [Catto et al. \(1998, p.17-18\)](#). Let $d = 2$ and consider the sequence of sets $(V_n)_{n \in \mathbb{N}}$ such that, for any $n \in \mathbb{N}$, the set $V_n \in \mathcal{B}$ is the union of a square of side 2^{n+1} centered in $\mathbf{0}$, and of 2^n bars that are 2^{n+1} long. The bars are placed so that $V_n \subset V_{n+1}$. See [Figure 2.14](#) for a representation of V_n . The sequence satisfies the two first conditions in [Definition 2.46](#) but not the third one : indeed, for fixed $n \in \mathbb{N}$, it holds $|\partial V_n \oplus B_1| > |V_n|$ (see [Figure 2.15](#)), and thus $\lim_{n \rightarrow +\infty} \frac{|\partial V_n \oplus B_{1/2}|}{|V_n|} \neq 0$. Nonetheless, it satisfies [\(iii\)](#) in [Definition 2.3](#). For any $n \in \mathbb{N}$, let W_n be a square of side 2^{n+1} . The limit in [\(iii\)](#) is actually the same for $(V_n)_{n \in \mathbb{N}}$ and $(W_n)_{n \in \mathbb{N}}$, and since $W_n \uparrow \mathbb{R}^d$, it is ultimately equal to 1.

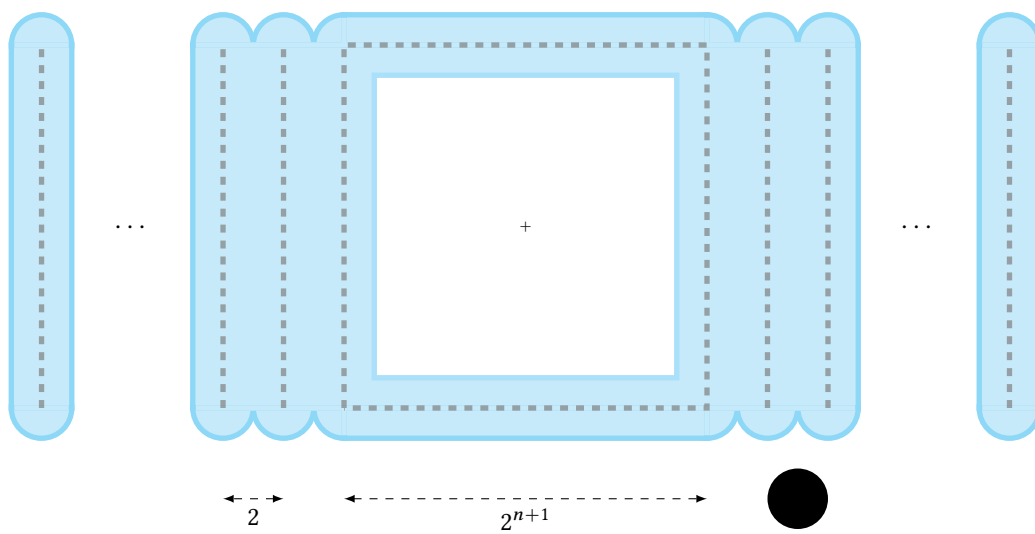


FIGURE 2.15 – Dilation (blue area) of ∂V_n (gray dashed lines) by the disk B_1 (black disk). It is the union of both dilation of the 2^n bars and of the $2^{n+1} \times 2^{n+1}$ square by the same structuring element B_1 . Their volumes are respectively equal to $2^{2(n+1)} + \pi 2^{n+1}$ and $2^{n+4} + 2\pi - 4$.

ESTIMATION OF THE EXTREMAL COEFFICIENT FUNCTION BASED ON A SINGLE OBSERVATION

Résumé *Considérons de nouveau un champ stationnaire max-stable simple. En utilisant les travaux présentés dans le chapitre précédent, un estimateur non paramétrique de sa fonction coefficient extrémal est proposé. Il dépend de l'estimateur de type Nadaraya-Watson du variogramme du champ des excès correspondant étudié par [García-Soidán et al. \(2004\)](#) et [García-Soidán \(2007\)](#). À partir de leurs travaux, les propriétés asymptotiques de ce nouvel estimateur sont établies quand celui-ci est évalué à partir d'un unique jeu de données spatialisées. En particulier, sous certaines hypothèses concernant la portée intégrale du champ des excès, nous montrons que cet estimateur est consistant et asymptotiquement normal. Une étude par simulation est menée afin de vérifier ces propriétés asymptotiques sur des échantillons de taille finie. Une méthode de validation croisée est notamment proposée pour sélectionner la largeur de la fenêtre associée à cette estimation non-paramétrique. Les résultats sont satisfaisants, excepté au voisinage de 0 : c'est une conséquence des effets de bords de l'estimateur à noyau du variogramme.*

3.1 INTRODUCTION

Consider a simple stationary max-stable random field Z defined on \mathbb{R}^d . We want to assess its dependence structure, but without assuming any specific model. As specified in [Chapter 1](#), due to high-dimensional distributional complexity, the study of the dependence is often limited to the bivariate distributions. Since Z is stationary, this amounts to estimating its extremal coefficient function (ECF) θ . Several estimators of θ , which do not require to assume a particular model for Z , have been proposed in the literature (see e.g. [Smith, 1990](#); [Capéraà et al., 1997](#); [Schlather and Tawn, 2003](#); [Cooley et al., 2006](#); [Bel et al., 2008](#)). They are generally used in a spatio-temporal context, when spatial replications of Z are observed through time. As detailed in [Chapter 1](#), to the best of our knowledge, only [Bel et al. \(2008\)](#) and [Naveau et al. \(2009\)](#) have estimated the extremal coefficient function from a single and partially observed realization of Z . However, the asymptotic properties of the estimators under study have not been theoretically investigated. This is done in [Dombry and Eyi-Minko \(2012\)](#) for some estimators of θ . In particular, they establish a central limit theorem for sample continuous max-id SRF defined

on \mathbb{Z}^d , when considering increasing domain asymptotics. Then, in the max-stable case, this result is used to obtain the asymptotic normality of three different estimators, among which the F-madogram estimator. This property holds under the condition that $2 - \theta(\mathbf{h})$ vanishes fast enough as $\|\mathbf{h}\| \rightarrow +\infty$. For all we know, no generalization to \mathbb{R}^d has been proposed so far. More generally, we are not aware of any other works about the asymptotic properties of estimators of θ , when having only one spatial set of observations. For any $z \in (0, +\infty)$, let I_z be the exceedance field above z associated with Z , defined in Eq. (2.26). In this chapter, we propose a new nonparametric estimator of θ , based on a Nadaraya-Watson estimator of the variogram of I_z proposed by García-Soidán (2007). From the asymptotic properties of this kernel estimator, which have been revealed in the paper, we deduce sufficient conditions on Z so that the nonparametric estimator of θ is asymptotically consistent and normal. These conditions are related to the mixing property of Z and the integral range A_z of I_z .

The chapter is structured as follows. We start off in Section 3.2 with the introduction of a few notation. In Section 3.3, the kernel estimator of the variogram of I_z , as well as its asymptotic properties, are presented. A special attention is given to the conditions under which the asymptotic results hold. In particular, some of these assumptions are modified so that they are more adapted to the extreme context of our study. Then, the new nonparametric estimator of θ is introduced and its asymptotic properties are derived. The results are illustrated in Section 3.4. In addition, the performances of our estimator of θ are compared with those of the F-madogram estimator. Assets and required improvements of our work are finally discussed in Section 3.5. Technical proofs and supplements are postponed to Section 3.6.

We shall point out that this work has been funded by Télécom Paris. It has been realized during a 6-month stay at Télécom Paris, under the supervision of E. Chautru (Mines ParisTech, PSL University) and A. Sabourin (Télécom Paris). It is a first version of an article that should be submitted in 2021.

3.2 SETTINGS

In this chapter, we shall employ the notation introduced in Chapter 2 (see Section 2.1). In addition, for any subsets $V, W \subset \mathbb{R}^d$, the distance $d(V, W)$ between V and W is given by $d(V, W) := \inf\{\|\mathbf{v} - \mathbf{w}\|, (\mathbf{v}, \mathbf{w}) \in V \times W\}$. Let also \xrightarrow{d} stands for the convergence in distribution.

In the sequel, unless specified otherwise, Z is a stochastically continuous simple max-stable SRF satisfying Assumption 2.1 and Assumption 2.2. It thus admits the spectral representation

given in Eq. (1.13). Let Y be the associated nonnegative spectral process. Let also $m \in \mathbb{N}^*$, $\mathbf{x}_1, \dots, \mathbf{x}_m \in \mathbb{R}^d$ and $z \in (0, +\infty)$. From Eq. (1.14) in Chapter 1 it holds

$$\mathbf{P}[Z(\mathbf{x}_1) \leq z, \dots, Z(\mathbf{x}_m) \leq z] = \exp \left\{ -\mathbf{E} \left[\max_{i \in \{1, \dots, m\}} \frac{Y(\mathbf{x}_i)}{z} \right] \right\}.$$

Now, define the coefficient $\vartheta(\{\mathbf{x}_1, \dots, \mathbf{x}_m\}) := \mathbf{E} \left[\max_{i \in \{1, \dots, m\}} Y(\mathbf{x}_i) \right]$. By definition of Y , $\vartheta(\{\mathbf{x}_1\}) = 1$. When $m \geq 2$, such a coefficient is termed *extremal coefficient* (see Smith, 1990); it is valued in $[1, m]$. As remarked e.g. in Schlather and Tawn (2002), when $Z(\mathbf{x}_1), \dots, Z(\mathbf{x}_m)$ are mutually independent, then

$$\mathbf{P}[Z(\mathbf{x}_1) \leq z, \dots, Z(\mathbf{x}_m) \leq z] = \exp \left\{ -\frac{m}{z} \right\}.$$

Hence, $\vartheta(\{\mathbf{x}_1, \dots, \mathbf{x}_m\})$ may be interpreted as the number of independent margins of the m -variate vector $(Z(\mathbf{x}_1), \dots, Z(\mathbf{x}_m))$; the case $\vartheta(\{\mathbf{x}_1, \dots, \mathbf{x}_m\}) = 1$ referring to (a.s.) equality between all its margins. In the sequel, for simplicity of notation, we shall write $\vartheta(\mathbf{x}_1, \dots, \mathbf{x}_m) = \vartheta(\{\mathbf{x}_1, \dots, \mathbf{x}_m\})$. Notice that, to all m -variate extremal coefficients $\vartheta(\mathbf{x}_1, \dots, \mathbf{x}_m)$, can be attached the function

$$(\mathbf{x}_1, \dots, \mathbf{x}_m) \in \mathbb{R}^{md} \mapsto \vartheta(\mathbf{x}_1, \dots, \mathbf{x}_m), \quad (3.1)$$

which is continuous since Z is continuous in probability (see Strokorb and Schlather, 2015, Lemma 23). In the following, the m -variate extremal coefficients and this function are indistinctly employed. Hence, depending on the context, $\vartheta(\mathbf{x}_1, \dots, \mathbf{x}_m)$ may also refer to the function (3.1) evaluated in $(\mathbf{x}_1, \dots, \mathbf{x}_m)$. We shall remark that for any $\mathbf{x}_1, \mathbf{x}_2 \in \mathbb{R}^d$, $\vartheta(\mathbf{x}_1, \mathbf{x}_2) = \theta(\mathbf{x}_1 - \mathbf{x}_2)$, where θ is the ECF of Z . Finally, set a threshold $z \in (0, +\infty)$. The stationary exceedance field above z is again denoted by I_z :

$$I_z(\mathbf{x}) = \mathbf{1}\{Z(\mathbf{x}) > z\}, \quad \mathbf{x} \in \mathbb{R}^d. \quad (3.2)$$

Besides $C_z : \mathbf{h} \in \mathbb{R}^d \mapsto \text{Cov}[I_z(\mathbf{0}), I_z(\mathbf{h})]$ and $\gamma_z : \mathbf{h} \in \mathbb{R}^d \mapsto \frac{1}{2} \mathbf{E}[(I_z(\mathbf{h}) - I_z(\mathbf{0}))^2]$ stand for its covariance function and its variogram, respectively.

3.3 A NEW NONPARAMETRIC VARIOGRAM BASED ESTIMATOR

3.3.1 Covariance or variogram ?

Set $z \in (0, +\infty)$ and recall from Chapter 2 that, for any $\mathbf{h} \in \mathbb{R}^d$,

$$C_z(\mathbf{h}) = \exp\{-\theta(\mathbf{h})/z\} - \exp\{-2/z\}. \quad (3.3)$$

Let $\mathbf{h} \in \mathbb{R}^d$. Since $\gamma(\mathbf{h}) = C(0) - C(\mathbf{h})$, it follows from [Eq. \(3.3\)](#) that

$$\gamma_z(\mathbf{h}) = \exp\{-1/z\} - \exp\{-\theta(\mathbf{h})/z\}. \quad (3.4)$$

Therefore, an estimator of θ may be obtained by considering an estimator of either the covariance function or the variogram. The objective is then to find, in the literature, an estimator of C_z or γ_z built on a single and partially observed realization of I_z , for which asymptotic properties have already been established. Furthermore, since we do not want to assume a particular model for the ECF, we focus on nonparametric estimators. We shall point out, even if the variogram and the covariance function are related, working with one or the other is in general not equivalent. As already mentioned in [Chapter 1](#), the estimation of the latter, contrary to the variogram, requires the knowledge of the expectation of I_z . When this expectation has to be estimated because it is unknown, this generates biased estimators of the correlation function. Hence, estimators of C_z and γ_z do not have necessarily the same properties. More generally, the variogram only needs the process to be intrinsically stationary to be well-defined, whereas the covariance function exists only for second-order stationary RF. That is why the variogram is usually preferred in geostatistical studies. Since, in our case, I_z is assumed to be stationary, the choice between considering C_z or γ_z shall mainly depend on the asymptotic properties of the respective estimators that are found in the literature. Before presenting them, we shall briefly discuss about asymptotic regime.

Remark 3.1 – Type of asymptotics. When considering asymptotic properties of estimators computed from only one spatial set of observation, the way the number of observations increases shall be defined; this constitutes the asymptotic regime of the study. Schematically, there exist two types of asymptotic regimes: the *infill* asymptotics and the *increasing domain* asymptotics. In the former framework, the number of observations grows in a fixed and bounded region, *i.e.* observations get denser. Consequently, they may be strongly dependent to each other and, as shown by [Lahiri \(1996\)](#), this can lead to inconsistent estimators. On the contrary, increasing domain asymptotics entails that the observations are always separated by a minimum distance, so that the region is expanding as the number of observations increases. As it is done hereafter, these two types of asymptotics may be combined.

Let Z be a second-order SRF defined on \mathbb{R}^d , with covariance function C and variogram γ . There is not a lot of nonparametric estimators of C and γ for which asymptotic properties have been investigated, when having only one set of spatial observations. We can first mention the seminal experimental variogram introduced in [Chapter 1](#) (see [Eq. \(1.18\)](#)) and the corresponding empirical estimator of the correlation function (see *e.g.* [Cressie, 1993](#), Equation 2.4.4). Under some conditions, their asymptotic normality has been established when considering increasing domain asymptotic. For the covariance function, this is shown in [Anderson](#)

(1971, Theorem 8.4.2) or Fuller (1996, Theorem 6.3.3), in the unidimensional case, when the time process Z is equal to a weighted sum of *i.i.d.* random variables. For the variogram, this is proved in Davis and Borgman (1982) when the spatial process Z is assumed to be m -dependent, for $m \in \mathbb{R}_+^*$. That is, when $(Z(\mathbf{x}))_{\mathbf{x} \in V}$ and $(Z(\mathbf{x}))_{\mathbf{x} \in W}$ are independent for any two subsets $V, W \subset \mathbb{R}^d$ separated by the distance m . Properties of non-parametric kernel estimators of C and γ have also been studied when considering both infill and increasing domain asymptotics. In the unidimensional case Hall et al. (1994) propose a Nadaraya-Watson estimator of C . Under appropriate mixing conditions, the authors show that it is consistent. In the d -dimensional case and under additional stronger mixing conditions, Hall and Patil (1994) demonstrates that the integrated squared error of this estimator, over a bounded set of locations $\mathbf{h} \in \mathbb{R}^d$, converges in distribution to the integral, over this same set, of a squared Gaussian RF. Along the lines of these works, García-Soidán et al. (2004) also propose a Nadaraya-Watson estimator of γ . When Z is isotropic and under similar conditions than in Hall et al. (1994), they show that it is consistent. García-Soidán (2007) generalizes these results to the anisotropic case. Furthermore, under additional stronger mixing conditions that are closed to the conditions in Hall and Patil (1994), the author establishes the asymptotic normality of this estimator. The results in García-Soidán (2007) are the most complete results we were able to find. We thus decide to based the estimator of the ECF on this nonparametric kernel estimator.

This estimator is detailed in the next subsection, when estimating the variogram of the exceedance field I_z of a simple max-stable SRF. We shall also introduce the assumptions under which its asymptotic properties are established. Before, let us conclude this part with the following remarks.

Remark 3.2 – *On conditionally negative-semidefiniteness.* Let Z be a second-order SRF on \mathbb{R}^d with covariance function C and variogram γ . As specified in Chapter 1, the latter are positive-semidefinite and conditionally negative-semidefinite, respectively. In particular, the conditionally negative-semidefiniteness of γ ensures that, when predicting Z at unobserved locations, the variance of the kriging error is nonnegative. The estimators of C and γ presented above do not fulfill these conditions. Hall et al. (1994), Hall and Patil (1994) and García-Soidán et al. (2004) propose some modifications of their estimators to ultimately obtain estimators that are themselves a covariance function or a variogram. These estimators are more complicated to handle and do not necessarily conserve the asymptotic properties of the original ones. For simplicity, and since we do not want later to perform some kriging methods, we shall not try to constrain the Nadaraya-Watson estimator of the variogram to be conditionally negative-semidefinite.

Remark 3.3 – *Ergodicity in the covariance.* Let Z be a second-order SRF on \mathbb{R}^d with expectation μ and covariance function C . Can the expectation be estimated starting from a single realization of Z ? As detailed in [Chapter 2](#), part of the answer is brought by the concepts of ergodicity in the mean and of integral range. When trying to estimate the covariance function from a unique realization, the equivalent condition of ergodicity in the mean is the so-called *ergodicity in the covariance*, see [Subsection 3.6.4](#). It could be interesting to investigate this notion and maybe introduce an equivalent concept of the integral range for the covariance function. Such a work is not conducted in this chapter. Besides, as shown later, for any $z \in (0, +\infty)$, having the integral range A_z of the indicator field I_z finite is a sufficient condition to derive asymptotic properties of the Nadaraya-Watson estimator of the variogram γ_z , when it is computed from a single and partially observed realization.

3.3.2 Nonparametric kernel estimator of the variogram: definition and assumptions

Definition

Set a threshold $z \in (0, +\infty)$ and let Z be a simple max-stable SRF on \mathbb{R}^d , a realization z of which is observed on a finite number $n \in \mathbb{N}^*$ of locations $\mathbf{x}_1, \dots, \mathbf{x}_n \in \mathbb{R}^d$. For simplicity, we shall assume that I_z (or equivalently Z) is isotropic. Since the results in [García-Soidán \(2007\)](#) also hold for anisotropic RF, we surmise that the results presented hereafter can readily be extended to the anisotropic case. Hence, for the simplicity of notation, γ_z now stands for the radial part of the variogram of I_z : for any $\mathbf{h} \in \mathbb{R}^d$,

$$\gamma_z(\|\mathbf{h}\|) := \frac{1}{2} \mathbb{E} \left[(I_z(\mathbf{h}) - I_z(\mathbf{0}))^2 \right].$$

Now, let K be a compactly supported, symmetric and bounded density function satisfying $K(0) > 0$. In nonparametric statistics, it is called a kernel. Let also $(\tau_n)_{n \in \mathbb{N}}$ be a sequence of positive real numbers representing bandwidths. From [García-Soidán et al. \(2003\)](#) and [García-Soidán \(2007\)](#), the Nadaraya-Watson estimator of γ_z is given, for any distance $t \in \mathbb{R}_+^*$, by

$$\hat{\gamma}_{z, \tau_n}(t) := \frac{\sum_{i=1}^n \sum_{j=1}^n K\left(\frac{t - \|\mathbf{x}_i - \mathbf{x}_j\|}{\tau_n}\right) [I_z(\mathbf{x}_i) - I_z(\mathbf{x}_j)]^2}{2 \sum_{i=1}^n \sum_{j=1}^n K\left(\frac{t - \|\mathbf{x}_i - \mathbf{x}_j\|}{\tau_n}\right)}, \quad (3.5)$$

where the denominator is supposed nonzero. In the sequel, it is assumed that K has compact support $[-C, C]$, with $C \in \mathbb{R}_+^*$. It is shown in [García-Soidán et al. \(2004\)](#) and [García-Soidán \(2007\)](#) that, for any $t \in \mathbb{R}_+$, the estimator $\hat{\gamma}_{z, \tau_n}(t)$ is consistent and asymptotically normal as

$n \rightarrow +\infty$. Before presenting these results, the required assumptions are introduced. We shall point out that some of the assumptions originally set by the authors was either not appropriate or difficult to check in the case of max-stable processes, and consequently, they have been weakened or modified. This is specified in the sequel. The proofs that the results in [García-Soidán et al. \(2004\)](#) and [García-Soidán \(2007\)](#) still hold under these alternative conditions are given later.

Assumptions

The two first conditions concern the sampling procedure of the observations. Recall from [Chapter 2](#) that \mathcal{B} represents the set of measurable bounded subsets of \mathbb{R}^d with positive volume. In addition, B_r stands for the closed ball of center $\mathbf{0}$ and radius $r \in (0, +\infty)$. For any $n \in \mathbb{N}^*$, it is supposed that the locations $\mathbf{x}_1, \dots, \mathbf{x}_n$ belongs to a set $V_n \subset \mathbb{R}^d$. The sequence of domains $(V_n)_{n \in \mathbb{N}^*}$ is taken such that $V_n = \lambda_n V$ where $V \subset \mathcal{B}$ contains a ball B_r with radius $r \in (0, +\infty)$ and $(\lambda_n)_{n \in \mathbb{N}}$ is an increasing sequence of positive real numbers which diverges to $+\infty$. In particular, $V_n \uparrow \mathbb{R}^d$. Fix $n \in \mathbb{N}^*$ and let $f_0 : V \rightarrow \mathbb{R}_+$ a density function such that $d_1 < f_0(\mathbf{x}) < d_2$, for any $\mathbf{x} \in V$ and for some $d_1, d_2 \in \mathbb{R}_+^*$. Similarly to [Hall et al. \(1994\)](#) and [Hall and Patil \(1994\)](#), a random design is assumed for $\mathbf{x}_1, \dots, \mathbf{x}_n$.

(A1) For any $i \in \{1, \dots, n\}$, $\mathbf{x}_i = \lambda_n \mathbf{u}_i$, where \mathbf{u}_i is a realization of the random variable $U_i \sim f_0$, and U_1, \dots, U_n are supposed mutually independent.

Then, for every $k \in \mathbb{N}^*$ and for any distinct indices $i, j_1, \dots, j_k \in \{1, \dots, n\}$, let f_k stands for the density function of the random vector $(U_i - U_{j_1}, \dots, U_i - U_{j_k})$. The following assumption is made

(A2) Let $\ell \in \{1, 2\}$. For every $k \in \{1, \dots, 4\ell - 1\}$, f_k is assumed to be continuously differentiable in a neighbourhood of $\mathbf{0}^+$.

It is also specified in [García-Soidán \(2007\)](#) that $f_1(\mathbf{0})$ should be positive. In fact, this condition is always fulfilled, since $f_0(\mathbf{0}) > 0$ and U_1, \dots, U_n are mutually independent. The assumptions **(A1)** and **(A2)** are for instance satisfied when f_0 is the uniform distribution on V .

The third assumption is related to the sequences $(\tau_n)_{n \in \mathbb{N}}$ and $(\lambda_n)_{n \in \mathbb{N}}$. It describes the asymptotic regime under which the asymptotic properties of γ_z are studied.

(A3) $\tau_n + \lambda_n^{-1} + (n\tau_n)^{-1} + \lambda_n d n^{-1} \xrightarrow{n \rightarrow +\infty} 0$

This assumption splits in 4 conditions:

- $\tau_n \xrightarrow{n \rightarrow +\infty} 0$,
- $\lambda_n \xrightarrow{n \rightarrow +\infty} +\infty$,
- $1/\tau_n = o(n)$ as $n \rightarrow +\infty$, and
- $\lambda_n^d = o(n)$ as $n \rightarrow +\infty$.

The second condition has already been set above. This establishes an increasing domain asymptotic regime. On the contrary, the last one means that the number of observations, in a fix domain, increases as $n \rightarrow +\infty$; this corresponds to infill asymptotics. Hence, the asymptotic regime defined by these conditions is a compromise between these two types of asymptotic structures. The other conditions are standard in nonparametric estimation studies. They express a trade-off between bias and variance (see e.g. [Tsybakov, 2009](#)).

The four last conditions affect the dependence structure of I_z .

(A4) For $t \in (0, +\infty)$, the first three derivatives of γ_z are continuous in a neighbourhood of t .

Remark that from [Eq. \(3.4\)](#), this condition may also be expressed in term of θ . Before introducing the two following conditions, define

$$g_1 : (\mathbf{x}_1, \mathbf{x}_2, \mathbf{x}_3) \in \mathbb{R}^{3d} \mapsto \text{Cov} \left[(I_z(\mathbf{0}) - I_z(\mathbf{x}_1))^2, (I_z(\mathbf{x}_2) - I_z(\mathbf{x}_3))^2 \right] \in \mathbb{R}, \quad (3.6)$$

and

$$g_2 : (\mathbf{x}_1, \mathbf{x}_2, \dots, \mathbf{x}_7) \in \mathbb{R}^{7d} \mapsto \mathbb{E} \left[\prod_{j=0}^3 \left([I_z(\mathbf{x}_{2j}) - I_z(\mathbf{x}_{2j+1})]^2 - \mathbb{E} \left[[I_z(\mathbf{x}_{2j}) - I_z(\mathbf{x}_{2j+1})]^2 \right] \right) \right] \in \mathbb{R}.$$

For any $\mathbf{x} \in \mathbb{R}^d$, $I_z(\mathbf{x})$ is Bernoulli-distributed: the (well-defined) functions g_1 and g_2 are bounded. Besides, they may be written in terms of extremal coefficients, including pair extremal coefficients (see [Eq. \(3.6\)](#)). Since the latter are continuous (see [Section 3.2](#)), thus so are g_1 and g_2 . Actually, [García-Soidán \(2007\)](#) further assumes that both functions are continuously differentiable on \mathbb{R}^{3d} and \mathbb{R}^{7d} , respectively. Such a condition does not seem appropriate for the context of our study. Indeed, recall for instance that the ECF θ is not differentiable at the origin unless $\theta(\mathbf{h}) = 1$ for every $\mathbf{h} \in \mathbb{R}^d$ (see [Theorem 1.16](#)). We show later that the continuity of g_1 and g_2 is sufficient to obtain the desired results.

(A5) For any $s \in (0, +\infty)$,

$$\mathcal{J}_1(s) = \int_{\substack{\|\mathbf{x}_1\| \leq s \\ \|\mathbf{x}_2 - \mathbf{x}_3\| \leq s}} |g_1(\mathbf{x}_1, \mathbf{x}_2, \mathbf{x}_3)| \, d\mathbf{x}_1 d\mathbf{x}_2 d\mathbf{x}_3 < +\infty.$$

(A6) For any $s \in (0, +\infty)$,

$$\mathcal{J}_2(s) = \int_{\substack{\|\mathbf{x}_1\| \leq s, \quad \|\mathbf{x}_2 - \mathbf{x}_3\| \leq s, \\ \|\mathbf{x}_4 - \mathbf{x}_5\| \leq s, \quad \|\mathbf{x}_6 - \mathbf{x}_7\| \leq s}} |g_2(\mathbf{x}_1, \dots, \mathbf{x}_7)| \, d\mathbf{x}_1 \dots d\mathbf{x}_7 < +\infty.$$

Notice that **(A6)** implies **(A5)**. Let A_z be the integral range of I_z . Actually we have shown that, if $2 - \theta(\mathbf{h})$ has a limit as $\|\mathbf{h}\| \rightarrow +\infty$, then the integrability of $2 - \theta(\mathbf{h})$ over \mathbb{R}^d , or equivalently a finite integral range A_z (see [Theorem 2.19](#)), is a sufficient condition for **(A5)** to be satisfied.

Proposition 3.4 Let Z be a simple max-stable SRF on \mathbb{R}^d with ECF θ . If $\lim_{\|\mathbf{h}\| \rightarrow +\infty} 2 - \theta(\mathbf{h}) = \ell \in [0, 1]$ then

$$\int_{\mathbb{R}^d} 2 - \theta(\|\mathbf{h}\|) d\mathbf{h} < +\infty \Rightarrow \text{(A5)}.$$

We refer to the [Subsection 3.6.1](#) for the proof. We also conjecture that [\(A7\)](#) entails [\(A6\)](#) too. The calculation is much more tedious than for [\(A5\)](#) and, until now, we did not manage to provide a complete proof. This is discussed at the end of [Subsection 3.6.1](#). Finally the last condition concerns the mixing property of Z (in the sense given in [Definition 2.26](#)).

$$\text{(A7)} \quad \lim_{\|\mathbf{h}\| \rightarrow +\infty} 2 - \theta(\mathbf{h}) = 0$$

This assumption is an alternative condition to (S10) in [García-Soidán \(2007\)](#), see [Remark 3.5](#).

Remark 3.5 – *ϱ -mixing condition.* For any $S \subset \mathbb{R}^d$, let $\sigma_Z(S_i)$ the σ -field generated by $\{Z(\mathbf{x}), \mathbf{x} \in S_i\}$. The correlation between two random variables W and Y is denoted $\text{Corr}[W, Y]$. In addition, we write $W \in \sigma_Z(S)$ if W is $\sigma_Z(S)$ -measurable. Finally, for any $r \in \mathbb{R}_+$, define the following (strong) ϱ -mixing coefficient

$$\varrho(r) := \sup_{\substack{S_1, S_2 \subset \mathbb{R}^d \\ d(S_1, S_2) > r}} \sup_{\substack{W_i \in \sigma_Z(S_i), i=1,2, \\ \mathbb{E}[W_i^2] < +\infty}} |\text{Corr}[W_1, W_2]|$$

The assumption (S10) in [García-Soidán \(2007\)](#) requires that

$$\varrho(r) \xrightarrow{r \rightarrow +\infty} 0. \quad (3.7)$$

According to [Bradley \(1993b\)](#), this mixing condition is equivalent to the convergence of the corresponding α -mixing coefficient to 0. To the best of our knowledge, only a few works have studied the mixing coefficients in a spatial extreme context (see [Dombry and Eyi-Minko, 2012](#); [Dombry and Kabluchko, 2018](#); [Koch et al., 2018](#)). When Z is sample continuous and defined on \mathbb{Z}^d , [Dombry and Eyi-Minko \(2012, Corollary 2.2\)](#) link the behaviour of the β -mixing coefficient with those of $2 - \theta(\mathbf{h})$, $\mathbf{h} \in \mathbb{Z}^d$. As mentioned in the previous chapter, when it is defined on \mathbb{R}^d , [Dombry and Kabluchko \(2018\)](#) show that the condition $\lim_{\|\mathbf{h}\| \rightarrow +\infty} Y(\mathbf{h}) = 0$, with Y the spectral process associated with Z , implies that Z is strongly β -mixing (in the sense given in the paper, when considering compact sets). However, they do not give explicit conditions on max-stable processes defined on \mathbb{R}^d such that [Eq. \(3.7\)](#) is satisfied. That is why we have tried to find an alternative condition to [Eq. \(3.7\)](#). As detailed in [Chapter 2](#), [\(A7\)](#) is a condition which is easy to check for standard max-stable processes.

Once the assumptions introduced, we shall now give the results about the asymptotics properties of $\hat{\gamma}_{z, \tau_n}(t)$ for any $t \in (0, +\infty)$.

3.3.3 Asymptotic properties

Let $z, t \in (0, +\infty)$. We shall first present the results about the consistency and normality of $\hat{\gamma}_{z, \tau_n}(t)$. These pointwise properties will be then extended to the estimator of the ECF θ suggested above, when it is based on $\hat{\gamma}_{z, \tau_n}$.

Nonparametric kernel estimator of the variogram

The next proposition certifies the asymptotic non-bias of $\hat{\gamma}_{z, \tau_n}(t)$ as $n \rightarrow +\infty$. First define

$$c_K = \int_{-C}^C h^2 K(t) dt.$$

Proposition 3.6 Set $z \in (0, +\infty)$. Let Z be an isotropic and simple max-stable SRF on \mathbb{R}^d and consider its corresponding exceedance field I_z with variogram γ_z . The second derivative of the latter is written γ_z'' . If (A1)-(A4) are satisfied, with $\ell = 1$, then

$$\mathbb{E} [\hat{\gamma}_{z, \tau_n}(t)] = \gamma_z(t) + \frac{c_K}{2} + \gamma_z''(t) \tau_n^2 + o(\tau_n^2) \quad \text{as } n \rightarrow +\infty,$$

and consequently, $\hat{\gamma}_{z, \tau_n}(t)$ is asymptotically unbiased.

This result stems from [García-Soidán et al. \(2004, Theorem 3.2\)](#), the proof of which is given in the paper. The second proposition establishes its consistency.

Proposition 3.7 Consider the same framework as in [Proposition 3.6](#). Under the additional assumption (A5), it also holds

$$\text{Var} [\hat{\gamma}_{z, \tau_n}(t)] = \frac{k_1(t) \lambda_n^d}{n^2 \tau_n} + \frac{k_2(t)}{\lambda_n^d} + o\left(\frac{\lambda_n^d}{n^2 \tau_n} + \frac{1}{\lambda_n^d} + \tau_n^4\right) \quad \text{as } n \rightarrow +\infty,$$

where $k_1(t), k_2(t) \in \mathbb{R}$. Hence, $\hat{\gamma}_{z, \tau_n}(t)$ converges in quadratic mean to $\gamma_z(t)$ and consequently, it is consistent.

This result is a consequence of Theorem 3.3 in [García-Soidán et al. \(2004\)](#) applied to I_z and explicit values of $k_1(t)$ and $k_2(t)$ are given in this paper. Recall that, contrary to [García-Soidán et al. \(2004\)](#) and [García-Soidán \(2007\)](#), we only suppose that g_1 in [Eq. \(3.6\)](#) is continuous on \mathbb{R}^{3d} . We show in [Subsection 3.6.2](#) that the proof of their theorem is still valid under this weaker assumption. Now, before setting the asymptotic normality of $\hat{\gamma}_{z, \tau_n}(t)$, some additional constraints on the convergence rates of the sequences $(\tau_n)_{n \in \mathbb{N}}$ and $(\lambda_n)_{n \in \mathbb{N}}$ need to be set.

(A8) $\lim_{n \rightarrow +\infty} \lambda_n^d n^{-c_0} = c_1$, for some positive real numbers c_0, c_1 .

(A9) $\lim_{n \rightarrow +\infty} \tau_n^5 \lambda_n^{-d} n^2 = c_2$, for a positive real number c_2 .

As claimed by [García-Soidán \(2007\)](#), these conditions imply that the variance of $\hat{\gamma}_{z,\tau_n}(t)$ is of the order of

$$v_n := n^{-4(2-c_0)/5} \mathbf{1}\{c_0 \geq 8/9\} + n^{-c_0} \mathbf{1}\{c_0 < 8/9\}.$$

Theorem 3.8 Consider the same framework as in [Proposition 3.6](#), with $\ell = 2$, and assume furthermore that [\(A6\)-\(A9\)](#) hold. Then

$$\frac{1}{\sqrt{v_n}} (\hat{\gamma}_{z,\tau_n}(t) - \gamma_z(t)) \xrightarrow[n \rightarrow +\infty]{d} \mathcal{N}(\mu(t), \sigma^2(t)), \quad (3.8)$$

where

$$\begin{aligned} - \mu(t) &= \frac{(c_1 c_2)^{2/5} c_K \gamma''(t)}{2} \mathbf{1}\{c_0 > 8/9\}, \\ - \sigma^2(h) &= (c_1^4 c_2^{-1})^{1/5} k_1(t) \mathbf{1}\{c_0 > 8/9\} + k_2(t) \mathbf{1}\{c_0 \leq 8/9\}, \end{aligned}$$

Again, this result stems from [García-Soidán et al. \(2004, Theorem 3.2\)](#), the proof of which is given in the paper. Similarly to [Proposition 3.7](#), its proof only necessitates that g_2 is continuous (see [Subsection 3.6.2](#)). In addition, we claimed that the assumption [\(A7\)](#) may replace the strong ϱ -mixing condition [\(3.7\)](#), which is required in [García-Soidán et al. \(2004\)](#). The proof is given in [Subsection 3.6.3](#). Another comment about [Theorem 3.8](#) is made in the next remark.

Remark 3.9 – *On the necessity of conditions [\(A6\)](#) and [\(A7\)](#).* In [García-Soidán \(2007\)](#), the proof of [Theorem 3.8](#) is divided in three parts, according to the value of c_0 in [\(A8\)](#). Let $t \in (0, +\infty)$. The assumptions [\(A6\)](#) and [\(3.7\)](#) (or equivalently [\(A7\)](#)) are only required to establish the asymptotic normality of $\hat{\gamma}_{z,\tau_n}(t)$ when $c_0 \leq 8/9$. When $c_0 > 8/9$, the framework of [Proposition 3.7](#), additionally to the boundedness of g_2 are sufficient to obtain the desired result.

From these statements, we shall now establish the asymptotic properties of an estimator of θ based on $\hat{\gamma}_{z,\tau_n}$.

Nonparametric variogram based estimator of θ

Since Z is supposed to be isotropic, there exists a function $\theta_0 : \mathbb{R}_+ \rightarrow [1, 2]$ such that, for any $\mathbf{h} \in \mathbb{R}^d$, $\theta(\mathbf{h}) = \theta_0(\|\mathbf{h}\|)$. It is referred to as the radial ECF in the sequel. Let $z_e \approx 1.44$ stands for the median of unit Fréchet distributed random variable. Define also, for any $z \in (0, +\infty)$, the function

$$\Psi_z : t \in [0, \exp\{-1/z\}) \mapsto -z \log [\exp\{-1/z\} - t] \in [1, +\infty).$$

From [Eq. \(3.4\)](#), we introduce a new nonparametric estimator of θ_0 given by

$$\hat{\theta}_{0,n,z}(t) = \Psi_z(\hat{\gamma}_{z,\tau_n}(t)),$$

for any $t \in (0, +\infty)$ and any threshold $z > z_e$ (see [Remark 3.10](#)). The (pointwise) consistency and asymptotic normality of this estimator are given in the following propositions

Remark 3.10 Let $z, t \in (0, +\infty)$. and remark that $\hat{\gamma}_{z, \tau_n}(t)$ is not necessarily lower than $\exp\{-1/z\}$. When it is larger, $\Psi_z(\hat{\gamma}_{z, \tau_n}(t))$ is not defined. However, notice that $\hat{\gamma}_{z, \tau_n}(t) \leq 1/2$. To be sure that it is well-defined, we shall take $z > z_e$ in the sequel. This inequality constrain is convenient if, in future works, we do not consider max-stable RF's but processes for which the pointwise maxima, taken over an infinite number of appropriately rescaled *i.i.d.* replications, converge in law to a max-stable process. In such a case, we will study the associated exceedance I_z field over a high threshold z .

Proposition 3.11 Set $z > z_e$ and let Z be an isotropic and simple max-stable SRF with ECF θ . If conditions [\(A1\)-\(A5\)](#), with $\ell = 1$, are satisfied then, for any $t \in (0, +\infty)$, $\hat{\theta}_{0, n, z}(t)$ is a consistent estimator.

This result is readily deduced from [Proposition 3.7](#): since [\(A1\)-\(A5\)](#) hold, the estimator $\hat{\gamma}_{z, \tau_n}(t)$ converges in probability to $\gamma_z(t)$, for any $t \in (0, +\infty)$. In addition, for any threshold $z > z_e$, Ψ_z is continuous. According to the continuous mapping theorem, this implies that $\hat{\theta}_{0, n, z}(t)$ is consistent.

Proposition 3.12 Consider the same framework as in [Proposition 3.11](#), with $\ell = 2$, and assume furthermore that [\(A6\)-\(A9\)](#) hold. Then, for any $t \in (0, +\infty)$,

$$\frac{1}{\sqrt{v_n}} \left(\hat{\theta}_{0, n, z}(t) - \theta_0(t) \right) \xrightarrow[n \rightarrow +\infty]{d} \mathcal{N} \left(\Psi'_z(\gamma_z(t)) \mu(t), \left[\Psi'_z(\gamma_z(t)) \right]^2 \sigma^2(t) \right),$$

where v_n , $\mu(t)$, and $\sigma^2(t)$ are given in [Theorem 3.8](#) and Ψ'_z stands for the derivative of Ψ_z .

Since Ψ_z is differentiable with derivative Ψ'_z and $v_n \rightarrow 0$ as $n \rightarrow +\infty$, this result directly follows from [Theorem 3.8](#) by using the Delta method. Let $z > z_e$ and suppose now that [\(A1\)-\(A4\)](#) are satisfied and that $\lim_{\|\mathbf{h}\| \rightarrow +\infty} 2 - \theta(\mathbf{h})$ exists. A sufficient condition for $\hat{\theta}_{0, n, z}(t)$ to be asymptotically normal is that the integral range A_z is finite (if the conjecture announced above about [\(A6\)](#) is true).

We shall now illustrate these asymptotic results with some numerical experiments.

3.4 NUMERICAL EXPERIMENTS

The asymptotic properties of the nonparametric variogram based estimator of θ are illustrated on simulations, then the performances of this estimator are compared to those of the F-madogram. First, we shall detail the experimental protocol of this study.

3.4.1 Experimental protocol

Setting

The study is conducted in the bidimensional case ($d = 2$). Consider the isotropic bivariate Smith and extremal Gaussian process **(i)** and **(iii)**, introduced in [Chapter 2](#). For both of them, the first three derivatives of γ_z are continuous, for $z \in (0, +\infty)$. Further, it has been shown that the Smith process satisfies

$$\int_{\mathbb{R}^d} 2 - \theta(\mathbf{h}) d\mathbf{h} < +\infty. \quad (3.9)$$

Set $t \in (0, +\infty)$. According to [Proposition 3.11](#) and [Proposition 3.4](#), under appropriate conditions on the sampling scheme and the sequence $(\tau_n)_{n \in \mathbb{N}}$ of bandwidth parameters, the estimator $\hat{\theta}_{0,n,z}(t)$ is thus consistent, as $n \rightarrow +\infty$. Conjecturing that [Eq. \(3.9\)](#) implies [\(A6\)](#), it is also asymptotically normal. On the contrary, the extremal Gaussian RF does not fulfil [Eq. \(3.9\)](#); as verified in [Chapter 2](#), it is even not mixing. We believe that, in this case, [\(A5\)](#) is not satisfied and consequently $\hat{\theta}_{0,n,z}(t)$ is neither consistent nor asymptotically normal. This is next illustrated on simulations.

Let $V = [-1, 1]^2$ and f_0 be the uniform density on V . Besides, for every $n \in \mathbb{N}$, take $\lambda_n = n^{8/9}$; this corresponds to $c_0 = 8/9$ and $c_1 = 1$ in [\(A8\)](#). As mentioned in [García-Soidán \(2007\)](#), this choice minimizes the order of the variance of $\hat{\gamma}_{z,\tau_n}(t)$, for any $t \in (0, +\infty)$. Three different irregular grids are considered, with number of locations $n = 300, 1000$ and 2000 , respectively. The locations $\mathbf{x}_1, \dots, \mathbf{x}_n \in \mathbb{R}^2$ of the grids are generated according to condition [\(A1\)](#). Then, for each grid, 500 simulations of the processes **(i)** and **(iii)** are performed, using the algorithm we propose in [Chapter 4](#) and the method implemented in the package `Randomfields`, respectively. Notice that, as required by the theoretical framework, the margins of these processes are unit-Fréchet distributed. In practice, with real data set, we do not know the margins of the underlying process; consequently, they have to be assessed to ultimately be transformed into unit-Fréchet margins. To test the robustness of our estimator, we thus carry out this estimation. For each simulation, we assume that the margins have a common distribution, the c.d.f. of which is estimated by the standard empirical c.d.f., computed from this single simulation. The latter is then transformed to obtain unit-Fréchet margins. Now, let the thresholds

$z_1 = 1.45$ and z_2 be the third quartile of a unit Fréchet distribution, *i.e.* $z_2 \approx 3.48$. From each modified simulation, the exceedance fields I_z , for $z = z_1, z_2$, are subsequently computed. Finally, from each dummy data set, the estimator $\hat{\theta}_{0,n,z}(t)$ is calculated for several distances t , using the Gaussian kernel given by

$$\forall t \in \mathbb{R} \quad K(t) := \frac{1}{\sqrt{2\pi}} \exp\left\{-\frac{t^2}{2}\right\}.$$

The later vanishes extremely fast. Even if its support is not compact, it can be numerically considered as such. The choice of the bandwidths is discussed next.

Bandwidth selection

Let $n \in \mathbb{N}$ and $t \in (0, +\infty)$. [García-Soidán \(2007\)](#) gives the expression of the optimal bandwidth parameter τ_n , which asymptotically minimize the mean square error of $\hat{\gamma}_{z,\tau_n}(t)$. To use this expression, which actually depends on t , some unknown quantities need to be assessed. [García-Soidán \(2007\)](#) propose to estimate them either parametrically or by employing again a nonparametric kernel methods. The first solution consists in assuming that the process under study is Gaussian: this is not adapted to our framework. The second one is a bit complex, mainly because the suggested nonparametric kernel methods also depend on bandwidth parameters that need to be chosen in turn. As it is often done in nonparametric studies, we have thus decided to select the bandwidth parameters by cross validation. It is known that the choice of the bandwidths is delicate, since they highly affect the outcome of a nonparametric estimation procedure. However the objective of these numerical experiments is not to propose an elaborate method to choose these parameters. That is why we set up a basic cross validation procedure. This could be ameliorated in future works.

Let $z \in \{z_1, z_2\}$ and consider a realization i_z of I_z , which is observed at $n \in \{300, 1000, 2000\}$ locations $\mathbf{x}_1, \dots, \mathbf{x}_n \in \mathbb{R}^d$. This data set is first divided into 10 clusters E_1, \dots, E_{10} of spatially closed observations with the k -means method. This limits the spatial dependence between the training and the testing sets. Let $\tau_n \in (0, +\infty)$ be a bandwidth. In addition, for any $t \in (0, +\infty)$ and any $k \in \{1, \dots, 10\}$, write $\hat{\gamma}_{z,\tau_n}^{-k}(t)$ the kernel estimation computed from all the observations that are not in E_k , *i.e.*

$$\hat{\gamma}_{z,\tau_n}^{-k}(t) := \frac{\sum_{j \notin E_k} \sum_{\ell \notin E_k} K\left(\frac{t - \|\mathbf{x}_j - \mathbf{x}_\ell\|}{\tau_n}\right) [i_z(\mathbf{x}_j) - i_z(\mathbf{x}_\ell)]^2}{2 \sum_{j \notin E_k} \sum_{\ell \notin E_k} K\left(\frac{t - \|\mathbf{x}_j - \mathbf{x}_\ell\|}{\tau_n}\right)}.$$

Define now the error

$$E_{\text{tot}} = \sum_{k=1}^{10} \sum_{\substack{j, \ell \in E_k \\ j \neq \ell}} \left| 2 \hat{\gamma}_{z,\tau_n}^{-k}(\|\mathbf{x}_j - \mathbf{x}_\ell\|) - (i_z(\mathbf{x}_j) - i_z(\mathbf{x}_\ell))^2 \right|.$$

For a given vector of bandwidths, we select the parameter that minimizes E_{tot} . Notice that this bandwidth does not depend on the distances t at which the estimator $\hat{\theta}_{0,n,z}$ will be subsequently evaluated.

Actually, it turns out that the selection by cross validation of the bandwidth was time-consuming, especially for data sets with 1000 or 2000 observations. We have thus decided, for each underlying processes (i) and (iii) and for each threshold z_1 and z_2 , to select the optimal bandwidth for only one data set among the 500 data sets with $n = 300$ observations. This parameter is then used to compute the Nadaraya-Watson estimator of the variogram for all the other data sets.

3.4.2 Tracking consistency and asymptotic normality

Let $n \in \{300, 1000, 2000\}$ and $z \in \{z_1, z_2\}$. Using the experimental protocol described in the last subsection, we have evaluated $\hat{\theta}_{0,n,z}$ for 50 distances t_1, \dots, t_{50} regularly spaced in $[0.2, 10]$. We shall notice that the optimal bandwidth has been selected among 15 bandwidths regularly spaced in the interval $[0.1, 2]$. These estimations are then used to track the consistency and the asymptotic normality of $\hat{\theta}_{0,n,z}(t_k)$, for $k \in \{1, \dots, 50\}$.

Smith process

Let $k \in \{1, \dots, 50\}$. As pointed out in the last subsection, in the case of the Smith process, $\hat{\theta}_{0,n,z}(t_k)$ should be consistent. This is graphically investigated. The left graphics in [Figure 3.1](#) display the mean curves obtained by averaging, for each $k \in \{1, \dots, 50\}$ and for each $n \in \{300, 1000, 2000\}$, the 500 estimates $\hat{\theta}_{0,n,z_1}(t_k)$ computed from the 500 realizations of the exceedance field I_{z_1} . They also show the corresponding 90% confidence envelopes built by computing, for each $k \in \{1, \dots, 50\}$ and for each $n \in \{300, 1000, 2000\}$, the sample quantiles of order 0.05 and 0.95 of the 500 estimates $\hat{\theta}_{0,n,z}(t_k)$. For comparison, the radial ECF θ_0 of the Smith process is also plotted on each graphic. The same information is shown in the right graphics when considering the threshold z_2 . We can observe that, except around $t = 0$, the mean curves fit well the θ_0 for both thresholds. Further the confidence envelopes become thinner as n increases. As agreed with the theoretical results, these graphics suggest that $\hat{\theta}_{0,n,z}(t_k)$ is consistent for distances t_k that are not too close to 0. Since the variogram γ_z is restricted to nonnegative value, the null distance is an endpoint. The unsatisfactory behaviour of the estimation near the endpoint is a well-known issue in nonparametric kernel estimation. [García-Soidán et al. \(2004\)](#) propose to modify the kernel K , accordingly to the method suggested in [Kyung-Joon and Schucany \(1998\)](#), to obtain satisfactory estimates near 0. This

is left for future improvements of the estimation method.

To illustrate the pointwise asymptotic normality of $\hat{\theta}_{0,n,z}$, we have selected the distance $t = 4.2$ among the 50 distances t_1, \dots, t_{50} . Then, for $n = 2000$ and $z = z_1$, we have considered the 500 estimates $\hat{\theta}_{0,n,z}(t)$: the corresponding histogram is displayed in [Figure 3.2](#). It is bell-shaped like a normal distribution. Further investigation should be carried out to test the normality of the estimates. This is not done in this study. As in [García-Soidán \(2007\)](#), we could also use the asymptotic normality property for building and testing confidence intervals. However, for any distance $t \in (0, +\infty)$, this requires to estimate the unknown quantities $\gamma''(t)$, $k_1(t)$ and $k_2(t)$ in [Theorem 3.8](#), which may be a bit delicate. This is not done in this study.

Extremal Gaussian process

In the case of the extremal Gaussian process, the consistency of $\hat{\theta}_{0,n,z}(t_k)$, for any $k \in \{1, \dots, n\}$ is also investigated. For $n = 300$, [Figure 3.3](#) displays the mean curves obtained by averaging, for each $k \in \{1, \dots, 50\}$ and for each threshold $z \in \{z_1, z_2\}$, the 500 estimates $\hat{\theta}_{0,n,z}(t_k)$ computed from the 500 realizations of the exceedance field I_z . The corresponding 90% confidence envelopes are also plotted as well as the radial ECF θ_0 of the extremal Gaussian. Contrary to the case of the Smith process, the mean curve does not fit at all the θ_0 : the estimates $\hat{\theta}_{0,n,z}(t_k)$ always overestimate the radial ECF. Similar results are obtained for $n = 1000$ and $n = 2000$. The estimation procedure of θ_0 has also been performed when the margins of the extremal Gaussian process are not estimated: the results are shown in [Figure 3.4](#). This time, the estimator $\hat{\theta}_{0,n,z}$ seems approximatively unbiased, except for distances $t_k \leq 2$, when $z = z_1$. On the other hand, the very large confidence envelopes indicate that the variability of the estimates is high and do not reduce as n increases. This would suggest that $\hat{\theta}_{0,n,z}(t_k)$ is not a consistent estimator. However, further investigations are needed. Indeed, it is for instance surprising that the confidence envelopes are larger than those obtained when the margins of the process are evaluated.

Finally, as for the Smith process, we have selected the distance $t = 4.2$. Then, for $n = 2000$ and $z = z_1$, we have considered the 500 estimates $\hat{\theta}_{0,n,z}(t)$: the corresponding histogram is displayed in [Figure 3.5](#). Contrary to the previous histogram, its shape does not look like the shape a Gaussian distribution at all.

3.4.3 *Comparison with the F-madogram estimator*

Let θ be the ECF of the Smith process [\(i\)](#). We shall now compare our estimator with the nonparametric F-madogram estimator suggested by [Cooley et al. \(2006\)](#), when assessing θ_0 .

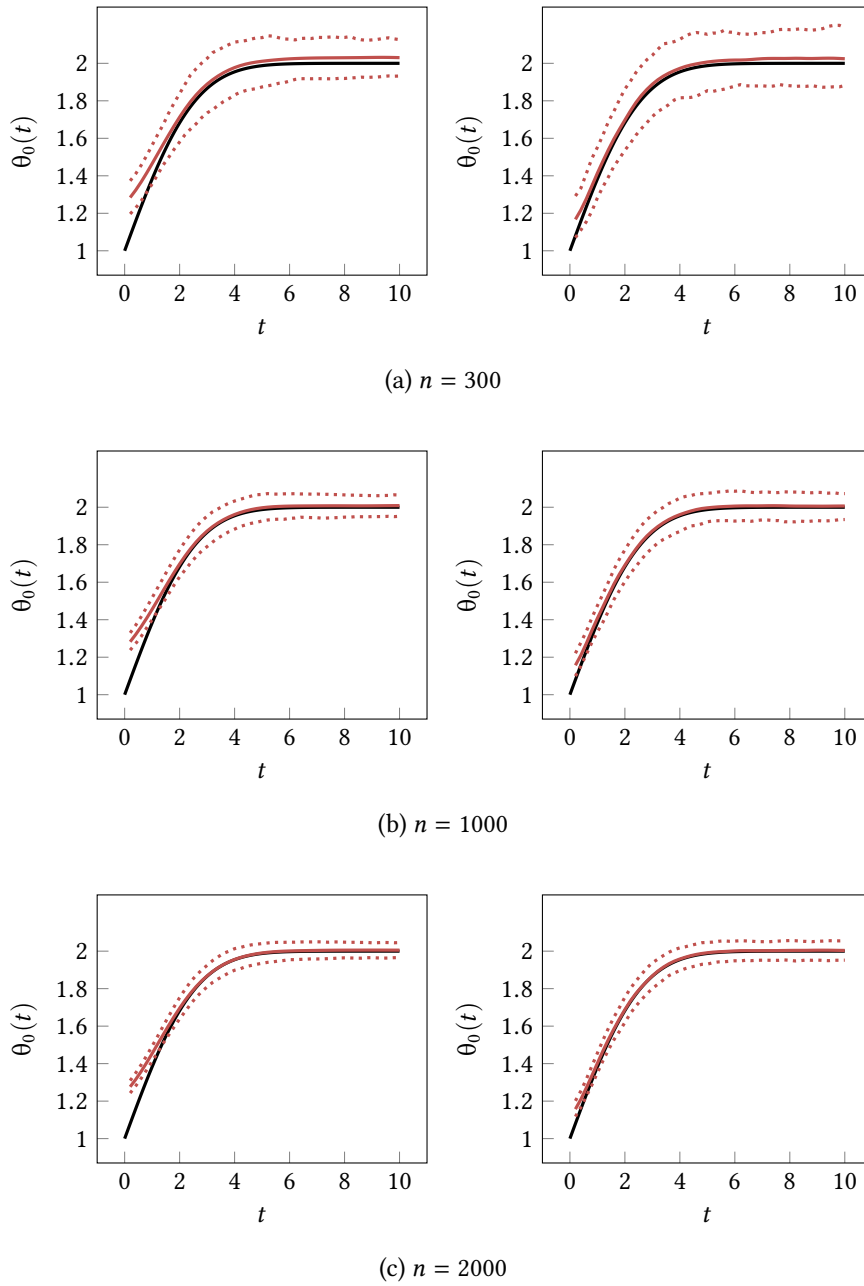


FIGURE 3.1 – The mean curve (red line) and the corresponding 90% confidence envelope (red dashed line) for thresholds z_1 (on the left) and z_2 (on the right). They are computed from 500 simulations of the Smith process (i) on irregular grids with size $n = 300, 1000, 2000$. For comparison, its radial ECF is also plotted (black line).

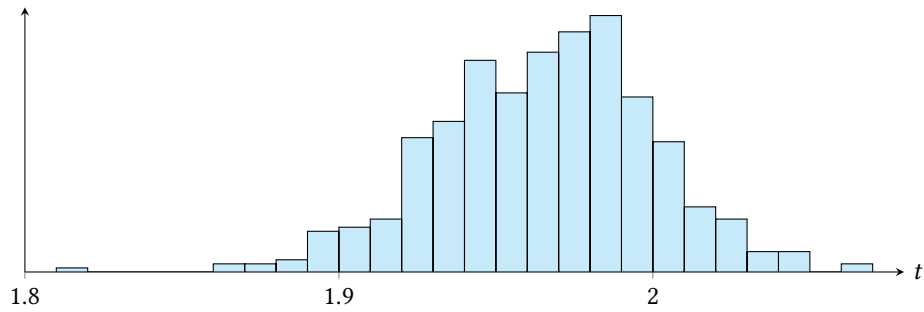


FIGURE 3.2 – Histogram of the 500 estimates $\hat{\theta}_{0,n,z}(t)$ (in lightblue), when $t = 4.2$, $n = 300$ and for threshold z_1 . The estimates have been computed from 500 simulations of the Smith process (iii) on an irregular grid with size n .

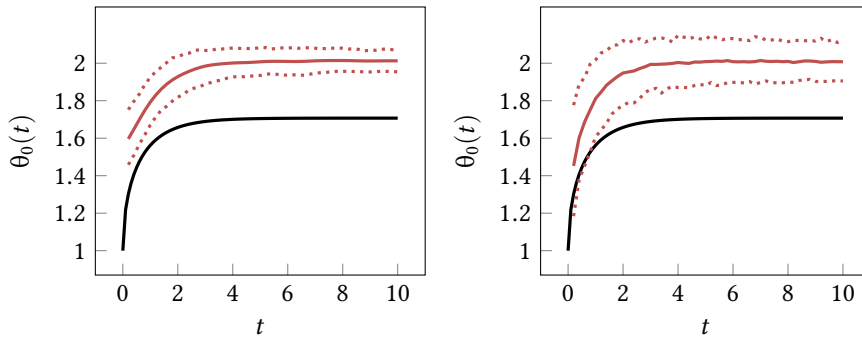


FIGURE 3.3 – The mean curve (red line) and the corresponding 90% confidence envelope (red dashed line) for thresholds z_1 (on the left) and z_2 (on the right). They are computed from 500 simulations of the Extremal Gaussian process (iii) on irregular grids with size $n = 300$. For comparison, its radial ECF is also plotted (black line).

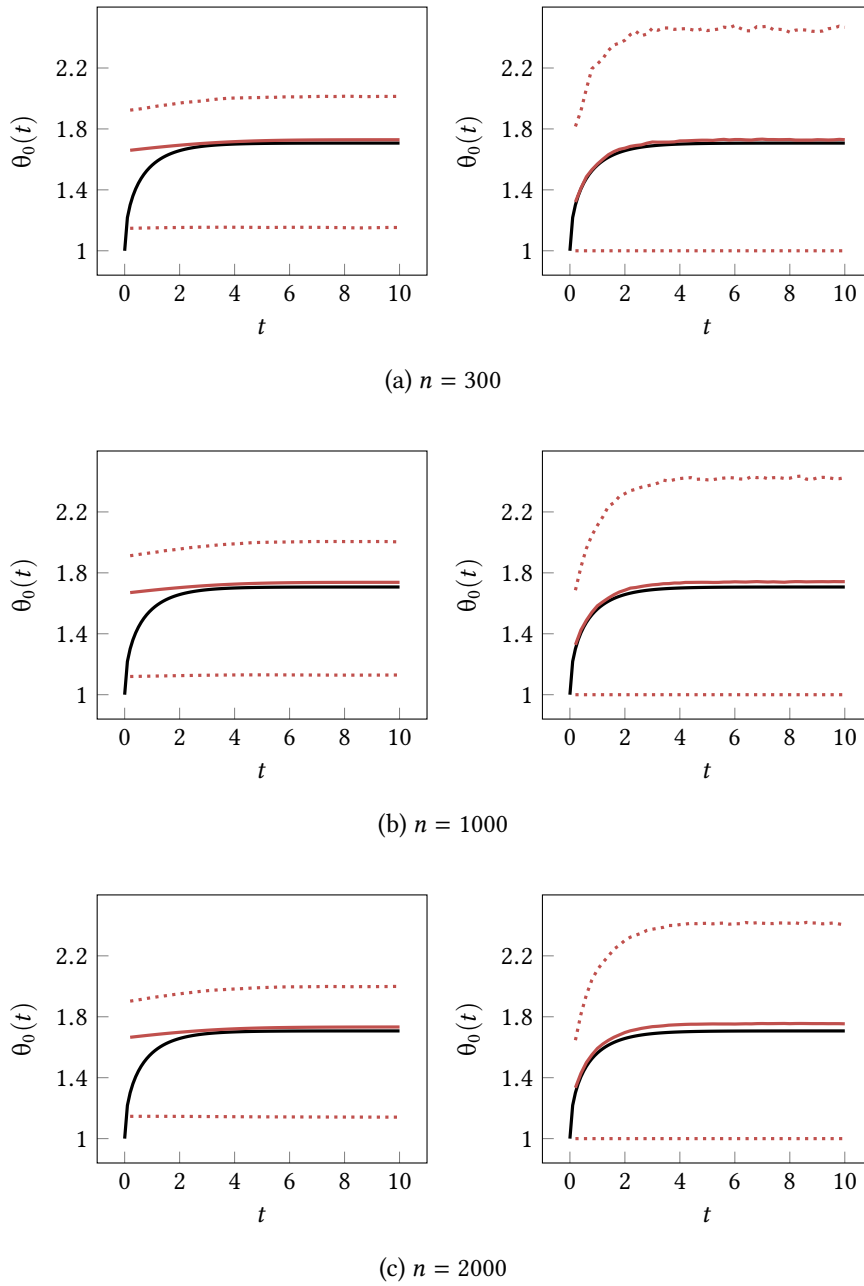


FIGURE 3.4 – The mean curve (red line) and the corresponding 90% confidence envelope (red dashed line) for thresholds z_1 (on the left) and z_2 (on the right) and for three different grids of size $n = 300, 1000, 2000$. They are all computed from 500 simulations of the Extremal Gaussian process (iii), for which the margins do not have been estimated. For comparison, the radial ECF of the model (iii) is also plotted (black line).

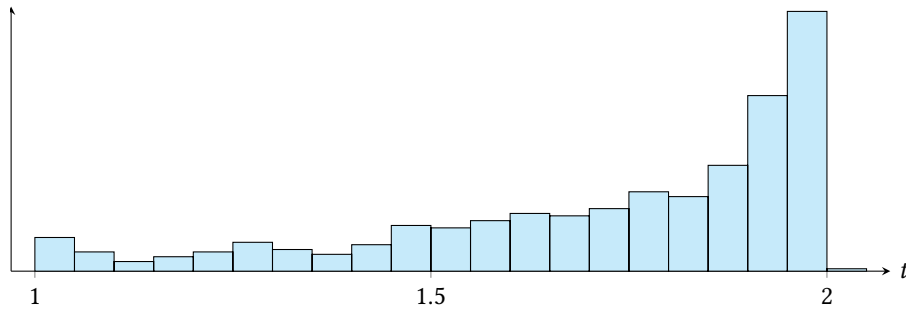


FIGURE 3.5 – Histogram of the 500 estimates $\hat{\theta}_{0,n,z}(t)$ (in lightblue), when $t = 4.2$, $n = 300$ and for threshold z_1 . They estimates have been computed from 500 simulations of the extremal Gaussian process (iii) on an irregular grid with size n .

Let Z stands for the max-stable process (i) or (iii) and let F be the c.d.f. of $Z(\mathbf{0})$. This estimator is based on the so-called F -madogram defined, for every $\mathbf{h} \in \mathbb{R}^d$, by

$$v_F(\mathbf{h}) := \frac{1}{2} \mathbf{E} [|F(Z(\mathbf{h})) - F(Z(\mathbf{0}))|].$$

Indeed, it is shown in Cooley et al. (2006) that for every $\mathbf{h} \in \mathbb{R}^d$

$$\theta(\mathbf{h}) = \frac{1 + 2v_F(\mathbf{h})}{1 - 2v_F(\mathbf{h})}.$$

Again, since Z is isotropic, there exists a function $v_{F,0} : \mathbb{R}_+ \rightarrow [0, 1]$ such that $v_F(\mathbf{h}) = v_{F,0}(\|\mathbf{h}\|)$, for any $\mathbf{h} \in \mathbb{R}^d$. Suppose that a realization of Z is observed at $n \in \mathbb{N}^*$ locations $\mathbf{x}_1, \dots, \mathbf{x}_n \in \mathbb{R}^d$ and let \hat{F} be an estimator of the c.d.f. F . According to Eq. (1.18) in Chapter 1, an empirical estimator of $v_{\hat{F},0}$ is given, for any $t \in (0, +\infty)$, by

$$\hat{v}_{\hat{F},0,n}(t) := \frac{1}{2|N_t|} \sum_{(\mathbf{x}_i, \mathbf{x}_j) \in N_t} |F(Z(\mathbf{x}_i)) - F(Z(\mathbf{x}_j))|, \quad (3.10)$$

where $N_t := \{(\mathbf{x}_i, \mathbf{x}_j) : \|\mathbf{x}_i - \mathbf{x}_j\| \in T_t, i, j = 1, \dots, k\}$, T_t is a tolerance region around t , and $|N_t|$ is the number of distinct pairs in N_t . For any $t \in (0, +\infty)$, the F -madogram estimator is then

$$\hat{\theta}_{0,n}^{\hat{F}}(t) = \frac{1 + 2\hat{v}_{\hat{F},0,n}(t)}{1 - 2\hat{v}_{\hat{F},0,n}(t)}.$$

Let t_1, \dots, t_{50} be the vector of distance considered in the last subsection. The same experimental protocol presented in Subsection 3.4.1 is used, when considering the Smith process, to obtain some estimates of $\hat{\theta}_{0,n}^{\hat{F}}(t_k)$, except that \hat{F} , empirical estimation of F , is used to obtain uniform margins and not unit-Fréchet margins. Besides the data are not ultimately transformed to obtain (some realizations of) exceedance fields. Notice also that the choice of the tolerance region T_t amounts to choose some bandwidth parameters: this is done with the same cross validation procedure presented above. The same graphics as before are displayed in Figure 3.6. For comparison, we also add the results previously obtained for our estimator

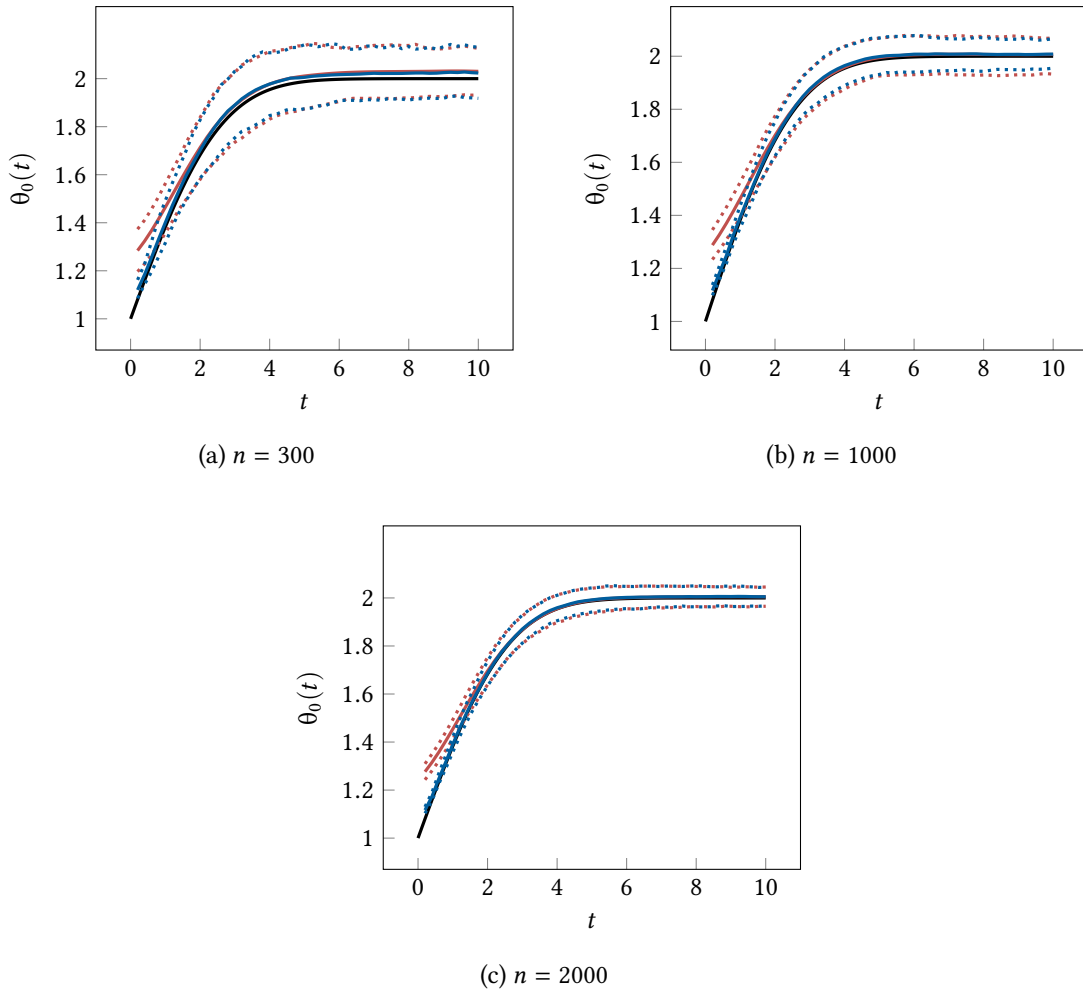


FIGURE 3.6 – The mean curves associated to $\hat{\theta}_{0,n}^{\hat{F}}$ (blue line) and $\hat{\theta}_{0,n,z_1}$ (red line) as well as the corresponding 90% confidence envelopes (blue and red dashed line, respectively). They are computed from 500 simulations of the Smith process (i) on irregular grids with size $n = 300, 1000, 2000$. The radial ECF of the process (i) is also plotted (black line).

$\hat{\theta}_{0,n,z}(t_k)$ when $z = z_1$. The curves for both estimators are very similar except near $t = 0$, where $\hat{\theta}_{0,n}^{\hat{F}}$ actually performs better.

3.5 DISCUSSION

In this chapter, we have introduced a new nonparametric estimator of the radial ECF θ of the simple max-stable SRF Z , which depends on the variogram γ_z of the corresponding exceedance field I_z above a positive threshold z . When γ_z is estimated by the Nadaraya-Watson estimator proposed in [García-Soidán \(2007\)](#), we derived from the latter asymptotic properties of our estimator when it is computed from a single and partially observed realization of Z . Namely, under some assumptions, we showed that it is asymptotically consistent and normal.

These conditions are modified versions of the assumptions required in [García-Soidán \(2007\)](#), which are more convenient to check when working with max-stable processes. In particular, they require that Z is mixing and that the integral range A_z of I_z is finite. This illustrates once more the relevance of the concept of integral range to study spatial extreme events when having only one set of spatial observations.

As detailed in this chapter, the asymptotic normality of the Nadaraya-Watson estimator of γ_z is obtained in [García-Soidán \(2007\)](#) under the condition that, for two subsets $V_1, V_2 \subset \mathbb{R}^d$, the associated ρ -mixing coefficient vanishes to 0 when the distance between V_1 and V_2 goes to infinity. As mentioned in [Chapter 2](#), some other studies require that such mixing coefficients decay fast enough to 0. The result of this chapter therefore encourages us to investigate further the link between integral range, ECF and strong mixing properties of Z . The relations between the β - and α -mixing conditions and θ have already been examined by [Dombry and Eyi-Minko \(2012\)](#) when Z is defined on \mathbb{Z}^d . More generally, when Z is defined on \mathbb{R}^d , they find an upper bound for the β -mixing coefficient, which involves the exponent measure of Z (see Theorem 2.1 in their paper). These seminal results constitute references for future work on the connection between integral range and strong mixing.

The results established in this chapter have been illustrated in [Section 3.4](#). It was underlined that the non parametric estimation of γ_z could be ameliorated, especially when selecting the bandwidth parameters. Besides, since θ does not depend on the threshold z , we could also try to aggregate estimators obtained for different thresholds. We have compared our new estimator of the ECF to the F-madogram estimator. Their performances were similar except for small distances. Comparisons with other estimators, like the maximum likelihood estimator proposed by [Schlather and Tawn \(2003\)](#), will be performed in forthcoming works. An application with real data (Bourgogne precipitation data set) should also be performed.

In this work, we have focused on the Nadaraya-Watson estimator of γ_z , since its asymptotic properties were already established. It would be interesting to study, at least with simulations, the performance of our estimator of θ when considering other estimators of γ_z . As it is commonly done in geostatistical studies, we could for instance use the estimator resulting from fitting a parametric model on the experimental variogram.

3.6 PROOFS AND SUPPLEMENTS

3.6.1 Finite integral range: a sufficient condition

In this subsection, we shall prove that, if $2 - \theta(\mathbf{h})$ admits a limit as $\|\mathbf{h}\| \rightarrow +\infty$, then

$$\int_{\mathbb{R}^d} 2 - \theta(\mathbf{h}) d\mathbf{h} < +\infty \quad \Rightarrow \quad \mathcal{I}_1 < +\infty.$$

The condition $\mathcal{I}_2 < +\infty$ is discussed after. Before, we shall introduce the next useful inequality between extremal coefficients.

Remark 3.13 – *About the extremal coefficients.* Set $n, m \in \mathbb{N}^*$ and let $\mathbf{x}_1, \dots, \mathbf{x}_n, \mathbf{y}_1, \dots, \mathbf{y}_m \in \mathbb{R}^d$. Since the spectral process Y associated with Z is nonnegative, it follows from Section 3.2 that

$$\begin{aligned} \vartheta(\mathbf{x}_1, \dots, \mathbf{x}_n, \mathbf{y}_1, \dots, \mathbf{y}_m) &= \mathbb{E} \left[\max \left(\max_{i \in \{1, \dots, n\}} Y(\mathbf{x}_i), \max_{i \in \{1, \dots, m\}} Y(\mathbf{y}_i) \right) \right] \\ &\leq \mathbb{E} \left[\max_{i \in \{1, \dots, n\}} Y(\mathbf{x}_i) \right] \mathbb{E} \left[\max_{i \in \{1, \dots, m\}} Y(\mathbf{y}_i) \right] \end{aligned}$$

Hence, $\vartheta(\mathbf{x}_1, \dots, \mathbf{x}_n, \mathbf{y}_1, \dots, \mathbf{y}_m) \leq \vartheta(\mathbf{x}_1, \dots, \mathbf{x}_n) \vartheta(\mathbf{y}_1, \dots, \mathbf{y}_m)$.

Integral \mathcal{I}_1

Set $\mathbf{x}_1, \mathbf{x}_2, \mathbf{x}_3 \in \mathbb{R}^d$ and remark that

$$g_1(\mathbf{x}_1, \mathbf{x}_2, \mathbf{x}_3) = \mathbb{P}[I_z(\mathbf{0}) \neq I_z(\mathbf{x}_1), I_z(\mathbf{x}_2) \neq I_z(\mathbf{x}_3)] - \mathbb{P}[I_z(\mathbf{0}) \neq I_z(\mathbf{x}_1)] \mathbb{P}[I_z(\mathbf{x}_2) \neq I_z(\mathbf{x}_3)].$$

By developing each term and using the formula of total probability, it follows

$$\begin{aligned} g_1(\mathbf{x}_1, \mathbf{x}_2, \mathbf{x}_3) &= \exp \left\{ -\frac{\vartheta(\mathbf{0}, \mathbf{x}_2)}{z} \right\} - \exp \left\{ \frac{-2}{z} \right\} + \exp \left\{ -\frac{\vartheta(\mathbf{x}_1, \mathbf{x}_2)}{z} \right\} - \exp \left\{ \frac{-2}{z} \right\} \\ &+ \exp \left\{ -\frac{\vartheta(\mathbf{0}, \mathbf{x}_3)}{z} \right\} - \exp \left\{ \frac{-2}{z} \right\} + \exp \left\{ -\frac{\vartheta(\mathbf{x}_1, \mathbf{x}_3)}{z} \right\} - \exp \left\{ \frac{-2}{z} \right\} - 2 \exp \left\{ -\frac{\vartheta(\mathbf{x}_1, \mathbf{x}_2, \mathbf{x}_3)}{z} \right\} \\ &- 2 \exp \left\{ -\frac{\vartheta(\mathbf{0}, \mathbf{x}_1, \mathbf{x}_3)}{z} \right\} - 2 \exp \left\{ -\frac{\vartheta(\mathbf{0}, \mathbf{x}_1, \mathbf{x}_2)}{z} \right\} - 2 \exp \left\{ -\frac{\vartheta(\mathbf{0}, \mathbf{x}_2, \mathbf{x}_3)}{z} \right\} \\ &+ 4 \exp \left\{ -\frac{(1 + \vartheta(\mathbf{x}_2, \mathbf{x}_3))}{z} \right\} + 4 \exp \left\{ -\frac{(1 + \vartheta(\mathbf{0}, \mathbf{x}_1))}{z} \right\} - 4 \exp \left\{ -\frac{(\vartheta(\mathbf{0}, \mathbf{x}_1) + \vartheta(\mathbf{x}_2, \mathbf{x}_3))}{z} \right\} \\ &+ 4 \exp \left\{ -\frac{\vartheta(\mathbf{0}, \mathbf{x}_1, \mathbf{x}_2, \mathbf{x}_3)}{z} \right\}. \end{aligned}$$

Now let $\mathbf{v}, \mathbf{w}, \mathbf{x}, \mathbf{y} \in \mathbb{R}^d$. Recall from Eq. (1.16) that

$$1 \leq \vartheta(\mathbf{x}, \mathbf{y}) \leq 2. \quad (3.11)$$

According to [Remark 3.13](#) it also holds

$$\vartheta(v, w, x) \leq 1 + \vartheta(w, x), \quad (3.12)$$

and

$$\vartheta(v, w, x, y) \leq \vartheta(v, w) + \vartheta(x, y). \quad (3.13)$$

Besides, from equation 13 in [Schlather and Tawn \(2002, page 92\)](#),

$$\begin{aligned} \vartheta(v, w, x) &\geq \vartheta(v, w) + \vartheta(v, x) + \vartheta(w, x) - 3 \\ &\geq [\vartheta(v, w) - 2] + [\vartheta(v, x) - 2] + \vartheta(w, x) + 1, \end{aligned} \quad (3.14)$$

and, from equation 23 in [Schlather and Tawn \(2002, page 95\)](#),

$$\vartheta(v, w, x, y) \geq [\vartheta(v, x) - 2] + [\vartheta(v, y) - 2] + [\vartheta(w, x) - 2] + [\vartheta(w, y) - 2] + \vartheta(v, w) + \vartheta(x, y). \quad (3.15)$$

Consequently, from equations [\(3.11\)](#), [\(3.12\)](#) and [\(3.13\)](#),

$$\begin{aligned} \left| g_1(\mathbf{x}_1, \mathbf{x}_2, \mathbf{x}_3) \right| &\leq \left(\exp \left\{ -\frac{\vartheta(\mathbf{0}, \mathbf{x}_2)}{z} \right\} - \exp \left\{ \frac{-2}{z} \right\} \right) + \left(\exp \left\{ -\frac{\vartheta(\mathbf{x}_1, \mathbf{x}_2)}{z} \right\} - \exp \left\{ \frac{-2}{z} \right\} \right) \\ &+ \left(\exp \left\{ -\frac{\vartheta(\mathbf{0}, \mathbf{x}_3)}{z} \right\} - \exp \left\{ \frac{-2}{z} \right\} \right) + \left(\exp \left\{ -\frac{\vartheta(\mathbf{x}_1, \mathbf{x}_3)}{z} \right\} - \exp \left\{ \frac{-2}{z} \right\} \right) \\ &+ 2 \left(\exp \left\{ -\frac{\vartheta(\mathbf{x}_1, \mathbf{x}_2, \mathbf{x}_3)}{z} \right\} - \exp \left\{ -\frac{(1 + \vartheta(\mathbf{x}_2, \mathbf{x}_3))}{z} \right\} \right) \\ &+ 2 \left(\exp \left\{ -\frac{\vartheta(\mathbf{0}, \mathbf{x}_1, \mathbf{x}_3)}{z} \right\} - \exp \left\{ -\frac{(1 + \vartheta(\mathbf{0}, \mathbf{x}_1))}{z} \right\} \right) \\ &+ 2 \left(\exp \left\{ -\frac{\vartheta(\mathbf{0}, \mathbf{x}_1, \mathbf{x}_2)}{z} \right\} - \exp \left\{ -\frac{(1 + \vartheta(\mathbf{0}, \mathbf{x}_1))}{z} \right\} \right) \\ &+ 2 \left(\exp \left\{ -\frac{\vartheta(\mathbf{0}, \mathbf{x}_2, \mathbf{x}_3)}{z} \right\} - \exp \left\{ -\frac{(1 + \vartheta(\mathbf{x}_2, \mathbf{x}_3))}{z} \right\} \right) \\ &+ 4 \left(\exp \left\{ -\frac{\vartheta(\mathbf{0}, \mathbf{x}_1, \mathbf{x}_2, \mathbf{x}_3)}{z} \right\} - \exp \left\{ -\frac{(\vartheta(\mathbf{0}, \mathbf{x}_1) + \vartheta(\mathbf{x}_2, \mathbf{x}_3))}{z} \right\} \right). \end{aligned}$$

Then, from equations [\(3.14\)](#) and [\(3.15\)](#) and the three following inequalities

$$\begin{aligned} - \exp \left\{ -\frac{(1 + \vartheta(\mathbf{0}, \mathbf{x}_1))}{z} \right\} &\leq 1, \\ - \exp \left\{ -\frac{(1 + \vartheta(\mathbf{x}_2, \mathbf{x}_3))}{z} \right\} &\leq 1, \\ - \exp \left\{ -\frac{(\vartheta(\mathbf{0}, \mathbf{x}_1) + \vartheta(\mathbf{x}_2, \mathbf{x}_3))}{z} \right\} &\leq 1, \end{aligned}$$

it yields

$$\begin{aligned} \left| g_1(\mathbf{x}_1, \mathbf{x}_2, \mathbf{x}_3) \right| &\leq \left(\exp \left\{ -\frac{\vartheta(\mathbf{0}, \mathbf{x}_2)}{z} \right\} - \exp \left\{ \frac{-2}{z} \right\} \right) + \left(\exp \left\{ -\frac{\vartheta(\mathbf{x}_1, \mathbf{x}_2)}{z} \right\} - \exp \left\{ \frac{-2}{z} \right\} \right) \\ &+ \left(\exp \left\{ -\frac{\vartheta(\mathbf{0}, \mathbf{x}_3)}{z} \right\} - \exp \left\{ \frac{-2}{z} \right\} \right) + \left(\exp \left\{ -\frac{\vartheta(\mathbf{x}_1, \mathbf{x}_3)}{z} \right\} - \exp \left\{ \frac{-2}{z} \right\} \right) \end{aligned}$$

$$\begin{aligned}
 & + 2 \left(\exp \left\{ \frac{[2 - \vartheta(\mathbf{x}_1, \mathbf{x}_2)] + [2 - \vartheta(\mathbf{x}_1, \mathbf{x}_3)]}{z} \right\} - 1 \right) + 2 \left(\exp \left\{ \frac{[2 - \vartheta(\mathbf{0}, \mathbf{x}_3)] + [2 - \vartheta(\mathbf{x}_1, \mathbf{x}_3)]}{z} \right\} - 1 \right) \\
 & + 2 \left(\exp \left\{ \frac{[2 - \vartheta(\mathbf{0}, \mathbf{x}_2)] + [2 - \vartheta(\mathbf{x}_1, \mathbf{x}_2)]}{z} \right\} - 1 \right) + 2 \left(\exp \left\{ \frac{[2 - \vartheta(\mathbf{0}, \mathbf{x}_2)] + [2 - \vartheta(\mathbf{0}, \mathbf{x}_3)]}{z} \right\} - 1 \right) \\
 & + 4 \left(\exp \left\{ \frac{[2 - \vartheta(\mathbf{0}, \mathbf{x}_2)] + [2 - \vartheta(\mathbf{0}, \mathbf{x}_3)] + [2 - \vartheta(\mathbf{x}_1, \mathbf{x}_2)] + [2 - \vartheta(\mathbf{x}_1, \mathbf{x}_3)]}{z} \right\} - 1 \right). \quad (3.16)
 \end{aligned}$$

Let $s \in \mathbb{R}_+^*$. We shall show that each difference in the right-handed part of Eq. (3.16) is integrable over $D := \{\mathbf{x}_1, \mathbf{x}_2, \mathbf{x}_3 \in \mathbb{R}^d : \|\mathbf{x}_1\| \leq s \text{ and } \|\mathbf{x}_2 - \mathbf{x}_3\| \leq s\}$, if $\int_{\mathbb{R}^d} 2 - \theta(\mathbf{h}) d\mathbf{h} < +\infty$.

First, recall from Eq. (2.27) that for any $\mathbf{v}, \mathbf{w} \in \mathbb{R}^d$

$$C_z(\mathbf{v} - \mathbf{w}) = C_z(\mathbf{w} - \mathbf{v}) = \exp \left\{ -\frac{\vartheta(\mathbf{v}, \mathbf{w})}{z} \right\} - \exp \left\{ \frac{-2}{z} \right\} \geq 0$$

Remark also that

$$\int_{\substack{\|\mathbf{x}_1\| \leq s \\ \|\mathbf{x}_2 - \mathbf{x}_3\| \leq s}} C_z(\mathbf{x}_2) d\mathbf{x}_1 d\mathbf{x}_2 d\mathbf{x}_3 = |\mathbb{B}_s| \int_{\mathbb{R}^d} \int_{\mathbb{B}_s(\mathbf{x}_2)} C(\mathbf{x}_2) d\mathbf{x}_2 d\mathbf{x}_3 = |\mathbb{B}_s|^2 \int_{\mathbb{R}^d} C(\mathbf{x}_2) d\mathbf{x}_2, \quad (3.17)$$

where \mathbb{B}_s stands for the centred ball of radius s , and

$$\int_{\substack{\|\mathbf{x}_1\| \leq s \\ \|\mathbf{x}_2 - \mathbf{x}_3\| \leq s}} C_z(\mathbf{x}_1 - \mathbf{x}_2) d\mathbf{x}_1 d\mathbf{x}_2 d\mathbf{x}_3 = |\mathbb{B}_s| \int_{\|\mathbf{x}_1\| \leq s} \int_{\mathbb{R}^d} C(\mathbf{x}_1 - \mathbf{x}_2) d\mathbf{x}_1 d\mathbf{x}_2 = |\mathbb{B}_s|^2 \int_{\mathbb{R}^d} C(\mathbf{y}) d\mathbf{y}. \quad (3.18)$$

Similarly, we have

$$\int_{\substack{\|\mathbf{x}_1\| \leq s \\ \|\mathbf{x}_2 - \mathbf{x}_3\| \leq s}} C_z(\mathbf{x}_3) d\mathbf{x}_1 d\mathbf{x}_2 d\mathbf{x}_3 = |\mathbb{B}_s|^2 \int_{\mathbb{R}^d} C(\mathbf{x}_3) d\mathbf{x}_3 \quad (3.19)$$

and

$$\int_{\substack{\|\mathbf{x}_1\| \leq s \\ \|\mathbf{x}_2 - \mathbf{x}_3\| \leq s}} C_z(\mathbf{x}_1 - \mathbf{x}_3) d\mathbf{x}_1 d\mathbf{x}_2 d\mathbf{x}_3 = |\mathbb{B}_s|^2 \int_{\mathbb{R}^d} C(\mathbf{y}) d\mathbf{y}. \quad (3.20)$$

Then, assume that

$$2 - \theta(\mathbf{h}) \xrightarrow{\|\mathbf{h}\| \rightarrow +\infty} 0,$$

and suppose that $\|\mathbf{x}_1\| \leq s$ and $\|\mathbf{x}_3 - \mathbf{x}_2\| \leq x$. When considering the Taylor series expansion of the exponential function in 0 at the first order, it gives that

$$\begin{aligned}
 & \exp \left\{ \frac{[2 - \vartheta(\mathbf{x}_1, \mathbf{x}_2)] + [2 - \vartheta(\mathbf{x}_1, \mathbf{x}_3)]}{z} \right\} - 1 \stackrel{\|\mathbf{x}_2\| \rightarrow +\infty}{=} \\
 & \left[1 + \frac{2 - \vartheta(\mathbf{x}_1, \mathbf{x}_2)}{z} + o\left(\frac{2 - \vartheta(\mathbf{x}_1, \mathbf{x}_2)}{z}\right) \right] \left[1 + \frac{2 - \vartheta(\mathbf{x}_1, \mathbf{x}_3)}{z} + o\left(\frac{2 - \vartheta(\mathbf{x}_1, \mathbf{x}_3)}{z}\right) \right] - 1 \stackrel{\|\mathbf{x}_2\| \rightarrow +\infty}{=} \\
 & \frac{1}{z} [2 - \vartheta(\mathbf{x}_1, \mathbf{x}_2) + o(2 - \vartheta(\mathbf{x}_1, \mathbf{x}_2)) + 2 - \vartheta(\mathbf{x}_1, \mathbf{x}_3) + o(2 - \vartheta(\mathbf{x}_1, \mathbf{x}_3))].
 \end{aligned}$$

Similarly,

$$\exp \left\{ \frac{[2 - \vartheta(\mathbf{0}, \mathbf{x}_3)] + [2 - \vartheta(\mathbf{x}_1, \mathbf{x}_3)]}{z} \right\} - 1 \stackrel{=}{=} \frac{1}{z} (2 - \vartheta(\mathbf{0}, \mathbf{x}_3) + o(2 - \vartheta(\mathbf{0}, \mathbf{x}_3)) + 2 - \vartheta(\mathbf{x}_1, \mathbf{x}_3) + o(2 - \vartheta(\mathbf{x}_1, \mathbf{x}_3))),$$

$$\exp \left\{ \frac{[2 - \vartheta(\mathbf{0}, \mathbf{x}_2)] + [2 - \vartheta(\mathbf{x}_1, \mathbf{x}_2)]}{z} \right\} - 1 \stackrel{=}{=} \frac{1}{z} (2 - \vartheta(\mathbf{0}, \mathbf{x}_2) + o(2 - \vartheta(\mathbf{0}, \mathbf{x}_2)) + 2 - \vartheta(\mathbf{x}_1, \mathbf{x}_2) + o(2 - \vartheta(\mathbf{x}_1, \mathbf{x}_2))),$$

$$\exp \left\{ \frac{[2 - \vartheta(\mathbf{0}, \mathbf{x}_2)] + [2 - \vartheta(\mathbf{0}, \mathbf{x}_3)]}{z} \right\} - 1 \stackrel{=}{=} \frac{1}{z} (2 - \vartheta(\mathbf{0}, \mathbf{x}_2) + o(2 - \vartheta(\mathbf{0}, \mathbf{x}_2)) + 2 - \vartheta(\mathbf{0}, \mathbf{x}_3) + o(2 - \vartheta(\mathbf{0}, \mathbf{x}_3))),$$

and

$$\exp \left\{ \frac{[2 - \vartheta(\mathbf{0}, \mathbf{x}_2)] + [2 - \vartheta(\mathbf{0}, \mathbf{x}_3)] + [2 - \vartheta(\mathbf{x}_1, \mathbf{x}_2)] + [2 - \vartheta(\mathbf{x}_1, \mathbf{x}_3)]}{z} \right\} - 1 \stackrel{=}{=} \frac{1}{z} \left(2 - \vartheta(\mathbf{0}, \mathbf{x}_2) + o(2 - \vartheta(\mathbf{0}, \mathbf{x}_2)) + 2 - \vartheta(\mathbf{0}, \mathbf{x}_3) + o(2 - \vartheta(\mathbf{0}, \mathbf{x}_3)) + 2 - \vartheta(\mathbf{x}_1, \mathbf{x}_2) + o(2 - \vartheta(\mathbf{x}_1, \mathbf{x}_2)) + 2 - \vartheta(\mathbf{x}_1, \mathbf{x}_3) + o(2 - \vartheta(\mathbf{x}_1, \mathbf{x}_3)) \right).$$

Now remember that it has been shown in [Chapter 2](#) that

$$\int_{\mathbb{R}^d} 2 - \theta(\mathbf{h}) d\mathbf{h} < +\infty \Leftrightarrow \forall z \in (0, +\infty) \int_{\mathbb{R}^d} C_z(\mathbf{h}) d\mathbf{h} < +\infty,$$

(see [Theorem 2.19](#)) and that, if $\lim_{\|\mathbf{h}\| \rightarrow +\infty} 2 - \theta(\mathbf{h})$ exists,

$$\int_{\mathbb{R}^d} 2 - \theta(\mathbf{h}) d\mathbf{h} < +\infty \Rightarrow 2 - \theta(\mathbf{h}) \xrightarrow{\|\mathbf{h}\| \rightarrow +\infty} 0.$$

Therefore, if $\lim_{\|\mathbf{y}\| \rightarrow +\infty} 2 - \theta(\mathbf{y})$ exists and if $\int_{\mathbb{R}^d} 2 - \theta(\mathbf{h}) d\mathbf{h} < +\infty$ thus so are the integrals in equations (3.17)-(3.20). Hence the integrals over D of each difference in the right-handed part of [Eq. \(3.16\)](#) is finite, and consequently $\mathcal{I}_1(x) < +\infty$.

Integral \mathcal{I}_2

First notice that if

$$\int_{\mathbb{R}^d} 2 - \theta(\mathbf{h}) d\mathbf{h} < +\infty, \tag{3.21}$$

then for any $s \in (0, +\infty)$,

$$\int_{\substack{\|\mathbf{x}_1\| \leq s, \quad \|\mathbf{x}_2 - \mathbf{x}_3\| \leq s, \\ \|\mathbf{x}_4 - \mathbf{x}_5\| \leq s, \quad \|\mathbf{x}_6 - \mathbf{x}_7\| \leq s}} \left(\exp \left\{ -\frac{\theta(\mathbf{y}_2, \tilde{\mathbf{y}}_2)}{z} \right\} - \exp \left\{ -\frac{2}{z} \right\} \right) \left(\exp \left\{ -\frac{\theta(\mathbf{y}_4, \tilde{\mathbf{y}}_4)}{z} \right\} - \exp \left\{ -\frac{2}{z} \right\} \right)$$

$$\times \left(\exp \left\{ -\frac{\theta(y_6, \tilde{y}_6)}{z} \right\} - \exp \left\{ -\frac{2}{z} \right\} \right) dx_1, \dots, x_7 < +\infty, \quad (3.22)$$

where the elements $y_2 \in \{\mathbf{x}_2, \mathbf{x}_3\}$, $y_4 \in \{\mathbf{x}_4, \mathbf{x}_5\}$, $y_6 \in \{\mathbf{x}_6, \mathbf{x}_7\}$, $\tilde{y}_2 \in \{\mathbf{0}, \mathbf{x}_1, \mathbf{x}_4, \mathbf{x}_5, \mathbf{x}_6, \mathbf{x}_7\}$, $\tilde{y}_4 \in \{\mathbf{0}, \mathbf{x}_1, \mathbf{x}_2, \mathbf{x}_3, \mathbf{x}_6, \mathbf{x}_7\}$, $\tilde{y}_6 \in \{\mathbf{0}, \mathbf{x}_1, \mathbf{x}_2, \mathbf{x}_3, \mathbf{x}_4, \mathbf{x}_5\}$ are such that the pairs $\{y_2, \tilde{y}_2\}$, $\{y_4, \tilde{y}_4\}$ and $\{y_6, \tilde{y}_6\}$ are distinct, with $\mathbf{0} \in \{\tilde{y}_2, \tilde{y}_4, \tilde{y}_6\}$ or $\mathbf{x}_1 \in \{\tilde{y}_2, \tilde{y}_4, \tilde{y}_6\}$.

Now, let $\mathbf{x}_0, \mathbf{x}_1, \dots, \mathbf{x}_7 \in \mathbb{R}^d$, with $\mathbf{x}_0 = \mathbf{0}$. We have

$$\begin{aligned} g_2(\mathbf{x}_1, \dots, \mathbf{x}_7) &= \mathbf{P} \left[\bigcap_{j=0}^3 I_z(\mathbf{x}_{2j}) \neq I_z(\mathbf{x}_{2j+1}) \right] \\ &- \sum_{i=0}^3 \mathbf{P} \left[\bigcap_{\substack{j \in \{0, \dots, 3\} \\ j \neq i}} I_z(\mathbf{x}_{2j}) \neq I_z(\mathbf{x}_{2j+1}) \right] \mathbf{P} [I_z(\mathbf{x}_{2i}) \neq I_z(\mathbf{x}_{2i+1})] \\ &+ \sum_{\substack{i, k \in \{0, \dots, 3\} \\ i \neq k}} \mathbf{P} \left[\bigcap_{\substack{j \in \{0, \dots, 3\} \\ j \neq i, k}} I_z(\mathbf{x}_{2j}) \neq I_z(\mathbf{x}_{2j+1}) \right] \mathbf{P} [I_z(\mathbf{x}_{2i}) \neq I_z(\mathbf{x}_{2i+1})] \mathbf{P} [I_z(\mathbf{x}_{2k}) \neq I_z(\mathbf{x}_{2k+1})] \\ &- 3 \prod_{j=0}^3 \mathbf{P} [I_z(\mathbf{x}_{2j}) \neq I_z(\mathbf{x}_{2j+1})]. \end{aligned} \quad (3.23)$$

As in the case of the integral \mathcal{I}_1 , we have conveniently decomposed Eq. (3.23) into 16 sums of 14 terms each. Then, using the inequalities for the extremal coefficients found by [Schlather and Tawn \(2002\)](#), we have tried to bound above the absolute value of these sums by the integrand in Eq. (3.22). Because each sum involves 14 terms, this task is more difficult than for \mathcal{I}_1 and, up to now, we did not manage to show that Eq. (3.21) implies that \mathcal{I}_2 is finite.

3.6.2 Continuity: an adequate assumption

As mentioned above, Theorem 3.2 in [García-Soidán et al. \(2004\)](#) and Theorem 3.1 in [García-Soidán \(2007\)](#) need for g_1 and g_2 to be continuously differentiable, respectively. Notice that if g_2 continuously differentiable then so is g_1 . When looking at the proof of Theorem 3.1 closely, it turns out that only the assumption on g_1 is involved. Hence, we shall prove that the continuity of g_1 is a sufficient condition for both theorems. Since the part of the proof where the continuity assumption is required are similar in both proofs, we shall only concentrate on Theorem 3.2 in [García-Soidán et al. \(2004\)](#).

First, recall that I_z is isotropic, for any $z \in (0, +\infty)$. Consequently, there exists a function $g : \mathbb{R}_+^4 \rightarrow \mathbb{R}$ such that,

$$\forall \mathbf{x}_1, \mathbf{x}_2, \mathbf{x}_3 \in \mathbb{R}^d \quad g_1(\mathbf{x}_1, \mathbf{x}_2, \mathbf{x}_3) = g(\|\mathbf{x}_2\|, \|\mathbf{x}_1 - \mathbf{x}_3\|, \|\mathbf{x}_3\|, \|\mathbf{x}_1 - \mathbf{x}_2\|).$$

Similarly to [García-Soidán et al. \(2004\)](#), we shall focus on g instead on g_1 . Recall that g_1 is assumed bounded: thus so is g . Now, set $t \in (0, +\infty)$, $n \in \mathbb{N}^*$ and let the random variables U_1, \dots, U_4 be independent, with same density f_0 . Define also

$$\alpha_1(t) := \mathbb{E} \left[\left(\mathbb{K} \left(\frac{t - \lambda_n \|U_1 - U_2\|}{\tau_n} \right) \right)^2 g(0, 0, \lambda_n \|U_1 - U_2\|, \lambda_n \|U_1 - U_2\|) \right],$$

$$\alpha_2(t) := \mathbb{E} \left[\mathbb{K} \left(\frac{t - \lambda_n \|U_1 - U_2\|}{\tau_n} \right) \mathbb{K} \left(\frac{t - \lambda_n \|U_1 - U_3\|}{\tau_n} \right) \right. \\ \left. \times g(0, \lambda_n \|U_2 - U_3\|, \lambda_n \|U_1 - U_3\|, \lambda_n \|U_1 - U_2\|) \right],$$

and

$$\alpha_3(t) := \mathbb{E} \left[\mathbb{K} \left(\frac{t - \lambda_n \|U_1 - U_2\|}{\tau_n} \right) \mathbb{K} \left(\frac{t - \lambda_n \|U_3 - U_4\|}{\tau_n} \right) \right. \\ \left. \times g(\lambda_n \|U_1 - U_3\|, \lambda_n \|U_2 - U_4\|, \lambda_n \|U_1 - U_4\|, \lambda_n \|U_2 - U_3\|) \right].$$

In the proof of Theorem 3.2 in [García-Soidán et al. \(2004\)](#), the assumption that g is continuously differentiable is invoked when calculating the expectation $\alpha_1(t)$, $\alpha_2(t)$ and $\alpha_3(t)$, but this computation is not detailed at all. We shall detail the calculus and show that the result is still valid when only assuming that g is continuous. Let us focus on $\alpha_1(t)$. Let $E_0 = \{\mathbf{x}_1 - \mathbf{x}_2 \in \mathbb{R}^d : \mathbf{x}_1, \mathbf{x}_2 \in V\}$. It follows

$$\alpha_1(t) = \int_{E_0} \left(\mathbb{K} \left(\frac{t - \lambda_n \|\mathbf{x}\|}{\tau_n} \right) \right)^2 g(0, 0, \lambda_n \|\mathbf{x}\|, \lambda_n \|\mathbf{x}\|) f_1(\mathbf{x}) d\mathbf{x},$$

Let $m_0 = \sup\{\|\mathbf{x}_1 - \mathbf{x}_2\| : \mathbf{x}_1, \mathbf{x}_2 \in V\}$. By an abuse of notation, we shall write, for any $y = (y_1, \dots, y_d) \in \mathbb{R}^d$, $f_1(y) = f_1(y_1, \dots, y_d)$. When switching to hyperspherical coordinates, it yields that

$$\alpha_1(t) = \int_0^{m_0} \int_0^\pi \dots \int_0^\pi \int_0^{2\pi} r^{d-1} \left(\mathbb{K} \left(\frac{t - \lambda_n r}{\tau_n} \right) \right)^2 J_d(\theta_1, \dots, \theta_{d-1}) g(0, 0, \lambda_n r, \lambda_n r) \\ \times f_1 \left(r \cos(\theta_1), \dots, r \prod_{j=1}^{d-1} \sin(\theta_j) \right) dr d\theta_1, \dots, d\theta_{d-1}, \quad (3.24)$$

where $J_d(\theta_1, \dots, \theta_{d-1}) = (\sin(\theta_1))^{d-2} (\sin(\theta_2))^{d-3} \dots \sin(\theta_{d-2})$. With substitution $s = (t - \lambda_n r)/\tau_n$, this becomes

$$\alpha_1(t) = \int_{(t - \lambda_n m_0)/\tau_n}^{s/\tau_n} \int_0^\pi \dots \int_0^\pi \int_0^{2\pi} \tau_n \lambda_n^{-d} (t - s\tau_n)^{d-1} (\mathbb{K}(s))^2 J_d(\theta_1, \dots, \theta_{d-1}) \\ \times g(0, 0, t - s\tau_n, t - s\tau_n) f_1 \left(\lambda_n^{-1} (t - s\tau_n) \cos(\theta_1), \dots, \lambda_n^{-1} (t - s\tau_n) \prod_{j=1}^{d-1} \sin(\theta_j) \right) ds d\theta_1, \dots, d\theta_{d-1}.$$

Then, by using the binomial expansion and the dominated convergence theorem, it holds

$$\begin{aligned} \alpha_1(t) &= \tau_n \lambda_n^{-d} t^{d-1} \int_{(t-\lambda_n m_0)/\tau_n}^{t/\tau_n} \int_0^\pi \cdots \int_0^\pi \int_0^{2\pi} (\mathbb{K}(s))^2 J_d(\theta_1, \dots, \theta_{d-1}) g(0, 0, t - s\tau_n, t - s\tau_n) \\ &\quad \times f_1 \left(\lambda_n^{-1}(t - s\tau_n) \cos(\theta_1), \dots, \lambda_n^{-1}(t - s\tau_n) \prod_{j=1}^{d-1} \sin(\theta_j) \right) ds d\theta_1, \dots, d\theta_{d-1} + o(\tau_n \lambda_n^{-d}), \end{aligned}$$

as $n \rightarrow +\infty$. Indeed, recall that $\tau_n \rightarrow 0$ and $\lambda_n \rightarrow +\infty$ as $n \rightarrow +\infty$. Notice also that

- \mathbb{K} is compactly supported on $[-C, C]$,
- $\lim_{n \rightarrow +\infty} \mathbf{1} \left\{ \max \left(-C, \frac{t - \lambda_n m_0}{\tau_n} \right) \leq s \leq \min \left(C, \frac{t}{\tau_n} \right) \right\} = \mathbf{1} \{-C \leq s \leq C\}$
- f_1 is a density function, which is continuous in $\mathbf{0}$ (see (A2)),
- g is bounded and is continuous in $(0, 0, t, t)$,
- $|g(0, 0, t, t)| f_1(\mathbf{0}) \int_{-C}^C \cdots \int_0^\pi \int_0^{2\pi} s^{d-1-k} (\mathbb{K}(s))^2 |J_d(\theta_1, \dots, \theta_{d-1})| dr d\theta_1, \dots, d\theta_{d-1} < +\infty$, for any $k \in \{0, \dots, d-2\}$.

By using the dominated convergence theorem, we obtain

$$\begin{aligned} &\lim_{n \rightarrow +\infty} \int_{(t-\lambda_n m_0)/\tau_n}^{t/\tau_n} \int_0^\pi \cdots \int_0^\pi \int_0^{2\pi} s^{d-1-k} (\mathbb{K}(s))^2 J_d(\theta_1, \dots, \theta_{d-1}) g(0, 0, t - s\tau_n, t - s\tau_n) \\ &\quad \times f_1 \left(\lambda_n^{-1}(t - s\tau_n) \cos(\theta_1), \dots, \lambda_n^{-1}(t - s\tau_n) \prod_{j=1}^{d-1} \sin(\theta_j) \right) ds d\theta_1, \dots, d\theta_{d-1} < +\infty \end{aligned}$$

and consequently,

$$\begin{aligned} &\tau_n \lambda_n^{-d} \sum_{k=0}^{d-2} C_{d-1}^k t^k (-\tau_n)^{d-1-k} \int_{(t-\lambda_n m_0)/\tau_n}^{t/\tau_n} \int_0^\pi \cdots \int_0^\pi \int_0^{2\pi} s^{d-1-k} (\mathbb{K}(s))^2 \\ &\quad \times J_d(\theta_1, \dots, \theta_{d-1}) g(0, 0, t - s\tau_n, t - s\tau_n) \\ &\quad \times f_1 \left(\lambda_n^{-1}(t - s\tau_n) \cos(\theta_1), \dots, \lambda_n^{-1}(t - s\tau_n) \prod_{j=1}^{d-1} \sin(\theta_j) \right) ds d\theta_1, \dots, d\theta_{d-1} \stackrel{n \rightarrow +\infty}{=} o(\tau_n \lambda_n^{-d}). \end{aligned}$$

Similarly, according to the dominated convergence theorem, we also have

$$\begin{aligned} &\lim_{n \rightarrow +\infty} \int_{(t-\lambda_n m_0)/\tau_n}^{t/\tau_n} \int_0^\pi \cdots \int_0^\pi \int_0^{2\pi} (\mathbb{K}(s))^2 J_d(\theta_1, \dots, \theta_{d-1}) \\ &\quad \times \left[g(0, 0, t - s\tau_n, t - s\tau_n) f_1 \left(\lambda_n^{-1}(t - s\tau_n) \cos(\theta_1), \dots, \lambda_n^{-1}(t - s\tau_n) \prod_{j=1}^{d-1} \sin(\theta_j) \right) \right. \\ &\quad \times \mathbf{1} \left\{ \max \left(-C, \frac{t - \lambda_n m_0}{\tau_n} \right) \leq s \leq \min \left(C, \frac{t}{\tau_n} \right) \right\} \\ &\quad \left. - g(0, 0, t, t) f_1(\mathbf{0}) \mathbf{1} \{-C \leq s \leq C\} \right] ds d\theta_1, \dots, d\theta_{d-1} \\ &= \int_{(t-\lambda_n m_0)/\tau_n}^{t/\tau_n} \int_0^\pi \cdots \int_0^\pi \int_0^{2\pi} (\mathbb{K}(s))^2 J_d(\theta_1, \dots, \theta_{d-1}) \end{aligned}$$

$$\begin{aligned}
 & \times \lim_{n \rightarrow +\infty} \left[g(0, 0, t - s\tau_n, t - s\tau_n) f_1 \left(\lambda_n^{-1}(t - s\tau_n) \cos(\theta_1), \dots, \lambda_n^{-1}(t - s\tau_n) \prod_{j=1}^{d-1} \sin(\theta_j) \right) \right. \\
 & \quad \times \mathbf{1} \left\{ \max \left(-C, \frac{t - \lambda_n m_0}{\tau_n} \right) \leq s \leq \min \left(C, \frac{t}{\tau_n} \right) \right\} \\
 & \quad \left. - g(0, 0, t, t) f_1(\mathbf{0}) \mathbf{1}\{-C \leq s \leq C\} \right] ds d\theta_1, \dots, d\theta_{d-1} \\
 & = 0
 \end{aligned}$$

Consequently, the result in [García-Soidán et al. \(2004\)](#) is retrieved:

$$\alpha_1(t) = d_K f_1(\mathbf{0}) t^{d-1} A_d g(0, 0, t, t) \tau_n \lambda_n^{-d} + o(\tau_n \lambda_n^{-d}), \quad (3.25)$$

with d_K and A_d defined as in [García-Soidán et al. \(2004\)](#).

We can also recover $\alpha_2(t)$ and $\alpha_3(t)$ in [García-Soidán et al. \(2004\)](#) by only using the assumption that g is continuous and not continuously differentiable. Since the calculus are similar, this is not presented here.

3.6.3 Finite integrale range: an alternative condition

Let $r \in \mathbb{R}_+$ and define

$$\tilde{q}(r) := \sup_{\substack{\mathbf{x}_1, \mathbf{x}_2 \in \mathbb{R}^d \\ \|\mathbf{x}_1 - \mathbf{x}_2\| \geq r}} (2 - \vartheta(\mathbf{x}_1, \mathbf{x}_2)).$$

In [García-Soidán \(2007\)](#), the asymptotic normality of the Nadaraya-Watson semivariogram estimator is obtained under the assumption that:

$$q(r) \xrightarrow{r \rightarrow +\infty} 0, \quad (3.26)$$

see [Remark 3.5](#). We shall prove that this condition may be replaced by

$$\tilde{q}(r) \xrightarrow{r \rightarrow +\infty} 0,$$

which is actually equivalent to $\lim_{\|\mathbf{h}\| \rightarrow +\infty} 2 - \theta(\mathbf{h}) = 0$ as $n \rightarrow +\infty$, see [Remark 3.14](#). Let us first introduce some notation. First recall from [Chapter 2](#) that the Minkowski sum of two bounded measurable subsets V and W of \mathbb{R}^d is defined as

$$V \oplus W := \{v + w, v \in V \text{ and } w \in W\}.$$

For any subset $V \in \mathbb{R}^d$ and for any $\lambda \in (0, +\infty)$, the set λV corresponds to the image of V after applying the homothety with center $\mathbf{0}$ and ratio λ . We shall stress that this notation slightly differs from [Chapter 2](#) where λV stood for image of V after applying the homothety with

ratio λ but with center equal to the barycenter of V .

Set $n \in \mathbb{N}$ and let $(C_{j,n})_{j \in \mathbb{N}^*}$ be a sequence of d -dimensional hypercubes of side α_n , which cover \mathbb{R}^d so that each hypercube is separated from its nearest neighbours by a spacing strip of width β_n . The sequences $(\alpha_n)_{n \in \mathbb{N}}$ and $(\beta_n)_{n \in \mathbb{N}}$ satisfy $\lim_{n \rightarrow +\infty} \alpha_n = +\infty$, $\lim_{n \rightarrow +\infty} \beta_n = +\infty$ and

$$\lambda_n^d \alpha_n^{-d} \varrho \left(\frac{\beta_n}{2} \right) \xrightarrow{n \rightarrow +\infty} 0. \quad (3.27)$$

Let also $\mathcal{J}_n := \{j \in \mathbb{N}^* : \lambda_n^{-1} C_j \cap V \neq \emptyset\}$, with number of elements J_n . Since $\mathbf{0} \in V$, $\lim_{n \rightarrow +\infty} J_n = +\infty$. In the sequel, for simplicity of notation, we shall write $C_j = C_{j,n}$ and $\mathcal{J} = \mathcal{J}_n$. Finally, let $W = \{\mathbf{y}_1 - \mathbf{y}_2 \in \mathbb{R}^d : \mathbf{y}_1, \mathbf{y}_2 \in V\}$ and define, for any $z, t \in (0, +\infty)$ and $j \in \mathbb{N}^*$,

$$Y_{2,j}(t) := \int_W \int_{\lambda_n^{-1} C_j \cap V} K \left(\frac{t - \lambda_n \|\mathbf{x}\|}{\tau_n} \right) \left([Z(\lambda_n \mathbf{x} + \lambda_n \mathbf{v}) - Z(\lambda_n \mathbf{v})]^2 - 2\gamma_z(\lambda_n \|\mathbf{x}\|) \right) \\ \times f_0(\mathbf{x} + \mathbf{v}) f_0(\mathbf{v}) d\mathbf{x} d\mathbf{v}.$$

Now, set $z, t \in (0, +\infty)$ and $j_0 \in \mathcal{J}$, and recall that the kernel K in Eq. (3.5) is compactly supported on $[-C, C]$, with $C \in (0, +\infty)$. In the proof of Theorem 3.1 in García-Soidán (2007) (see the appendix, section 5), Eq. (3.26) intervenes at the end of the page 498 to get

$$A := \mathbb{E} \left[Y_{2,j_0}(t) \sum_{j \in \mathcal{J} \setminus j_0} Y_{2,j}(t) \right] = O \left(\lambda_n^{-3d} \tau_n^2 \varrho(\beta_n - 2[t + C]) \right) \quad \text{as } n \rightarrow +\infty. \quad (3.28)$$

The author does not give any details about the different steps to get Eq. (3.28). This result together with Eq. (3.27) and Eq. (3.26) is then used in an intermediate step to ultimately obtain the asymptotic normality of $\hat{\gamma}_{z, \tau_n}(t)$. Similarly to Eq. (3.27), assume without any inconvenience that $(\alpha_n)_{n \in \mathbb{N}}$ and $(\beta_n)_{n \in \mathbb{N}}$ satisfy

$$\lambda_n^d \alpha_n^{-d} \tilde{\varrho} \left(\frac{\beta_n}{2} \right) \xrightarrow{n \rightarrow +\infty} 0. \quad (3.29)$$

We shall demonstrate that

$$A = O \left(\lambda_n^{-3d} \tau_n^2 \tilde{\varrho}(\beta_n - 2[t + C]) \right) \quad \text{as } n \rightarrow +\infty.$$

Proof. We have

$$A = \sum_{j \in \mathcal{J} \setminus j_0} \int_W \int_{\lambda_n^{-1} C_j \cap V} \int_W \int_{\lambda_n^{-1} C_{j_0} \cap V} K \left(\frac{t - \lambda_n \|\mathbf{x}_1\|}{\tau_n} \right) K \left(\frac{t - \lambda_n \|\mathbf{x}_2\|}{\tau_n} \right) \\ \times \mathbb{E} \left[\left\{ [Z(\lambda_n \mathbf{x}_1 + \lambda_n \mathbf{v}_1) - Z(\lambda_n \mathbf{v}_1)]^2 - 2\gamma_z(\lambda_n \|\mathbf{x}_1\|) \right\} \right. \\ \left. \times \left\{ [Z(\lambda_n \mathbf{x}_2 + \lambda_n \mathbf{v}_2) - Z(\lambda_n \mathbf{v}_2)]^2 - 2\gamma_z(\lambda_n \|\mathbf{x}_2\|) \right\} \right] \\ \times f_0(\mathbf{x}_1 + \mathbf{v}_1) f_0(\mathbf{v}_1) f_0(\mathbf{x}_2 + \mathbf{v}_2) f_0(\mathbf{v}_2) d\mathbf{x}_1 d\mathbf{v}_1 d\mathbf{x}_2 d\mathbf{v}_2,$$

Since

$$\begin{aligned} & E \left[\left\{ [Z(\lambda_n \mathbf{x}_1 + \lambda_n \mathbf{v}_1) - Z(\lambda_n \mathbf{v}_1)]^2 - 2\Upsilon_z(\lambda_n \|\mathbf{x}_1\|) \right\} \right. \\ & \quad \left. \times \left\{ [Z(\lambda_n \mathbf{x}_2 + \lambda_n \mathbf{v}_2) - Z(\lambda_n \mathbf{v}_2)]^2 - 2\Upsilon_z(\lambda_n \|\mathbf{x}_2\|) \right\} \right] \\ & = \text{Cov} \left[(Z(\lambda_n \mathbf{x}_1 + \lambda_n \mathbf{v}_1) - Z(\lambda_n \mathbf{v}_1))^2, (Z(\lambda_n \mathbf{x}_2 + \lambda_n \mathbf{v}_2) - Z(\lambda_n \mathbf{v}_2))^2 \right], \end{aligned}$$

and by assumption, $\sup_{\mathbf{x} \in V} f_0(\mathbf{x}) < +\infty$, the following inequality holds

$$\begin{aligned} A & \leq \left(\sup_{\mathbf{x} \in V} f_0(\mathbf{x}) \right)^4 \sum_{j \in \mathcal{J} \setminus j_0} \int_W \int_{\lambda_n^{-1} C_j \cap V} \int_W \int_{\lambda_n^{-1} C_{j_0} \cap V} K \left(\frac{t - \lambda_n \|\mathbf{x}_1\|}{\tau_n} \right) K \left(\frac{t - \lambda_n \|\mathbf{x}_2\|}{\tau_n} \right) \\ & \quad \times \text{Cov} \left[(Z(\lambda_n \mathbf{x}_1 + \lambda_n \mathbf{v}_1) - Z(\lambda_n \mathbf{v}_1))^2, (Z(\lambda_n \mathbf{x}_2 + \lambda_n \mathbf{v}_2) - Z(\lambda_n \mathbf{v}_2))^2 \right] d\mathbf{x}_1 d\mathbf{v}_1 d\mathbf{x}_2 d\mathbf{v}_2, \end{aligned}$$

In addition K is nonnegative and compactly supported on $[-C, C]$. Hence,

$$\begin{aligned} A & \leq \left(\sup_{\mathbf{x} \in V} f_0(\mathbf{x}) \right)^4 \sum_{j \in \mathcal{J} \setminus j_0} \int_{\substack{\mathbf{x}_1 \text{ s.t.} \\ t - C\tau_n \leq \lambda_n \|\mathbf{x}_1\| \leq t + C\tau_n}} \int_{\lambda_n^{-1} C_j \cap V} \int_{\substack{\mathbf{x}_2 \text{ s.t.} \\ t - C\tau_n \leq \lambda_n \|\mathbf{x}_2\| \leq t + C\tau_n}} \\ & \int_{\lambda_n^{-1} C_{j_0} \cap V} K \left(\frac{t - \lambda_n \|\mathbf{x}_1\|}{\tau_n} \right) K \left(\frac{t - \lambda_n \|\mathbf{x}_2\|}{\tau_n} \right) \\ & \quad \times \left| \text{Cov} \left[(Z(\lambda_n \mathbf{x}_1 + \lambda_n \mathbf{v}_1) - Z(\lambda_n \mathbf{v}_1))^2, (Z(\lambda_n \mathbf{x}_2 + \lambda_n \mathbf{v}_2) - Z(\lambda_n \mathbf{v}_2))^2 \right] \right| d\mathbf{x}_1 d\mathbf{v}_1 d\mathbf{x}_2 d\mathbf{v}_2. \end{aligned}$$

Let now $W_t := \{\mathbf{x} \in \mathbb{R}^d : 0 \leq \lambda_n \|\mathbf{x}\| \leq t + C\}$. Consequently, for n large enough so that $\tau_n \leq \min(t/C, 1)$,

$$\begin{aligned} A & \leq \left(\sup_{\mathbf{x} \in V} f_0(\mathbf{x}) \right)^4 \sum_{j \in \mathcal{J} \setminus j_0} \int_{W_t} \int_{\lambda_n^{-1} C_j \cap V} \int_{W_t} \int_{\lambda_n^{-1} C_{j_0} \cap V} K \left(\frac{t - \lambda_n \|\mathbf{x}_1\|}{\tau_n} \right) K \left(\frac{t - \lambda_n \|\mathbf{x}_2\|}{\tau_n} \right) \\ & \quad \times \left| \text{Cov} \left[(Z(\lambda_n \mathbf{x}_1 + \lambda_n \mathbf{v}_1) - Z(\lambda_n \mathbf{v}_1))^2, (Z(\lambda_n \mathbf{x}_2 + \lambda_n \mathbf{v}_2) - Z(\lambda_n \mathbf{v}_2))^2 \right] \right| d\mathbf{x}_1 d\mathbf{v}_1 d\mathbf{x}_2 d\mathbf{v}_2. \quad (3.30) \end{aligned}$$

Let $\mathbf{x}_1, \mathbf{x}_2 \in W_t$, $\mathbf{v}_1 \in (\lambda_n^{-1} C_j \cap V)$, and $\mathbf{v}_2 \in (\lambda_n^{-1} C_{j_0} \cap V)$. Remembering that for any $j_0 \in \mathcal{J}$ and for any $j \in \mathcal{J} \setminus j_0$, $d(C_{j_0}, C_j) \geq \beta_n$, notice that,

$$d(\lambda_n W_t \oplus (C_j \cap \lambda_n V), \lambda_n W_t \oplus (C_{j_0} \cap \lambda_n V)) \geq \beta_n - 2(t + C). \quad (3.31)$$

We shall now prove that

$$\left| \text{Cov} \left[(Z(\lambda_n \mathbf{x}_1 + \lambda_n \mathbf{v}_1) - Z(\lambda_n \mathbf{v}_1))^2, (Z(\lambda_n \mathbf{x}_2 + \lambda_n \mathbf{v}_2) - Z(\lambda_n \mathbf{v}_2))^2 \right] \right| \leq \tilde{q}_{n,t}, \quad (3.32)$$

with

$$\tilde{q}_{n,t} = 16 \left(\exp \left\{ \frac{4\tilde{\varrho}(\beta - 2[t + C])}{z} \right\} - 1 \right).$$

For simplicity, write $\mathbf{y}_1 = \lambda_n \mathbf{x}_1$, $\mathbf{y}_2 = \lambda_n \mathbf{x}_1 + \lambda_n \mathbf{v}_1 - \lambda_n \mathbf{x}_2 - \lambda_n \mathbf{v}_2$ and $\mathbf{y}_3 = \lambda_n \mathbf{x}_1 + \lambda_n \mathbf{v}_1 - \lambda_n \mathbf{v}_2$.

From Eq. (3.16),

$$\left| \text{Cov} \left[(Z(\lambda_n \mathbf{x}_1 + \lambda_n \mathbf{v}_1) - Z(\lambda_n \mathbf{v}_1))^2, (Z(\lambda_n \mathbf{x}_2 + \lambda_n \mathbf{v}_2) - Z(\lambda_n \mathbf{v}_2))^2 \right] \right|$$

$$\begin{aligned}
&= \left| \text{Cov} \left[(Z(\mathbf{0}) - Z(\mathbf{y}_1))^2, (Z(\mathbf{y}_2) - Z(\mathbf{y}_3))^2 \right] \right| \\
&\leq \left(\exp \left\{ -\frac{\vartheta(\mathbf{0}, \mathbf{y}_2)}{z} \right\} - \exp \left\{ \frac{-2}{z} \right\} \right) + \left(\exp \left\{ -\frac{\vartheta(\mathbf{y}_1, \mathbf{y}_2)}{z} \right\} - \exp \left\{ \frac{-2}{z} \right\} \right) \\
&+ \left(\exp \left\{ -\frac{\vartheta(\mathbf{0}, \mathbf{y}_3)}{z} \right\} - \exp \left\{ \frac{-2}{z} \right\} \right) + \left(\exp \left\{ -\frac{\vartheta(\mathbf{y}_1, \mathbf{y}_3)}{z} \right\} - \exp \left\{ \frac{-2}{z} \right\} \right) \\
&+ 2 \left(\exp \left\{ \frac{[2 - \vartheta(\mathbf{y}_1, \mathbf{y}_2)] + [2 - \vartheta(\mathbf{y}_1, \mathbf{y}_3)]}{z} \right\} - 1 \right) + 2 \left(\exp \left\{ \frac{[2 - \vartheta(\mathbf{0}, \mathbf{y}_3)] + [2 - \vartheta(\mathbf{y}_1, \mathbf{y}_3)]}{z} \right\} - 1 \right) \\
&+ 2 \left(\exp \left\{ \frac{[2 - \vartheta(\mathbf{0}, \mathbf{y}_2)] + [2 - \vartheta(\mathbf{y}_1, \mathbf{y}_2)]}{z} \right\} - 1 \right) + 2 \left(\exp \left\{ \frac{[2 - \vartheta(\mathbf{0}, \mathbf{y}_2)] + [2 - \vartheta(\mathbf{0}, \mathbf{y}_3)]}{z} \right\} - 1 \right) \\
&+ 4 \left(\exp \left\{ \frac{[2 - \vartheta(\mathbf{0}, \mathbf{y}_2)] + [2 - \vartheta(\mathbf{0}, \mathbf{y}_3)] + [2 - \vartheta(\mathbf{y}_1, \mathbf{y}_2)] + [2 - \vartheta(\mathbf{y}_1, \mathbf{y}_3)]}{z} \right\} - 1 \right).
\end{aligned}$$

Consider the right-handed part of this inequality. According to Eq. (3.31), the four first terms, the four following terms and the last term are less than $\exp \{ \tilde{\varrho}(\beta_n - 2[h + C])/z \} - 1$, $2(\exp \{ 2\tilde{\varrho}(\beta_n - 2[h + C])/z \} - 1)$ and $4(\exp \{ 4\tilde{\varrho}(\beta_n - 2[h + C])/z \} - 1)$, respectively. Hence Eq. (3.32) is satisfied. Coming back to Eq. (3.30), it follows that

$$\begin{aligned}
A &\leq \tilde{\varrho}_{n,t} \left(\sup_{\mathbf{x} \in V} f_0(\mathbf{x}) \right)^4 \sum_{j \in \mathcal{J} \setminus j_0} \int_{W_t} \int_{\lambda_n^{-1} C_j \cap V} \int_{W_t} \int_{\lambda_n^{-1} C_{j_0} \cap V} \\
&\quad \mathbb{K} \left(\frac{t - \lambda_n \|\mathbf{x}_1\|}{\tau_n} \right) \mathbb{K} \left(\frac{t - \lambda_n \|\mathbf{x}_2\|}{\tau_n} \right) d\mathbf{x}_1 d\mathbf{v}_1 d\mathbf{x}_2 d\mathbf{v}_2 \\
&\leq \tilde{\varrho}_{n,t} \left(\sup_{\mathbf{x} \in V} f_0(\mathbf{x}) \right)^4 \lambda_n^{-2d} (J_n - 1) |C_j \cap \lambda_n V| |C_{j_0} \cap \lambda_n V| \\
&\quad \times \int_{W_t} \int_{W_t} \mathbb{K} \left(\frac{t - \lambda_n \|\mathbf{x}_1\|}{\tau_n} \right) \mathbb{K} \left(\frac{t - \lambda_n \|\mathbf{x}_2\|}{\tau_n} \right) d\mathbf{x}_1 d\mathbf{x}_2,
\end{aligned}$$

For every $j \in \mathcal{J}$, $|C_j| = \alpha_n^d$ and, since V is bounded, there exists $b_3 \in \mathbb{R}_+^*$ such that $J_n \leq b_3 (\lambda_n \alpha_n^{-1})^d$. Hence, for large enough n ,

$$A \leq \tilde{\varrho}_{n,t} \left(\sup_{\mathbf{x} \in V} f_0(\mathbf{x}) \right)^4 b_3 \alpha_n^d \lambda_n^{-d} \int_{W_t} \int_{W_t} \mathbb{K} \left(\frac{t - \lambda_n \|\mathbf{x}_1\|}{\tau_n} \right) \mathbb{K} \left(\frac{t - \lambda_n \|\mathbf{x}_2\|}{\tau_n} \right) d\mathbf{x}_1 d\mathbf{x}_2. \quad (3.33)$$

If additionally n is such that $b_3 \alpha_n^d \leq 1$, then

$$A \leq \tilde{\varrho}_{n,t} \left(\sup_{\mathbf{x} \in V} f_0(\mathbf{x}) \right)^4 \lambda^{-d} \int_{W_t} \int_{W_t} \mathbb{K} \left(\frac{t - \lambda_n \|\mathbf{x}_1\|}{\tau_n} \right) \mathbb{K} \left(\frac{t - \lambda_n \|\mathbf{x}_2\|}{\tau_n} \right) d\mathbf{x}_1 d\mathbf{x}_2. \quad (3.34)$$

Let $R_t = \{r \in \mathbb{R}_+, 0 \leq \lambda_n r \leq t + C\}$, and let $n \in \mathbb{N}$ such that $(t + C)/\lambda_n \leq 1$. When switching to polar coordinates, we thus obtain that

$$A \leq \tilde{\varrho}_{n,t} \left(\sup_{\mathbf{x} \in V} f_0(\mathbf{x}) \right)^4 \lambda^{-d} d |B_1| \int_{R_t} \int_{R_t} r_1^{d-1} r_2^{d-1} \mathbb{K} \left(\frac{t - \lambda_n r_1}{\tau_n} \right) \mathbb{K} \left(\frac{t - \lambda_n r_2}{\tau_n} \right) dr_1 dr_2$$

With substitutions $s_1 = (t - \lambda_n r_1)/\tau_n$ and $s_2 = (t - \lambda_n r_2)/\tau_n$, it follows that

$$A \leq \tilde{\varrho}_{n,t} \left(\sup_{\mathbf{x} \in V} f_0(\mathbf{x}) \right)^4 \lambda^{-3d} \tau_n^2 d |B_1| \int_{s_1 \in \mathbb{R}_+ \text{ s.t. } \frac{t-C}{\tau_n} \leq s_1 \leq \frac{t}{\tau_n}} \int_{s_2 \in \mathbb{R}_+ \text{ s.t. } \frac{t-C}{\tau_n} \leq s_2 \leq \frac{t}{\tau_n}} (t - \tau_n s_1)^{d-1} (t - \tau_n s_2)^{d-1}$$

$$\begin{aligned} & \times K(s_1) K(s_2) ds_1 ds_2 \\ & \leq \tilde{Q}_{n,t} \left(\sup_{\mathbf{x} \in V} f_0(\mathbf{x}) \right)^4 \lambda^{-3d} \tau_n^2 d |\mathbb{B}_1| (\tau_n + C)^{2(d-1)} \int_{\substack{s_1 \in \mathbb{R}_+ \\ \frac{-C}{\tau_n} \leq s_1 \leq \frac{t}{\tau_n}}} \int_{\substack{s_2 \in \mathbb{R}_+ \\ \frac{-C}{\tau_n} \leq s_2 \leq \frac{t}{\tau_n}}} K(s_1) K(s_2) ds_1 ds_2. \end{aligned}$$

For large enough n , since K is a density function compactly supported on $[-C, C]$, it yields

$$A \leq \tilde{Q}_{n,t} \left(\sup_{\mathbf{x} \in V} f_0(\mathbf{x}) \right)^4 \lambda^{-3d} \tau_n^2 d |\mathbb{B}_1| (\tau_n + C)^{2(d-1)}.$$

When assuming that $\lim_{r \rightarrow +\infty} \tilde{Q}(r) = 0$, and since $\lim_{n \rightarrow +\infty} \beta_n = +\infty$, it gives

$$A = O\left(\lambda^{-3d} \tau_n^2 \tilde{Q}_{n,t}\right) \quad \text{as } n \rightarrow +\infty,$$

which is equivalent to

$$A = O\left(\lambda^{-3d} \tau_n^2 \tilde{Q}(\beta_n - 2[t + C])\right) \quad \text{as } n \rightarrow +\infty,$$

since $\exp\{x\} - 1 \sim x$ as $x \rightarrow +0$. This concludes the proof. ■

Remark 3.14 The two following propositions are equivalent:

$$(i) \quad \tilde{Q}(r) \xrightarrow{r \rightarrow +\infty} 0$$

$$(ii) \quad 2 - \theta(\mathbf{0}, \mathbf{h}) \xrightarrow{\|\mathbf{h}\| \rightarrow +\infty} 0$$

The implication (i) \Rightarrow (ii) is straightforward. Now, let $\epsilon \in \mathbb{R}_+^*$. The condition (ii) guarantees that it exists $\mathbf{h}_1^\epsilon \in \mathbb{R}^d$ such that for any $\mathbf{h} \in \mathbb{R}^d$ satisfying $\|\mathbf{h}\| \geq \|\mathbf{h}_1^\epsilon\|$,

$$0 \leq 2 - \theta(\mathbf{0}, \mathbf{h}) < \epsilon.$$

Hence, for any $r \geq \|\mathbf{h}_1^\epsilon\|$,

$$0 \leq \sup_{\substack{\mathbf{x}_1, \mathbf{x}_2 \in \mathbb{R}^d \\ \|\mathbf{x}_1 - \mathbf{x}_2\| \geq r}} (2 - \theta(\mathbf{x}_1, \mathbf{x}_2)) \leq \epsilon,$$

and consequently (ii) implies (i).

3.6.4 Ergodicity in the covariance

Let Z be a second-order SRF on \mathbb{R}^d with expectation μ and covariance function C . In this subsection, we shall digress briefly from the possibility of estimating the covariance function

from a unique realization of Z , which is observed everywhere. Remind the notation introduced in [Chapter 2](#): consider a sequence $V_n \uparrow \mathbb{R}^d$. Let $\mathbf{h} \in \mathbb{R}^d$ and for any $n \in \mathbb{N}$, define $V_n^{\mathbf{h}} := V_n \cap (V_n + \mathbf{h})$; obviously $V_n^{\mathbf{h}} \uparrow \mathbb{R}^d$. An empirical estimator of $C(\mathbf{h})$ is thus given by

$$\begin{aligned}\hat{C}_n(\mathbf{h}) &= \frac{1}{|V_n^{\mathbf{h}}|} \int_{V_n^{\mathbf{h}}} \left[Z(\mathbf{x}) - Z(V_n^{\mathbf{h}}) \right] \left[Z(\mathbf{x} + \mathbf{h}) - Z(V_n^{\mathbf{h}}) \right] d\mathbf{x} \\ &= \frac{1}{|V_n^{\mathbf{h}}|} \int_{V_n^{\mathbf{h}}} Z(\mathbf{x})Z(\mathbf{x} + \mathbf{h}) d\mathbf{x} - \left[Z(V_n^{\mathbf{h}}) \right]^2,\end{aligned}$$

where

$$Z(V_n^{\mathbf{h}}) := \frac{1}{|V_n^{\mathbf{h}}|} \int_{V_n^{\mathbf{h}}} Z(\mathbf{x}) d\mathbf{x}.$$

This estimator is biased:

$$\mathbb{E} [\hat{C}_n(\mathbf{h})] = C(\mathbf{h}) - \mathbb{E} \left[\left(Z(V_n^{\mathbf{h}}) - \mu \right)^2 \right].$$

It is asymptotically unbiased if Z is assumed to be ergodic in the mean (see [Definition 2.5](#)), since this implies that $Z(V_n^{\mathbf{h}})$ converges to μ in the mean square sense as $n \rightarrow +\infty$. Similarly, under appropriate conditions on the fourth-order moments of Z , we could also suppose that Z is *ergodic in the covariance*, i.e.

$$\lim_{n \rightarrow +\infty} \text{Var} [\hat{C}_n(\mathbf{h})] = 0, \tag{3.35}$$

for any $\mathbf{h} \in \mathbb{R}^d$. This means that $\hat{C}_n(\mathbf{h})$ is consistent (in the mean square sense); $C(\mathbf{h})$ can be estimated from a single realization of Z with any desirable degree of accuracy provided that the latter is observed on a sufficiently large domain. Suppose also that the random field $Y_{\mathbf{h}} = (Z(\mathbf{x})Z(\mathbf{x} + \mathbf{h}))_{\mathbf{x} \in \mathbb{R}^d}$ is second-order stationary, with covariance function $C_{Y_{\mathbf{h}}}$. It is easy to show that an equivalent condition to [Eq. \(3.35\)](#) is

$$\lim_{n \rightarrow +\infty} \frac{1}{|V_n|} \int_{V_n} C_{Y_{\mathbf{h}}}(\mathbf{y}) d\mathbf{y} = 0.$$

CONTINUOUS SIMULATION OF STORM PROCESSES

Résumé *Ce chapitre porte sur la simulation exacte de processus tempête. Ces processus constituent des prototypes pour modéliser les extrêmes spatiaux. La plupart des algorithmes existants permettent de simuler ces processus de manière exacte sur un ensemble fini de points dans un domaine donné. Lorsque la fonction de forme associée à ces processus est déterministe, nous proposons un nouvel algorithme pour obtenir de telles simulations sur un domaine continu comme des pavés ou des boules. Il consiste à générer des ingrédients de base qui peuvent ensuite être utilisés pour assigner une valeur à n'importe quel point du champ de simulation. Cette approche est particulièrement adaptée à l'étude des propriétés géométriques des processus tempêtes. Une attention particulière est dédiée à l'efficacité de cette procédure : en introduisant et en exploitant la notion de domaine d'influence, le temps de simulation est considérablement réduit. De plus, la plupart des étapes de la méthode de simulation ont été construites afin d'être parallélisables. Cet algorithme est enfin utilisé pour simuler trois processus tempête différents.*

When working on the relation between integral range and extremal coefficient function, we needed to find a mixing max-stable process for which the integral range of the corresponding exceedance field above a finite threshold was infinite. The objective was to show how the method we had proposed to estimate the integral range behaved when the latter was infinite. We proved that the M2 process Z with Cauchy density shape function satisfied these conditions. Algorithms to perform exact simulations of such processes has been suggested by [Dombry et al. \(2016\)](#) or [Oesting et al. \(2018\)](#) but actually no package in R have implemented them. Further, like most algorithms, these procedures only apply to simulation domains made of a finite number of points. When investigating *e.g.* the geometrical properties of random fields, it may be convenient to perform simulation in continuous domains, especially if the geometric feature under study involves different scales of observations. This motivated us to propose and implement a new method for simulating storm processes like Z exactly in continuous domain of \mathbb{R}^d . This work is presented in this chapter. It actually corresponds to a paper written in collaboration with R. Carnec, E. Chautru, and C. Lantuéjoul (Mines ParisTech, PSL University) and recently submitted for publication. The notation may slightly differ from the other chapters. For instance, to avoid confusion, a dot shall sit on top of random elements. In

addition, for any measurable subset V of \mathbb{R}^d , its volume with respect to the Lebesgue measure in \mathbb{R}^d is written $v_d(V)$ instead $|V|$.

4.1 INTRODUCTION

In the last decades, max-stable processes (or random fields, random functions) have become a prevalent model for spatial extremes in environmental sciences, see for instance [Davison et al. \(2019\)](#) and references therein. An important class is the *storm process*, often referred to as a mixed moving maxima process. First introduced by [Smith \(1990\)](#), then extended by [Schlather \(2002\)](#) to model convective precipitations, it has subsequently been studied and applied, mainly in climatology (*cf. e.g.* [Coles, 1993](#), [Coles and Walshaw, 1994](#), [Coles and Tawn, 1996](#), [de Haan and Pereira, 2006](#), [Bel et al., 2008](#), [Smith and Stephenson, 2009](#), [Padoan et al., 2010](#), [Cooley et al., 2010](#) and [Lantuéjoul et al., 2011](#)). It is defined as follows: let $d \in \mathbb{N}^*$, $\dot{\Pi}$ be a homogeneous Poisson point process with intensity $\mu \in (0, +\infty)$ on $\mathbb{R}^d \times (0, +\infty)$ and $(\dot{Y}_\tau, \tau > 0)$ be independent copies of a nonnegative process \dot{Y} defined on \mathbb{R}^d with integrable expectation on \mathbb{R}^d . Then the storm process is written $\dot{Z} := (\dot{Z}(\mathbf{x}), \mathbf{x} \in \mathbb{R}^d)$ with

$$\forall \mathbf{x} \in \mathbb{R}^d \quad \dot{Z}(\mathbf{x}) = \max_{(\dot{s}, \dot{\tau}) \in \dot{\Pi}} \left\{ \frac{\dot{Y}_{\dot{\tau}}(\mathbf{x} - \dot{s})}{\dot{\tau}} \right\}.$$

To fix ideas, \dot{Y} is referred to as a storm, \dot{s} as its location and $1/\dot{\tau}$ as its magnitude. It can be shown that the margins of \dot{Z} are 1-Fréchet distributed. More generally, the spatial distribution of \dot{Z} is given by

$$\mathbf{P} \left[\max_{i \in I} \frac{\dot{Z}(\mathbf{s}_i)}{z_i} < 1 \right] = \exp \left\{ -\mu \int_{\mathbb{R}^d} \mathbf{E} \left\{ \max_{i \in I} \frac{\dot{Y}(\mathbf{s} - \mathbf{s}_i)}{z_i} \right\} d\mathbf{s} \right\}$$

for all finite sets of indices $I \subset \mathbb{N}$ and all families of points $(\mathbf{s}_i, i \in I)$ and values $(z_i, i \in I)$. However, it is well known that all statistical properties of \dot{Z} are not conveyed by its spatial distribution. Besides standard questions like the differentiability of its realizations or their connectivity above a certain level, there are a number of specific issues, such as what is the extension of a storm versus its magnitude? How do the magnitudes of neighbouring storms compare? To a large extent, the spatial distribution of \dot{Z} says very little about the geometry of its realizations.

Of course, these questions should be addressed from a mathematical point of view, but this might be quite a delicate exercise. For that reason simulations are considered as a first alternative approach. Several algorithms can be found in the literature to simulate storm processes, *e.g.* [Schlather \(2002\)](#), [Dombry et al. \(2016\)](#), [Oesting et al. \(2018\)](#). They are exact and applicable to any workspace dimension. The most two recent algorithms have been designed to be fast, either by simulating only the *active* storms, *i.e.* those that have an impact on the simulation

(Dombry et al., 2016), or by ingeniously choosing a spectral representation of the process with suitable properties (Oesting et al., 2018). However, these algorithms apply to simulation domains made of a finite number of points, which may not be appropriate if the geometric feature under study involves different scales of observation.

This is what prompted us to develop an algorithm for simulating storm processes exactly in a *continuous* domain of \mathbb{R}^d , such as a hyperrectangle or a hyperball. At first sight, this may look overambitious, but a previous paper (Lantuéjoul et al., 2011) showed that this is feasible, at least in the particular case where the storms are indicator functions of Poisson polytopes. The idea is to generate a finite family of storms that includes all active storms. This family is subsequently used to assign a value to any point of the simulation domain.

It has been observed on simulations that most storms have limited influence, or even no influence at all. In order to get faster simulations, this should definitely be taken into account. To each storm with given location and magnitude, it is possible to assign a *domain of influence* that delimits the part of the simulation domain where it contributes to the realization of the storm process, given other storms of larger magnitude.

For the sake of simplicity, the present paper deals mainly with deterministic storms. It is organized as follows. Section 4.3 presents a general algorithm to generate the active storms and clarifies the concept of domain of influence. A simple but general procedure is proposed to enclose it. Section 4.4 shows examples with different deterministic storms (Gaussian, Student, power exponential). For each type of storm, emphasis is put on the explicit construction of its domain of influence. Then follows Section 4.5 that discusses a number of issues regarding the shape of the simulation domain, the efficiency of the proposed algorithm, and its range of applicability towards models with random storms. A brief conclusion terminates this paper in Section 4.6.

4.2 NOTATION AND SETTING

Notation

Throughout this paper, the workspace is the d -dimensional Euclidean space \mathbb{R}^d . Points are boldface type to distinguish them from their coordinates. The Euclidean distance separating two points $\mathbf{x} = (x_1, \dots, x_d)$ and $\mathbf{y} = (y_1, \dots, y_d)$ is denoted by $\|\mathbf{x} - \mathbf{y}\|$ and their scalar product by $\langle \mathbf{x}, \mathbf{y} \rangle$.

More generally, let I be a nonempty subset of $\{1, \dots, d\}$ with $k(I)$ elements. For each $\mathbf{x} \in \mathbb{R}^d$, let \mathbf{x}_I be the family of the coordinates of \mathbf{x} that are indexed by I . In other words $\mathbf{x}_I = (x_i, i \in I)$. The space \mathbb{R}^I of all \mathbf{x}_I 's can be equipped with the distance $\|\mathbf{x}_I - \mathbf{y}_I\|_I = \sqrt{\sum_{i \in I} (x_i - y_i)^2}$, and $B_I(r) := \{\mathbf{x}_I \in \mathbb{R}^I : \|\mathbf{x}_I\|_I \leq r\}$ is the closed ball of \mathbb{R}^I with radius r , centered at the origin. When $I = \{1, \dots, d\}$, the standard notation $B_d(r)$ is used. In addition, many scalar operations shall be applied component by component, e.g. the absolute value $|x_i|$, the sign $\text{sign}(x_i)$, and inequalities $x_i \leq y_i$.

Subsets of dimension k are represented by uppercase, lightface letters. If V is such a subset, then its intrinsic boundary is written ∂V and its relative complement in \mathbb{R}^k by V^c . Assuming V measurable, we shall denote by $v_k(V)$ its k -volume (number of elements in 0 dimension, length in 1 dimension, and so on). In the particular case where V is a ball of radius r , the standard notation ω_k is used for the unit ball, so that $v_k(V) = \omega_k r^k$ and $v_{k-1}(\partial V) = k\omega_k r^{k-1}$. The uniform distribution on V is abbreviated $\mathcal{U}(V)$. Similarly, given $\lambda \in (0, +\infty)$, $\mathcal{E}(\lambda)$ stands for the exponential distribution with expectation $1/\lambda$. Finally, to avoid any confusion, a dot shall sit on top of random elements.

Setting

Equipped with this notation, we shall focus on deterministic and radial storms. Precisely, the typical storm is written $\dot{Y}(\mathbf{s}) = f(\|\mathbf{s}\|)$, where f is a function from \mathbb{R}_+ to $[0, 1]$ that is non-increasing and satisfies $f(0) = 1$. Attached to f are its moments

$$\forall k \in \{0, \dots, d-1\} \quad m_k := \int_0^\infty f(u) u^k du, \quad (4.1)$$

and its weighted probability density functions

$$\forall k \in \{0, \dots, d-1\} \quad \forall u \geq 0 \quad f_k(u) := \frac{f(u) u^k}{m_k}. \quad (4.2)$$

The assumption that the storms are integrable is expressed by the condition $m_{d-1} < +\infty$.

The simulation field is a hyperrectangle of dimension d , termed R . Its edge lengths are denoted by $2\ell_1, \dots, 2\ell_d$. There is no inconvenience in assuming R centered at the origin and its edges parallel to the coordinate axes, so that its 2^d vertices have coordinates of the form $(\epsilon_1 \ell_1, \dots, \epsilon_d \ell_d)$ with $\epsilon_i = \pm 1$ for each $i = 1, \dots, d$.

4.3 AN ALGORITHM FOR CONTINUOUS SIMULATION

For this simulation exercise, since the storms are deterministic, only the Poisson points need to be simulated. At first, the task looks daunting because the Poisson process is made of infinitely many points. However, it can be surmised that points with at least one large spatial or temporal coordinate are likely not to affect the result of the simulation. This prompts us to distinguish between the *active* points, *i.e.* all the Poisson points $(\dot{s}, \dot{\tau}) \in \dot{\Pi}$ such that there exists $\mathbf{x} \in \mathbb{R}$ for which

$$\dot{Z}(\mathbf{x}) = \frac{f(\|\mathbf{x} - \dot{s}\|)}{\dot{\tau}}, \quad (4.3)$$

and the other *passive* points. Each active point $(\dot{s}, \dot{\tau})$ can be assigned a *domain of influence*, which is formed by all $\mathbf{x} \in \mathbb{R}$ that satisfy (4.3). Our first objective is to delimit the part of $\mathbb{R}^d \times (0, +\infty)$ where the active Poisson points are situated. To do this, it is convenient to split the Poisson process $\dot{\Pi}$ into two smaller independent Poisson point processes $\dot{\Pi}_{\text{in}}$ and $\dot{\Pi}_{\text{out}}$, the points of which have their spatial component respectively inside and outside the simulation field:

$$\dot{\Pi}_{\text{in}} = \{(\dot{s}, \dot{\tau}) \in \dot{\Pi} : \dot{s} \in \mathbb{R}\} \quad \text{and} \quad \dot{\Pi}_{\text{out}} = \{(\dot{s}, \dot{\tau}) \in \dot{\Pi} : \dot{s} \notin \mathbb{R}\}.$$

Starting from the two point processes, two independent random fields are defined on \mathbb{R}^d :

$$\forall \mathbf{x} \in \mathbb{R}^d \quad \begin{cases} \dot{Z}_{\text{in}}(\mathbf{x}) = \max_{(\dot{s}, \dot{\tau}) \in \dot{\Pi}_{\text{in}}} \frac{f(\|\mathbf{x} - \dot{s}\|)}{\dot{\tau}}, \\ \dot{Z}_{\text{out}}(\mathbf{x}) = \max_{(\dot{s}, \dot{\tau}) \in \dot{\Pi}_{\text{out}}} \frac{f(\|\mathbf{x} - \dot{s}\|)}{\dot{\tau}}, \end{cases}$$

so that $\dot{Z} = \max(\dot{Z}_{\text{in}}, \dot{Z}_{\text{out}})$.

4.3.1 Contribution of the inner process

Since the number of Poisson points in a compact subset is finite, the Poisson points of $\dot{\Pi}_{\text{in}}$ can be ordered by decreasing order of magnitude. Thus we can write

$$\forall \mathbf{x} \in \mathbb{R}^d \quad \dot{Z}_{\text{in}}(\mathbf{x}) = \max_{k \geq 1} \frac{f(\|\mathbf{x} - \dot{s}_k\|)}{\dot{\tau}_k}, \quad (4.4)$$

where the \dot{s}_k 's are independent and uniform points of \mathbb{R} and, independently, the $\dot{\tau}_k$'s are the constitutive points of a homogeneous Poisson process with intensity $\mu v_d(\mathbb{R})$ on $(0, +\infty)$. A problem with (4.4) is that it involves infinitely many points. Can the inner storm process be exactly generated using only a finite number of Poisson points?

To answer this question, consider a finite covering \mathcal{C} of \mathbb{R} by domains such as balls or hyperrectangles. A population of points on \mathbb{R} is said to be \mathcal{C} -dispersed if each domain of the

covering contains at least one point of the population. Define \dot{n} as the minimum number of Poisson points generated once \mathcal{C} -dispersion has taken place:

$$\dot{n} := \min \{n \in \mathbb{N}^* : \forall C \in \mathcal{C} \ C \cap \{\dot{s}_1, \dots, \dot{s}_n\} \neq \emptyset\}.$$

Let $\delta := \max_{C \in \mathcal{C}} \max_{\mathbf{x}, \mathbf{y} \in C} \|\mathbf{x} - \mathbf{y}\|$ be the diameter of the covering, and \mathbf{x} be an arbitrary point of \mathbb{R}^c . The previous definitions ensure $\min_{1 \leq k \leq \dot{n}} \|\mathbf{x} - \dot{s}_k\| \leq \delta$, which implies in turn $\max_{1 \leq k \leq \dot{n}} f(\|\mathbf{x} - \dot{s}_k\|) \geq f(\delta)$ since f is non-increasing. Using the sequential construction of the $\dot{\tau}_k$'s, it follows

$$\max_{1 \leq k \leq \dot{n}} \frac{f(\|\mathbf{x} - \dot{s}_k\|)}{\dot{\tau}_k} \geq \max_{1 \leq k \leq \dot{n}} \frac{f(\|\mathbf{x} - \dot{s}_k\|)}{\dot{\tau}_{\dot{n}}} \geq \frac{f(\delta)}{\dot{\tau}_{\dot{n}}}.$$

This is true for all $\mathbf{x} \in \mathbb{R}^c$, therefore

$$\min_{\mathbf{x} \in \mathbb{R}^c} \max_{1 \leq k \leq \dot{n}} \frac{f(\|\mathbf{x} - \dot{s}_k\|)}{\dot{\tau}_k} \geq \frac{f(\delta)}{\dot{\tau}_{\dot{n}}}. \quad (4.5)$$

This shows that the current inner storm process is lower bounded by a strictly positive value as soon as the \mathcal{C} -dispersion condition is satisfied. Now let \dot{n}_{in} be the random index defined as follows:

$$\dot{n}_{\text{in}} := \min \left\{ n > \dot{n} : \frac{1}{\dot{\tau}_n} < \frac{f(\delta)}{\dot{\tau}_{\dot{n}}} \right\}. \quad (4.6)$$

Then the assumption $f \leq 1$ as well as (4.6) and (4.5) imply that for any $n \geq \dot{n}_{\text{in}}$

$$\begin{aligned} \frac{f(\|\mathbf{x} - \dot{s}_n\|)}{\dot{\tau}_n} &\leq \frac{1}{\dot{\tau}_n} \leq \frac{1}{\dot{\tau}_{\dot{n}_{\text{in}}}} < \frac{f(\delta)}{\dot{\tau}_{\dot{n}}} \\ &\leq \min_{\mathbf{x} \in \mathbb{R}^c} \max_{1 \leq k \leq \dot{n}} \frac{f(\|\mathbf{x} - \dot{s}_k\|)}{\dot{\tau}_k} \leq \min_{\mathbf{x} \in \mathbb{R}^c} \max_{1 \leq k \leq n} \frac{f(\|\mathbf{x} - \dot{s}_k\|)}{\dot{\tau}_k}. \end{aligned} \quad (4.7)$$

It appears that all storms of index $n \geq \dot{n}_{\text{in}}$ cannot affect the current simulation. As a consequence, the inner Poisson process needs not be simulated beyond index \dot{n}_{in} .

The algorithm to simulate the inner storm process can therefore be seen in two distinct stages: first generate Poisson points so as to meet the \mathcal{C} -dispersion condition, then resume the generation of Poisson points until constraint (4.6) is satisfied. Of course, the efficiency of this algorithm depends largely on the choice of the parameter δ . The discussion on this matter is deferred to [Section 4.5](#).

Here is the algorithm for simulating the inner process:

4.3.2 Contribution of the outer process

Once the inner process has been generated, the simulation of the outer process can start. Among all outer Poisson points, only those that are susceptible to modify the inner process need be considered. These points are located in the random domain

$$\dot{D}_{\text{out}} := \left\{ (\mathbf{s}, \tau) \in \mathbb{R}^c \times (0, +\infty) : \exists \mathbf{x} \in \mathbb{R}^c \ \frac{f(\|\mathbf{x} - \mathbf{s}\|)}{\tau} > \max_{k < \dot{n}_{\text{in}}} \frac{f(\|\mathbf{x} - \dot{s}_k\|)}{\dot{\tau}_k} \right\}.$$

Algorithm 1: Simulation of $\dot{\Pi}_{\text{in}}$

-
- (i) set $\tau = 0$ and $S = T = \emptyset$;
 - (ii) generate $\epsilon \sim \mathcal{E}(\mu v_d(\mathbb{R}))$, put $\tau = \tau + \epsilon$ and insert τ to T ;
 - (iii) generate $s \sim \mathcal{U}(\mathbb{R})$ and insert s to S ;
 - (iv) if $C \cap S = \emptyset$ for some $C \in \mathcal{C}$, then goto (ii);
 - (v) put $n = v_0(S)$ and $\tau_n = \tau$;
 - (vi) generate $\epsilon \sim \mathcal{E}(\mu v_d(\mathbb{R}))$, put $\tau = \tau + \epsilon$ and insert τ to T ;
 - (vii) generate $s \sim \mathcal{U}(\mathbb{R})$ and insert s to S ;
 - (viii) if $\tau f(\delta) < \tau_n$, then goto (vi);
 - (ix) return S, T and τ_n ;
-

Unfortunately, this domain is difficult to handle because it involves the points of \mathbb{R} . Consider instead the random domain

$$\dot{D} := \left\{ (s, \tau) \in \mathbb{R}^c \times (0, +\infty) : \frac{f(d(s, \mathbb{R}))}{\tau} > \frac{f(\delta)}{\dot{\tau}_{\dot{n}}} \right\}, \quad (4.8)$$

where $d(s, \mathbb{R}) := \min_{\mathbf{x} \in \mathbb{R}} \|s - \mathbf{x}\|$ denotes the distance from s to \mathbb{R} . This domain possesses three distinctive features:

- Its definition does not rely on any point of \mathbb{R} .
- It contains the domain of interest: $\dot{D} \supset \dot{D}_{\text{out}}$. Let $(s, \tau) \in \mathbb{R}^c \times (0, +\infty)$ and let $\mathbf{x} \in \mathbb{R}$ be chosen as in the definition of \dot{D}_{out} . The inclusion results from the following chain of inequalities:

$$\frac{f(d(s, \mathbb{R}))}{\tau} \geq \frac{f(\|\mathbf{x} - s\|)}{\tau} > \max_{k < \dot{n}_{\text{in}}} \frac{f(\|\mathbf{x} - \dot{s}_k\|)}{\dot{\tau}_k} \geq \frac{f(\delta)}{\dot{\tau}_{\dot{n}}}.$$

Indeed, starting from $d(s, \mathbb{R}) \leq \|s - \mathbf{x}\|$, the first inequality stems from the assumption that f is non-increasing. The second inequality is provided by the definition of \dot{D}_{out} , and the third one derives from (4.7).

- It has finite volume: $v_{d+1}(\dot{D}) < +\infty$. This directly stems from the fact that the storms are integrable.

As a consequence, given $\dot{\tau}_{\dot{n}}$, the number \dot{n}_{out} of points of $\dot{\Pi}_{\text{out}}$ in \dot{D} is Poisson distributed with mean $\mu v_{d+1}(\dot{D})$. Moreover, these points are uniform and independent in \dot{D} . Starting from this, a natural idea for simulating the outer process consists in generating each Poisson point of $\dot{\Pi}_{\text{out}}$ in \dot{D} and computing its contribution to the storm process. However, there is still a pending problem: how to simulate a uniform point $(\dot{s}, \dot{\tau})$ in \dot{D} ? This question is addressed now. In the sequel, the probability density function (p.d.f.) of a random variable \dot{u} shall be denoted by $f_{\dot{u}}$, eventual conditioning being made explicit by writing $f_{\dot{u}}(\cdot | \cdot)$.

Suppose that Algorithm 1 returns the value τ_n for $\dot{\tau}_n$. Then \dot{D} is a deterministic domain, say D . Given $\dot{s} = s$, the definition of D shows that $\dot{\tau}$ is uniform on the segment $[0, \tau_n f(d(s, R))/f(\delta)]$. Thus, the main problem is the simulation of \dot{s} . The definition of D also suggests to perform the simulation of $d(\dot{s}, R)$ prior to that of \dot{s} , according to the randomization formula

$$\forall s \in \mathbb{R}^c \quad f_{\dot{s}}(s) = \int_0^\infty f_{d(\dot{s}, R)}(u) f_{\dot{s}}(s | u) du. \quad (4.9)$$

The distribution of $d(\dot{s}, R)$ has an expression that depends on the closest point of R to \dot{s} . It is therefore convenient to write it as a mixture of p.d.f.'s, which can be done by introducing the following family of domains (cf. Figure 4.1):

$$\forall I \subset \{1, \dots, d\} \quad E_I := \left\{ s \in \mathbb{R}^d : \forall i \in I \ |s_i| > \ell_i, \quad \forall j \notin I \ |s_j| \leq \ell_j \right\}.$$

Further define the distribution p that gives each $I \subset \{1, \dots, d\}$ the probability $p_I := \mathbf{P}[\dot{s} \in E_I]$ of being selected, and the conditional p.d.f.'s

$$\forall I \subset \{1, \dots, d\} \quad \forall u \geq 0 \quad f_{d(\dot{s}, R)}(u | I) := \frac{f(u) u^{k(I)-1}}{m_{k(I)-1}} \quad (4.10)$$

that can be written $f_{d(\dot{s}, R)}(u | I) = f_{k(I)-1}(u)$ owing to (4.2). Then, the randomization formula (4.9) becomes

$$\forall s \in \mathbb{R}^c \quad f_{\dot{s}}(s) = \sum_{I \neq \emptyset} p_I \int_0^\infty f_{k(I)-1}(u) f_{\dot{s}}(s | I, u) du.$$

Writing I^c the complement of I in $\{1, \dots, d\}$ and putting $R_{I^c} := \prod_{j \in I^c} [-\ell_j, +\ell_j]$, one explicitly finds

$$\forall I \subset \{1, \dots, d\} \quad p_I = \frac{v_{k(I^c)}(R_{I^c}) k(I) \omega_{k(I)} m_{k(I)-1}}{\sum_{J \neq \emptyset} v_{k(J^c)}(R_{J^c}) k(J) \omega_{k(J)} m_{k(J)-1}}. \quad (4.11)$$

The proofs of formulae (4.10) and (4.11) are deferred to Subsection 4.7.1.

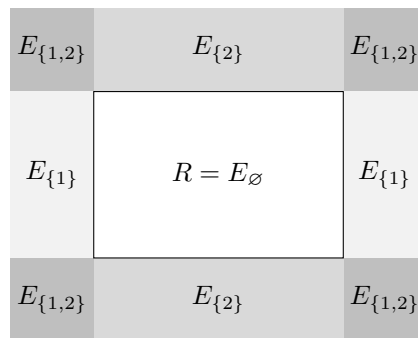


FIGURE 4.1 – Illustration when $d = 2$: to each point exterior to the simulation domain, its closest face is associated.

Remark 4.1 The probability p_I admits a geometric interpretation. Given two subsets A and B of \mathbb{R}^d , recall that a point $z \in \mathbb{R}^d$ belongs to the Minkowski's sum $A \oplus B$ of A and B if there exist $x \in A$ and $y \in B$ such that $z = x + y$. In the case where A and B lie in two orthogonal subspaces of respective dimensions i and j , then $v_{i+j}(A \oplus B) = v_i(A) v_j(B)$. It can be easily shown that p_I is proportional to the expected value of $v_{d-1}(R_I^c \oplus \partial B_I(\dot{u}))$, where \dot{u} is a random variable with p.d.f. proportional to f .

Suppose that the moments of f have been calculated, which must be done on a case by case basis. Then the simulation of p is rather simple using the standard inversion method. Once a subset I has been generated, the conditional simulation of $f_{k(I)-1}$ is also often straightforward. In certain situations, it may be helpful to interpret this distribution as that of the modulus of a random vector with $k(I)$ components. Having thus generated the positive real number u , there just remains to simulate $f_s(\cdot | I, u)$, which is a bit more tricky.

A symmetry argument shows that the distribution of \dot{s} given I and u is uniform over $E_I \cap \partial(R \oplus B_d(u))$. Let $s \in E_I \cap \partial(R \oplus B_d(u))$, and let x be its projection onto R . Owing to the definition of E_I , $|x_I| = \ell_I$ and $-\ell_{I^c} \leq x_{I^c} \leq +\ell_{I^c}$. It follows that s satisfies $s_I = x_I + y_I$ with $y_I \in \mathbb{R}^I$ such that $\text{sign}(y_I) = \text{sign}(x_I)$ and $\|y_I\|_I = u$, as well as $s_{I^c} = x_{I^c}$. By construction, the point y_I can be generated uniformly over a sphere of radius u in $k(I)$ dimensions. Its sign specifies to which face it should be affected (see Figure 4.2).

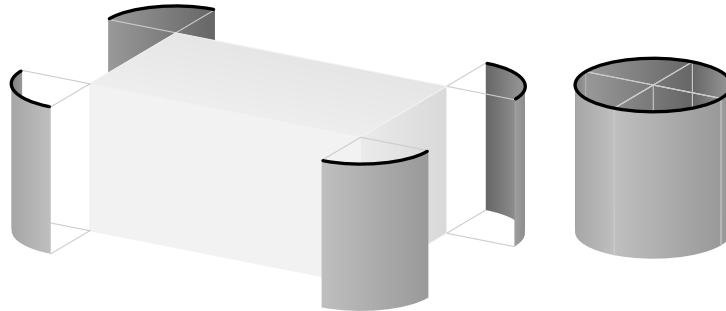


FIGURE 4.2 – Illustration when $d = 3$: when considering the Minkowski sum of R (in light grey) with a sphere, the contribution of each vertical edge is a quarter of a cylinder (in dark grey). The point y_I is generated uniformly on its circular basis (drawn in bold).

Finally, here is the algorithm for simulating each point of the outer process:

Algorithm 2: Simulation of $(\dot{s}, \dot{\tau}) \in \dot{\Pi}_{\text{out}}$

- (i) generate $I \sim p$;
 - (ii) generate $u \sim f_{k(I)-1}$;
 - (iii) generate $s_{I^c} \sim \mathcal{U}(\mathbb{R}_{I^c})$;
 - (iv) generate $y_I \sim \mathcal{U}(\partial B_I(u))$;
 - (v) put $s_I = \text{sign}(y_I) + y_I$;
 - (vi) $\tau \sim \mathcal{U}([0, \tau_n f(u)/f(\delta)])$;
 - (vii) return $s = (s_i, i = 1, \dots, d)$ and τ .
-

4.3.3 Efficient computation of maxima

Once all Poisson points of interest have been generated, the next question is how to compute the values of the storm process at a given population of points within the simulation field. A natural idea consists in computing the maximum of the generated storms at each point of the population. It turns out that this standard procedure is squarely long time consuming. A finer approach is therefore required.

Considering the inner process, one can surmise that except the first Poisson points, all others have a limited influence on the final outcome of the simulation. The following lemma should clarify this idea:

Lemma 4.2 Let (s, τ) and (s_0, τ_0) be two points of $\mathbb{R}^d \times (0, +\infty)$ satisfying $\tau_0 < \tau$. There does not exist any point $\mathbf{x} \in \mathbb{R}^d$ satisfying

$$\frac{f(\|\mathbf{x} - s_0\|)}{\tau_0} < \frac{f(\|\mathbf{x} - s\|)}{\tau} \quad (4.12)$$

in the closed half-space H_0 limited by the mediator hyperplane of s_0 and s and containing s_0 .

Proof. By contradiction, suppose that there exists $\mathbf{x} \in H_0$ such that (4.12) holds. Since $\mathbf{x} \in H_0$, then $\|\mathbf{x} - s_0\| \leq \|\mathbf{x} - s\|$, which implies $f(\|\mathbf{x} - s_0\|) \geq f(\|\mathbf{x} - s\|)$ because f is non-increasing. Moreover, $\tau_0 < \tau$ implies $1/\tau_0 > 1/\tau$. Then, multiplying both inequalities gives $f(\|\mathbf{x} - s_0\|)/\tau_0 > f(\|\mathbf{x} - s\|)/\tau$, which contradicts (4.12). ■

Suppose now that a population of \mathcal{C} -dispersed Poisson points has been generated. Then Lemma 4.2 can be used to delimit the *domain of influence* of each newly generated point (s, τ) , i.e. the region $A \subset \mathbb{R}$ where it affects the realization of the storm process. The circumscription of A can subsequently be exploited when simulating the storm process on a grid. It suffices

to consider only the Poisson points that may influence each grid point. Note that the domain of influence of each Poisson point of the outer process can also be delimited once they have been sorted into decreasing orders of magnitude.

Now it should be pointed out that [Lemma 4.2](#) is a general result that can give only a crude approximation of the domains of influence. In particular, it does not state that many of them are in fact empty. The case-by-case study of the following examples will make their delimitation much more precise.

4.4 EXAMPLES

In this section, the algorithm is detailed for three different types of storm (Gaussian, Student and power exponential). This includes the calculation of the moments [\(4.1\)](#) of f , the simulation of the weighted distributions [\(4.2\)](#) involved in [\(4.10\)](#) and a more refined conscription of the domains of influence built from f . In all illustrations presented hereunder, the simulation domain is a 600×400 rectangle. In addition, the intensity μ of $\tilde{\Pi}$ is always chosen so that the realizations have standard Fréchet margins.

From now onward, we shall call *relative domain of influence* of $(s, \tau) \in \mathbb{R}^d \times (0, +\infty)$ over some reference point $(s_0, \tau_0) \in \mathbb{R}^d \times (0, \tau)$ the set

$$A_0 := \left\{ \mathbf{x} \in \mathbb{R}^d : \frac{f(\|\mathbf{x} - \mathbf{s}\|)}{\tau} > \frac{f(\|\mathbf{x} - \mathbf{s}_0\|)}{\tau_0} \right\}. \quad (4.13)$$

It is trivially empty when $\mathbf{s} = \mathbf{s}_0$. In addition, the symbols Γ and B shall refer respectively to the gamma and beta functions.

4.4.1 Gaussian storms

This is one of the cases treated by [Smith \(1990\)](#): given a scale parameter $a \in (0, +\infty)$,

$$\forall u \geq 0 \quad f(u) = \exp \left\{ - \left(\frac{u}{a} \right)^2 \right\}. \quad (4.14)$$

Moments of the storm: straightforward calculations give

$$\forall k \in \{0, \dots, d-1\} \quad m_k = \frac{a^{k+1}}{2} \Gamma \left(\frac{k+1}{2} \right).$$

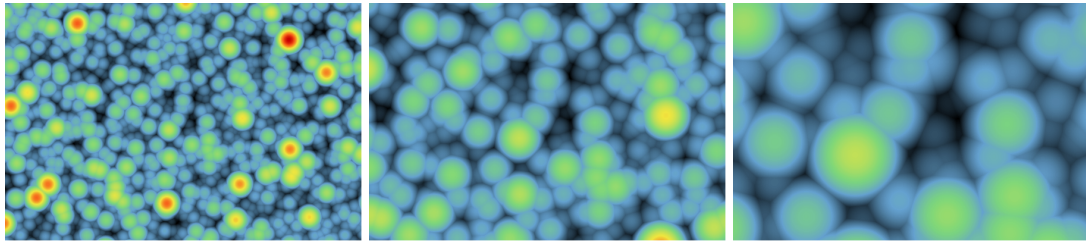


FIGURE 4.3 – Realization of a Gaussian storm process at three different scales, on grids 600×400 . All the grids are centered at the same point and, from left to right, their mesh sizes are respectively 1, 0.5 and 0.25.

Simulation of the weighted distributions: for each $k \in \{0, \dots, d-1\}$, the probability density function f_k takes the form

$$\forall u \geq 0 \quad f_k(u) = \frac{\frac{2}{a} \left(\frac{u}{a}\right)^k \exp\left\{-\left(\frac{u}{a}\right)^2\right\}}{\Gamma\left(\frac{k+1}{2}\right)},$$

which is that of the square root of a random variable that is distributed like a Gamma variable with shape parameter $(k+1)/2$ and scale factor a^2 . The simulation of Gamma distributions is standard (Devroye, 1986).

Domains of influence: let $(\mathbf{s}, \tau) \in \mathbb{R}^d \times (0, +\infty)$ and $(\mathbf{s}_0, \tau_0) \in \mathbb{R}^d \setminus \{\mathbf{s}\} \times (0, \tau)$. Given (4.14), the relative domain of influence of (\mathbf{s}, τ) over (\mathbf{s}_0, τ_0) defined in (4.13) directly simplifies into

$$A_0 = \left\{ \mathbf{x} \in \mathbb{R} : \langle \mathbf{x}, \mathbf{s} - \mathbf{s}_0 \rangle > \frac{1}{2} \left(a^2 \ln\left(\frac{\tau}{\tau_0}\right) + \|\mathbf{s}\|^2 - \|\mathbf{s}_0\|^2 \right) \right\}.$$

This corresponds to the intersection between \mathbb{R} and an open half-space in \mathbb{R}^d . Therefore, the domain of influence of (\mathbf{s}, τ) is included in the intersection between \mathbb{R} and a polyhedron.

Illustrations: we are now fully equipped to perform a simulation. Consider a bidimensional Gaussian storm process with scale factor $a = 10$. The results obtained about the domains of influence have been incorporated to the algorithm, which leads to a drastic reduction of the number of Poisson points to consider. For the inner and the outer processes, only 2 221 out of 134 344 and 630 out of 10 252 Poisson points have been respectively detained as potentially active. Hence, in total, 98% of the Poisson points have been removed. The remaining points are then used to generate a realization of the storm process on three different grids of 600×400 pixels. All are centered at the origin and have the same orientation. Their mesh sizes are respectively equal to 1, 0.5 and 0.25. The corresponding results are displayed in Figure 4.3. Everything happens exactly as if the simulation had been zoomed around the origin.

4.4.2 Student storms

With scale $a \in (0, +\infty)$ and shape $\alpha \in (d/2, +\infty)$, the storm f is now given by

$$\forall u \geq 0 \quad f(u) = \left(1 + \frac{u^2}{a^2}\right)^{-\alpha}; \quad (4.15)$$

taking $\alpha > d/2$ ensures that f is integrable. It has the same form as a multivariate t-distribution.

Moments of the storm: like before, straightforward calculations give

$$\forall k \in \{0, \dots, d-1\} \quad m_k = \frac{a^{k+1}}{2} \text{B}\left(\frac{k+1}{2}, \alpha - \frac{k+1}{2}\right).$$

Simulation of the weighted distributions: for each $k \in \{0, \dots, d-1\}$, the previous equality yields

$$\forall u \geq 0 \quad f_k(u) = \frac{u^k \left(1 + \frac{u^2}{a^2}\right)^{-\alpha}}{\frac{a^{k+1}}{2} \text{B}\left(\frac{k+1}{2}, \alpha - \frac{k+1}{2}\right)}.$$

Simulating such a density is less direct than in the Gaussian case; it involves the mixture of two distributions. Precisely, let \dot{w} be a Gamma distributed random variable with shape $\alpha - (k+1)/2$ and scale 1. For any $w \in (0, +\infty)$ consider the Gamma distributed random variable \dot{u}_w with shape $(k+1)/2$ and scale a^2/w , independent from \dot{w} . Then, the compound random variable $\sqrt{\dot{u}_w}$ has density f_k .

Domains of influence: let $(\mathbf{s}, \tau) \in \mathbb{R}^d \times (0, +\infty)$ and $(\mathbf{s}_0, \tau_0) \in \mathbb{R}^d \setminus \{\mathbf{s}\} \times (0, \tau)$. To simplify the notation, also put $\lambda := \tau^{1/\alpha}$ and $\lambda_0 = \tau_0^{1/\alpha}$. Given (4.15), the relative domain of influence of (\mathbf{s}, τ) over (\mathbf{s}_0, τ_0) defined in (4.13) becomes

$$A_0 = \left\{ \mathbf{x} \in \mathbb{R} : \left\| \mathbf{x} - \frac{\lambda \mathbf{s} - \lambda_0 \mathbf{s}_0}{\lambda - \lambda_0} \right\|^2 < \frac{\lambda \lambda_0}{(\lambda - \lambda_0)^2} \|\mathbf{s} - \mathbf{s}_0\|^2 - a^2 \right\}.$$

This set is non-empty if and only if the coefficient

$$\rho^2 := \frac{\lambda \lambda_0}{(\lambda - \lambda_0)^2} \|\mathbf{s} - \mathbf{s}_0\|^2 - a^2$$

is positive. In this case, A_0 is the intersection between \mathbb{R} and an open ball in \mathbb{R}^d with center $(\lambda \mathbf{s} - \lambda_0 \mathbf{s}_0)/(\lambda - \lambda_0)$ and radius ρ . Therefore, the domain of influence of (\mathbf{s}, τ) is either empty or contained in the intersection between \mathbb{R} and an intersection of balls in \mathbb{R}^d .

Illustrations: three bidimensional Student storm processes have been simulated with the same scale factor $a = 10$, but different shape parameters ($\alpha = 5, 3$ and 1.5 , respectively). In the case $\alpha = 1.5$, f has the form of a bivariate Cauchy distribution. These simulations, performed on a regular grid 600×400 with unit mesh size, are displayed in Figure 4.4.

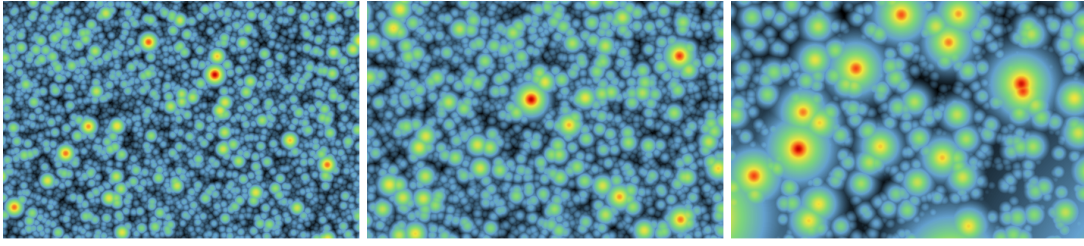


FIGURE 4.4 – Realization of a Student storm process on a grid 600×400 with unit mesh size. The scale factor of the typical storm is equal to 10 and its shape parameter takes, from left to right, the values 5, 3 and 1.5.

4.4.3 Power exponential storms

Let $a, \alpha \in (0, +\infty)$ be scale and shape parameters, and consider the following storm

$$\forall u \geq 0 \quad f(u) = \exp \left\{ - \left(\frac{u}{a} \right)^\alpha \right\}. \quad (4.16)$$

It has the form of a power exponential distribution (see *e.g.* Gómez et al., 1998). In particular, when $\alpha = 2$, it corresponds to the Gaussian storm introduced above. When $d = 1$ and $\alpha = 1$, the well-known Laplace distribution is retrieved.

Moments of the storm: similarly to the Gaussian case,

$$\forall k \in \{0, \dots, d-1\} \quad m_k = \frac{a^{k+1}}{\alpha} \Gamma \left(\frac{k+1}{\alpha} \right).$$

Simulation of the weighted distributions: for each $k \in \{0, \dots, d-1\}$, the previous equation gives

$$\forall u \geq 0 \quad f_k(u) = \frac{\frac{\alpha}{a} \left(\frac{u}{a} \right)^k \exp \left\{ - \left(\frac{u}{a} \right)^\alpha \right\}}{\Gamma \left(\frac{k+1}{\alpha} \right)}.$$

This is the density function of a Gamma distributed random variable, with shape $(k+1)\alpha^{-1}$ and scale a^α , raised to the power $1/\alpha$.

Domains of influence: let $(s, \tau) \in \mathbb{R}^d \times (0, +\infty)$ and $(s_0, \tau_0) \in \mathbb{R}^d \setminus \{s\} \times (0, \tau)$. Also define the positive real number

$$c_\alpha := \left(\frac{a}{\|s - s_0\|} \right)^\alpha \ln \left(\frac{\tau}{\tau_0} \right).$$

Then, given (4.16), the relative domain of influence of (s, τ) over (s_0, τ_0) defined in (4.13) is

$$A_0 = \left\{ \mathbf{x} \in \mathbb{R}^d : \|\mathbf{x} - s_0\|^\alpha - \|\mathbf{x} - s\|^\alpha > c_\alpha \|\mathbf{s} - s_0\|^\alpha \right\}.$$

Consider the closed half-space H_0 limited by the mediator hyperplane of \mathbf{s}_0 and \mathbf{s} and containing \mathbf{s}_0 . [Lemma 4.2](#) guarantees that $A_0 \subset H_0^c$. When $\alpha > 2$, there is little hope to find a better approximation of the relative domain of influence, which has a complex form. It is, however, explicit in the case $\alpha = 2$, which was treated in [Subsection 4.4.1](#). The following proposition shows that when $\alpha < 2$, it is actually possible to further circumscribe A_0 . In some specific situations, it is even found to be bounded. The proof is deferred to [Subsection 4.7.2](#).

Proposition 4.3 Consider the objects defined in [Subsection 4.4.3](#). Let $\lambda \in (1/2, +\infty)$ and define $H_\lambda := H_0 + (\lambda - 1/2)(\mathbf{s} - \mathbf{s}_0)$ so that $H_\lambda^c \subset H_0^c$. Then, for $\alpha \in (0, 2)$, taking

$$\lambda = \begin{cases} 1 - \left(2^{-\alpha} - \frac{c_\alpha}{2}\right)^{1/\alpha} & \text{if } \alpha \in (0, 1), \\ \frac{c_1 + 1}{2} & \text{if } \alpha = 1, \\ 1 & \text{if } \alpha \in (1, 2) \text{ and } c_\alpha = 1, \\ \left(2^{-\alpha} + \frac{c_\alpha}{2}\right)^{1/\alpha} & \text{if } \alpha \in (1, 2) \text{ and } c_\alpha < 1, \\ 2 + \frac{c_\alpha - 2^\alpha + 1}{\alpha(2^{\alpha-1} - 1)} & \text{if } \alpha \in (1, 2) \text{ and } c_\alpha > 1, \end{cases}$$

yields $A_0 \subset H_\lambda^c$. Moreover, when $\alpha \in (0, 1)$ and $c_\alpha < 1$, set the real numbers

$$\lambda := 1 + \frac{1}{2} \left(\left(\frac{c_\alpha}{\alpha} \right)^{1/(\alpha-1)} - \left(2^{-\alpha} - \frac{c_\alpha}{2} \right)^{1/\alpha} \right)$$

and $\rho := \frac{1}{2} \left(\left(\frac{c_\alpha}{\alpha} \right)^{1/(\alpha-1)} + \left(2^{-\alpha} - \frac{c_\alpha}{2} \right)^{1/\alpha} \right).$

Then, A_0 is included in the ball centered at $(1 - \lambda)\mathbf{s}_0 + \lambda\mathbf{s}$ with radius ρ .

As a consequence, the domain of influence of (\mathbf{s}, τ) is always included in the intersection between R and either a polyhedron, an intersection of balls, or an intersection of balls and half-spaces in \mathbb{R}^d .

Illustrations: consider three bidimensional power exponential storm processes with the same scale factor $a = 10$, but different shape parameters ($\alpha = 2, 1$ and 0.5 , respectively). They have all been simulated on a regular grid 600×400 , with unit mesh size. The result is displayed in [Figure 4.5](#).

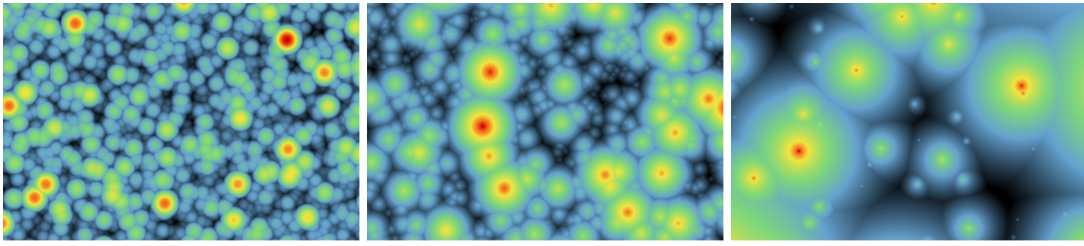


FIGURE 4.5 – Realization of a power exponential storm process on a grid 600×400 with unit mesh size. The scale factor of the typical storm is equal to 10 and its shape parameter takes, from left to right, the values 2, 1 and 0.5.

4.5 DISCUSSION

4.5.1 On the covering

One important parameter that can be used to minimize the running time is the number of generated storms. This is the sum $\dot{n}_{\text{in}} + \dot{n}_{\text{out}}$ of the storms generated in the inner and the outer process. Both depend largely on the diameter δ of the covering domains. Starting from (4.6) and (4.8), trite calculations give

$$\begin{aligned} \mathbf{E}[\dot{n}_{\text{in}}] &= 1 + \frac{\mathbf{E}[\dot{n}]}{f(\delta)} \approx \frac{\mathbf{E}[\dot{n}]}{f(\delta)}, \\ \mathbf{E}[\dot{n}_{\text{out}}] &= \frac{\mathbf{E}[\dot{\tau}_{\dot{n}}]}{f(\delta)} \int_{\mathbb{R}^c} f(d(\mathbf{s}, \mathbf{R})) \, d\mathbf{s} \propto \frac{\mathbf{E}[\dot{\tau}_{\dot{n}}]}{f(\delta)}. \end{aligned}$$

Now, the relation $\mathbf{E}[\dot{\tau}_{\dot{n}}] \propto \mathbf{E}[\dot{n}]$ also holds. It follows, roughly speaking, that the number of storms to generate is proportional to the ratio

$$\varrho := \frac{\mathbf{E}[\dot{n}]}{f(\delta)}.$$

Given $n_1, \dots, n_d \in \mathbb{N}^*$, suppose that the covering \mathcal{C} is a partition of hyperrectangular domains of edge lengths $\ell'_1 = \ell_1/n_1, \dots, \ell'_d = \ell_d/n_d$. The number of domains of \mathcal{C} is thus $v_0(\mathcal{C}) = 2^d n_1 \dots n_d$. A standard probability exercise (Feller, 1968) shows that

$$\mathbf{E}[\dot{n}] = v_0(\mathcal{C}) \sum_{j=1}^{v_0(\mathcal{C})} \frac{1}{j} \approx v_0(\mathcal{C}) (\ln v_0(\mathcal{C}) + \gamma),$$

where $\gamma = 0.577 \dots$ is Euler's constant. If δ is close to 0, then $f(\delta)$ is close to 1 and $\mathbf{E}[\dot{n}]$ is large. Conversely, if δ is large compared to the diameter of the simulation domain, then $\mathbf{E}[\dot{n}]$ is slightly greater than 1, but $f(\delta)$ may be quite small. In both cases, ϱ is large. As a consequence, an intermediate value for δ should be retained. Strictly speaking, δ should be optimized via the edge lengths of the covering domains, but this procedure is delicate. As a rule of thumb, we recommend a δ value such that $f(\delta) \approx 0.5$. This corresponds to $\varrho \approx 2 v_0(\mathcal{C}) (\ln v_0(\mathcal{C}) + \gamma)$.

4.5.2 About the simulation domain

In this paper, we present an algorithm for simulating storm processes in a hyperrectangle $R \subset \mathbb{R}^d$. This procedure may be readily adapted when the domain of simulation is a hyperball. Let $r \in (0, +\infty)$ and consider the ball $B_d(r)$. The part of the algorithm that concerns the inner process remains unchanged, but building the covering \mathcal{C} is a bit more intricate. Indeed, there is no partition of congruent domains. As a result, evaluating the mean number of generated storms is not straightforward.

Conversely, the simulation of the uniform point $(\dot{s}, \dot{\tau}) \in \dot{D}$ of the outer process becomes much easier. The reason is that \dot{D} is a radial domain: the distance of a point $s \notin B_d(r)$ to the simulation domain is $d(s, B_d(r)) = \|s\| - r$. It can be found that

$$\forall u \geq 0 \quad f_{d(\dot{s}, B_d(r))}(u) = \frac{\sum_{k=0}^{d-1} \binom{d-1}{k} r^{d-1-k} f(u) u^k}{\sum_{k=0}^{d-1} \binom{d-1}{k} r^{d-1-k} m_k},$$

where m_k is still given by (4.1). Again, this can be rewritten in the form of a finite mixture model:

$$\forall u \geq 0 \quad f_{d(\dot{s}, B_d(r))}(u) = \sum_{k=0}^{d-1} p_k f_k(u),$$

where p is the distribution that gives each $k \in \{0, \dots, d-1\}$ a probability

$$p_k := \frac{\binom{d-1}{k} r^{d-1-k} m_k}{\sum_{\ell=0}^{d-1} \binom{d-1}{\ell} r^{d-1-\ell} m_\ell}$$

of being generated, and the f_k 's are the weighted distributions defined in (4.2).

The simulation of p is rather simple using the standard inversion method. An alternative approach consists in generating a candidate value k according to a binomial distribution of index $d-1$ and parameter $(r+1)^{-1}$. It is then accepted with probability $m_k / (\sum_{\ell=0}^{d-1} m_\ell)$ and rejected otherwise, in which case the procedure is repeated.

4.5.3 Improving computation efficiency

There are a few practical ways to further improve the efficiency of our algorithm.

First of all, using domains of influence helps reduce the number of potential active storms, leading to a more efficient computation of maxima. However, it also requires a large number of time-consuming comparisons between the generated Poisson points; a compromise must be found to optimize the final running time. By construction, storms have a limited range

of action, and have no chance of having influence over spatially distant competitors. This suggests to compare a candidate storm to its nearest spatial neighbours only. To do so, it is convenient to use the grid generated by the covering, so that a candidate storm has its spatial component in one of the cells. Then, restricting comparisons to those located in its extended Moore neighborhood (8-connectivity in two dimensions, and 26-connectivity in three dimensions) of order 2 was found to be efficient in practice.

Second, the simulation of the outer process turns out to be parallelizable. Computation time can easily be saved by exploiting this asset and distributing calculations.

Finally, because we worked in a continuous setting, the computation of maxima is independent from the generation of storms. It is, in addition, fully parallelizable. This attractive feature, exploited in [Subsection 4.4.1](#), makes high-resolution simulations technically possible in a limited amount of time.

4.5.4 *Random storms*

Although the storm process has been defined in the introduction of this paper in terms of random storms, only deterministic storms have been considered so far. The ensuing question is whether the algorithm designed for continuous simulations can be applied to storm processes with random storms? This is certainly possible if each realization of a random storm is completely characterized by a limited number of parameter values or ingredients. An example was shown in [Lantuéjoul et al. \(2011\)](#), where storms consist of indicator functions of Poisson polytopes. In this case, each realization of a Poisson polytope is specified by the hyperplanes supporting its $(d - 1)$ -faces. A simple way to design a random storm is to start from a deterministic storm and make one or several of its parameters random. A typical example is the Gaussian storm with random scale factor. Despite the complexity introduced, the construction of the domains of influence remains possible. More precisely, consider two Gaussian storms located at (s_0, τ_0) and (s, τ) , with respective scale factors a_0 and a . Suppose $\tau_0 < \tau$. The inequality

$$\frac{1}{\tau_0} \exp\left(-\frac{\|\mathbf{x} - \mathbf{s}_0\|^2}{a_0^2}\right) < \frac{1}{\tau} \exp\left(-\frac{\|\mathbf{x} - \mathbf{s}\|^2}{a^2}\right)$$

holds if and only if

$$\frac{\|\mathbf{x} - \mathbf{s}_0\|^2}{a_0^2} - \frac{\|\mathbf{x} - \mathbf{s}\|^2}{a^2} > \ln\left(\frac{\tau}{\tau_0}\right),$$

that is if and only if \mathbf{x} belongs to a domain limited by a two sheeted hyperboloid.

4.6 CONCLUSION

Motivated by the exploration of geometrical properties of storm processes, we proposed in [Section 4.3](#) an algorithm for the continuous simulation of deterministic, isotropic, non-increasing storms on a hyperrectangle in arbitrary dimension. It consists of the succession of two independent tasks: first identify all the potentially active Poisson points, with spatial component located inside then outside the domain of simulation, then compute the value of the storm process at any chosen point within the domain. As illustrated in [Section 4.4](#) and discussed in [Section 4.5](#), this structure, made possible by working in a continuous framework, allows for fast and efficient simulations. In particular, both the generation of the outer active points and the calculation of maxima are parallelizable, which makes high-resolution simulations accessible.

Possible improvements of our algorithm were also brought up in [Section 4.5](#), thereby suggesting avenues for future research. For instance, the running time could be reduced even more by optimizing the covering. More general, random storms could also be considered. Another natural extension, which shall be the focus of forthcoming work, is the adaptation of our results to conditional simulations. Taking into account either point or regional data exceeding a critical value in a portion of space would make our algorithm full of potentialities in real-world applications. Finally, simulations could be performed on non-Euclidean spaces like spheres, which is of special interest in climatology.

4.7 PROOFS

4.7.1 *Distribution of \dot{s}*

To simplify mathematical expressions, the indicator function of any condition C is denoted by $\mathbf{1}\{C\}$. It is equal to 1 if C is true and 0 otherwise.

Calculation of p_I

Recall that $D = \{(s, \tau) \in \mathbb{R}^c \times (0, +\infty) : f(d(s, R))/\tau > f(\delta)/\tau_n\}$, and let $I \neq \emptyset$. Since $(\dot{s}, \dot{\tau})$ is uniformly distributed on D , then we have

$$p_I = \frac{\int_D \mathbf{1}\{s \in E_I\} d\tau ds}{\int_D d\tau ds} = \frac{\int_{E_I} f(d(s, R)) ds}{\int_{\mathbb{R}^c} f(d(s, R)) ds} = \frac{\int_{E_I} f(d(s, R)) ds}{\sum_{J \neq \emptyset} \int_{E_J} f(d(s, R)) ds}.$$

To calculate the numerator

$$\int_{E_I} f(d(\mathbf{s}, \mathbf{R})) d\mathbf{s} = \int_{\mathbb{R}^d} f(d(\mathbf{s}, \mathbf{R})) \mathbf{1}\{|\mathbf{s}_I| \geq \ell_I\} \mathbf{1}\{|\mathbf{s}_{I^c}| < \ell_{I^c}\} d\mathbf{s},$$

the crux is to observe that

$$\forall \mathbf{s} \in E_I \quad d(\mathbf{s}, \mathbf{R}) = \|\mathbf{s}_I - \ell_I\|.$$

This shows that the integrand does not depend on \mathbf{s} but only on $|\mathbf{s}|$, that is the absolute values of its coordinates. Accordingly, integration needs to take place only in the positive hyperoctant, in which case the relation $d(\mathbf{s}, \mathbf{R}) = \|\mathbf{s}_I - \ell_I\|_I$ holds. It follows:

$$\int_{E_I} f(d(\mathbf{s}, \mathbf{R})) d\mathbf{s} = 2^d \int_{\mathbb{R}_+^d} f(\|\mathbf{s}_I - \ell_I\|_I) \mathbf{1}\{\mathbf{s}_I \geq \ell_I\} \mathbf{1}\{0 \leq \mathbf{s}_{I^c} < \ell_{I^c}\} d\mathbf{s}.$$

Denoting by $k(I)$ the number of elements of I , and putting $\mathbf{R}_I = \prod_{i \in I} [-\ell_i, \ell_i]$, this integral becomes

$$\int_{E_I} f(d(\mathbf{s}, \mathbf{R})) d\mathbf{s} = 2^{k(I)} v_{k(I^c)}(\mathbf{R}_{I^c}) \int_{\mathbb{R}_+^{k(I)}} f(\|\mathbf{s}_I - \ell_I\|_I) \mathbf{1}\{\mathbf{s}_I \geq \ell_I\} d\mathbf{s}_I.$$

The changes of variables $\mathbf{s}_I - \ell_I \rightarrow \mathbf{s}_I$ yields

$$\int_{E_I} f(d(\mathbf{s}, \mathbf{R})) d\mathbf{s} = 2^{k(I)} v_{k(I^c)}(\mathbf{R}_{I^c}) \int_{\mathbb{R}_+^{k(I)}} f(\|\mathbf{s}_I\|_I) d\mathbf{s}_I.$$

Then, a change into polar coordinates gives

$$\begin{aligned} \int_{E_I} f(d(\mathbf{s}, \mathbf{R})) d\mathbf{s} &= v_{k(I^c)}(\mathbf{R}_{I^c}) \int_{\mathbb{R}^{k(I)}} f(\|\mathbf{s}_I\|_I) d\mathbf{s}_I \\ &= v_{k(I^c)}(\mathbf{R}_{I^c}) k(I) \omega_{k(I)} \int_0^\infty f(\tau) \tau^{k(I)-1} d\tau \\ &= v_{k(I^c)}(\mathbf{R}_{I^c}) k(I) \omega_{k(I)} m_{k(I)-1}. \end{aligned}$$

Calculation of $f_{d(\dot{\mathbf{s}}, \mathbf{R})}(u | I)$

This p.d.f. is calculated via its complementary distribution function. Starting from the fact that $(\dot{\mathbf{s}}, \dot{\mathbf{t}})$ is uniform over D , it appears that

$$\mathbf{P}[d(\dot{\mathbf{s}}, \mathbf{R}) > u | I] = \frac{\int_{E_I} f(d(\mathbf{s}, \mathbf{R})) \mathbf{1}\{d(\mathbf{s}, \mathbf{R}) > u\} d\mathbf{s}}{\int_{E_I} f(d(\mathbf{s}, \mathbf{R})) d\mathbf{s}}.$$

The denominator was obtained in the previous section. Regarding the numerator, it is calculated exactly the same way. All calculations done, the result is

$$\mathbf{P}[d(\dot{\mathbf{s}}, \mathbf{R}) > u | I] = \frac{\int_u^\infty f(\tau) \tau^{k(I)-1} d\tau}{\int_0^\infty f(\tau) \tau^{k(I)-1} d\tau},$$

which finally gives

$$\forall u > 0 \quad f_{d(\dot{\mathbf{s}}, \mathbf{R})}(u | I) = \frac{f(u) u^{k(I)-1}}{m_{k(I)-1}}.$$

4.7.2 Domains of influence of power exponential storms

This section is dedicated to the proof of [Proposition 4.3](#). We shall first establish some preliminary results. In what follows, consider the same notation as in [Subsection 4.4.3](#) and recall that

$$A_0 = \left\{ \mathbf{x} \in \mathbb{R}^d : \|\mathbf{x} - \mathbf{s}_0\|^\alpha - \|\mathbf{x} - \mathbf{s}\|^\alpha > c_\alpha \|\mathbf{s} - \mathbf{s}_0\|^\alpha \right\}. \quad (4.17)$$

Also denote by $M := \{\mathbf{x} \in \mathbb{R}^d : \|\mathbf{x} - \mathbf{s}_0\| = \|\mathbf{x} - \mathbf{s}\|\}$ the mediator hyperplane of the segment with endpoints \mathbf{s}_0 and \mathbf{s} , and by $L := \{(1 - \lambda)\mathbf{s}_0 + \lambda\mathbf{s} : \lambda \geq 1/2\}$ the half-line with initial point $(\mathbf{s} + \mathbf{s}_0)/2 \in M$ and direction $\mathbf{s} - \mathbf{s}_0$. The distance between two subsets A and B of \mathbb{R}^d shall be denoted by $d(A, B) := \inf \{\|\mathbf{x} - \mathbf{y}\| : (\mathbf{x}, \mathbf{y}) \in A \times B\}$.

Lemma 4.4 The following properties are equivalent:

- (i) $A_0 = \emptyset$,
- (ii) $A_0 \cap L = \emptyset$,
- (iii) $\alpha \leq 1$ and $c_\alpha \geq 1$.

Proof. The proof of this lemma relies on the definition of A_0 given in [\(4.17\)](#).

First of all, (i) clearly implies (ii).

To check that (ii) implies (iii), consider the contrapositive. First take $c_\alpha < 1$, then $\mathbf{s} \in L$ is also trivially in A_0 . Now consider $\alpha > 1$ and $c_\alpha \geq 1$. Because $u \in (0, +\infty) \mapsto u^\alpha$ is increasing and continuous, it is easy to check that $-c_\alpha \mathbf{s}_0 + (c_\alpha + 1)\mathbf{s} \in L$ is also in A_0 . Therefore, in both cases, $A_0 \cap L \neq \emptyset$.

The proof is concluded by showing the last entailment: (iii) implies (i). First take $\alpha = 1$. The triangular inequality $\|\mathbf{x} - \mathbf{s}_0\| \leq \|\mathbf{x} - \mathbf{s}\| + \|\mathbf{s} - \mathbf{s}_0\|$ directly implies that $A_0 = \emptyset$ if $c_\alpha \geq 1$. Now let $\alpha < 1$. Since $u \in (0, +\infty) \mapsto u^\alpha$ is concave and increasing with $u^\alpha \rightarrow 0$ as $u \rightarrow 0$,

$$\|\mathbf{x} - \mathbf{s}_0\|^\alpha \leq (\|\mathbf{x} - \mathbf{s}\| + \|\mathbf{s} - \mathbf{s}_0\|)^\alpha \leq \|\mathbf{x} - \mathbf{s}\|^\alpha + \|\mathbf{s} - \mathbf{s}_0\|^\alpha,$$

therefore $A_0 = \emptyset$ if $c_\alpha \geq 1$. ■

Lemma 4.5 A_0 is bounded if $\alpha < 1$ and $c_\alpha < 1$.

Proof. Let $\alpha < 1$ and $c_\alpha < 1$. Because the function $u \in (0, +\infty) \mapsto u^\alpha$ is concave and differentiable, its graph lies under all of its tangents, which yields

$$\forall \mathbf{x} \in \mathbb{R}^d \quad \|\mathbf{x} - \mathbf{s}_0\|^\alpha - \|\mathbf{x} - \mathbf{s}\|^\alpha \leq \alpha \|\mathbf{x} - \mathbf{s}\|^{\alpha-1} (\|\mathbf{x} - \mathbf{s}_0\| - \|\mathbf{x} - \mathbf{s}\|).$$

Taking $\mathbf{x} \in A_0$, this implies in turn that

$$\left(\frac{c_\alpha}{\alpha}\right)^{1/(\alpha-1)} \|\mathbf{s} - \mathbf{s}_0\| \geq \|\mathbf{x} - \mathbf{s}\|,$$

which means that \mathbf{x} is contained in the closed ball in \mathbb{R}^d of center \mathbf{s} and radius $(c_\alpha/\alpha)^{1/(\alpha-1)} \|\mathbf{s} - \mathbf{s}_0\|$. ■

Lemma 4.6 If $\alpha < 1$ and $c_\alpha < 1$, there exist positive real numbers λ_* and λ^* satisfying

$$1 - \left(2^{-\alpha} - \frac{c_\alpha}{2}\right)^{1/\alpha} \leq \lambda_* < 1 \quad \text{and} \quad 1 < \lambda^* \leq 1 + \left(\frac{c_\alpha}{\alpha}\right)^{1/(\alpha-1)}$$

such that the the relative domain of influence A_0 meets the half-line L on the open segment with endpoints $(1 - \lambda_*) \mathbf{s}_0 + \lambda_* \mathbf{s}$ and $(1 - \lambda^*) \mathbf{s}_0 + \lambda^* \mathbf{s}$:

$$A_0 \cap L = \{(1 - \lambda) \mathbf{s}_0 + \lambda \mathbf{s} : \lambda \in (\lambda_*, \lambda^*)\}.$$

Proof. Let $\alpha < 1$, $c_\alpha < 1$ and $\mathbf{x} \in A_0 \cap L$. By definition, there exists $\lambda > 1/2$ such that

$$\begin{cases} \|\mathbf{x} - \mathbf{s}_0\|^\alpha - \|\mathbf{x} - \mathbf{s}\|^\alpha > c_\alpha \|\mathbf{s} - \mathbf{s}_0\|, \\ \mathbf{x} = (1 - \lambda) \mathbf{s}_0 + \lambda \mathbf{s}, \end{cases}$$

which is equivalent to $\lambda^\alpha + |\lambda - 1|^\alpha > c_\alpha$.

Consider the function $\phi_\alpha : \lambda \in (1/2, +\infty) \mapsto \lambda^\alpha + |\lambda - 1|^\alpha$. It is continuous on its domain of definition, and differentiable separately on $(1/2, 1)$ and $(1, +\infty)$. A study of its variations shows that when $\alpha < 1$, it is increasing on $(1/2, 1)$, going from $\phi_\alpha(1/2) = 0$ to $\phi_\alpha(1) = 1$, then decreasing on $(1, +\infty)$, tending to 0 as $\lambda \rightarrow +\infty$. Therefore, the intermediate value theorem guarantees that there exist $\lambda_* \in (1/2, 1)$ and $\lambda^* \in (1, +\infty)$ such that $\phi_\alpha(\lambda_*) = \phi_\alpha(\lambda^*) = c_\alpha \in (0, 1)$ and $\phi_\alpha > c_\alpha$ on (λ_*, λ^*) .

More refined bounds can be obtained for those two real numbers using the concavity and differentiability of $u \in (0, +\infty) \mapsto u^\alpha$. Indeed, the three chords lemma applied to $1 - \lambda_* < 1/2 < \lambda_*$ gives

$$1 - \left(2^{-\alpha} - \frac{c_\alpha}{2}\right)^{1/\alpha} \leq \lambda_*,$$

and the subgradient inequality $c_\alpha = \phi_\alpha(\lambda^*) \leq \alpha(\lambda^* - 1)^{\alpha-1}$ yields

$$\lambda^* \leq 1 + \left(\frac{c_\alpha}{\alpha}\right)^{1/(\alpha-1)}.$$

■

Lemma 4.7 If $\alpha = 1$ and $c_\alpha < 1$ or $\alpha > 1$, there exists $\lambda_* > 1/2$ such that the relative domain of influence A_0 meets the half-line L on the open half-line L_* with initial point $(1 - \lambda_*) \mathbf{s}_0 + \lambda_* \mathbf{s}$ and direction $\mathbf{s} - \mathbf{s}_0$:

$$A_0 \cap L = \{(1 - \lambda) \mathbf{s}_0 + \lambda \mathbf{s} : \lambda > \lambda_*\} =: L_*.$$

Moreover, λ_* satisfies

$$\left\{ \begin{array}{ll} \lambda_* = \frac{c_1 + 1}{2} & \text{if } \alpha = 1 \text{ and } c_1 < 1, \\ \left(2^{-\alpha} + \frac{c_\alpha}{2}\right)^{1/\alpha} \leq \lambda_* < 1 & \text{if } 1 < \alpha < 2 \text{ and } c_\alpha < 1, \\ \lambda_* = 1 & \text{if } 1 < \alpha < 2 \text{ and } c_\alpha = 1, \\ 2 + \frac{c_\alpha - 2^\alpha + 1}{\alpha(2^{\alpha-1} - 1)} \leq \lambda_* & \text{if } 1 < \alpha < 2 \text{ and } c_\alpha > 1. \end{array} \right.$$

Proof. Let $\mathbf{x} \in A_0 \cap L$ and $\phi_\alpha : \lambda \in (1/2, +\infty) \mapsto \lambda^\alpha + |\lambda - 1|^\alpha$. Like in the proof of [Lemma 4.6](#), $\mathbf{x} \in A_0 \cap L$ means that there exists $\lambda > 1/2$ such that $\phi_\alpha(\lambda) > c_\alpha$.

First consider the case where $\alpha = 1$ and $c_\alpha < 1$. Then ϕ_1 simplifies to

$$\phi_1(\lambda) = \begin{cases} 2\lambda - 1 & \text{if } \lambda \in (1/2, 1), \\ 1 & \text{if } \lambda \in [1, +\infty). \end{cases}$$

Therefore, the equation $\phi_1(\lambda) = c_1 \in (0, 1)$ admits a unique solution $\lambda_* = \frac{c_1 + 1}{2}$ and $\phi_1 > c_1$ on $(\lambda_*, +\infty)$.

Now turn to the case where $\alpha > 1$. Studying the variations of ϕ_α yields that it is increasing on its domain of definition, going from $\phi_\alpha(1/2) = 0$ to $\phi_\alpha(1) = 1$ then to $+\infty$ as $\lambda \rightarrow +\infty$. Invoking once more the intermediate value theorem, there exists $\lambda_* > 1/2$ such that $\phi_\alpha(\lambda_*) = c_\alpha$ and $\phi_\alpha > c_\alpha$ on $(\lambda_*, +\infty)$.

Moreover, when $c_\alpha < 1$, then $\lambda_* \in (1/2, 1)$. Because $u \in (0, +\infty) \mapsto u^\alpha$ is convex for $\alpha > 1$, the three chords lemma can be applied to $1 - \lambda_* < 1/2 < \lambda_*$, which yields

$$\left(2^{-\alpha} + \frac{c_\alpha}{2}\right)^{1/\alpha} \leq \lambda_*.$$

When $c_\alpha = 1$, the equation $\phi_\alpha(\lambda) = 1$ admits a unique solution $\lambda_* = 1$.

Finally, when $c_\alpha > 1$, differentiating ϕ_α twice shows that it is convex. Then, the subgradient inequality $\phi_\alpha(\lambda_*) - \phi_\alpha(2) \geq \phi'_\alpha(2)(\lambda_* - 2)$ gives

$$2 + \frac{c_\alpha - 2^\alpha + 1}{\alpha(2^{\alpha-1} - 1)} \leq \lambda_*.$$

■

Lemma 4.8 If $\alpha \leq 2$, then $d(A_0, M) = d(A_0 \cap L, M)$.

Proof. Let $\mathbf{x} \in A_0$ and consider P the $d \times d$ orthogonal projection matrix onto the line passing through \mathbf{s}_0 and \mathbf{s} . We shall prove that $P\mathbf{x} \in A_0$. Indeed, by the Pythagorean theorem,

$$\|P\mathbf{x} - \mathbf{s}_0\|^\alpha - \|P\mathbf{x} - \mathbf{s}\|^\alpha = \left(\|P\mathbf{x} - \mathbf{s}_0\|^2\right)^{\alpha/2} - \left(\|P\mathbf{x} - \mathbf{s}\|^2\right)^{\alpha/2}$$

$$\begin{aligned}
 &= \left(\|\mathbf{x} - \mathbf{s}_0\|^2 - \|\mathbf{P}\mathbf{x} - \mathbf{x}\|^2 \right)^{\alpha/2} - \left(\|\mathbf{x} - \mathbf{s}\|^2 - \|\mathbf{P}\mathbf{x} - \mathbf{x}\|^2 \right)^{\alpha/2} \\
 &= \|\mathbf{x} - \mathbf{s}_0\|^\alpha - \|\mathbf{x} - \mathbf{s}\|^\alpha \\
 &\quad + \left(\left(\|\mathbf{x} - \mathbf{s}_0\|^2 - \|\mathbf{P}\mathbf{x} - \mathbf{x}\|^2 \right)^{\alpha/2} - \|\mathbf{x} - \mathbf{s}_0\|^\alpha \right) \\
 &\quad - \left(\left(\|\mathbf{x} - \mathbf{s}\|^2 - \|\mathbf{P}\mathbf{x} - \mathbf{x}\|^2 \right)^{\alpha/2} - \|\mathbf{x} - \mathbf{s}\|^\alpha \right)
 \end{aligned}$$

In addition, for any $c \geq 0$ the function $u \in (\sqrt{c}, +\infty) \mapsto (u^2 - c)^{\alpha/2} - u^\alpha$ is differentiable and non-decreasing. Taking $c = \|\mathbf{P}\mathbf{x} - \mathbf{x}\|^2$ and $u = \|\mathbf{x} - \mathbf{s}_0\| > \|\mathbf{x} - \mathbf{s}_1\|$ (because $A_0 \subset H_0^c$), this yields

$$\|\mathbf{P}\mathbf{x} - \mathbf{s}_0\|^\alpha - \|\mathbf{P}\mathbf{x} - \mathbf{s}\|^\alpha \geq \|\mathbf{x} - \mathbf{s}_0\|^\alpha - \|\mathbf{x} - \mathbf{s}\|^\alpha > c_\alpha \|\mathbf{s} - \mathbf{s}_0\|^\alpha.$$

In other words, $\mathbf{P}\mathbf{x} \in A_0$. Since L is orthogonal to M by construction, it directly follows that $d(A_0, M) = d(A_0 \cap L, M)$. ■

We are now fully equipped to handle the proof of [Proposition 4.3](#). Indeed, the inclusion given for $\alpha \in (0, 2)$ is a direct consequence of [Lemmas 4.6](#) and [4.7](#) combined with [Lemma 4.8](#). Observe that this also holds when $\alpha \leq 1$ and $c_\alpha \geq 1$, in which case $A_0 = \emptyset$ ([Lemma 4.4](#)). For $\alpha \in (0, 1)$ and $c_\alpha < 1$, the inclusion of A_0 in the given ball directly stems from [Lemma 4.5](#) combined with [Lemmas 4.6](#) and [4.8](#). This concludes the proof of [Proposition 4.3](#).

BIBLIOGRAPHY

- R. J. Adler. *The Geometry of Random Fields*. Wiley series in probability and statistics. John Wiley & Sons Inc, 1981. ISBN 0471278440.
- T. W. Anderson. *The statistical analysis of time series*. Wiley Classics Library. Wiley, New York, 1971.
- D. Azzimonti, F. Willot, and D. Jeulin. Optical properties of deposit models for paints: full-fields fft computations and representative volume element. *Journal of Modern Optics*, 60(7): 519–528, 2013. doi:[10.1080/09500340.2013.793778](https://doi.org/10.1080/09500340.2013.793778).
- M. Baake, M. Birkner, and R. V. Moody. Diffraction of stochastic point sets: Explicitly computable examples. *Communications in Mathematical Physics*, 293(3):611, 2009. doi:[10.1007/s00220-009-0942-x](https://doi.org/10.1007/s00220-009-0942-x).
- J. N. Bacro and G. Toulemonde. Measuring and modelling multivariate and spatial dependence of extremes. *Journal de la Société Française de Statistique*, 154(2):139–155, 2013. ISSN 2102-6238.
- A. A. Balkema and L. de Haan. Residual life time at great age. *Ann. Probab.*, 2(5):792–804, 10 1974. doi:[10.1214/aop/1176996548](https://doi.org/10.1214/aop/1176996548).
- A. A. Balkema and S. I. Resnick. Max-infinite divisibility. *Journal of Applied Probability*, 14(2): 309–319, 1977. doi:[10.2307/3213001](https://doi.org/10.2307/3213001).
- J. Beirlant, Y. Goegebeur, J. Segers, and J. L. Teugels. *Statistics of Extremes: Theory and Applications*. John Wiley & Sons Inc, 2004.
- L. Bel, J. N. Bacro, and C. Lantuéjoul. Assessing extremal dependence of environmental spatial fields. *Environmetrics*, 19(2):163–182, 2008. doi:[10.1002/env.863](https://doi.org/10.1002/env.863).
- P. Billingsley. *Probability and Measure*. John Wiley and Sons, Inc, New-York, third edition, 1995. ISBN 978-8126517718.
- R. C. Bradley. Equivalent mixing conditions for random fields. *Ann. Probab.*, 21(4):1921–1926, 10 1993a. doi:[10.1214/aop/1176989004](https://doi.org/10.1214/aop/1176989004).
- R. C. Bradley. Equivalent mixing conditions for random fields. *Ann. Probab.*, 21(4):1921–1926, 10 1993b. doi:[10.1214/aop/1176989004](https://doi.org/10.1214/aop/1176989004).

- L. Breiman. *Probability*. Classics in Applied Mathematics. SIAM, 1992. ISBN 978-0-898712-96-4.
- B. M. Brown and S. I. Resnick. Extreme values of independent stochastic processes. *Journal of Applied Probability*, 14(4):732–739, 1977. doi:[10.2307/3213346](https://doi.org/10.2307/3213346).
- P. Capéraà, A.-L. Fougères, and C. Genest. A nonparametric estimation procedure for bivariate extreme value copulas. *Biometrika*, 84(3):567–577, 1997. doi:[10.1093/biomet/84.3.567](https://doi.org/10.1093/biomet/84.3.567).
- D. Castro-Camilo and R. Huser. Local likelihood estimation of complex tail dependence structures, applied to u.s. precipitation extremes. *Journal of the American Statistical Association*, 0(0):1–29, 2019. doi:[10.1080/01621459.2019.1647842](https://doi.org/10.1080/01621459.2019.1647842).
- S. Castruccio, R. Huser, and M. G. Genton. High-order composite likelihood inference for max-stable distributions and processes. *Journal of Computational and Graphical Statistics*, 25(4):1212–1229, 2016. doi:[10.1080/10618600.2015.1086656](https://doi.org/10.1080/10618600.2015.1086656).
- I. Catto, C. Le Bris, and P.-L. Lions. *The Mathematical Theory of Thermodynamic Limits: Thomas-Fermi Type Models*. Oxford university press, 1998.
- J.-P. Chilès and P. Delfiner. *Geostatistics: Modeling Spatial Uncertainty*. Wiley series in probability and statistics. John Wiley & Sons Inc, second edition, 2012. doi:[10.1002/9781118136188](https://doi.org/10.1002/9781118136188).
- S. Coles. *An Introduction to Statistical Modeling of Extreme Values*. Springer-Verlag London, 2001. doi:[10.1007/978-1-4471-3675-0](https://doi.org/10.1007/978-1-4471-3675-0).
- S. G. Coles. Regional modelling of extreme storms via max-stable processes. *Journal of the Royal Statistical Society. Series B (Methodological)*, 55(4):797–816, 1993. ISSN 00359246.
- S. G. Coles and J. A. Tawn. Modelling extremes of the areal rainfall process. *Journal of the Royal Statistical Society: Series B (Methodological)*, 58(2):329–347, 1996. doi:[10.1111/j.2517-6161.1996.tb02085.x](https://doi.org/10.1111/j.2517-6161.1996.tb02085.x).
- S. G. Coles and D. Walshaw. Directional modelling of extreme wind speeds. *Journal of the Royal Statistical Society. Series C (Applied Statistics)*, 43(1):139–157, 1994. doi:[10.2307/2986118](https://doi.org/10.2307/2986118).
- D. Cooley, P. Naveau, and P. Poncet. *Variograms for spatial max-stable random fields*, pages 373–390. Springer New York, New York, NY, 2006. doi:[10.1007/0-387-36062-X_17](https://doi.org/10.1007/0-387-36062-X_17).
- D. Cooley, R. A. Davis, and P. Naveau. The pairwise beta distribution: A flexible parametric multivariate model for extremes. *Journal of Multivariate Analysis*, 101(9):2103 – 2117, 2010. doi:[10.1016/j.jmva.2010.04.007](https://doi.org/10.1016/j.jmva.2010.04.007).

- U. Cormann and R.-D. Reiss. Generalizing the pareto to the log-pareto model and statistical inference. *Extremes*, 12(1):93–105, Mar 2009. doi:[10.1007/s10687-008-0070-6](https://doi.org/10.1007/s10687-008-0070-6).
- N. Cressie. *Statistics for Spatial Data*. Wiley series in probability and statistics. John Wiley & Sons Inc, 1993. doi:[10.1002/9781119115151](https://doi.org/10.1002/9781119115151).
- B. M. Davis and L. E. Borgman. A note on the asymptotic distribution of the sample variogram. *Journal of the International Association for Mathematical Geology*, 14:189–193, 12 1982. doi:[10.1007/BF01083951](https://doi.org/10.1007/BF01083951).
- A. Davison, R. Huser, and E. Thibaud. Spatial extremes. In A. Gelfand, M. Fuentes, J. Hoeting, and R. Smith, editors, *Handbook of Environmental and Ecological Statistics*. CRC Press, 2019. doi:[10754/631198](https://doi.org/10754/631198).
- A. C. Davison and M. M. Gholamrezaee. Geostatistics of extremes. *Proceedings of the Royal Society A: Mathematical, Physical and Engineering Sciences*, 468(2138):581–608, 2012. doi:[10.1098/rspa.2011.0412](https://doi.org/10.1098/rspa.2011.0412).
- A. C. Davison, S. A. Padoan, and M. Ribatet. Statistical modeling of spatial extremes. *Statist. Sci.*, 27(2):161–186, 05 2012. doi:[10.1214/11-STS376](https://doi.org/10.1214/11-STS376).
- R. de Fondeville. *Functional Peaks-Over-Threshold Analysis for Complex Extreme Events*. PhD thesis, EPFL, Lausanne, 2018.
- L. de Haan. A spectral representation for max-stable processes. *Ann. Probab.*, 12(4):1194–1204, 1984. doi:[10.1214/aop/1176993148](https://doi.org/10.1214/aop/1176993148).
- L. de Haan and A. Ferreira. *Extreme Value Theory: An Introduction*. Springer-Verlag New York, 2006. doi:[10.1007/0-387-34471-3](https://doi.org/10.1007/0-387-34471-3).
- L. de Haan and T. T. Pereira. Spatial extremes: Models for the stationary case. *Ann. Statist.*, 34(1):146–168, 02 2006. doi:[10.1214/009053605000000886](https://doi.org/10.1214/009053605000000886).
- N. Desassis and D. Renard. Automatic variogram modeling by iterative least squares: Univariate and multivariate cases. *Mathematical Geosciences*, 45, 05 2012. doi:[10.1007/s11004-012-9434-1](https://doi.org/10.1007/s11004-012-9434-1).
- L. Devroye. *Non-Uniform random Variate Generation*. Springer-Verlag New York, 1986.
- D. Dey and J. Yan. *Extreme value modeling and risk analysis: Methods and applications*. Chapman and Hall/CRC, 2016. doi:[10.1201/b19721](https://doi.org/10.1201/b19721).
- J. Dirrenberger, S. Forest, and D. Jeulin. Towards gigantic rve sizes for 3d stochastic fibrous networks. *International Journal of Solids and Structures*, 51(2):359 – 376, 2014. doi:[10.1016/j.ijsolstr.2013.10.011](https://doi.org/10.1016/j.ijsolstr.2013.10.011).

- C. Dombry and F. Eyi-Minko. Strong mixing properties of max-infinitely divisible random fields. *Stochastic Processes and their Applications*, 122(11):3790 – 3811, 2012. doi:[10.1016/j.spa.2012.06.013](https://doi.org/10.1016/j.spa.2012.06.013).
- C. Dombry and Z. Kabluchko. Ergodic decompositions of stationary max-stable processes in terms of their spectral functions. *Stochastic Processes and their Applications*, 127(6):1763 – 1784, 2017. doi:[10.1016/j.spa.2016.10.001](https://doi.org/10.1016/j.spa.2016.10.001).
- C. Dombry and Z. Kabluchko. Random tessellations associated with max-stable random fields. *Bernoulli*, 24(1):30–52, 02 2018. doi:[10.3150/16-BEJ817](https://doi.org/10.3150/16-BEJ817).
- C. Dombry and M. Ribatet. Functional regular variations, pareto processes and peaks over threshold. *Statistics and its interface*, 8(1):9–17, 2015. doi:[10.4310/SII.2015.v8.n1.a2](https://doi.org/10.4310/SII.2015.v8.n1.a2).
- C. Dombry, S. Engelke, and M. Oesting. Exact simulation of max-stable processes. *Biometrika*, 103(2):303–317, 05 2016. doi:[10.1093/biomet/asw008](https://doi.org/10.1093/biomet/asw008).
- I. Domowitz and M. A. El-Gamal. A consistent test of stationary-ergodicity. *Econometric Theory*, 9(4):589–601, 1993. doi:[10.2307/3532676](https://doi.org/10.2307/3532676).
- I. Domowitz and M. A. El-Gamal. A consistent nonparametric test of ergodicity for time series with applications. *Journal of Econometrics*, 102(2):365 – 398, 2001. ISSN 0304-4076. doi:[10.1016/S0304-4076\(01\)00058-6](https://doi.org/10.1016/S0304-4076(01)00058-6).
- J. L. Doob. *Stochastic processes*. Wiley Classics Library. Wiley-Interscience, 1990.
- P. Doukhan. *Mixing, Properties and Examples*. Springer-New-York, 1994. doi:[10.1007/978-1-4612-2642-0](https://doi.org/10.1007/978-1-4612-2642-0).
- N. Dunford. A mean ergodic theorem. *Duke Math. J.*, 5(3):635–646, 09 1939a. doi:[10.1215/S0012-7094-39-00552-1](https://doi.org/10.1215/S0012-7094-39-00552-1).
- N. Dunford. An ergodic theorem for n-parameter groups. *Proceedings of the National Academy of Sciences*, 25(4):195–196, 1939b. doi:[10.1073/pnas.25.4.195](https://doi.org/10.1073/pnas.25.4.195).
- J. H. J. Einmahl and J. R. Magnus. Records in athletics through extreme-value theory. *Journal of the American Statistical Association*, 103(484):1382–1391, 2008. doi:[10.1198/016214508000000698](https://doi.org/10.1198/016214508000000698).
- J. J. Einmahl, J. H. J. Einmahl, and L. de Haan. Limits to human life span through extreme value theory. *Journal of the American Statistical Association*, 114(527):1075–1080, 2019. doi:[10.1080/01621459.2018.1537912](https://doi.org/10.1080/01621459.2018.1537912).
- P. Embrechts, C. Klüppelberg, and T. Mikosch. *Modelling Extremal Events: for insurance and finance*. Springer-Verlag Berlin Heidelberg, 1997. doi:[10.1007/978-3-642-33483-2](https://doi.org/10.1007/978-3-642-33483-2).

- S. Engelke, R. De Fondeville, and M. Oesting. Extremal behaviour of aggregated data with an application to downscaling. *Biometrika*, 106(1):127–144, 12 2018. doi:[10.1093/biomet/asy052](https://doi.org/10.1093/biomet/asy052).
- W. Feller. *Introduction to Probability Theory and its Applications*. Wiley, New York, 1968.
- A. Ferreira and L. de Haan. The generalized pareto process; with a view towards application and simulation. *Bernoulli*, 20(4):1717–1737, 11 2014. doi:[10.3150/13-BEJ538](https://doi.org/10.3150/13-BEJ538).
- A. Ferreira, L. de Haan, and C. Zhou. Exceedance probability of the integral of a stochastic process. *Journal of Multivariate Analysis*, 105(1):241–257, 2012.
- R. A. Fisher and L. H. C. Tippett. Limiting forms of the frequency distribution of the largest or smallest member of a sample. *Mathematical Proceedings of the Cambridge Philosophical Society*, 24(2):180–190, 1928. doi:[10.1017/S0305004100015681](https://doi.org/10.1017/S0305004100015681).
- W. A. Fuller. *Introduction to Statistical Time Series*. John Wiley & Sons, Inc., 2 edition, 1996. doi:[10.1002/9780470316917](https://doi.org/10.1002/9780470316917).
- P. García-Soidán. Asymptotic normality of the nadaraya–watson semivariogram estimators. *TEST*, 16(3):479–503, Dec 2007. doi:[10.1007/s11749-006-0016-8](https://doi.org/10.1007/s11749-006-0016-8).
- P. H. García-Soidán, W. González-Manteiga, and M. Febrero-Bande. Local linear regression estimation of the variogram. *Statistics & Probability Letters*, 64(2):169–179, 2003. doi:[10.1016/S0167-7152\(03\)00149-4](https://doi.org/10.1016/S0167-7152(03)00149-4).
- P. H. García-Soidán, M. Febrero-Bande, and W. González-Manteiga. Nonparametric kernel estimation of an isotropic variogram. *Journal of Statistical Planning and Inference*, 121(1): 65 – 92, 2004. doi:[10.1016/S0378-3758\(02\)00507-4](https://doi.org/10.1016/S0378-3758(02)00507-4).
- J.-B. Gasnier, F. Willot, H. Trumel, B. Figliuzzi, D. Jeulin, and M. Biessy. A fourier-based numerical homogenization tool for an explosive material. *Matériaux & Techniques*, 103(3): 308, 2015. doi:[10.1051/mattech/2015019](https://doi.org/10.1051/mattech/2015019).
- E. Gómez, M. Gomez-Viilegas, and J. Marín. A multivariate generalization of the power exponential family of distributions. *Communications in Statistics - Theory and Methods*, 27(3): 589–600, 1998. doi:[10.1080/03610929808832115](https://doi.org/10.1080/03610929808832115).
- B. Gnedenko. Sur la distribution limite du terme maximum d’une serie aleatoire. *Annals of Mathematics*, 44(3):423–453, 1943. doi:[10.2307/1968974](https://doi.org/10.2307/1968974).
- P. Hall and P. Patil. Properties of nonparametric estimators of autocovariance for stationary random fields. *Probability Theory and Related Fields*, 99(3):399–424, Sep 1994. doi:[10.1007/BF01199899](https://doi.org/10.1007/BF01199899).

- P. Hall, N. I. Fisher, and B. Hoffmann. On the nonparametric estimation of covariance functions. *Ann. Statist.*, 22(4):2115–2134, 12 1994. doi:[10.1214/aos/1176325774](https://doi.org/10.1214/aos/1176325774).
- R. Huser and A. C. Davison. Composite likelihood estimation for the Brown–Resnick process. *Biometrika*, 100(2):511–518, 02 2013. doi:[10.1093/biomet/ass089](https://doi.org/10.1093/biomet/ass089).
- R. Huser and M. Genton. Non-stationary dependence structures for spatial extremes. *JABES*, 21:470–491, 2016. doi:[10.1007/s13253-016-0247-4](https://doi.org/10.1007/s13253-016-0247-4).
- IPCC. *Managing the Risks of Extreme Events and Disasters to Advance Climate Change Adaptation*. Cambridge university press, 2012.
- A. F. Jenkinson. The frequency distribution of the annual maximum (or minimum) values of meteorological elements. *Quarterly Journal of the Royal Meteorological Society*, 81(348):158–171, 1955. doi:[10.1002/qj.49708134804](https://doi.org/10.1002/qj.49708134804).
- D. Jeulin. Variance scaling of boolean random varieties. Technical report, 2011.
- Z. Kabluchko. Spectral representations of sum- and max-stable processes. *Extremes*, 12(4):401, Apr 2009. doi:[10.1007/s10687-009-0083-9](https://doi.org/10.1007/s10687-009-0083-9).
- Z. Kabluchko and M. Schlather. Ergodic properties of max-infinitely divisible processes. *Stochastic Processes and their Applications*, 120(3):281 – 295, 2010. ISSN 0304-4149. doi:[10.1016/j.spa.2009.12.002](https://doi.org/10.1016/j.spa.2009.12.002).
- Z. Kabluchko, M. Schlather, and L. de Haan. Stationary max-stable fields associated to negative definite functions. *Ann. Probab.*, 37(5):2042–2065, 09 2009. doi:[10.1214/09-AOP455](https://doi.org/10.1214/09-AOP455).
- E. Koch. Spatial risk measures and applications to max-stable processes. *Extremes*, 20(3):635–670, 2017. doi:[10.1007/s10687-016-0274-0](https://doi.org/10.1007/s10687-016-0274-0).
- E. Koch. Spatial risk measures and rate of spatial diversification. *Risks*, 7(2), 2019. doi:[10.3390/risks7020052](https://doi.org/10.3390/risks7020052).
- E. Koch, C. Dombry, and C. Y. Robert. A central limit theorem for functions of stationary max-stable random fields on \mathbb{R}^d . *Stochastic Processes and their Applications*, 2018. doi:[10.1016/j.spa.2018.09.014](https://doi.org/10.1016/j.spa.2018.09.014).
- C. Kyung-Joon and W. R. Schucany. Nonparametric kernel regression estimation near endpoints. *Journal of Statistical Planning and Inference*, 66(2):289 – 304, 1998. ISSN 0378-3758. doi:[10.1016/S0378-3758\(97\)00082-7](https://doi.org/10.1016/S0378-3758(97)00082-7).
- S. Lahiri, M. Kaiser, N. Cressie, and N. Hsu. Prediction of spatial cumulative distribution functions using subsampling. *Journal of the American Statistical Association*, 94(445):86–97, 1999. doi:[10.2307/2669680](https://doi.org/10.2307/2669680).

- S. N. Lahiri. On inconsistency of estimators based on spatial data under infill asymptotics. *Sankhyā: The Indian Journal of Statistics, Series A (1961-2002)*, 58(3):403–417, 1996. doi:[10.2307/25051119](https://doi.org/10.2307/25051119).
- C. Lantuéjoul. Ergodicity and integral range. *Journal of Microscopy*, 161(3):387–403, 1991. doi:[10.1111/j.1365-2818.1991.tb03099.x](https://doi.org/10.1111/j.1365-2818.1991.tb03099.x).
- C. Lantuéjoul. *Geostatistical simulation*. Springer, Berlin, Heidelberg, 2002. doi:[10.1007/978-3-662-04808-5](https://doi.org/10.1007/978-3-662-04808-5).
- C. Lantuéjoul, J. N. Bacro, and L. Bel. Storm processes and stochastic geometry. *Extremes*, 14:413–428, 2011. doi:[10.1007/s10687-010-0121-7](https://doi.org/10.1007/s10687-010-0121-7).
- M. Leadbetter. Extremes and local dependence in stationary sequences. *Zeitschrift für Wahrscheinlichkeitstheorie und Verwandte Gebiete*, 65:291–306, 1983. doi:[10.1007/BF00532484](https://doi.org/10.1007/BF00532484).
- H.-Y. Lee, H.-J. Park, and H.-M. Kim. A clarification of the cauchy distribution. *Communications for Statistical Applications and Methods*, 21, 03 2014. doi:[10.5351/CSAM.2014.21.2.183](https://doi.org/10.5351/CSAM.2014.21.2.183).
- J.-Y. Lee, R. V. Moody, and B. Solomyak. Pure point dynamical and diffraction spectra. *Annales Henri Poincaré*, 3(5):1003–1018, 2002. doi:[10.1007/s00023-002-8646-1](https://doi.org/10.1007/s00023-002-8646-1).
- D. Lenz and P. Stollmann. An ergodic theorem for delone dynamical systems and existence of the integrated density of states. *Journal d'Analyse Mathématique*, 97(1):1–24, 2005. doi:[10.1007/BF02807400](https://doi.org/10.1007/BF02807400).
- H. Madsen, C. P. Pearson, and D. Rosbjerg. Comparison of annual maximum series and partial duration series methods for modeling extreme hydrologic events: 2. regional modeling. *Water Resources Research*, 33(4):759–769, 1997. doi:[10.1029/96WR03849](https://doi.org/10.1029/96WR03849).
- G. Maruyama. The harmonic analysis of stationary stochastic processes. *Memoirs of the Faculty of Science, Kyushu University. Series A, Mathematics*, 4(1):45–106, 1949. doi:[10.2206/kyushumfs.4.45](https://doi.org/10.2206/kyushumfs.4.45).
- G. Matheron. *Traité de Geostatistique Appliquée*, volume 14 of *Mémoires du Bureau de Recherches Géologiques et Minières, Tome I*. Editions Technip, Paris, 1962.
- G. Matheron. *Les variables régionalisées et leur estimation. Une application de la théorie des fonctions aléatoires aux Sciences de la Nature*. PhD thesis, Masson, Paris, 1965.
- G. Matheron. *The Theory of Regionalized Variables and Its Applications*, volume 5 of *Cahiers du Centre de Morphologie Mathématique*. École des Mines de Paris, 1971.

- G. Matheron. *Random Sets and Integral Geometry*. John Wiley and Sons, Inc, 1975. ISBN 978-0471576211.
- G. Matheron. *Estimating and Choosing*. Springer-Verlag, Berlin, 1989. doi:[10.1007/978-3-642-48817-7](https://doi.org/10.1007/978-3-642-48817-7).
- B. Matérn. *Spatial Variation*, volume 36 of *Lecture Notes in Statistics*. Springer, New York, NY, 1986. doi:[10.1007/978-1-4615-7892-5](https://doi.org/10.1007/978-1-4615-7892-5).
- L. E. McPhillips, H. Chang, M. V. Chester, Y. Depietri, E. Friedman, N. B. Grimm, J. S. Kominoski, T. McPhearson, P. Méndez-Lázaro, E. J. Rosi, and J. Shafiei Shiva. Defining extreme events: A cross-disciplinary review. *Earth's Future*, 6(3):441–455, 2018. doi:[10.1002/2017EF000686](https://doi.org/10.1002/2017EF000686).
- I. Molchanov. *Random Sets and Random Functions*, pages 451–552. Springer London, London, 2017. doi:[10.1007/978-1-4471-7349-6_5](https://doi.org/10.1007/978-1-4471-7349-6_5).
- R. V. Moody and N. Strungaru. Point sets and dynamical systems in the autocorrelation topology. *Canadian Mathematical Bulletin*, 47(1):82–99, 2004. doi:[10.4153/CMB-2004-010-8](https://doi.org/10.4153/CMB-2004-010-8).
- P. Naveau, A. Guillou, D. Cooley, and J. Diebolt. Modelling pairwise dependence of maxima in space. *Biometrika*, 96(1):1–17, 03 2009. doi:[10.1093/biomet/asp001](https://doi.org/10.1093/biomet/asp001).
- M. Oesting, Z. Kabluchko, and M. Schlather. Simulation of brown–resnick processes. *Extremes*, 15:89–107, 2012. doi:[110.1007/s10687-011-0128-8](https://doi.org/110.1007/s10687-011-0128-8).
- M. Oesting, M. Ribatet, and C. Dombry. Simulation of max-stable processes. In *Extreme Value Modeling and Risk Analysis: Methods and Applications*, page chapter 10. Chapman and Hall / CRC, 2015.
- M. Oesting, M. Schlather, and C. Zhou. Exact and fast simulation of max-stable processes on a compact set using the normalized spectral representation. *Bernoulli*, 24(2):1497–1530, 05 2018. doi:[10.3150/16-BEJ905](https://doi.org/10.3150/16-BEJ905).
- S. A. Padoan, M. Ribatet, and S. A. Sisson. Likelihood-based inference for max-stable processes. *Journal of the American Statistical Association*, 105(489):263–277, 2010. doi:[10.1198/jasa.2009.tm08577](https://doi.org/10.1198/jasa.2009.tm08577).
- C. Peyrega and D. Jeulin. Estimation of acoustic properties and of the representative volume element of random fibrous media. *Journal of Applied Physics*, 113(10):104901, 2013. doi:[10.1063/1.4794501](https://doi.org/10.1063/1.4794501).
- J. Potthoff. Sample properties of random fields. i. separability and measurability. *Communications on Stochastic Analysis*, 3:143–153, 2009. ISSN 2688-6669.

- S. I. Resnick. *Extreme Values, Regular Variation and Point Processes*. Springer-Verlag New York, 1987. doi:[10.1007/978-0-387-75953-1](https://doi.org/10.1007/978-0-387-75953-1).
- M. Ribatet. Spatial extremes: Max-stable processes at work. *Journal de la Société Française de Statistique*, 154(2):156–177, 2013. ISSN 2102-6238.
- J. Rivoirard, C. Demange, X. Freulon, A. Lécureuil, and N. Bellot. A top-cut model for deposits with heavy-tailed grade distribution. *Mathematical Geosciences*, 45:967–982, 2013. doi:[10.1007/s11004-012-9401-x](https://doi.org/10.1007/s11004-012-9401-x).
- D. Ruelle. *Thermodynamic Formalism: The Mathematical Structure of Equilibrium Statistical Mechanics*. Cambridge Mathematical Library. Cambridge University Press, 2 edition, 2004. doi:[10.1017/CBO9780511617546](https://doi.org/10.1017/CBO9780511617546).
- F. Salmon. Recipe for disaster: The formula that killed wall street. *Wired*, February 2009. URL <https://www.wired.com/2009/02/wp-quant/>.
- C. Scarrott and A. MacDonald. A review of extreme value threshold estimation and uncertainty quantification. *Revstat Statistical Journal*, 10:33–60, 03 2012.
- M. Schlather. Models for stationary max-stable random fields. *Extremes*, 5(1):33–44, 2002. doi:[10.1023/A:1020977924878](https://doi.org/10.1023/A:1020977924878).
- M. Schlather and J. Tawn. Inequalities for the extremal coefficients of multivariate extreme value distributions. *Extremes*, 5(1):87–102, Mar 2002. doi:[10.1023/A:1020938210765](https://doi.org/10.1023/A:1020938210765).
- M. Schlather and J. Tawn. A dependence measure for multivariate and spatial extreme values: Properties and inference. *Biometrika*, 90(1):139–156, 2003. doi:[10.1093/biomet/90.1.139](https://doi.org/10.1093/biomet/90.1.139).
- E. L. Smith and A. G. Stephenson. An extended gaussian max-stable process model for spatial extremes. *Journal of Statistical Planning and Inference*, 139(4):1266 – 1275, 2009. doi:[10.1016/j.jspi.2008.08.003](https://doi.org/10.1016/j.jspi.2008.08.003).
- R. Smith. Max-stable processes and spatial extremes. unpublished manuscript, 1990.
- E. Spodarev. *Limit Theorems for Excursion Sets of Stationary Random Fields*, pages 221–241. Springer International Publishing, Cham, 2014. doi:[10.1007/978-3-319-03512-3_13](https://doi.org/10.1007/978-3-319-03512-3_13).
- D. B. Stephenson. Definition, diagnosis, and origin of extreme weather and climate events. In H. F. Diaz and R. J. Murnane, editors, *Climate Extremes and Society*, page 11–23. Cambridge University Press, 2008. doi:[10.1017/CBO9780511535840.004](https://doi.org/10.1017/CBO9780511535840.004).
- S. A. Stoev. On the ergodicity and mixing of max-stable processes. *Stochastic Processes and their Applications*, 118(9):1679 – 1705, 2008. doi:[10.1016/j.spa.2007.10.013](https://doi.org/10.1016/j.spa.2007.10.013).

- S. A. Stoev. *Max-Stable Processes: Representations, Ergodic Properties and Statistical Applications*, pages 21–42. Springer Berlin Heidelberg, Berlin, Heidelberg, 2010. doi:[10.1007/978-3-642-14104-1_2](https://doi.org/10.1007/978-3-642-14104-1_2).
- K. Strokorb and M. Schlather. An exceptional max-stable process fully parameterized by its extremal coefficients. *Bernoulli*, 21(1):276–302, 02 2015. doi:[10.3150/13-BEJ567](https://doi.org/10.3150/13-BEJ567).
- J. Tawn, R. Shooter, R. Towe, and R. Lamb. Modelling spatial extreme events with environmental applications. *Spatial Statistics*, 28:39 – 58, 2018. doi:[10.1016/j.spasta.2018.04.007](https://doi.org/10.1016/j.spasta.2018.04.007).
- J. A. Tawn. Estimating probabilities of extreme sea-levels. *Journal of the Royal Statistical Society: Series C (Applied Statistics)*, 41(1):77–93, 1992. doi:[10.2307/2347619](https://doi.org/10.2307/2347619).
- A. Tsybakov. *Introduction to Nonparametric Estimation*. Springer, New York, 2009. doi:[10.1007/b13794](https://doi.org/10.1007/b13794).
- S. Vettori, R. Huser, and M. Genton. Bayesian modeling of air pollution extremes using nested multivariate max-stable processes. *Biometrics*, 75, 03 2018. doi:[10.1111/biom.13051](https://doi.org/10.1111/biom.13051).
- R. von Mises. La distribution de la plus grande de n valeurs. *Rev. Math. Union Interbalcanique*, 1:141–160, 1936. Reproduced in: Selected Papers of Richard von Mises, Amer. Math. Soc., Vol. 2, 271-294 (1964).
- Y. Wang, P. Roy, and S. A. Stoev. Ergodic properties of sum- and max-stable stationary random fields via null and positive group actions. *Ann. Probab.*, 41(1):206–228, 01 2013. doi:[10.1214/11-AOP732](https://doi.org/10.1214/11-AOP732).
- N. Wiener. The ergodic theorem. *Duke Math. J.*, 5(1):1–18, 03 1939. doi:[10.1215/S0012-7094-39-00501-6](https://doi.org/10.1215/S0012-7094-39-00501-6).
- A. Yaglom. *Correlation Theory of Stationary and Related Random Functions*. Springer-Verlag New York, 1987. doi:[10.1002/9781118136188](https://doi.org/10.1002/9781118136188).

RÉSUMÉ

La théorie spatiale des valeurs extrêmes permet de modéliser et prédire la fréquence d'évènements extrêmes ayant une étendue spatiale comme, par exemple, des pluies ou des températures extrêmes. Elle s'adapte bien aux données temporelles. Parfois de telles données ne sont pas accessibles : seulement un ou quelques enregistrements sont disponibles. C'est le cas, par exemple, des études sur l'évaluation de la pollution des sols. Au contraire, c'est un cadre d'analyse auquel la Géostatistique s'intéresse particulièrement. L'objectif de cette thèse est d'établir des connexions mathématiques entre ces deux disciplines afin de mieux appréhender les évènements extrêmes et en particulier leur structure de dépendance spatiale, lorsque le phénomène spatial sous-jacent n'est observé qu'une seule fois. Dans un premier temps, un lien est établi à travers le concept de portée intégrale. Issu de la théorie géostatistique, ce paramètre caractérise les fluctuations, à large échelle, d'un champ aléatoire stationnaire. Lorsque ce dernier est max-stable simple, nous montrons que sa fonction coefficient extrémal (ECF), qui est une mesure de dépendance spatiale, est fortement liée à la portée intégrale du champ des excès, au dessus d'un certain seuil, correspondant. À partir de ces travaux, un nouvel estimateur non-paramétrique de l'ECF est ensuite proposé. Ses propriétés asymptotiques sont établies lorsqu'il est évalué à partir d'un unique jeu de données spatialisées : sous certaines hypothèses concernant la portée intégrale du champ des excès, nous montrons qu'il est consistant et asymptotiquement normal. Enfin, nous proposons un algorithme efficient permettant de simuler de manière exacte des processus max-stables tempête sur un domaine continu, lorsque la fonction de forme associée est déterministe. Il se distingue de la plupart des autres procédures existantes qui s'utilisent lorsque le domaine de simulation est composé d'un nombre fini de points. La plupart des étapes de cet algorithme ont été construites afin d'être parallélisables.

MOTS CLÉS

Théorie spatiale des valeurs extrêmes, Fonction coefficient extrémal, Géostatistique, Portée intégrale, Réalisation unique, Algorithme de simulation.

ABSTRACT

Spatial extreme value theory helps model and predict the frequency of extreme events in a spatial context like, for instance, extreme precipitations, extreme temperatures. It is well adapted to time series. However, in some cases, such types of data cannot be accessed: only one or just a few records are made available. This is the case, for instance in soil contamination evaluation. This situation is rarely addressed in the spatial extremes community, contrary to Geostatistics, which typically deals with such issues. The aim of this thesis is to make some connections between both disciplines, in order to better handle the study of spatial extreme events, and especially their spatial dependence structure, when having only one set of spatial observations. A link is first established through the concept of integral range. It is a geostatistical parameter that characterizes the statistical fluctuations of a stationary random field at large scale. When the latter is max-stable, we show that its extremal coefficient function (ECF), which is a measure of spatial dependence, is closely related to the integral range of the corresponding exceedance field above a threshold. From this, we move to proposing a new nonparametric estimator of the ECF. Its asymptotic properties are derived when it is computed from a single and partially observed realization of a stationary max-stable random field. Specifically, under some assumptions on the aforementioned integral range, we prove that it is consistent and asymptotically normal. Finally, we develop a novel algorithm to perform exact simulations in a continuous domain of storm processes with deterministic shape function. It distinguishes itself from most existing procedures, which apply to simulation domains made of a finite number of points. Most part of the algorithm are designed to be parallelizable.

KEYWORDS

Spatial extreme value theory, Extremal coefficient function, Geostatistics, Integral range, Single realization, Simulation algorithm.